



University of HUDDERSFIELD

University of Huddersfield Repository

Gray, Nicholas

The Optimisation of the Floating Ball Valve Seat Component Design Methodology

Original Citation

Gray, Nicholas (2019) The Optimisation of the Floating Ball Valve Seat Component Design Methodology. Masters thesis, University of Huddersfield.

This version is available at <http://eprints.hud.ac.uk/id/eprint/35148/>

The University Repository is a digital collection of the research output of the University, available on Open Access. Copyright and Moral Rights for the items on this site are retained by the individual author and/or other copyright owners. Users may access full items free of charge; copies of full text items generally can be reproduced, displayed or performed and given to third parties in any format or medium for personal research or study, educational or not-for-profit purposes without prior permission or charge, provided:

- The authors, title and full bibliographic details is credited in any copy;
- A hyperlink and/or URL is included for the original metadata page; and
- The content is not changed in any way.

For more information, including our policy and submission procedure, please contact the Repository Team at: E.mailbox@hud.ac.uk.

<http://eprints.hud.ac.uk/>

**THE OPTIMISATION OF THE FLOATING BALL
VALVE SEAT COMPONENT DESIGN
METHODOLOGY**

MR N. D. GRAY

A thesis submitted to the University of Huddersfield in partial fulfilment of the requirements for the degree of Master of Science

The University of Huddersfield

July 2019

Copyright statement

- i. The author of this thesis (including any appendices and/or schedules to this thesis) owns any copyright in it (the "Copyright") and s/he has given The University of Huddersfield the right to use such copyright for any administrative, promotional, educational and/or teaching purposes.
- ii. Copies of this thesis, either in full or in extracts, may be made only in accordance with the regulations of the University Library. Details of these regulations may be obtained from the Librarian. This page must form part of any such copies made.
- iii. The ownership of any patents, designs, trademarks and any and all other intellectual property rights except for the Copyright (the "Intellectual Property Rights") and any reproductions of copyright works, for example graphs and tables ("Reproductions"), which may be described in this thesis, may not be owned by the author and may be owned by third parties. Such Intellectual Property Rights and Reproductions cannot and must not be made available for use without the prior written permission of the owner(s) of the relevant Intellectual Property Rights and/or Reproductions

Abstract

Nicholas Gray, Computing and Engineering, The University of Huddersfield

Abstract of Master's by Research Thesis, Submitted **July 2019**:

The objective of this thesis is to optimise the design methodology through which the design of floating ball valves seats are designed. The lack of an established and accepted design methodology has led to numerous part-solutions being applied to the design process. The variations in design methodology lead to significant variations in designs produced and significant variations in the performance of these designs. In establishing an optimised design methodology this thesis takes the fundamental functions of a floating ball valve and develops a design methodology which when applied achieves a consistent and robust seat design for floating ball valves.

To develop the optimised floating ball valve seat design method this thesis first develops an understanding of the mechanics governing the fundamental features of the seat and its interaction with the ball component. The development of the understanding is started through the establishment of theoretical models describing the mechanics of the seat component based on established works. To further ensure the understanding of the seat component is correct a realistic computational model is developed. Through the evaluation of the data from the computational model the theoretical models can be compared to the realistic function of the seat component. Where there are differences between the results from the theoretical and computational models, the theoretical models are improved to be able to be applied to the computational model and generate representative results. Following on from the validation of the theoretical models, the theoretical models are re-arranged and combined in such a way that the models used to describe the mechanics can be used to determine design parameters. The design equations developed are combined into a complete design methodology through which a floating ball valve seat can be designed. Following the establishment of the floating ball valve seat design methodology, the methodology is applied to a case study to demonstrate the robustness and appropriateness of the methodology to designing floating ball valve seats.

Table of Contents

Chapter 1 - Introduction.....	14
1.1 Thesis Overview.....	15
1.2 General Introduction.....	16
1.3 Floating Ball General Principles	21
1.4 Seat Designs	23
1.5 Gaps in General Knowledge	24
1.6 Motivation of the Work.....	25
1.7 Aims of Research	25
Chapter 2 - Literature Review	27
2.1 General Approach.....	28
2.2 Mechanistic Theoretical Models	29
2.2.1 Theoretical Sealing Models – Ball Valves	29
2.2.2 Theoretical Sealing Model – Seals.....	38
2.2.3 Requirements of the ball valve seat.....	42
2.2.4 Theoretical Contact Models.....	43
2.2.5 Theoretical Functional Model (Torque)	56
2.2.6 Section Outcomes	59
2.3 Analytical Methods and Validation.....	60
2.3.1 Section Outcomes	64
2.4 Design Methodologies	65
2.4.1 Section Outcomes	67
2.5 Summary	69
2.6 Scope of the Work.....	72
2.7 Specific Research Objectives.....	73
Chapter 3 – Research Methods.....	75
3.1 Finite Element Analysis	76
3.1.1 Analysis Steps	76
3.1.2 Study Properties	79
3.1.3 Geometry of the Valve	79
3.1.4 Material	82
3.1.5 Loads and Fixtures	83
3.1.6 Contact Definitions	87
3.1.7 Elements and Mesh	88
3.1.8 Results Processing.....	90
3.1.9 Instrumental Uncertainties	91
3.1.10 Instrumental Developments.....	91
Chapter 4 – Theoretical Mechanistic Model Development	92
4.1 Pressure-load theoretical mechanistic model development.....	93

4.2	Seat deflection theoretical mechanistic model development	97
4.3	Bending stress theoretical mechanistic model development	103
4.4	Conclusions	104
Chapter 5 – Validation of established theoretical models through the use of finite element analysis.....		107
5.1	Finite element analysis.....	108
5.1.1	Pressure-load	108
5.1.2	Seat deflection.....	126
5.1.3	Bending Stress	138
5.2	Comparison of finite element analysis results to theoretical results.....	148
5.2.1	Pressure-load	148
5.2.2	Seat Deflection	149
5.2.3	Bending Stress	150
5.3	Modification of theoretical models.....	151
5.3.1	Pressure-load	151
5.3.2	Seat deflection.....	153
5.3.3	Bending Stress	155
5.4	Conclusions	155
Chapter 6 – Development of a Design Methodology		157
6.1	Proposal of design equations.....	158
6.1.1	Pressure Load	158
6.1.2	Initial Deflection – Seat Preload	163
6.1.3	Bending Stress	165
6.2	Develop of design methodology	166
6.2.1	Initial Analysis (Step 1).....	166
6.2.2	Application of a Seat Preload (Step 2).....	168
6.2.3	Evaluation of the Combined Load (Step 3).....	169
6.2.4	Validation of Bending Stress in Seat Component (Step 4).....	171
6.2.5	Determination of Valve Torque (Step 5)	172
6.2.6	Design Methodology Flowchart.....	173
6.3	Application of design methodology to a case study	176
6.4	Conclusions	184
Chapter 7 - Summary		186
7.1	Research Problem Synopsis	187
7.2	Research Aims and Major Achievements.....	188
7.3	Recommendations	189
Appendix 1 – Contact Width Comparisons		191
Appendix 2 – O-Ring Load and Sealing Calculations		193
Appendix 3 – Simulation Convergence Studies (Data)		195
Appendix 4 – Theoretical Mean Contact Stress Calculations.....		196
Appendix 5 – Theoretical Seat Bending Stress Calculations		199

Bibliography201

Word count: 61,640 words

List of Figures

- Figure 1 - Floating Ball Valve Rendering (Grant, 2019) 16
- Figure 2 - Full and Reduced Bore Floating Ball Valves (Zoombd24, 2019) 17
- Figure 3 – (Axial) End-Entry Floating Ball Valve (British Standards Institution, 2015) 18
- Figure 4 - Ball Valve Body Styles (British Standards Institute, 1974)..... 19
- Figure 5 - Axial Entry Floating Ball Valve (Velan Inc, 2019)..... 20
- Figure 6 - Two-Piece Floating Ball Valve (Velan Inc, 2019)..... 20
- Figure 7 - Three-Piece Floating Ball Valve (Velan Inc, 2014) 21
- Figure 8 - Ball Valve Assembly, Initial Pressure Application 22
- Figure 9- Ball Valve Assembly, Body Cavity Pressurised..... 22
- Figure 10 – Seat Design Type Comparison (Velan Inc, 2019) 29
- Figure 11 - Ball Valve Assembly 31
- Figure 12 - Minimum Seat Deflection (Canada Patent No. 3,384,341, 1964) 32
- Figure 13 - Maximum Seat Deflection (Canada Patent No. 3,384,341, 1964)..... 32
- Figure 14 - Flexible Seat, Ball Contact (Metso, 2011) 33
- Figure 15 - Ball Valve Design Assessed (G.V.Bozhko, 2000)..... 34
- Figure 16 - Seat Design Assessed (G.V.Bozhko, 2000) 35
- Figure 17 - Flanged Head Designs [UG34], (American Society of Mechanical Engineers, 2017) 36
- Figure 18 - Trunnion Mounted Ball Valve Seat (Boiko, Regush, Semenov, & Regush, 1986) 37
- Figure 19 - Schematic of cylinders (left) and spheres (right) in contact (Dwyer-Joyce, 1997) 44
- Figure 20 - Pressure Profile Developed on Contact (Dwyer-Joyce, 1997)..... 46
- Figure 21 - Geometry of Spherical Indentation (Fleck, 1998) 47
- Figure 22 - Contour Plot of Radial Stress Component (Lee, 2006) 50
- Figure 23 - Lip-Seal Initial Interference Stress Distribution (Kim, 1997) 51
- Figure 24 - Comparison of Uniform Pressure and Hertz Pressure (K.L.Johnson, 2003) 52
- Figure 25 – Radial Lip Seal Schematic diagram (a), interference of seal lip and shaft (XiaoHong, et al., 2014)..... 60
- Figure 26 – Finite element Model (XiaoHong, et al., 2014)..... 61
- Figure 27 - 3D Modelling of ball valve and seat (Song, Wang, & Park, 2009)..... 62
- Figure 28 - Von Mises Stress under Load condition A (a), and Load condition A+B (b) (Song, Wang, & Park, 2009) 63
- Figure 29 - Finite element analysis process flowchart 77
- Figure 30 – General Seat Design Layout to be Optimised..... 79
- Figure 31 - Seat Design Detail Drawing 80
- Figure 32 - Supplementary Seat Dimensions..... 81

Figure 33 - Mean seal diameter	83
Figure 34 - Applied Load.....	84
Figure 35 - Loads and Fixtures Applied to Model Geometry	85
Figure 36 - Diagram of seat component being supported by housing.....	86
Figure 37 - Finite Element Solver Comparison (Courtesy of SolidSolutions).....	87
Figure 38 - Spherical Indentation Mesh (Fleck, 1998).....	88
Figure 39 - Mesh Applied to Model Geometry	89
Figure 40 - Curvature-Based Mesh Convergence Study with Element Growth Ratio of 1.1 .	90
Figure 41 - Mean Seat Contact Diameter	93
Figure 42 - Pressure Load Components τ	94
Figure 43 - Seat Angle	94
Figure 44 - Roark's theory of stress and strain, Table 11.2, Case 1c diagram	98
Figure 45 - Roark's theory of stress and strain, Table 11.2, Case 1d, diagram.....	99
Figure 46 - Roark's theory of stress and strain, Table 11.2, Case 1h diagram.....	99
Figure 47 - Radial Seat Distance Definitions.....	100
Figure 48 – A plot of the von mises stress from FEA when a 400lb-f (1779.3N) load is applied to the model.....	109
Figure 49 – A plot of the von mises stress from FEA when a 600lb-f (2668.9N) load is applied to the model.....	110
Figure 50 – A plot of the von mises stress from FEA when a 800lb-f (3558.6N) load is applied to the model.....	111
Figure 51 – A plot of the von mises stress from FEA when a load of 1000lb-f (4448.2N) is applied to the model.....	112
Figure 52 – A plot of the von mises stress from FEA when a load of 1200lb-f (5337.9N) is applied to the model.....	113
Figure 53 – A plot of the von mises stress from FEA when a load of 1400lb-f (6227.5N) is applied to the model.....	114
Figure 54 – A plot of the von mises stress from FEA when a load of 1600lb-f (7117.2N) is applied to the model.....	115
Figure 55 – Contact Pressure against Location of Stress in Half-Contact	119
Figure 56 – A plot of the magnitude of contact pressure against location in contact half-width	120
Figure 57 – A plot of the magnitude of contact pressure against location in contact half-width, including 440lb-f (1957.2N) data	121
Figure 58 – A plot of the magnitude of contact pressure against location in contact half-width determined from the FEA stress profile	122
Figure 59 – A plot of the seat deflection from FEA when a 600lb-f (2668.9N) load is applied	127
Figure 60 – A plot of the seat deflection from FEA when a 800lb-f (3558.6N) load is applied	128
Figure 61 – A plot of the seat deflection from FEA when a 1000lb-f (4448.2N) load is applied	129

Figure 62 – A plot of the seat deflection from FEA when a 1200lb-f (5337.9N) load is applied	130
Figure 63 – A plot of the seat deflection from FEA when a 1400lb-f (6227.5N) load is applied	131
Figure 64 – A plot of the seat deflection from FEA when a 1600lb-f (7117.2N) load is applied.....	132
Figure 65 – A graph showing the deflection results plotted against distance of the result from point of contact	134
Figure 66 – Graph showing a plot of deflection/max. deflection against distance from centre/contact half-width.....	135
Figure 67 – A plot showing the probe of von mises stresses when a load of 600lb-f (2668.9N) is applied	139
Figure 68 – A plot showing the probe of von mises stresses when a load of 800lb-f (3558.6N) is applied	140
Figure 69 – A plot showing the probe of von mises stresses when a load of 1000lb-f (4448.2N) is applied	141
Figure 70 – A plot showing the probe of von mises stresses when a load of 1200lb-f (5337.9N) is applied	142
Figure 71 – A plot showing the probe of von mises stresses when a load of 1400lb-f (6227.5N) is applied	143
Figure 72 – A plot showing the probe of von mises stresses when a load of 1600lb-f (7117.2N) is applied	144
Figure 73 – Review of the load components	151
Figure 74 – Design Pressure-Area Definition	158
Figure 75 - Seat Angle for Design Calculations	159
Figure 76 – Applied load components used for the determination of sealing mechanics ...	159
Figure 77 - Flowchart of the design methodology.....	174
Figure 78 - Dimensions of seat and ball component for case study.....	176
Figure 79 - Von Mises stress plot with case study geometry and applied loads	180
Figure 80 - Figure showing radial distances of the case study annular disc.....	182
Figure 81 - Chord Length Variable Definitions (Tutor Vista, 2019).....	191

List of Tables

Table 1 - Minimum duration for pressure tests (International Organisation for Standardization, 2008).....	43
Table 2 - Tabulation of Hertz Contact Mechanics Equations (K.L.Johnson, 2003).....	44
Table 3 - Comparison of O-Ring and Hertz Peak Contact Stress'	49
Table 4 - Tabulation of Torque Evaluation (EPRI, 1999).....	56
Table 5 - ASTM A182 F316 Material Properties	82
Table 6 - PTFE Material Properties	83
Table 7 - Theoretical contact pressures from the applied pressure load	97
Table 8 - Theoretical seat material radial lengths.....	101
Table 9 - Theoretical radial seat dimensions.....	101
Table 10 - Roark's theory of stress and strain Table 11.2, Case 1c, deflection results.....	102
Table 11 - Radial and tangential stresses from Table11.2, Case 1c	103
Table 12 - Von Mises Bending Stress.....	104
Table 13 – Average contact pressure from stress profile from FEA results (pressure load)	116
Table 14 - Percentage change in average contact stress from the stress profile of the FEA results	117
Table 15 – Percentage change in average contact pressure per percentage change in load from stress profile FEA results.....	118
Table 16 – Table of average contact pressures determined from contact stress profile FEA results	123
Table 17 – Table of the percentage change in load an average contact pressure from FEA data.....	123
Table 18 - Percentage change in contact pressure per percentage change in applied pressure load	124
Table 19 - Finite Element Analysis Deflection Results	136
Table 20 - Percentage change in FEA deflection results.....	136
Table 21 - Percentage change in maximum deflection per percentage change in applied load	137
Table 22 – Tabulated stress values from probes of von mises stress plots at each load increment.....	145
Table 23 – Filtered stress values from probes of von mises stress plots at each load increment.....	145
Table 24 - Average bending stress values determined from the results of the probe data	146
Table 25 - Percentage change in average bending stresses from probing von mises stress plots	146
Table 26 – Percentage change in bending stress per percentage change in applied load ..	147
Table 27 – Comparison of theoretical and computational average contact pressure by applied load	148

Table 28 - Comparison of theoretical and computational maximum seat deflection by applied load	149
Table 29 - Table showing the comparison of theoretical and computational bending stresses	150
Table 30 – Comparison of revised average computational contact pressures to analytical results by applied load	152
Table 31 - Comparison of the amended theoretical deflections to the computational results by applied load.....	153
Table 32 – Comparison of the revised theoretical deflections to the computational results by applied load.	154
Table 33 - Case study max. contact pressure finite element analysis results	181
Table 34 - O-Ring 72-0945-30 Dimensions	191
Table 35 - Contact width results compared to chord lengths	192
Table 36 – Tabulated max. contact pressure results for Hertz analysis of an o-ring	193
Table 37 - Convergence Study Settings and Results.....	195

List of Abbreviations

Symbol	Definition	Units
α	Sealing load component angle	Degrees
β	Included seat angle	Degrees
σ_1	Principle stress 1	psi [N.mm ⁻²]
σ_2	Principle stress 2	psi [N.mm ⁻²]
σ_v	Equivalent / von mises stress	psi [N.mm ⁻²]
θ	Angular deflection of seat	Degrees
θ_b	Angular deflection of seat at location b	Degrees
μ	Seat coefficient of friction	N/A
a	Contact half-width	in [mm]
a_1	Contact half-width from pressure-load application	in [mm]
a_2	Contact half-width from preload application	in [mm]
a_3	Contact half-width from combined load application	in [mm]
a_{400}	Contact half-width from 400lb-f load application	in [mm]
a_{600}	Contact half-width from 600lb-f load application	in [mm]
a_{800}	Contact half-width from 800 lb-f load application	in [mm]
a_{1000}	Contact half width from 1000lb-f load application	in [mm]
a_{1200}	Contact half-width from 1200 lb-f load application	in [mm]
a_{1400}	Contact half-width from 1400 lb-f load application	in [mm]
a_{1600}	Contact half-width from 1600 lb-f load application	in [mm]
b	O-ring contact width	in [mm]
d_1	O-ring section diameter	in [mm]
D	Plate constant	N/A
D_i	O-ring outside diameter	in [mm]
D_M	O-ring mean diameter	in [mm]
D_o	O-ring outside diameter	in [mm]
D_{MS}	Mean seat contact diameter	in [mm]
E	Modulus of elasticity	psi [N.mm ⁻²]
E^*	Reduced modulus	psi [N.mm ⁻²]
G_3	Calculation constant	N/A

f'	Maximum o-ring contact pressure	psi [N.mm ⁻²]
f'_{10}	Maximum o-ring contact pressure 10% compressed	psi [N.mm ⁻²]
f'_{15}	Maximum o-ring contact pressure 15% compressed	psi [N.mm ⁻²]
f'_{20}	Maximum o-ring contact pressure 20% compressed	psi [N.mm ⁻²]
F	Applied load	lb-f [N]
F_{10}	Load required to compress o-ring by 10%	lb-f [N]
F_{15}	Load required to compress o-ring by 15%	lb-f [N]
F_{20}	Load required to compress o-ring by 20%	lb-f [N]
F_2	Calculation constant	N/A
F_3	Calculation constant	N/A
F_7	Calculation constant	N/A
F_9	Calculation constant	N/A
F_t	Shear load	lb-f [N]
F_{PL}	Pressure load	lb-f [N]
F_{SS}	Sealing load	lb-f [N]
L	Contact length	in [mm]
L_c	Chord length	in [mm]
M_r	Radial bending moment	in-lb [N.mm]
M_{rb}	Bending moment at location b	in-lb [N.mm]
M_t	tangential bending moment	in-lb [N.mm]
P	Applied pressure (fluid pressure)	psi [N.mm ⁻²]
P_1	Load per unit length from pressure load	lb-in ⁻¹ [N.mm ⁻¹]
P_3	Combined load per unit lengths	psi [N.mm ⁻²]
p_0	Maximum contact pressure	psi [N.mm ⁻²]
p_{01}	Maximum contact pressure under pressure load	psi [N.mm ⁻²]
p_e	Effective contact pressure from preload	psi [N.mm ⁻²]
p_{gs}	Gas sealing contact pressure	psi [N.mm ⁻²]
p_{ls}	Liquid sealing contact pressure	psi [N.mm ⁻²]
p_m	Mean contact pressure	psi [N.mm ⁻²]
p_{m400}	Mean contact pressure with 400lb-f applied	psi [N.mm ⁻²]
p_{m600}	Mean contact pressure with 600lb-f applied	psi [N.mm ⁻²]
p_{m800}	Mean contact pressure with 800lb-f applied	psi [N.mm ⁻²]

p_{m1000}	Mean contact pressure with 1000lb-f applied	psi [N.mm ⁻²]
p_{m1200}	Mean contact pressure with 1200lb-f applied	psi [N.mm ⁻²]
p_{m1400}	Mean contact pressure with 1400lb-f applied	psi [N.mm ⁻²]
p_{m1400}	Mean contact pressure with 1600lb-f applied	psi [N.mm ⁻²]
q	Sealing contact pressure	psi [N.mm ⁻²]
Q_b	Shear stress at location b	psi [N.mm ⁻²]
R	Radius	in [mm]
R_e	Equivalent radius	in [mm]
r	O-ring section radius	in [mm]
r_0	radius of applied load	in [mm]
r_a	External radial seat span	in [mm]
r_b	Internal radial seat span	in [mm]
S_r	Principle radial stress	psi [N.mm ⁻²]
S_t	Principle tangential stress	psi [N.mm ⁻²]
t	Seat thickness	in [mm]
ν	Poisson's ratio	N/A
w	Deflection load per unit length	lb-in ⁻¹ [N.mm ⁻¹]
x	O-ring compression	in [mm]
y	Seat component deflection	in [mm]
y_b	Seat deflection at location b	in [mm]

Chapter 1 - Introduction

This chapter forms an introduction to the subject area of the thesis. The introduction is formed of information about the general subject area of valves in general initial and then following that ball valves, following this a detailed description of floating ball valves is included. Once the floating ball valve is introduced in this chapter, context for the problem investigated by this thesis is created by discussing the function of the seat component in a floating ball valve and the general issues that surround the form, function and design of these components.

In addition to introducing the subject area this chapter includes an overview of this thesis. The overview of the thesis details the chapters included in this thesis and the works contained within each of the chapters.

1.1 Thesis Overview

This thesis is comprised of seven chapters, each of these chapters achieves an aim which contributes to the achievement of the optimisation of the design methodology of a floating ball valve seat.

Chapter 1 forms the introduction to this thesis, in this chapter a general introduction to the subject area of valves is presented with a focus on floating ball valves. From floating ball valves, the area of interest of this thesis, the seat component and the design of the seat component is introduced. From the review of the basis established in this chapter the aims of this thesis are developed.

Chapter 2 is the literature review of this thesis. In chapter 2 any applicable works are reviewed to determine whether they hold knowledge that can be applied to the aims defined in chapter 1. Through reviewing the available literature this chapter identifies where there exist gaps in the knowledge required to complete the aims of the thesis. From the gaps in the knowledge around the aims the research objectives are formed.

Chapter 3 covers the research methods used in this thesis. The research methods applied to the work presented in this thesis are presented and explained to ensure that the research completed is robust and accurate.

Chapter 4 contains the development of theoretical models. The theoretical models established in chapter 4 describe the mechanics of the floating ball valve seat component when a load is applied to the seat. The description of the mechanics of the floating ball valve seat component is achieved through the application of established theories to the geometry of the ball and seat and load applied.

Chapter 5 covers the validation and modification of the theoretical models of the previous chapter. Computational models are developed in this chapter which are used to provide realistic data from the interaction of the ball and seat components when subjected to a load. The results of the computational models are compared with the theoretical models results and the differences between them identified. Finally, in this chapter the assumptions made in Chapter 4 to establish the theoretical models are reviewed to develop valid theoretical models which describe the mechanics of the floating ball valve seat.

Chapter 6 of this thesis developed the design methodology. The valid theoretical models describing the mechanics are developed to describe by the choice of inputs and outputs the parameters needed to analyse a seat component while designing it. The design equations are then formulated into a design methodology through which a floating ball valve seat can be designed. With the design methodology established it is then applied to a case study to ensure the results gained are valid. In applying the design method to a case study it is evaluated numerically and by a computational model to ensure the results are comparable.

Chapter 7 is the summary of the thesis. In this chapter the works completed previously are summarised, achievements, aims and objectives met are discussed. Where there are opportunities for future work based on the work of this thesis these are highlighted here.

1.2 General Introduction

A valve is a fluid control device used in a number of industries where it is installed in a pipeline. Valves are included in pipelines for the purpose of regulating the flow of fluid in the pipeline. When a ball valve is used in a pipeline it is typically used for the purpose of on/off fluid flow control, when in the closed position the ball valve isolates the downstream sections of the pipeline.

Valves are broadly split into a number of groups based on their design, these groups are: Ball, Butterfly, Check, Diaphragm, Gate, Globe, Needle, Pinch, Plug and Pressure-Relief Valves. Each of these valve types have inherent advantages and disadvantages because of the features associated with that type of valve. When specifying valves for a pipeline the valve type whose features best suit the application should be chosen. Despite the various types of valves available this thesis is concerned only with ball valves, and more specifically the sub-group of floating ball valves and within that sub-group the soft-seated ball valves constituents. Soft-seated ball valves are a form of ball valve where the seat component is manufactured from a non-metallic material, this material is typically a form of polymer such as PTFE.

Ball valves are basically defined as "a species of plug valves having a ball shaped closure member." (Zappe, 1998) this can be expanded on further, where a "ball valve is basically a ported sphere in a housing. Rotation of the sphere by 90° changes the position from open to closed." (Lyons & Askland, 1975). Figure 1 shows a rendered sectional image of a floating ball valve illustrating the description of having a ported ball closure located in a housing defining the floating ball valve construction.

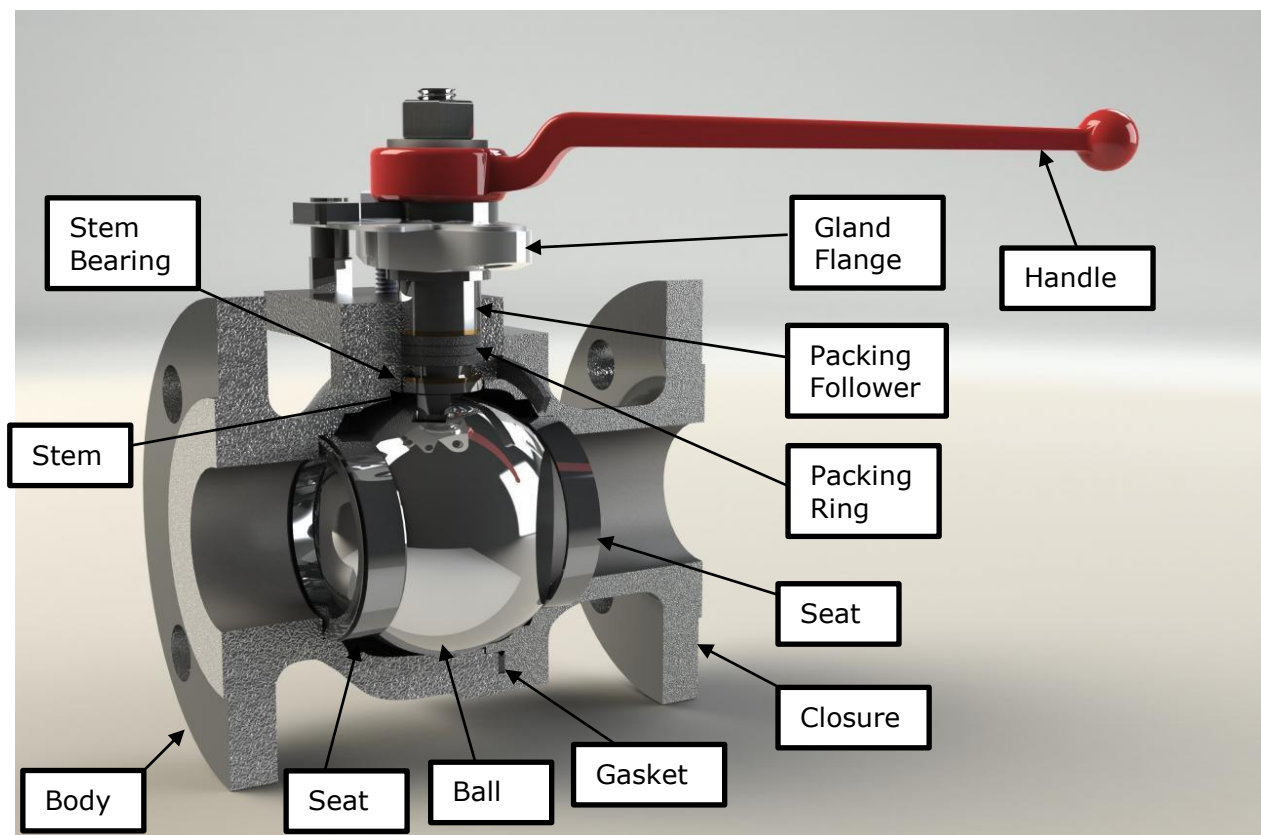


Figure 1 - Floating Ball Valve Rendering (Grant, 2019)

In Figure 1 we see a ball with a cylindrical port through the middle of it, this port allows passage of fluid through the valve when the valve is in the open position. On either side of the ball is located the seats. The function of the seats is primarily to create a seal between itself and the ball component to prevent the fluid from flowing through the valve when the valve is in the closed position. Driving the ball is the stem, the stem transmits the load applied to the handle to the ball allowing the valve to be moved between the open and closed positions. Retaining the ball, seats and stem are the body and closure components, these components form the pressure-containing boundary. The pressure-containing components are those which contain the pressurised fluid when applied to the valve in either the open or closed position. Sealing the body and closure components is a gasket. The gaskets purpose is to create a seal between the body and closure components preventing the fluid from leaking from the valve to the atmosphere. The stem bearing sits between the stem and body. The stem bearing provides a surface for the shoulder of the stem to run against which prevents the two components from galling when the surfaces run against each other. Sealing the stem is the gland packing, packing follower and gland flange arrangement. The gland arrangement compresses the gland packing creating a seal between the body and stem components. The handle converts the applied mechanical force to a torque applied to the valve stem which in turn operates the valve moving it between the open and closed positions.

Further to the basic definition a ball valves construction the valve “may be of a fixed or floating design and full or reduced port” (Lyons & Askland, 1975). For the purpose of this thesis we shall only be considering floating ball valve; further to this as explained later in this section the distinction between full and reduced port is considered to have no bearing on the outcome of this thesis. Figure 2 shows a comparison between a full and reduced bore valve illustrating the reduction of the passage through the valve.

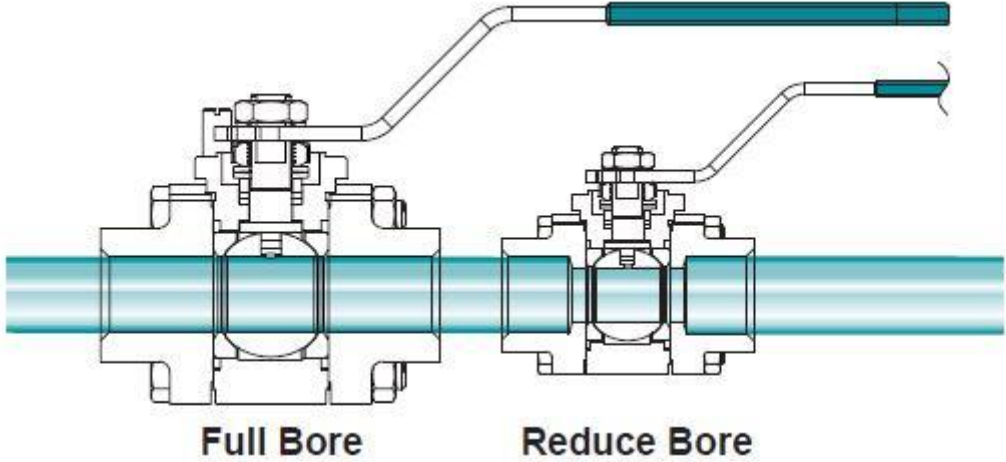


Figure 2 - Full and Reduced Bore Floating Ball Valves (Zoombd24, 2019)

A typical floating ball valve can be seen in the following figure, (Figure 3). Although it is not obvious how the seats (12) have been designed, it can be seen that the ball (3) is located between the two seats (12) and is therefore 'floating' with no components either supporting or locating the ball to any other component within the valve assembly. It should be noted that the valve is shown in the open position, when moved to the closed position the ball will be able to move freely in the upstream and downstream directions.

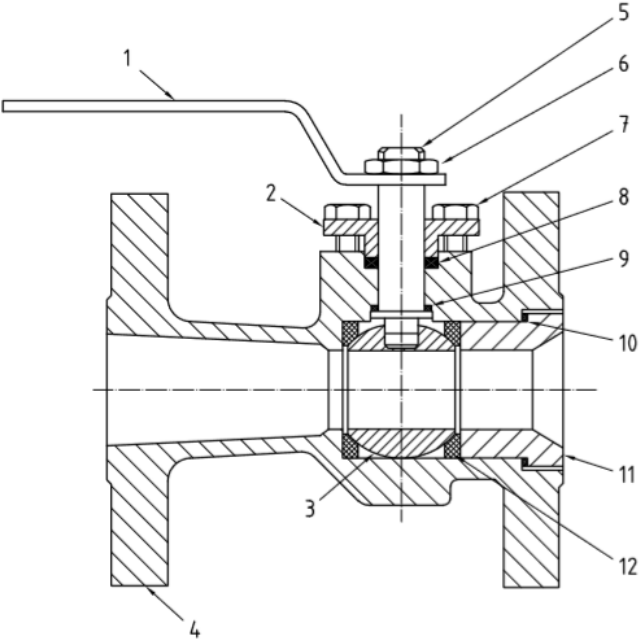


Figure 3 – (Axial) End-Entry Floating Ball Valve (British Standards Institution, 2015)

The components shown in Figure 3 are as follows, 1 – Handle (lever type), 2 – Gland, 3 – Ball, 4 – Body, 5 – Stem, 6 – Stem nut, 7 – Gland bolting, 8 – Stem seal, 9 – Thrust washer, 10 – Body seal, 11 – Body insert, 12 – seat.

The previous figure, Figure 3, shows an (axial) end-entry ball valve, this however is only one design of floating ball valve. The construction of the pressure-envelope, achieved by screwing a body insert (11), into the body (4) defines this particular valve as an (axial) end-entry floating ball valve. The design of the pressure-envelope will vary as illustrated diagrammatically in Figure 4 (this figure also includes top-entry and trunnion mounted ball valves).

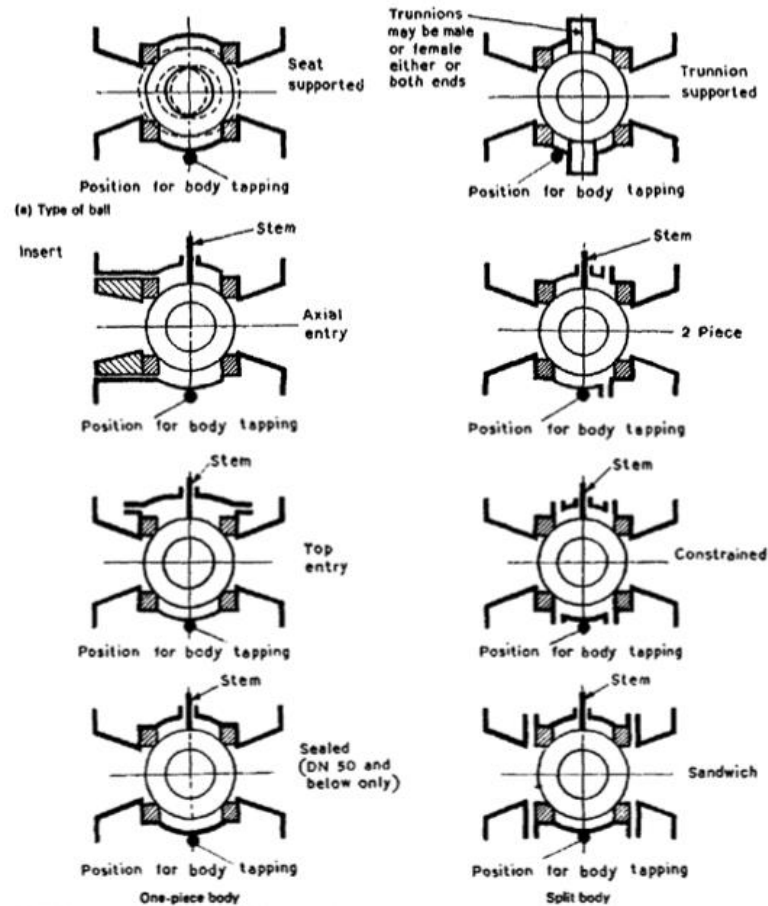


Figure 4 - Ball Valve Body Styles (British Standards Institute, 1974)

Looking at the construction of the pressure envelope of the floating ball valves shown in Figure 4 there are many differences between the designs but also some similarities. In all the valve designs (with the exception of the trunnion mounted design) the ball is solely supported between the two seats. The valve body holds the seats in alignment with each other therefore, the seats are held in alignment with the ball therefore giving the uniform circumferential sealing stress as previously referenced; this function of the design is common to all the illustrations of the floating ball valves. Also common across all the designs of the floating ball valves is the loading of the seats by the closure, be that by an insert (axial-entry), Adaptor (2-piece) or Adaptors (3-piece, sandwich and constrained).

Figure 5 shows an axial-entry floating ball valve where the ball and a seat are installed in the valve body, the closure of the housing is achieved through an insert threaded into the valve body which contains the second seat as well as means for achieving a seal between the valve body and insert components. The load generated by threading the insert into the body is distributed across both the seats to provide a pre-load for both seats at the point contact with the ball.

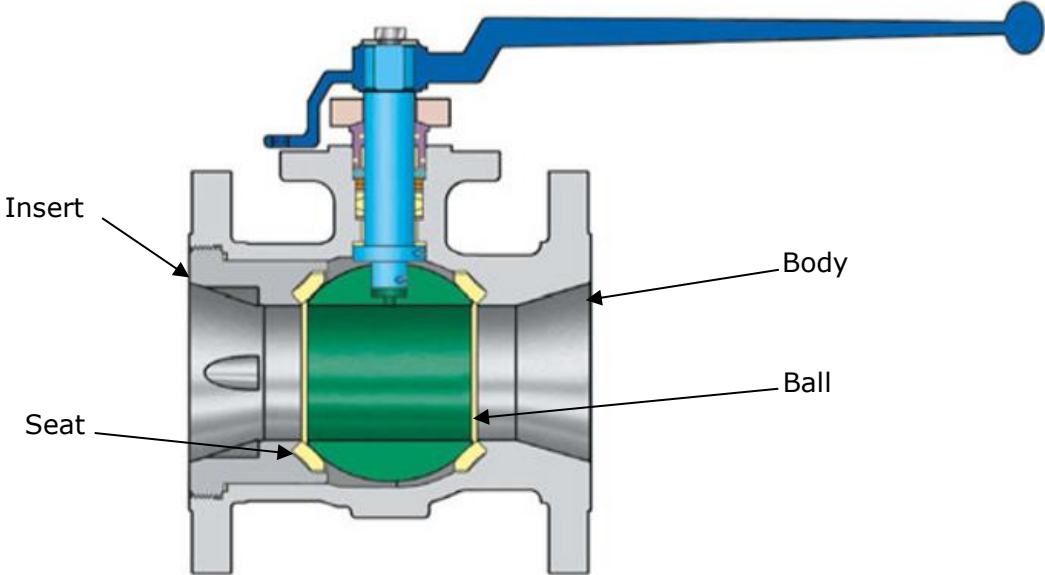


Figure 5 - Axial Entry Floating Ball Valve (Velan Inc, 2019)

Figure 6 shows a two-piece floating ball valve where the ball and a seat are installed in the valve body, the closure of the housing is achieved through the bolting of a closure (adaptor) onto the body. The adaptor contains the second seat and the seal for the purpose of achieving a seal between the valve body and adaptor component. The load generated by the bolting in compressing the seal between the body and the adaptor is also used to provide a pre-load for both seats where they contact the ball.

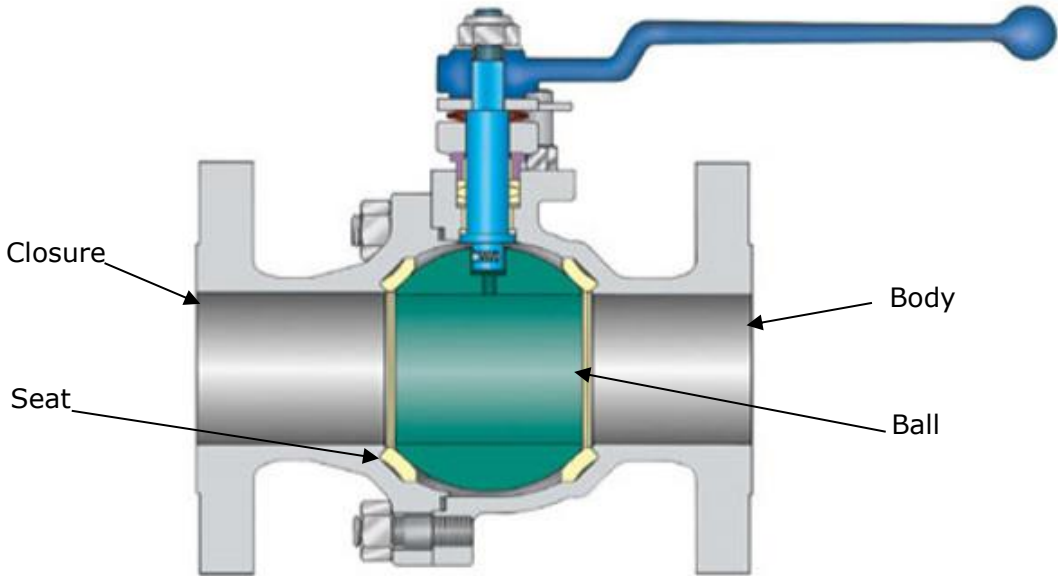


Figure 6 - Two-Piece Floating Ball Valve (Velan Inc, 2019)

Figure 7 illustrates a three-piece floating ball valve design where the ball and seats are retained within a central body section, the closure of the housing is achieved through the bolting of a closure (adaptor) onto each side of the body. The load generated by the bolting in compressing the seal between the body and adaptors is also used to provide a pre-load for both seats where they contact the ball.

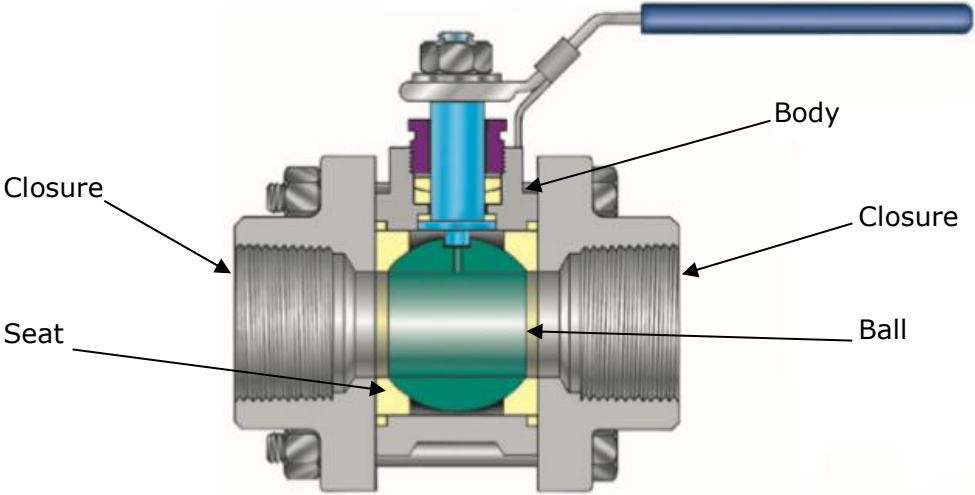


Figure 7 - Three-Piece Floating Ball Valve (Velan Inc, 2014)

While the design of the pressure-envelope may change due to the body style selected the design of the ball, seats and stem (collectively referred to as the trim), should be identical across body styles for the same valve size and pressure rating.

1.3 Floating Ball General Principles

As described earlier floating ball valve seats are the core of a floating ball valve in providing support to the ball, determining the operating torque profile and sealing performance of the valve. A simplified model of the construction of a floating ball valve is shown in Figure 8. Figure 8 is comprised of the ball (1), which is supported by two seats (2). The seats (2) are retained within the valve body (3) "two round seats are fixed on the upstream and downstream side of the ball, this is commonly called double seating." (Skousen, 1997). As discussed on page 19, the exact construction of the valve body is not important when considering the design and function of the trim, therefore the construction of it has been neglected from this figure. Finally, the stem (4) is shown, this operates the valve by turning the ball from the open position to the closed position (closed position shown).

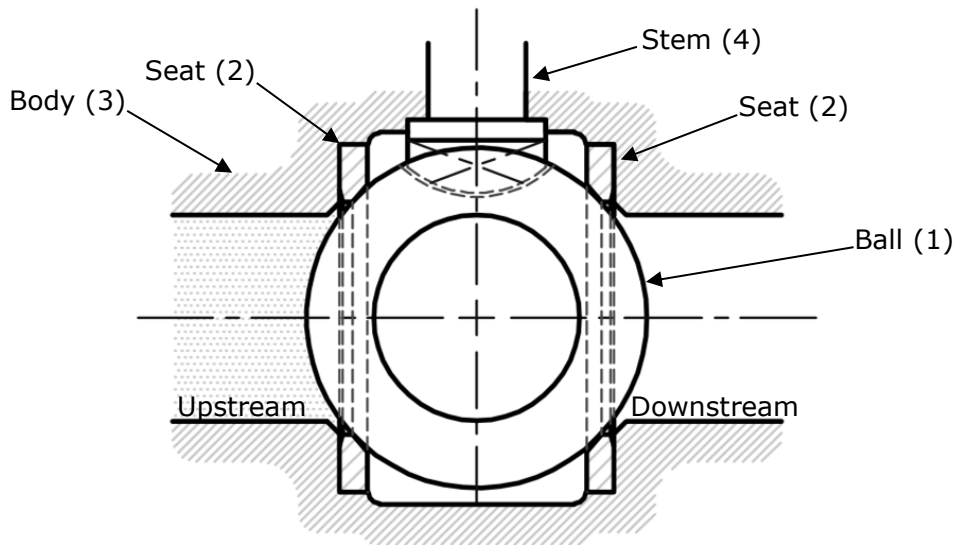


Figure 8 - Ball Valve Assembly, Initial Pressure Application

When the ball valve is 'operated', the valve is turned from the open position to the closed position, as "the balls opening begins to move perpendicular to the flowstream with the edges of the port rotating through the seat. When the full quarter-turn is reached, the port is completely perpendicular to the flowstream, blocking the flow" (Skousen, 1997). When the port is completely perpendicular to the flowstream, in the closed position, the upstream cavity will become pressurised as shown in Figure 8. Initially as the upstream cavity fills and starts to become pressurised the upstream seat seals against the ball, however, there will come a point where the pressure acting over the ball will overcome this seal. As "the ball is not fixed to the stem and is allowed some freedom of movement through the key slot." (Skousen, 1997) this freedom of movement allows the pressure acting over the ball to 'push' the ball away from the upstream seat. With the ball 'pushed' away from the upstream seat the body cavity will fill with fluid from the upstream section of the valve as shown in the following figure:

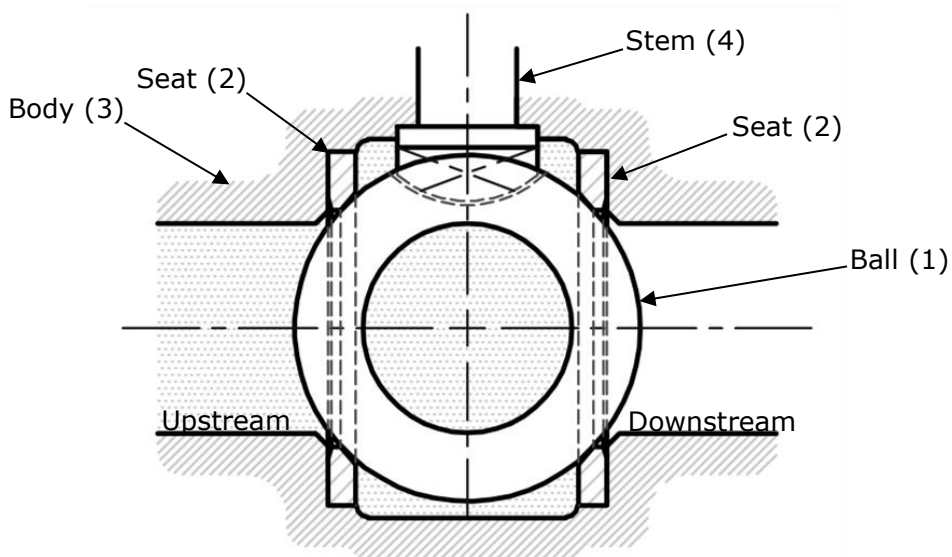


Figure 9- Ball Valve Assembly, Body Cavity Pressurised

Figure 9 shows the body cavity becoming pressurised by the fluid from the upstream pipeline. The result of the body cavity becoming pressurised is the ball have a pressure drop acting over the ball and the unpressurised downstream cavity. "The force of the upstream pressure acting over the ball pushes the ball hard against the downstream seat" (BVAA, 2007), this pushing of the ball into the downstream seat, "the upstream fluid pressure assists the seal by pushing the ball back against a rear or downstream seat." (Skousen, 1997), the upstream fluid filling the cavity and acting over the ball will increase the load on the seat therefore increasing the seal between the ball and seat.

There are a couple of conditions that appear applicable to the previously described general principles of the floating ball valve seat and mechanics; firstly, that when the flow direction is reversed, i.e. the downstream pipeline is pressurised "the ball seats in the reverse direction" (BVAA, 2007) this shows that both seats in the valve must be identical to allow this to be possible within the same process conditions. While the general principles shown previously shows the pressure as the main element in the mechanics of the floating ball valve under "low pressure conditions springs may be incorporated or the seats may be pre-loaded or pre-formed" (BVAA, 2007) indicating that at lower pressures the fluid pressure alone may be insufficient to achieve the load required to generate a seal. Conversely "the higher the pressure the more sealing force and torque are required to operate the valve" (BVAA, 2007) eludes to a relationship between the pressure in the valve and the load needed to achieve a seal between the ball and seat. The quote also indicates that there is a relationship between the fluid pressure and the operating torque of the valve with an increase in the fluid pressure resulting in an increased operating torque.

1.4 Seat Designs

With the design of the seat being critical to both the performance and function of the valve it is an area where a greater understanding of the mechanics at play is required to optimise the performance of the seat, "Several different seat design principles are used to achieve good sealing and low torque requirements." (Nesbitt, 2001). There are various design principles which will need to be assessed to ensure the suitability of them with regards to the optimisation of the seat as well as the applicability of the work contained in further sections of this thesis to the furthering of knowledge with regards to the design of floating ball valve seats.

When considering the design of seats in general the following is referenced as the applicable design methodologies depending on the type/style of seat used. "The intimate contact between the seatings of ball valves may be achieved in a number of ways. Some of the ones more frequently used are:

1. By the fluid pressure forcing the ball against the seat.
2. By the fluid forcing a floating seat ring against a trunnion-supported ball.
3. By relying mainly on the installed prestress between the seat and a trunnion-supported ball.
4. By means of a mechanical force, which is introduced to the ball and seat on closing." (Zappe, 1998)

For floating ball valves, the "first sealing method, in which the seating load is regulated by the fluid pressure acting on the ball, is the most common one. The permissible operating pressure is limited in this case by the ability of the downstream seat ring to withstand the fluid loading at operating temperature without permanent gross deformation." (Zappe, 1998).

In addition to the pressure load being applied to the seat “flat seats tangential to the ball surface have a theoretical line contact but very quickly bed-in to create a narrow band.” (Nesbitt, 2001); this principle shall be explored further in the literature review to determine whether a consensus can be reached in relation to the mechanics governing the formation of a narrow band at the contact between the ball and seat.

Further to the tangential seat sealing face, the seat rings of floating ball valves are typically “provided with a cantilevered lip, which is designed so that the ball contacts initially only the tip of the lip. As the upstream and downstream seats are pre-stressed on assembly against the ball, the lips deflect and put the seat rings into torsion. When the valve is being closed against the line pressure, the lip of the downstream seat deflects still further until finally the entire seat surface matches the ball. By this design, the seats have some spring action that promotes good sealing action at low fluid pressures. Furthermore, the resilient construction keeps the seats from being crushed at high fluid loads.” (Zappe, 1998).

The seat rings of floating ball valves are typically “provided with peripheral slots which are known as pressure-equalizing slots. These slots reduce the effect of the upstream pressure on the total valve torque. This is achieved by letting the upstream pressure filter by the upstream seat ring into the valve body cavity so that the upstream seat ring becomes pressure balanced.” (Zappe, 1998). In addition to the peripheral groove on the outside diameter of the seat rings other methods of achieving cavity relief include making the lip flexible enough to bend and relieve the pressure.

1.5 Gaps in General Knowledge

The general knowledge around the subject area predominately relates to the definition of the floating ball valve and the basic function of the assembled valve, as well as the performance and requirements of the valve. There is limited available open literature relating to the design of the seat component in detail. When the seat component design is considered in the general knowledge literature there are only generic qualitative descriptions of the design function and process results without any methodologies or theories used to achieve the designed component or how the design of the seat will impact its performance under the specified conditions. The reflection of the lack of any design methodology is reflected in practice where it is known that many manufacturers of floating ball valves apply seat designs to their products which are achieved solely through trial and error. The lack of a design methodology and application of ‘trial and error’ designing leads to a significant number of issues where manufactured valves do not match the performance definitions under which they are sold. Typically, the operating torque is higher than published due to additional compression on the seat to achieve a seal, this is a significant issue for a valve as it means it cannot be operated correctly.

This section makes clear that there is no unified design methodology for the design of a floating ball valve seat but rather a number of varying methods which would imply varying results are being obtained from these methods. Further to the sealing performance of the seat there is limited available literature related to the effect of the seat design to the valves operating torque of a floating ball valve. Finally, when considering the performance of the seat, there are a small number of articles that are available which relate to the specific designs, features and requirements of standards these articles detail an amount of information on the design and function of the seat component however this is limited to qualitative information with no information provided that could be used to generate a design from. There is currently limited open literature which covers the design methodology and theory for the design of a seat for a floating ball valve that will relieve an over pressurised body cavity through the deformation of the seat component alone.

1.6 Motivation of the Work

Currently the widely accepted and used method for designing a floating ball valve seat includes an amount of 'trial and error' and a significant number of undefined variables which are not considered in the design method. The lack of definition and consideration given to the variables in the current design method results in an over engineered design. In using the current design methodology, the thickness of a seat component and the compression as a function of the thickness is considered to determine a sealing stress. Should the seat fail the compression of the seat is increased until a seal is achieved using the specified material. The current design method described in this paragraph is a significant disadvantage and undesirable due to the lack of control and lack of definition of the design based on the variable of the seat component.

The available open literature shows limited evidence of a design methodology which is validated and therefore accepted for use in designing the seat component in a floating ball valve. The each of the literature sources reviewed in the general literature section describes the same function of a floating ball valves seat component when considering the design, function and operation of the component. There is no expansion in any of the literature sources into appropriate theories or methodologies and their application to a floating ball valve's seat component.

The lack of a theoretical model and the validation of the use of that theoretical model is missing from all of the general knowledge reviewed in this section. A comprehensive theoretical model linking the variables of the seat design to its performance and function is a critical element in the design of a floating ball valve seat. The design of the floating ball valves are critical to the function of the overall performance of the valve. The design of the floating ball valve seat is a critical component of the valve to be understood when designing the valve prior to manufacturing the design, due to the many performance factors it affects. In designing a floating ball valve a theoretical model will allow the seats design to be optimised and therefore the components which are designed based on the parameters which are affected by the seat design, such as operating torque, to be optimised also.

1.7 Aims of Research

This thesis sets out to generate new knowledge which fills the gaps identified in the general literature review in this research area. The addition of new knowledge will be required to define each of the aspects of the theoretical model which defines the mechanistic function of the ball valve seat component and its interaction with the ball component.

In achieving the above a major step forward will be taken in the understanding of the mechanics governing the design of a floating ball valve seat and the effect of the seat on the sealing performance of the seat and the operating torque of the valve as a whole. With the development of the theoretical model the theories defining each of the components of the seat component can be combined into a comprehensive design method. The comprehensive theoretical model shall encompass all the elements involved in the design of the seat as well as the performance factors that the design effects, such as operating torque.

The variations in design method will give variations in the performance of the seat components used while the mechanics of the interaction between the ball and the seat components are governed. By achieving theories which describe each of the mechanics that govern the response of the seat component under various conditions, it shall be possible to combine the theories describing the mechanics into a single theoretical model. From a single theoretical model it will be possible to develop a single design method and therefore achieve a consistent performance from the seat components designed through this method.

To generate the new knowledge and satisfy the motivation for this work this thesis has been designed and planned to fulfil the following three aims:

1. Development of mechanistic theoretical models based on established theoretical models.

This aim sets out to develop theoretical models which describe the mechanics of the areas of the seat component which must be defined to create a complete definitions of the interaction between the ball and the seat component and the response of the seat to the loads applied to it. By using and applying established theoretical models there may be assumptions made to ensure applied models suit the function in which they are applied. This will enable development of design equations for this complex component.

2. Validation of theoretical models through finite element analysis.

The purpose of this aim is to validate the application of the theoretical models to the geometry and function of the floating ball valve seat. This is particularly true as the theoretical models are based on simplifying assumptions. It is important to test the effects of the assumptions made on the important design parameters through comprehensive FEA analysis. By validating the application of the theoretical models to the geometry of a floating ball valve seat design it is possible to evaluate the assumptions made. Any differences between the theoretical models and computational results can be evaluated and the theoretical models modified to take into account any changes that need to be made to the assumptions made. As FEA methods have been developed to make the analysis of complex components possible where close form solutions may not be possible, it is hoped that the close form solutions developed in aim 1 can be tested for their effectiveness through the use of FEA.

3. Development of a design methodology.

This aim takes the validated theoretical models and develops them into a design methodology. The combination of theoretical models allows for a method through which it is possible to design a seat component to be created. Through the creation of the design methodology the application of the design method to an example case would demonstrate the function and use of the established design methodology in a practical manner.

By fulfilling the three aims of the thesis shall deliver a significant and theoretically sound step forward in the understanding and development of an optimised theoretical floating ball valve seat design methodology.

Chapter 2 - Literature Review

This chapter contains the literature review which is developed around the three specific research aims established on pages 25 and 26 of the previous chapter to identify the gaps in the available knowledge. First the literature review covers the mechanistic theoretical models which either describe the floating ball valves seat design in full, a component of the design of the seat or a seal which may have transferable knowledge to the floating ball valve seat design. By considering the mechanistic theoretical model as a whole and as constituent components all of the relevant areas which contribute knowledge towards this subject area are reviewed in the detail required to evaluate the current knowledge presently available. The literature covering the approach through which the floating ball valve is analysed is reviewed next. By reviewing the literature where a floating ball valve either in part or in whole is performed allows for the seat component to be analysed in a way which is in-line with previous work completed. The previous work completed is reviewed to determine where there are gaps in the knowledge presented with the analytical methods implemented, these areas will result in a short fall of knowledge generated. The lack of knowledge required for this thesis from the previously completed works can be addressed through research objectives in this thesis. For the second research aim, the literature reviewed for the development of a design methodology sits between the literature reviewed for the first aim and literature covering the creation of a design methodology. The numerical methods for the theoretical models reviewed for the first aim form the technical part of the final aim, these design equations have already been reviewed and the gaps in the equations and methods themselves identified. Through the review of the design methodology literature the processes through which a design is created and evaluated are assessed. By reviewing the literature on design methods, the areas where these methods do not meet the requirements of this thesis are identified. By identifying the areas where there are gaps in the current design processes it is possible to generate new knowledge in creating the design method which satisfies the requirements of the design methodology for the design of a floating ball valve seat. Through the completion of the literature review based on the available literature, knowledge gaps are identified which shall be addressed by the development of new knowledge and understanding of the subject area.

2.1 General Approach

The aim of this literature review is to review what information exists with regards to each of the aims of this thesis. By reviewing the literature which applies to each of the research aims it is possible to identify where gaps exist in the current knowledge. By identifying where the gaps exist in the current knowledge it is possible to formulate research objectives to fill these gaps and generating new knowledge it will be possible to work towards creating a comprehensive design methodology.

The theoretical models surrounding the theoretical description of the floating ball valve and specifically the design and function of the seat component are reviewed to determine where current knowledge and design processes exist. In reviewing the currently available knowledge and design methods the gaps and shortfalls of these existing methods can be identified. Following the review of floating ball valve seat design methodology general seal designs are reviewed, while the subject matter of this thesis is not in regard to other seal designs seal designs have been around for a long time and have been subject to a significant amount of research. The research on seal design may include knowledge which can be transferred from seal design and applied to the design of a floating ball valve seat. Once the areas of the floating ball valve and seal theoretical models have been reviewed the areas where the knowledge from these subject areas is lacking are reviewed to determine whether there is any further knowledge is available and where gaps in this knowledge exist. Following the design methods, the requirements of the ball valve seats performance and function are reviewed to ensure the complete set of requirements and variables effected by the design of the floating ball valves seat are understood. By understanding the full scope of requirements this allows for a comprehensive solution to be found. The requirements reviewed will enable the design method to be developed in a manner whereby these requirements are guaranteed to be satisfied.

The review of the literature with regards to the computational methods used to assess a floating ball valves shall follow the methods used in general as well as those methods previously used to achieve a successful set of data from a computational model. The general methods used to establish and run a finite element analysis model shall be reviewed to ensure that the methods used in this thesis are in line with the best practice for the type of analysis being performed. In reviewing the current methods for finite element analysis the areas where these methods do not meet the requirements of the work in this thesis there area shall be highlighted as areas for the development of new knowledge. The literature where the analysis has been performed on a floating ball valve shall be reviewed for the application of finite element analysis to the analysis of a floating ball valve. The methods through which finite element analysis is applied to the shall be reviewed to determine whether they are applicable to the requirements of this thesis. Where the methods applied to floating ball valves are applicable they shall be adopted, where the methods applied are not applicable or do not satisfy the requirements of the analyses of this thesis these gaps shall be identified as areas for the creation of new knowledge.

The design methodologies literature is covered partly by the literature reviewed for the first aim, where this literature is not applicable to the first aim it shall be reviewed in the final section of this chapter. The design methods currently in existence shall be reviewed with a view of applying them to the process of designing a floating ball valve seat. Where existing design methods do not cover the requirements of designing a floating ball valve seat these areas shall be highlighted as areas for the development of new knowledge.

2.2 Mechanistic Theoretical Models

This section looks at the existing literature that may be used to describe the mechanics that govern the interaction between the ball and seat. Through reviewing the available literature on the subject of the theoretical models which describe the mechanics of floating ball valves and applicable related subject areas it is possible to identify where the gaps in the available knowledge are. By identifying the gaps in the current knowledge this thesis can generate the new knowledge required to create a mechanistic theoretical model of the floating ball valve seat.

2.2.1 Theoretical Sealing Models – Ball Valves

This section reviews the literature relating to theoretical sealing models. The literature reviewed is focused on the literature of seals which are directly applicable to the design of ball valve seats. The basic design of a soft-seated floating ball valve was discussed on page 22 of section 1.3, this section builds on that by reviewing specialist literature about the theoretical design of the seat component with the aim of developing an understanding of the design theories and methodologies used to effect a seal between the ball and seat components. When considering the design of a floating ball valve seat there are “several different seat design principles are used to achieve good sealing and low torque requirements” (Nesbitt, 2001). Of these various seat designs the following figure taken from Velan’s product literature illustrates this by showing three different methods of designing a seat:

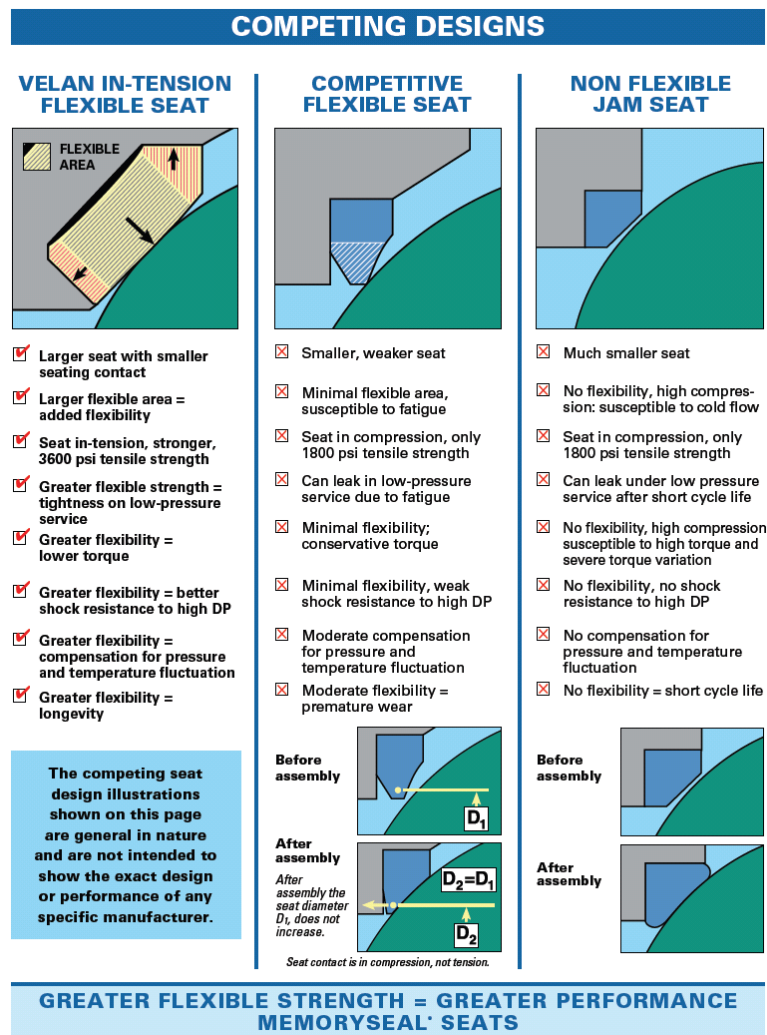


Figure 10 – Seat Design Type Comparison (Velan Inc, 2019)

Figure 10 shows the comparison of three different floating ball valve seat designs the material in each of the seat designs is subject to a different form of loading. The Velan in-tension seat puts the seat material in tension, the competitive flexible seat puts the material in bending and the jam seat puts the material under compression. The Velan in-tension seat has a flexible central section to the seat with support on the internal and external edge. The competitive flexible seat design has support around the outside diameter of the seat. The non-flexible jam seat is supported on the outside diameter and the back-face of the seat. Each of the supports of the competing seat designs provide different characteristics when considering the seat design. The Velan in-tension seat will be a more robust seat design as the internal and external support will limit the amount of flexibility in the seat but the increased degree of support will ensure no excessive deformation will occur. The competitive flexible seat design has support retaining the seat in the seat-pocket of the body or closure however the sealing lip has no support, it is assumed that if this design was incorrectly specified that gross deformation could occur permanently deforming the sealing lip and degrading the components performance with respect to achieving a seal. The non-flexible jam seat has support surrounding the external edge and the back-face, therefore the compression of the seat is fixed by the compression of the ball onto the seat component with not adjustment possible from the flexibility of the seat component. The Velan in-tension seat being a more robust and better supported seat design could be assumed to have a higher torque than the competitive flexible seat design as there will be a higher load imparted on the ball when the seat is compressed by the ball. A valve with the competitive flexible seat design can be assumed to have the lowest torque of the three designs as the greater degree of flexibility in the seat will lower the initial load acting on the ball by the seat component. A valve with the non-flexible jam seat design in it will have the highest torque of all the designs shown, the lack of flexibility will result in all the compressive load being generated by the compression of the seat section being transmitted back to the contact with the ball therefore increasing the overall valve torque. None of the three designs shown in Figure 10 demonstrate a complete design which can be viewed as superior to the other designs shown. Individual features from these designs can be seen to benefit the parts of the overall valve performance which are related to the seat. The level of support of the in-tension seat design with an internal and external support is the best support arrangement of the three designs. The flexibility of the competitive flexible seat design gives the best performance related properties of the three designs. By combining the support methods of the Velan in-tension seat design and the flexibility of the competitive flexible seat design it would be possible to create a seat design that combines the most beneficial features of these three seat designs.

Figure 10 shows a number of different floating ball valve seat designs, however, it is also part of the Velan advertising material. Therefore the analysis shown in Figure 10 is written in a biased manner to show the Velan in-tension seat design as the superior floating ball valve seat design.

Regardless of the design of the seat the resulting assembled valve contains the same components, as generically shown Figure 11.

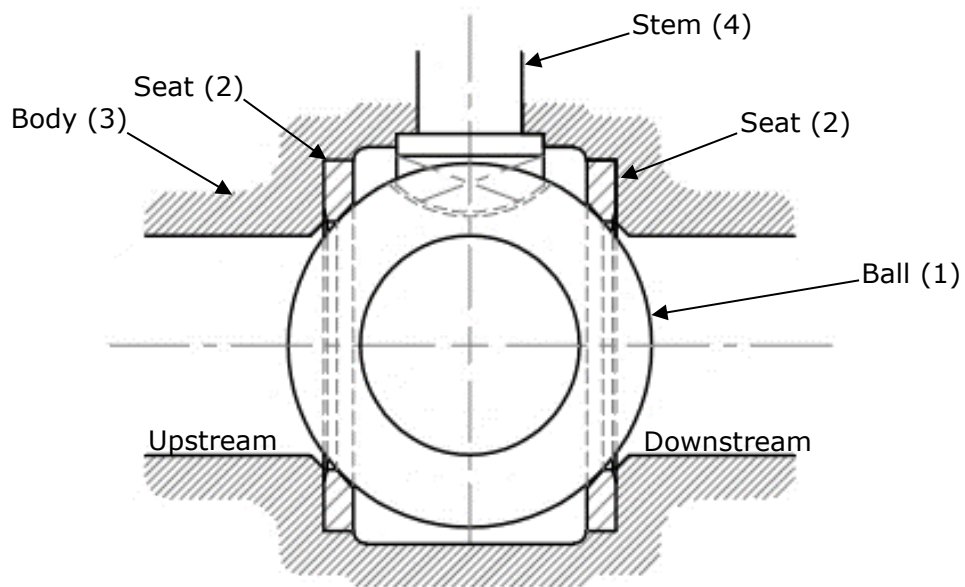


Figure 11 - Ball Valve Assembly

Here we have the valve body (3), housing the method of operating the valve, the stem (4). Inside the valve there is a solid ball (1) which 'floats' between a pair of seats (2). The idea that the ball 'floats' between the pair of seats highlights the expectation that the seat components should be flexible enough so that the ball is able to be able to 'float'. The "two seats are designed to conform to the ball's sealing surface." (Skousen, 1997), this is further confirmed by this quote from Zappe "These seats are designed to be circular so that the sealing stress is circumferentially uniform." (Zappe, 1998) further to this "soft seats conform to the ball contours to establish a seal" (Nesbitt, 2001).

Figure 12 shows a detailed view of the initial compression of a proprietary in-tension flexible seat where there are "convex surfaces of the seat running against the ball" (Canada Patent No. 3,384,341, 1964). The interaction of the two convex surfaces running against each other will not be possible to be described by the application of plane stresses to the problem, therefore it is assumed that some other form of mechanics is to be applied to this area of the design to describe this interaction. The arcuate profile of the seat section is inherently strong, therefore there is little concern about the design of the seats ability to handle the loads applied to it.

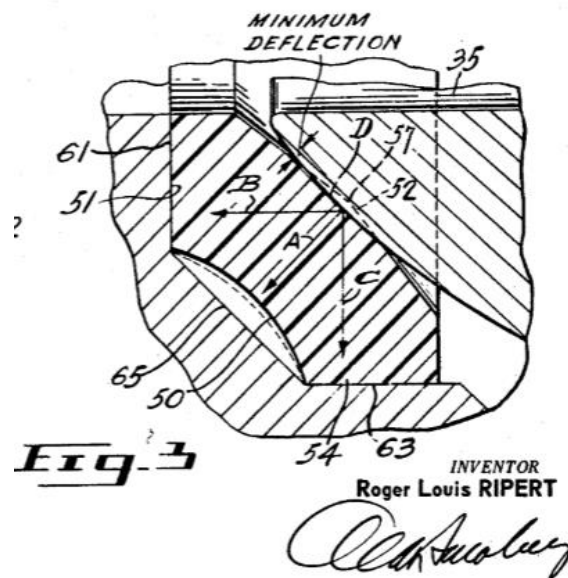


Figure 12 - Minimum Seat Deflection (Canada Patent No. 3,384,341, 1964)

The design of the flexible in-tension seat shown in Figure 12 does not show much beyond the initial deflection of the seat to accommodate the ball after assembly of the valve. The area of most interest in Figure 13 is the seat is the only component defined as deflecting or distorting, therefore assuming that the ball remains rigid throughout the function of the seat.

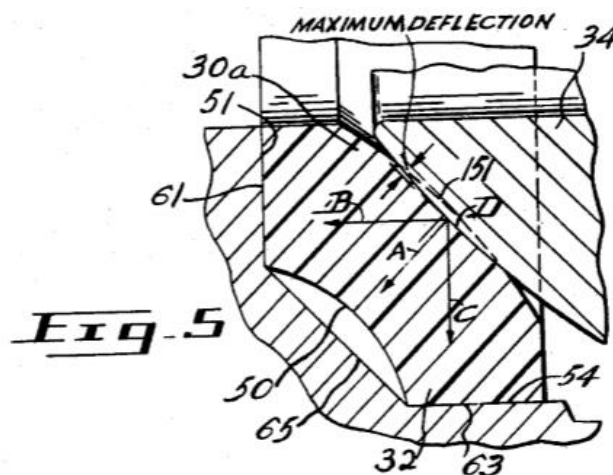


Figure 13 - Maximum Seat Deflection (Canada Patent No. 3,384,341, 1964)

These figures taken from the patent demonstrate the operation of the seat is based on the deflection of it by a load transferred onto it by the ball either through assembly (as with the minimum deflection figure), of the line pressure (as with the maximum deflection figure).

With the arcuate structure of the seat the core of the seats function it may be possible to replicate the function of the seat i.e. the deflection of the central section of the seat to obtain the desirable effects of the function of this seat design without infringing the patent claims shown previously. As discussed previously this support function of the internal and external edge of the seat component is the ideal solution to this application however the compression of the arcuate profile is too rigid to give the low torque value that is desirable in the optimal solution. The floating ball valve seat design and associated information provided in the patent does not provide any significant amount of information with regards to the design of the seat. The most significant knowledge found in this source is the application of an initial deflection when the valve is assembled, and that this deflection increases when the seat component is subject to a pressure-load. There is minimal information provided in any of the Velan documents which does anything past describe the general function of the seat design; there is no relationship provided which links the seat design to the geometry of the components involved or the material properties selected or to the achievement of a seal by the seat design.

The finite analysis stress plot of the flexible seat shown in Figure 14 shows a stress plot where the stress distribution confirms that the stress model describing the interaction between the ball and seat components is not described by the application of plane stress mechanics. The stress distribution shown in Figure 14 resembles a form of contact mechanics, the identification of the exact form of contact mechanics shall be discussed in the following sections.



Figure 14 - Flexible Seat, Ball Contact (Metso, 2011)

Figure 14 shows a flexible lip type floating ball valve seat design. The stresses shown in the figure cannot be quantified as no scale for the stresses is provided, however the general pattern is that of a non-uniform distribution further demonstrating that plane stresses are not involved in the analysis of the seat design. It is possible to identify that the seat has not been grossly deflected and therefore permanently deformed due to the lower stress shown in the central region which is subject to bending. The stresses shown identify two localised areas of high stress within the seat component and a corresponding area of high stress in the ball component, it is assumed that these stresses are the result of contact mechanics and therefore are defined as contact stresses. Where the ball and seat contact the magnitude of the stresses show the greater stress is generated in the soft non-metallic

component, therefore it should be assumed that the material properties factor in the magnitude of the stress achieved in the seat component to effect a seal between itself and the ball. Also at the point of contact between the ball and seat components the figure shows the seat component deforming to conform to the profile of the ball, this is a key function of the contact mechanics which have been assumed to be most applicable manner to describe the interaction of these two components. This literature source shows a level of detail which has been interpreted to provide guidance on the applicability of theoretical models to the design of a floating ball valve seat component. While the interpretation of the figure has provided guidance to the application of theories to the design of the component the identification of the exact theoretical models would have to be determined.

A different design of a floating ball valve is shown in Figure 15, this design is of the valve design assessed by G.V.Bozhko in the paper 'Force analysis for a Ball-seating valve with a PTFE Seal' (G.V.Bozhko, 2000). The type of seal considered in this paper is of an elastomer-energised jam seat design, where the seat is manufactured from PTFE (2) the elastomer an O-Ring (3).

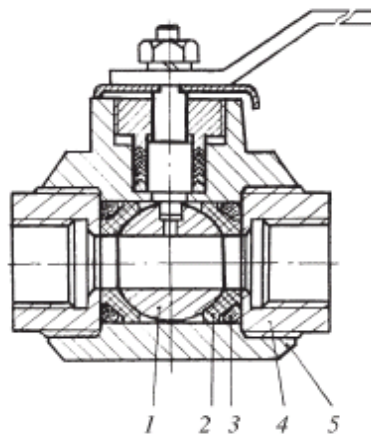


Figure 15 - Ball Valve Design Assessed (G.V.Bozhko, 2000)

The components shown in Figure 15 are defined as follows, 1 – Ball, 2 – Seat, 3 – O-Ring, 4 – Closure, 5 – Body.

The design shown in Figure 15, where an O-Ring energised seat is shown is not an acceptable solution for a floating ball valve seat design, as specified by the standardised supplemental industrial specification, "Elastomeric O-ring seat inserts shall not be permitted." (International Association of Oil & Gas Producers, 2019). Despite the use of an O-ring seat insert the analysis of the sealing load on the seat can be used as a basis from which the project can be built from.

The assumption that is made in this paper is that the profile of the seat component conforms perfectly to the ball and does not deform when a load is applied to it. When considering the mechanics of fluoropolymers this can be judged to be an incorrect assumption; the seat will deform by varying amounts depending on the magnitude of the load applied to it. The magnitude of the load applied to the sealing surface will vary depending on the location of it on the seat face. The paper assumes the load to be homogeneous about the spherical contact between the ball and seat components. This paper does not take into account the deformation of the seat, this is dependant on factors such as the dimensions of the bodies in contact and the material properties of the bodies in contact, specifically properties such as the flexural rigidity and Poisson's ratio.

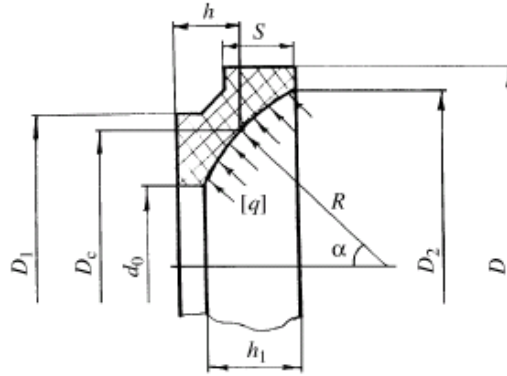


Figure 16 - Seat Design Assessed (G.V.Bozhko, 2000)

The O-Ring used to energise the seat is located in the recess at the back of the seat, part of the sealing force is created by the compression of this O-ring. As shown in the quote from the International Association of Oil and Gas Producers on page 34, the use of a secondary 'active' element such as an O-ring is not acceptable. Based on this requirement, it is possible to determine the requirement that the seat component must be manufactured from a single homogeneous material or a single composite material; these requirements are imposed by a number of Oil and Gas Majors under the International Association of Oil and Gas Producers. The initial sealing load is generated by the compression of the O-ring, this sealing load then increases with the pressure being applied to the valve. This literature source provides a sealing stress equation for the determination of the sealing stress when a gas of up to 6MPa is applied to the valve, this is shown in Equation 1.

$$[q] = 7.5 + 1.5p$$

Equation 1 - Gas Sealing Stress Determination (G.V.Bozhko, 2000)

Where:

[q] = Required sealing stress, MPa

p = Pressure to seal, MPa

This equation is provided for applications where a gas is the medium considered, however there is no evidence provided that applying this relationship to a valve will result in a seal being achieved. Also there is a significant limitation that the required sealing stress determined is only applicable to gases with a pressure of 6MPa or less, this excludes a significant portion of applications where a floating ball valve seat is applied. Beyond determining the sealing pressure for a gas this source does not provide any quantifiable method for determining whether the seal achieved with other media. While it would be possible to create a design to the method provided in this paper there are significant gaps in the knowledge and the application to other media. While this paper does not match the previous sources in the application of plane stress for the contact between the ball and the seat and the use of an O-ring to preload the seat some similarities can be seen across the literature reviewed so far. All of the seat designs reviewed so far have used a form of preload generated by the seat as part of the sealing function, this has been supplemented by the action of the pressure load to generate a full seal. All of the sources reviewed in this section so far have used a preload of some sort combined with a pressure-load to generate the total load which achieves a leak-tight seal.

The load from which the sealing stress is derived is applied to the seat shown in Figure 16 from the contact with the ball is set at an angle (α) to the direction of axial loading between

the ball and seat. The derivation of the force acting on the seat is representative of the action of the ball loading the seat. In this paper the angle is set to the middle of the contact area of the seat, typically this is the location taken for pressure areas when considering seat seals and seals in general, as shown by the flanged head designs in Figure 17 taken from ASME VIII Division 1.

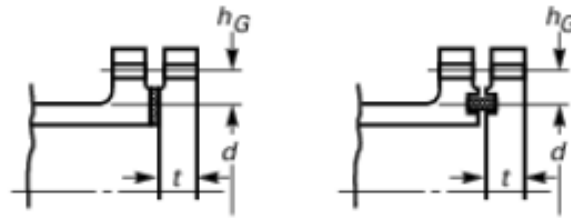


Figure 17 - Flanged Head Designs [UG34], (American Society of Mechanical Engineers, 2017)

The design rules associated with the diagrams shown in Figure 17 are taken from ASME VIII Division 1, these rules have been developed by the American Society of Mechanical Engineers to be used for the design flanged covers for piping and associated equipment when subject to an internal pressure. The flanged head designs shown in Figure 17 assume the internal pressure within the piping is acting over the area bound by the mean diameter of the seal, diameter 'd' from the figure. When applying this design philosophy to a typical floating ball valve seat design the mean contact diameter between the ball and seat component would be considered as the equivalent to diameter 'd' from Figure 17 over which any pressure within the valve would act. When the ASME VIII Div. 1 equivalent diameter 'd' is combined with the information related to the seat design method shown in Figure 17. This assumption is further confirmed in the following quote, "On condition that in the closed valve position the working medium penetrates to the centre of the sealing surface." (Boiko, Regush, Semenov, & Regush, 1986), therefore, the mean seat diameter should be considered at which any pressure should be considered to be acting when evaluating the mechanics of a seat design.

The paper entitled 'Analysis and optimization of nitrile butadiene rubber sealing mechanism of ball valve' by Xue-Guan Song achieves part of the work proposed in this thesis using a nitrile butadiene rubber seat in the place of a plastic one. The paper assessed the seat under 'full' working conditions "divided into three kinds: installation in the seat with an initial interference fit (load condition A), the effect of fluid pressure (load condition B), the ball rotation or opening (load condition A+B)." (Song, Wang, & Park, 2009). This paper is limited to the use of nitrile rubber as a seat material due to applying the Mooney-Rivlin hyperelastic material model to describe the seal material; while the Mooney-Rivlin model is the best choice for describing an elastomer due to its historical use in doing so it is not suitable for describing other materials. This paper did not provide any evidence as to the method through which the optimisation was completed. From the information presented in the paper it is assumed that the optimisation was carried through iterative finite element analyses. The general approach of this paper, breaking down the design into its constituent elements, is a useful approach to develop the required understanding of the mechanics of the components. The lack of applicability of the outcomes of this paper to any design or material type other than the one evaluated and optimised in the paper itself is a significant limitation of this work.

In the seat design in the paper 'Calculation of polymer seals for ball valves' (Boiko, Regush, Semenov, & Regush, 1986) the design methodology uses an initial spring load and a pressure load acting across a seat seal to generate the sealing load and therefore the contact pressure. The approach of this paper to designing seats, (shown in Figure 18), is generally the approach taken when designing seats for trunnion mounted ball valves.

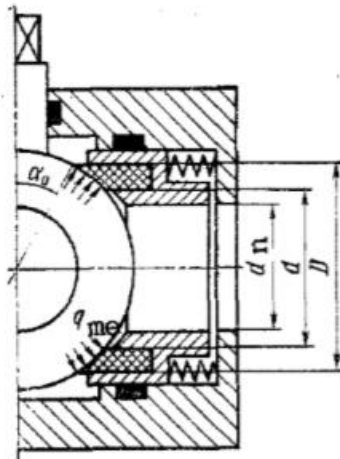


Figure 18 - Trunnion Mounted Ball Valve Seat (Boiko, Regush, Semenov, & Regush, 1986)

As can be seen from Figure 18 the ball is not supported; when the ball is loaded by the springs and pressure from one end of the valve the ball will not be supported and will simply compress the upstream seat as well as the downstream seat. While this lack of support does not make the model usable in a practical situation if the ball is assumed to be rigid in respect to axial movement then the methodology behind the seat design may be assessed to understand the theory applied to the seat in isolation. The design of the seat relies on achieving a specific stress in the seating material as defined by:

$$q_h = a + b \cdot p$$

Equation 2 - Sealing Stress Calculation (Boiko, Regush, Semenov, & Regush, 1986)

Where:

p = Pressure of medium sealed, MPa

q_h = Specific seal pressure, MPa

The variables, 'a', 'b', are not defined beyond being defined by experimental methods in the paper 'Calculation of polymer seals for ball valves' (Boiko, Regush, Semenov, & Regush, 1986). While the issue with the application of this method to the valve design is the lack of axial support for the ball to prevent its movement in the axial direction none of the terms in the above equation are defined in this paper. If the valve is considered to be a typical trunnion mounted i.e. the ball is fixed in horizontal position with respect to the valve body then the ball will react against the load acting on it is making the above equation true should q_h represent the full axial load of the seat acting on the ball, a be a spring load and $b \cdot p$ being a pressure-related load acting on the seat. The seat contact does seem flawed with it being assumed that it acts across the whole seating surface while at the same time considering that the seating surface is flat and runs tangentially to the ball. As shown in the previous designs discussed there is evidence of that the use of contact mechanics is optimal method through which the mechanics of this interaction can be described.

The works reviewed in this section have both provided guidance through consensus' being found in specific areas while also identifying area where there is a lack of knowledge in the available literature. The various designs of ball valve seat, with the exception of the jam seat design, reviewed each in their own way identified the mechanics of loading the seat component as being achieved through a pre-load and a load generated by the pressure.

Where in the literature reviewed there were no springs or O-rings present in the design a pre-load is created through the deflection or compression of the seat component itself. Through the various seat design methods assessed in this section presented numerical models where the design method used a mean seal diameter as the diameter on which the calculations are based. The mean seat diameter was used particularly as a point across which a pressure acted to create a pressure-load. In each case where the numerical model is presented a combination of pre-load and pressure-load was used to determine the sealing stress in the seat component.

The knowledge gained from reviewing the works in this section failed to provide a solution to designing a floating ball valve seat. Where the seats were manufactured from a single material, and the design method considered the material properties, design geometry and performance requirements of the design. The literature only presented information in a qualitative manner with regards to the function of a fluoropolymer seat components function, while this information is useful in providing guidance on the function of the design there is no knowledge available on the use of specific design methods to achieve these functional requirements. A couple of works reviewed presented methods which were claimed to define the required sealing stress through which a leak-tight joint is achieved. No source provided evidence to substantiate the determination of the methods of calculating these sealing stresses and of the works reviewed a consensus could not be reached as to a common method from which a basis could be formed. The mechanics through which the sealing stress was determined in the numerical models reviewed did not match the mechanics which have been presented in the computational work previously undertaken in other works. There are significant disparities between the numerical models and the computational models reviewed. The numerical models present results which match those predicted by contact mechanics; while the numerical models determine the sealing stress though the application of plain stresses.

In summary there are gaps in knowledge where there is no mechanical model which describe in a quantitative manner the mechanics of the seat component itself. Following this there is a lack of a unified method of understanding the interaction between the ball and seat components. When determining the contact stress there is no model available which can reliably provide a required sealing stress for the range of applications to which the seat design could be applied.

2.2.2 Theoretical Sealing Model – Seals

In this section theoretical sealing models and the associated literature which are not directly applicable to a floating ball valve seat are reviewed. Due to the lack of information openly available with regards to achieving a seal between the ball and seat components, the review of literature may make it possible to identify knowledge which fills the gaps identified in the ball valve seat section.

When setting out to achieve a zero-leakage (hermetic) seal there is research available that describes the design of the seal and related components; when designing “components for strength and hermetic sealing, one of the basic parameters is the minimum specific load, q , on the sealing surface at which the required level of hermetic sealing is ensured in the working conditions.” (Bozhko, Kalabekov, Vinogradov, & Denisov, 1992). When looking to achieve a hermetic seal, “the dependence of the specific load of hermetic sealing [q] on gas pressure in the cavity of the test model for specimens with varying widths of contact” (Bozhko, Kalabekov, Vinogradov, & Denisov, 1992) shows the specific load can be determined based on the contact width for a variety of applied loads. The relationship between the specific load of hermetic sealing [q] and the gas pressure can be described numerically as shown in Equation 3 on page 39.

$$q = A \cdot P_g^c$$

Equation 3 – Specific load of hermetic sealing (Bozhko, Kalabekov, Vinogradov, & Denisov, 1992)

Where the coefficient 'A' is described in terms of seating face width as:

$$A = \frac{(6.8 - 2.7 \cdot b)}{(1.8 - 0.7 \cdot b)}$$

Equation 4 – Coefficient 'A' (Bozhko, Kalabekov, Vinogradov, & Denisov, 1992)

Where:

'b' – width of contact

Exponent 'c' is defined as:

$$c = 0.12 + 0.4 \cdot b$$

Equation 5 – Exponent 'c' (Bozhko, Kalabekov, Vinogradov, & Denisov, 1992)

By substituting Equation 4 and Equation 5 into Equation 3 it is possible to define the required specific load of hermetic sealing in terms of seal width, as shown in Equation 6.

$$q = \frac{6.8 - 2.7 \cdot b}{1.8 - 0.7b} \cdot P_g^{0.12+0.4 \cdot b}$$

Equation 6 – Hermetic sealing load in terms of contact width (Bozhko, Kalabekov, Vinogradov, & Denisov, 1992)

From Equation 6, "it can be seen that, as 'b' decreases, the required specific load of hermetic sealing decreases at constant pressure of the medium sealed." (Bozhko, Kalabekov, Vinogradov, & Denisov, 1992) This equation demonstrated a relationship between the specific stress in the sealing contact and the pressure being sealed and contact width of the seal itself. By relating these three variables it would be possible to evaluate any given geometry so long as the contact width can be determined and gas is the medium being sealed. This method to determine the required sealing stress when gas is the pressurised medium fills the gap in knowledge identified in the previous section as it provides a numerical solution which is not limited by the pressure or other factors.

When considering other seal designs which may have available literature that can contribute knowledge towards the aims of this thesis the seal type referred to as mechanical face seals would be considered one of the best seal designs to start with. As one of the most researched and well developed seal designs the information on this seal design is widely available. Mechanical face seals are designed around the principle of achieving a specific contact pressure to ensure that a seal is achieved, typically the effectiveness of the seal is determined by the value of ΔP_{crit} as defined below.

$$\Delta P_{crit} = \frac{F_s}{A_f \cdot (1 - B_a)}$$

Equation 7 – Critical Pressure (Brink, Czernik, & Horve, 1993)

Where F_s , "the sum of the spring force" (Brink, Czernik, & Horve, 1993), is combined with the balance ratio to determine the critical pressure at the interface area at which the mechanical seal will develop an effective seal.

Here "the balance ratio is employed to describe that fraction of the internal pressure is acting to close the seal faces. It is defined as the ratio of hydraulic loading area to the seal interface ratio. As the balance ratio decreases, the closing force, due to the internal pressure also decreases" (Brink, Czernik, & Horve, 1993). The following equations define the balance ratio for both internally and externally energised seal arrangements.

$$B_e = \frac{\text{Hydraulic load area}}{\text{Seal interface area}} = \frac{1/4 \cdot \pi \cdot (D_{fo}^2 - D_s^2)}{1/4 \cdot \pi \cdot (D_{fo}^2 - D_{fi}^2)} = \frac{D_{fo}^2 - D_s^2}{D_{fo}^2 - D_{fi}^2}$$

Equation 8 – Externally Energised Balance Ratio (Brink, Czernik, & Horve, 1993)

$$B_i = \frac{\text{hydraulic load area}}{\text{seal interface area}} = \frac{1/4 \cdot \pi \cdot (D_s^2 - D_{fi}^2)}{1/4 \cdot \pi \cdot (D_{fo}^2 - D_{fi}^2)} = \frac{D_s^2 - D_{fi}^2}{D_{fo}^2 - D_{fi}^2}$$

Equation 9 – Internally Energised Balance Ratio (Brink, Czernik, & Horve, 1993)

By adjusting the relative geometries which define the balance area, particularly the ratio of the hydraulic load area to seal interface area it is possible to alter the effect the pressure has on the seal design. By changing increasing the hydraulic area and maintaining the seal interface area the balance ratio increases, while reducing the seal interface area has the same effect on the balance ratio. Conversely reducing the hydraulic load area or increasing the seal interface area has the effect of reducing the balance ratio. Changing the balance ratio effects the outcome of the critical pressure, as determine by Equation 7. Both the spring force and balance ratio are combined to give the total closing force acting on the seal, as shown by Equation 10.

$$F_{cl} = F_s + F_h = F_s + A_f \cdot B_a \cdot \Delta P + A_f \cdot P_o$$

Equation 10 – Total Closing force (Brink, Czernik, & Horve, 1993)

The interface area, A_f , is defined by the following equation:

$$A_f = 1/4 \cdot \pi \cdot (D_{fo}^2 - D_{fi}^2)$$

Equation 11 – Interface Area (Brink, Czernik, & Horve, 1993)

Where:

F_{cl} = closing force, N

F_s = Spring Force, N

F_h = Hydraulic Force, N

A_f = Interface Area, mm²

B_a = Balance Ratio

B_e = Balance Ratio (externally pressurised)
 B_i = Balance Ratio (Internally pressurised)
 ΔP = Pressure Drop ($P_i - P_o$), $N.mm^{-2}$
 D_{fo} = outside interface diameter, mm
 D_{fi} = inside interface diameter, mm
 D_s = Effective Sealing Diameter, mm
 P_i = Upstream (system) pressure, $N.mm^{-2}$
 P_o = Downstream (usually atmospheric) Pressure, $N.mm^{-2}$

The equations and general function of a mechanical face seal match the description and function of the seat (and seat insert) of a trunnion-mounted ball valve, as referred to in Figure 18 on page 37. Here we can see both a mechanical face seal and a trunnion-mounted ball have a spring force and a hydrostatic (pressure-energised) force contributing to a load acting over an interface area which seals against a counter-face. Although not directly applicable to a floating ball valve this common description does demonstrate the applicability of the mechanics which describe a face seal to a ball valve seat design model.

When designing a mechanical face seal a number of factors have to be considered to ensure the face seal is designed in a way which achieves a seal between the sealing face and the counter-face. The factors considered include the "face deformation due to hydrostatic and centrifugal forces generated between the faces as well as shaft eccentricity, misalignment and vibration" (Brink, Czernik, & Horve, 1993) these are typical factors which can be assessed numerically and resolved in the design phase but do not have to be considered in a mechanistic model. In addition to these factors there are a number of factors which "tend to increase leakage, other than those that cause seal face damage are:

- High fluid viscosity (typically 30-cP or 32-cST)
- Low seal balance (60 to 65 percent range)
- Low face pressure due to unloading forces
- Very narrow faces (<0.100 in) – Edge chipping, surface damage and wear have a more dramatic effect on leakage than wider face widths
- Face treatments or special lapping techniques to increase sealing gap
- Composite face materials (due to rougher surface finish)
- Excessive converging sealing gap due to thermal distortions
- Excessive divergent sealing gap due to pressure distortion
- Wiping action of seal face over mating ring
- Distorted seal faces (high and low spots from some mechanical conditions)"
(Fluid Sealing Association, 2008)

All of the factors shown above are of importance to be considered in the design of a floating ball valve, as they have been identified in causing leakage in face seals. It is highly likely that these factors will produce the same effect of increasing leakage if not considered when designing a floating ball valve seat and therefore should be considered if possible in the design methodology.

The review of seals, face seals and the design factors considered in the design of these seal types has filled a gap in the knowledge of the previous section. The numerical solution for determining the required sealing stress to achieve hermetic sealing with gas as the medium to be sealed fills a gap from the section reviewing the ball valve seat design methods as the method shown is not limited by the pressure of the medium being sealed and is therefore appropriate for the full range of applications a ball valve seat could be designed for. This section has not been able to provide a method for determining the required sealing stress

for the floating ball valve seat when a liquid is the medium being sealed, this is a gap in the knowledge which has not been filled by the ball valve seat information or the available seal information. The mechanics of the seals reviewed have not yielded any knowledge which can be used to describe the movement of the seat component under load or its interaction with the ball component.

2.2.3 Requirements of the ball valve seat

This section assesses the literature with regards to the requirements that are placed on the final solution when it has been manufactured and is under acceptance test and in-service conditions. While not an area of this thesis where knowledge must be understood and gaps established it is important that the requirements placed on the design created by the application of the design methodology are understood. By understanding the requirements placed on in their entirety it ensures the design methodology and the designs created by its application meet the requirements.

The seat is required to seal under various operating and test conditions, these are usually specified by the end-user, (the person who will operate the valve) although they are typically defined by international standards as a minimum, this section contains the review of one of those standards. "The equipment used by the valve manufacturer to perform the required pressure test shall not apply external forces that affect seat leakage. If an end-clamping fixture is used, the valve manufacturer shall be able to demonstrate that the test fixture does not affect the sealing capability of the valve being tested. End clamping is allowed for valves designed to function between mating flanges, such as wafer check and wafer butterfly valves." (American Petroleum Institute, 2009)

There are a number of requirements placed directly on the seat component. Some requirements are placed on the valve design, here the design and performance of the seat influences the compliance of the complete valve to these requirements. The primary function of the seat is to seal against the ball under pressure, (as discussed previously), to validate the sealing performance of a valve the valve is typically subjected to factory acceptance testing. With regards to the performance of the seat, it is always subjected to a pneumatic test where "the closure test pressure shall be 6 bar \pm 1 bar" (International Organisation for Standardization, 2008). The pneumatic closure test is specified as being mandatory "in the case of resilient seated valves, a high-pressure closure test may degrade the subsequent sealing performance in low-pressure applications" (International Organisation for Standardization, 2008). Despite this the high-pressure closure test defined as a test where "the closure test pressure shall be a minimum of x 1.1 the CWP" (International Organisation for Standardization, 2008), where the CWP (cold-rated working pressure) is defined as the " maximum fluid pressure assigned to a valve for operation at a fluid temperature of -20°C to 38°C" (International Organisation for Standardization, 2008). During testing the acceptable leakage rates are shown in the standard ISO 5208. A resilient-seated valve shall have a leakage rate of Rate A, this is defined as "No visually detectable leakage for the duration of the test" (International Organisation for Standardization, 2008). These tests are maintained for a minimum duration, as specified in Table 1.

Valve size	Minimum test duration ^a			
	Shell	Optional backseat	Closure	
	All valves	When relevant	Isolation valves	Check valves
DN ≤ 50	15	15	15	60
65 ≤ DN ≤ 150	60	60	60	60
200 ≤ DN ≤ 300	120	60	120	120
DN ≥ 300	300	60	120	120
a The test duration is the period of time for inspection after the test valve is fully prepared and under pressure				

Table 1 - Minimum duration for pressure tests (International Organisation for Standardization, 2008)

This section highlights the sealing requirements of a floating ball valve seat when it is tested under factor acceptance test conditions. While the valve must function in the in-service conditions the additional requirements of being able to pass a test on air (gas) and test fluid (liquid) at the pressures stated shows the requirement of the seat to be seal against both gases and liquids is a requirement of the design methodology.

2.2.4 Theoretical Contact Models

This section considers the available literature which can provide a numerical model to describe the interaction between the ball and seat components. As discussed previously the contact shown between the ball and seat is based on contact mechanics. It is necessary to determine what knowledge is available and what available knowledge is applicable to the design of a ball valve seat and where the gaps in the knowledge are.

When considering the interaction between the ball and seat this interaction can be separated into two elements; the mechanics of the contact between the ball and seat components, and how the mechanics of the contact affects achieving a seal. This section looks to describe the contact initially and then how that description of the contact describes the sealing stress. From the general literature review it is found that Nesbitt's quote is useful to the analysis, this quote states that "flat seats tangential to the ball surface have a theoretical line contact but very quickly bed-in to create a narrow band" (Nesbitt, 2001). Considering the interaction between the ball and seat in its most basic form, as described by Nesbit, this interaction is that of a contact; therefore it is reasonable to assume the application of contact mechanics is valid as contact mechanics are "concerned with the stresses and deformation which arise when the surface of the two solid bodies are brought into contact." (K.L.Johnson, 2003).

Contact mechanics can be generally split into conforming contacts where the "surfaces of the two bodies 'fit' together or even closely without deformation" and non-conforming contacts where the "bodies have dissimilar profiles", When brought into contact without deformation they will touch first at a point - 'point contact' or along a line - 'line contact'",

(K.L.Johnson, 2003). This quote from Johnson introduces a theoretical model for a 'line contact' which builds on the quote from Nesbitt. When the two forms of contact models are evaluated against the general geometry of the interaction between the ball and seat, i.e. a spherical surface and a flat surface, as previously defined by Nesbitt; this geometry leads to a definition of this interaction as being a non-conforming interaction due to the bodies having dissimilar profiles. Figure 19 illustrates the two non-conforming contact mechanics models; the first model is a 'point contact' model while the second is a 'line contact' model.

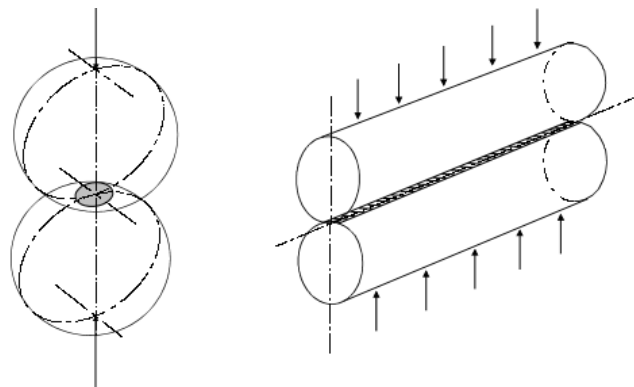


Figure 19 - Schematic of cylinders (left) and spheres (right) in contact (Dwyer-Joyce, 1997)

Considering the geometry of the components involved in the interaction between the ball and seat as well as the quote "flat seats tangential to the ball surface have a theoretical line contact but very quickly bed-in to create a narrow band." (Nesbitt, 2001), the most appropriate model that agrees with the quotes and the contact geometry is that of a line contact. The equations for both the line and point contacts are shown in Table 2.

Parameters	Line Contact	Point Contact
	Contact half width, a	Load per unit length, P
Material Properties, E_1, ν_1, E_2, ν_2	Material Properties, E_1, ν_1, E_2, ν_2	Applied Load, P
Contact Radii, R_1, R_2	Contact Radii, R_1, R_2	Material Properties, E_1, ν_1, E_2, ν_2
Relative radius of Curvature, R	$\frac{1}{R} = \frac{1}{R_1} + \frac{1}{R_2}$	
Reduced Modulus, E	$\frac{1}{E^*} = \frac{1 - \nu_1^2}{E_1} + \frac{1 - \nu_2^2}{E_2}$	
Dimensions of the contact	$a = \sqrt{\frac{4 \cdot P \cdot R}{\pi \cdot E^*}}$	$a = \sqrt[3]{\frac{3 \cdot P \cdot R}{4 \cdot E^*}}$
Max. Contact Pressure, p_0	$p_0 = \frac{2P}{\pi a} = \sqrt[2]{\left(\frac{PE^*}{\pi R}\right)}$	$p_0 = \frac{3P}{2\pi a^2} = \sqrt[3]{\left(\frac{6PE^{*2}}{\pi^3 R^2}\right)}$

Table 2 - Tabulation of Hertz Contact Mechanics Equations (K.L.Johnson, 2003)

Table 2 shows the properties and equations related to determining the properties of a contact in accordance with Hertz contact mechanics. The material properties of each

material include the modulus of elasticity and Poisson's ratio these material properties describe how the material responds when a load is applied to it, therefore these properties play a key role in being applied to the geometry within the contact area as it is expected that the bodies shall deform when in contact. The radii of the two bodies in contact are input parameters, these radii will determine the dimensions of the contact. It is anticipated that larger radii are closer to resembling a flat surface and therefore likely to have an effect on the size of the contact between the two bodies. The relative radius is based on two curved bodies coming into contact whereby the relative radius, derived from the radii of the two bodies, is used in the calculations regarding the contact. With both bodies being considered in determining the relative radius of curvature this ensures that variables, particularly the contact half-space, and mechanics determined represent the contact of these two bodies in a considered manner which ensures the solution is appropriate to the geometry involved. The reduced modulus is an equivalent material property used in the contact calculations that uses the Poisson's ratio and the Modulus of Elasticity of each of the materials in contact to determine a single value for the mechanical properties of the materials. With the dimensions of the contact the differences between a point contact and a line contact start to show the differences between the two types of contact. The dimensions of the contact being determined are the half-contact widths as shown in Figure 20. From the results of the previously describe equations the maximum contact pressure for either case can be determined, typically this will be at the point of contact between the two bodies.

Typically, the equations shown in Table 2 are used to solve contact problems between to metallic bodies such as balls running within a bearing track. When used to solve contact problems the equations shown are used to determine the maximum contact pressure. The geometry, material properties and applied load are usually known. From the geometry it is possible to determine the relative radius of curvature. The material properties of the bodies in contact are used to calculate the reduced modulus. With the relative dimensions and reduced modulus determined it is possible to evaluate the half-contact width, 'a'. The maximum contact pressure is calculated from the determined properties as well as the half-contact width. Where contact mechanics are used to determine the contact pressure between two bodies the usual constraint placed on the problem is that the maximum contact pressure should be less than the yield stress of either of the bodies in contact to ensure that the design is considered valid. Should the contact pressure be greater than the yield strength of either body the component design which effects the contact pressure would need to be modified before being re-evaluated.

Further to the equations shown in Table 2, there is a relationship between the maximum contact pressure and the average contact stress across the contact width, this is shown in Equation 12 below:

$$p_0 = \frac{2P}{\pi a} = \frac{4}{\pi} p_m = \left(\frac{PE^*}{\pi R} \right)^{1/2}$$

Equation 12 - Mean and Max. Contact Pressure Relationship (K.L.Johnson, 2003)

The Hertz contact mechanics equations shown in Table 2 are used to describe non-confirming contacts between two curved bodies, as shown in Figure 19; however "for the contact of a cylinder or a sphere on a flat plane, set $R_2 = \infty$ " (Dwyer-Joyce, 1997) therefore it is possible to adapt the equations to describe a line contact of a cylindrical body on a flat plane. To make this representative of the line contact between the ball and the seat it would be logical to set R_1 equal to the radius of the ball and R_2 equal to ∞ .

When considering the ball and seat contact length, the length of the contact shall be equal to the length of the contact when it has been un-revolved i.e. the contact diameter multiplied by pi. While these adaptations allow the basic theory to be applied to the floating ball valve seat geometry there may be other issues raised by applying a linear model to an axis-symmetric problem. When comparing an axis-symmetric problem to a linear problem the symmetry involved in the axis-symmetric problem influences the method through which the problem is solved; while literature sources state that the stress in the seat ring is axis-symmetric meaning this ideally will not present an issue it shall be considered that there is a possible source of disparity by applying this assumption to the model. The orientation of the load applied to the contact is considered to be perpendicular to the point of contact between the two bodies. When the geometry of the ball and seat is considered the load applied to the seat acts in the direction of the flow axis of the valve not perpendicular to the contact. In applying mechanics and assumptions to derive a load to satisfy the input requirements of the contact mechanics equations it is possible that the load used may result in variance in the resulting outputs from the contact mechanics equations.

Evidence has been gathered through experimentation that shows that “while the Hertz theory of contact was quite good there were cases where the theory did not match to experimentation. This experimentation showed that limitations to the Hertz theory at smaller loads.” (Taylor, 2016) This paper uses the following equation to determine the dimensions of the contact half-space for a line contact:

$$b = \left(\frac{4R_e}{\pi L E^*} \right)^{1/3}$$

Equation 13 – Contact half-space equation (Taylor, 2016)

When compared with other literature and the spherical contact equation it is found that the load term is missing. When compared to other sources of Hertz contact mechanics equations the load term was always found to be present. As this is the only literature source which excludes the load term it would be reasonable to consider this an error in the literature source. By including the load term Equation 14 is derived.

$$b = \sqrt[3]{\frac{4R_e F}{\pi L E^*}}$$

Equation 14 – Contact half-space from Taylor with load term

The contact geometry of the flat plane with a cylindrical body acting on it is shown in Figure 20.

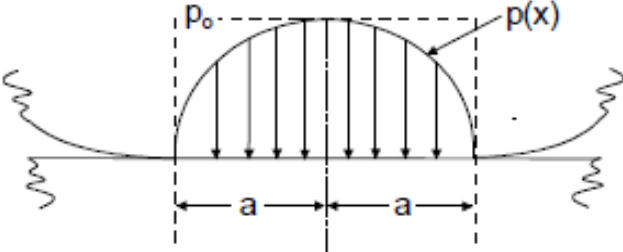


Figure 20 - Pressure Profile Developed on Contact (Dwyer-Joyce, 1997)

In Figure 20 the extents of the pressure profile shown is bound by the contact half-space defined as 'a'. The contact shown in Figure 20 shows the cylindrical body deforming and the flat plane remaining undistorted, it is assumed that with a metallic cylindrical body and a non-metallic plane that the cylindrical body will not distort while the non-metallic plane will.

The results of the calculation for contact pressure can give the mean contact pressure, as shown previously, as well as the maximum contact pressure created by the contact of the two surfaces. Further to this the stress distribution can be determined in the x, y and z-axis to fully evaluate the stresses in the contact area. "The contact area between non-conforming bodies is generally small compared with the dimensions of the bodies themselves; the stresses are highly concentrated in the region close to the contact zone and are not greatly influenced by the shape of the bodies at a distance from the contact area" (K.L.Johnson, 2003). It is possible to derive from the equations shown in Table 2 an equation which can determine the contact pressure at the locations within the contact half-space, when applied to a number of scenarios the evaluation of the contact pressure at various points in the contact half-space agrees with the contact pressure profile shown in shown in Figure 20.

The equations shown in Table 2 that describe non-conforming Hertz contact mechanics are used exclusively to describe the contact between two metallic bodies. When we consider the ball and seat components, the ball can be modelled as a cylindrical metallic component, (as discussed previously), while the seat can be modelled as a non-metallic (plastic) flat plane. To make the equations presented in Table 2 applicable to this problem a degree of adaption is required; this adaption is required to include the behaviour of the non-metallic (plastic) plane. The work that has been presented in the paper 'Spherical indentation of Elastic-Plastic Solids' (Fleck, 1998), demonstrates the development of a point contact model based on a spherical metal body called an indenter being pressed into a flat elastic-plastic plane. The resulting output from the paper is a range of theoretical models which describe the behaviour of the elastic-plastic plane within specified boundary conditions. The general problem to which the solutions are generated to solve is shown in Figure 21.

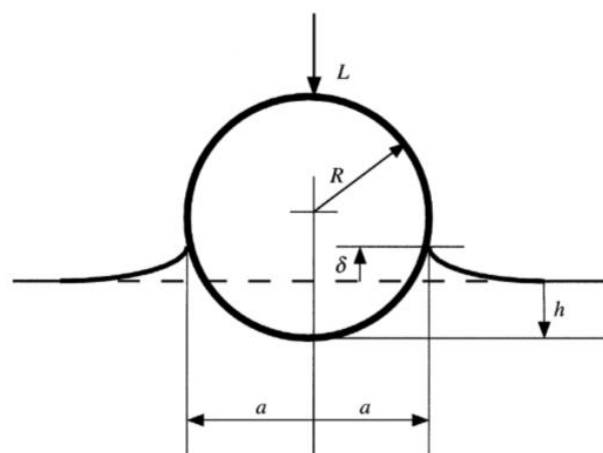


Figure 21 - Geometry of Spherical Indentation (Fleck, 1998)

The definition of terms shown in Figure 21 - Geometry of Spherical Indentation Figure 21 is as follows: L , the load that is applied normal to the surface, R , the radius of the spherical indenter, a , the contact radius (half-space), h , indent depth and δ , for material pile-up (if applicable). The material pile-up denoted as δ may be positive for material pile up or negative for material sink in. The indenter is considered rigid and therefore excluded from the scope of analysis of the thesis.

When considering the spherical indenter in the paper by Fleck et al, it was found that “initially, elastic indentation occurs and the classical solution of Hertz is reproduced for the frictionless indenter” (Fleck, 1998), this was found to be applicable “for small indent depths, the response is elastic and is given by the Hertz elastic solution for frictionless indentation” (Fleck, 1998). The paper presents a number of different models that described the indentation and response of the plastic plane. However the area of interest is the initial regime which is considered as the elastic regime “the elastic regime pertains when Mises stress within the half-space is less than the rigid strength of the solid” (Fleck, 1998), this is satisfied for the relationship shown in Equation 15.

$$\frac{a}{R} < \frac{2.5 \cdot \sigma_0}{E^*}$$

Equation 15 - Hertz Contact Mechanics, Applicability

Where:

a – half-space width

R – indenter (ball) Radius

E* - reduced modulus

σ_0 – Von Mises Stress

Equation 15 can be re-arranged to determine a limiting factor whereby Hertz contact mechanics have been proven to be applicable by the work of Fleck et al. Equation 16 shows the re-arrangement to give the limiting factor.

$$\sigma_0 > \frac{a \cdot E^*}{2.5 \cdot R}$$

Equation 16 - Hertz Contact, Von Mises Stress Limit

In the case of a rigid indenter the “Poisson’s ratio ν appears combined with the Young’s modulus E in the form of a single elastic constant” (Fleck, 1998) as shown below:

$$E^* \equiv \frac{E}{(1 - \nu^2)}$$

Equation 17 - Elastic Constant (Fleck, 1998)

Equation 17 shows a different calculation of the reduced modulus to that shown in Table 2; the elastic constant presented in Equation 17 only considered the properties of the plastic plane and not the rigid indenter. In addition to the amended elastic constant the application of Hertz contact mechanics to this problem required the following assumptions to be applied to the problem:

- The size of the contact area is small compared with the size of the curved bodies.
- Both contacting surfaces are smooth and frictionless
- The deformation is elastic and can be calculated by treating each body as an elastic half space. (An elastic half space is the term given to a flat surface on an infinite elastic solid.)

To further understand the application of contact mechanics involved in the designing of a seating component and validate the assumptions made, the following part of this section reviews the literature where contact mechanics have previously been applied to the design of a seal.

To start with the contact mechanics of a low-pressure O-ring seal shall be considered, in this case it is considered that the seal is achieved by the compression of the O-ring into the groove (housing) alone, i.e. the effect of the pressure acting on the O-ring in the groove is neglected. When considering these mechanics of the O-ring we are presented with the following equation:

$$f' = \frac{4F}{\pi^2 b D_m}$$

Equation 18 - O-Ring Contact Stress (Hertz, 1979)

Where:

- b – seal contact width
- f' – peak contact stress
- F – compressive load
- D_m – Mean seal diameter

Equation 18 is compared to the equation for maximum contact pressure for a cylindrical contact taken from Table 2, this is shown in Table 3.

Variable	O-Ring	Hertz Contact Mechanics
Peak Stress	$f' = \frac{4F}{\pi^2 b D_m}$	$P_0 = \frac{2P}{\pi a}$

Table 3 - Comparison of O-Ring and Hertz Peak Contact Stress'

Here we find the term ' $\frac{F}{\pi \cdot D_m}$ ' is equivalent to the term 'P' as the load per unit length. The calculated term for load per unit length, ' $\frac{F}{\pi \cdot D_m}$ ', from EQ.5 is determined by taking the mean O-Ring diameter and multiplying that by pi giving the circumferential length of the mean diameter, dividing the total compressive load by the circumferential length of the mean diameter gives the load per unit length equivalent to 'P'. If the term 'P' is substituted into the O-ring equation, this becomes:

$$f' = \frac{4 \cdot P}{\pi \cdot b}$$

Equation 19 - Max. Contact Stress with load per unit length

Here we see the differences are that the seal contact width, 'b' is determined by the compression of the circular cross-section as shown by Equation 20.

$$b = 2.4x$$

Equation 20 - Seal Contact Width (Hertz, 1979)

Where:

b – seal contact width

x – seal deflection

The seal contact width is equivalent to the half-space width of Hertz contact mechanics however it is unclear whether the equivalence is direct i.e. a is equal to b or whether b is equal to 2a.

The seal contact width, b, has been compared to the chord length of the section of a 72-0945-30 O-Ring, as shown in Appendix 1, here it is seen that the seal contact width determined in Equation 20 is equivalent to the half-space in the Hertz Contact equation. With the contact widths being shown to be the same this therefore leaves a factor of two difference between the two equations; however, it cannot be said as to whether this factor is to take into account the axis-symmetry or not.

As has been shown previously Hertz contact mechanics can be applied to the contact between seals (non-metallic bodies) and metallic bodies, when assessing “sealing contact areas and sealing stresses these are determined in accordance with contact mechanics” (Hertz, 1979), as shown in the following figure:

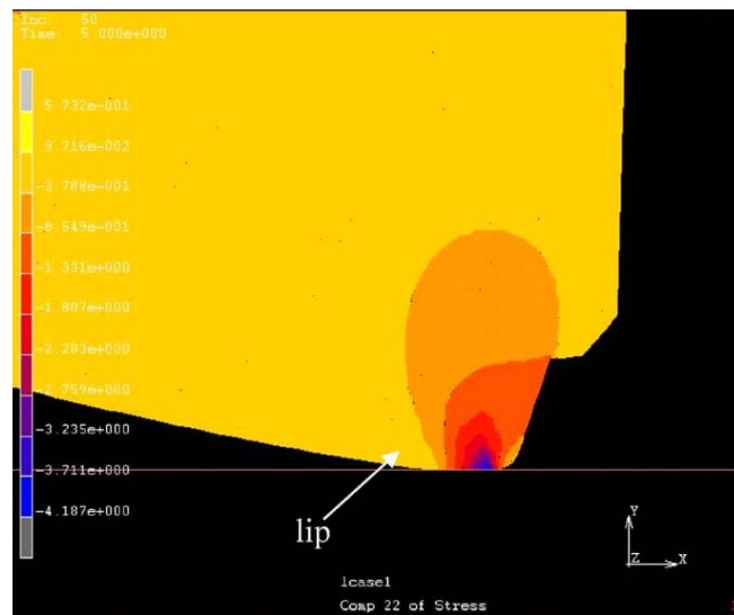
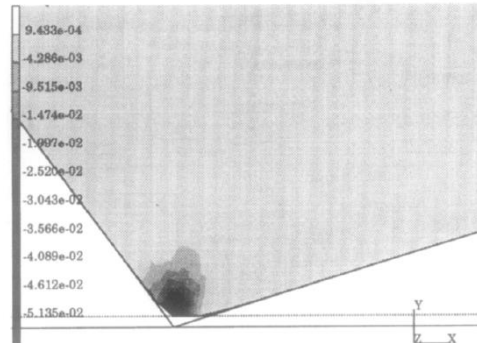


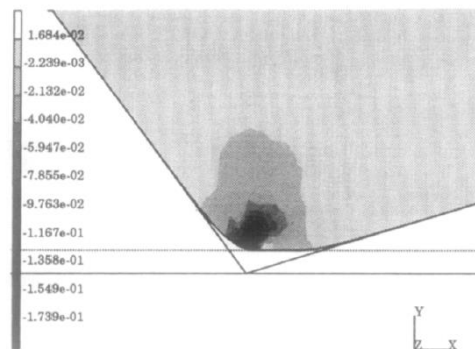
Figure 22 - Contour Plot of Radial Stress Component (Lee, 2006)

Figure 22 shows the stress plot of the radial stresses in a lip seal, not “this radial stress component at the contact surface represents the contact pressure” (Lee, 2006) this contact pressure acts perpendicular to the shaft being sealed therefore based on Hertz contact mechanics the force generating this contact pressure must be acting in the same direction (i.e. perpendicular to the shaft).

Figure 23 shows a lip seal with two different interferences between the shaft and seal, in both these images the interference causes radial seal deflection and radial contact pressure.



(a) Interference $\delta=0.2\text{mm}$



(b) Interference $\delta=0.3\text{mm}$

Figure 23 - Lip-Seal Initial Interference Stress Distribution (Kim, 1997)

When the interference presented in Figure 23 with the equations defined in Equation 18 we find that the greater the compression of the seal the greater the maximum contact pressure is, (A full set of these calculations are shown in Appendix 2), this is in agreement with the magnitude of the stresses shown in Figure 23 where the greater the interference the greater the maximum contact pressure is.

In both Figure 22 and Figure 23 the lip seals display the same radial pressure distribution patterns; the "contact stress has an elliptical distribution across the contact zone" (Budynas & Nisbett, 2015) this is predicted by the Hertz contact mechanics model as shown in the following figure.

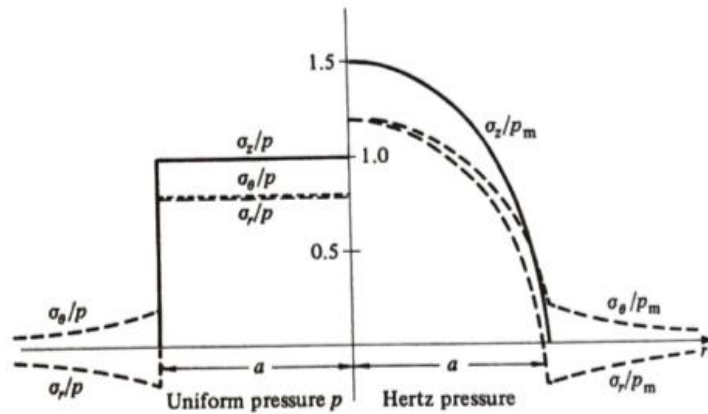


Figure 24 - Comparison of Uniform Pressure and Hertz Pressure (K.L.Johnson, 2003)

From Figure 22, Figure 23 and Figure 24 it can be seen that the theoretical model (Figure 24), predicts the results that are shown in the simulations of the lip seal contacts (Figure 22 and Figure 23). While it is numerically impossible to evaluate the contact mechanics shown in the two figures it is possible to make a qualitative comparison and a judgement as to whether this is an appropriate theoretical model to use as a basis for developing a theoretical model. The use of the evaluation of the contact pressure profile of a Hertz contact model and the plots of the contact stresses of the non-metallic sealing components presented in these figures allow for the comparison to be made which supports the assumption made that the most representative theoretical contact model available to describe the contact between the seal and counter-face is Hertz contact mechanics. The contact pressure shown in the stress contours shown in the three plots in the two figures are closer in resemblance to Hertz contact pressure profiles than to the uniform pressure profile shown. Therefore it is assumed that the Hertz contact theoretical model is applicable based on the previously stated reasoning and shall be used as the basis for determining the contact between the ball and seat components in this thesis.

With the mechanics describing the contact between the ball and seat components identified from the literature reviewed. The following works reviewed seek to identify whether there is knowledge available which describes the function of a seal through contact mechanics or whether there is a consensus between the available materials on both subject areas.

When considering seals in general we find that "sealing performance depends largely on a suitable unit load being maintained at the seal-shaft interface" (Lee, 2006) this is further confirmation of the findings of the previous section. When combined with the understanding that "resilient flow is produced by closure loading, stressing the seal in compression. Contact pressure is then maintained by stored elastic strain energy" (Warring, 1981).

In general sealing is considered to be effective when "the sealing pressure is thus higher than the applied fluid pressure" (Warring, 1981). When looking beyond the general concepts of sealing seals are broadly categorised into static and dynamic seals; "Static seals aim at providing a complete physical barrier in a potential leak path to which they are applied. They are zero leakage seals. To achieve this the seal must be resilient enough to flow into and fill any irregularities in the surfaces being sealed and at the same time remain rigid enough to resist extrusion onto the clearance gap between the surfaces under the full system pressure being sealed." (Warring, 1981).

A second seal category referred to as dynamic seals is split into the following two categories.

- (i) "Contact seals where the seal bears against its mating surface under positive pressure.
- (ii) Clearance seal which operate with a positive clearance (i.e. no rubbing contact)." (Brown, 1990).

When considering a static O-Ring seal, where an O-Ring is used in a low-pressure application; in a low-pressure application the pressure-energised function of the O-Ring is considered to be negligible. In designing an O-Ring seal the "sealing contact areas and sealing stresses are determined in accordance contact mechanics" (Hertz, 1979); further to this the design of the seal is considered to be effective when " f is greater than the system pressure, the O-Ring will seal the joint" (Hertz, 1979), where f is being defined as the peak contact stress. The dynamic seal category defines the types of seals which it covers as being defined as being contact seals.

Comparing the descriptions of static and dynamic seals to the function of a floating ball valve seat as defined in section 1.3 the positive pressure against the mating surface is in agreement with the seat preload combined with the pressure load. Dynamic seals can be designed as pressure-energised seals, these "seals fall into two categories. The first comprises of solid elastomeric rings (such as O-Rings and rectangular rings) which are assembled in grooves with an interference fit. This imparts a 'squeeze' or preload pressure, providing sealing in the static condition (they may also be used as static seals). Under fluid pressure acting on one side of the seal through the clearance gap the elastomeric section is deformed, increasing the interference pressure by an amount equal to the fluid pressure. If the preload pressure is p and the fluid pressure is P , the effective pressure under working conditions is $P+p$ because this is greater than the actual fluid pressure, P , sealing is maintained" (Brown, 1990), this description of a pressure-energised dynamic seal is identical to the general principles of the floating ball valve seats function; here the initial interference between the ball and seat is achieved on assembly like with the preload, p , then when in the closed position and under 'working conditions' a pressure load, P , is introduced by the pressure acting over the ball. The pressure load, P , and the interference load, p , combined together, $P+p$, is expected to be greater than the fluid pressure as with the dynamic seals mechanics previously described.

The main difference between the seal from the ball valve seat and the pressure-energised dynamic seal is that the ball moves under pressure to energise the seat whereas in the seal the pressure acts on the seal energising the seal itself against the mating face.

When looking at lip seals in more detail some "pressure-energised seals 'employs a hollow section' with a flexible lip or lips. Again it is assembled with an interference fit giving a preload pressure" (Brown, 1990), this can be made equivalent to ' p '. With "lip type seals the interference load can vary with lip radial thickness, length of the flexible leg(s) and the modulus of elasticity of the material. The distribution of the interference load depends on the section geometry." (Warring, 1981). This interference load may be "achieved by pre-loading when assembled (i.e. the free inner diameter of the seal is an interference fit); or more usually by a certain degree of preload together with mechanical pressure applied by a garter spring." (Warring, 1981). In addition to the interference or pre-load "the fluid pressure (P) acting on the section further increases the interface pressure to $P+p$ " (Brown, 1990). Once again the function of the pressure-energised seal is comparable to function of the floating ball valve seats function.

As discussed earlier the seal needs to fill the irregularities in the mating face for the seal to be leak-tight. When considering the surface of the mating face the surface irregularities need to be minimised to reduce the work the seal has to do to achieve this, with this in mind the surface finish is "usually specified as 10 to 20 CLA, with a finer finish being acceptable" (Machine Design, 1993) to achieve surface finish a "plunge-ground shaft is preferred, although any process that generates the specified finish without a lead is acceptable" (Machine Design, 1993).

Once the surface finish has been defined the longevity of this surface finish of the mating face needs to be maintained when its "hardness should be held to 55Rc minimum when possible" (Machine Design, 1993), this ensures that the seal itself is the component that will wear instead of the mating face. When considering the interaction between the mating surface and the seal with respect to the radial stress profile of the mating surface is key "maximum bore to shaft misalignment is normally 0.38mm TIR" (Machine Design, 1993), therefore the radial stress can only possibly vary by the radial misalignment, this will reduce the radial stress on one side but increase it on the other side, the reduction of radial stress may if too severe reduce the contact pressure below the value required for the seal to be leak-tight.

Irrespective of the type of seal, a load is generated between the seal contact point and the mating area. This interface load depends on the amount of interference or 'squeeze' produced when the seal is assembled, together with the modulus of elasticity of the material." (Warring, 1981)

In both Figure 22 and Figure 23 the only part being assessed is the seal itself, this indicates that the analysis of the effectiveness of the seal is dependent only on the contact pressure present in the interface between the shaft and the seal but only in the seal component. A "seal must be resilient enough to flow into and fill irregularities in the surfaces being sealed and at the same time remain rigid enough to resist extrusion" (Warring, 1981).

Of all the literature reviewed with regards to the contact models, in-particular the Hertz contact model there are limited works which present a link the contact pressure and the required sealing load for a particular material or set of materials. By looking at the literature reviewed in this section as a whole it is apparent that it is possible to determine the contact pressure (proposed to be the sealing stress) based on the material properties, geometries of the components and the forces applied to the contact of the two bodies effecting a seal. With a known geometry of the sealing component and counter-face, known material properties and a known load it is possible to determine the relative radius of curvature and elastic constant. From the calculated variables it would be possible to evaluate the contact half-space and therefore the peak contact stress in the seal. By determining the peak contact stress in the seal it is possible to consider this as the sealing stress in the seal component.

This section has reviewed the literature available with regards to the contact between two bodies, starting with two metallic bodies being in contact determining Hertz Contact mechanics as the accepted solution for cases with two metallic bodies. Using the literature related to spherical indentation of plastic-elastic solids the application of Hertz contact mechanics was broadened to include non-metallic bodies as well. While this literature shows that it is possible to use Hertz contact mechanics to describe the interaction between a metallic and non-metallic body these mechanics were not used to describe the stresses in the contact half-width which was identified as a probable determining factor in whether a seal is achieved or not.

Literature relating to applying contact mechanics to seals were reviewed, starting with the low-pressure O-Ring where it was seen that Hertz Contact mechanics are used to determine the contact pressure induced by compressing the O-ring in the housing and the relation of this to the pressure to be sealed by the O-Ring.

Following the understanding of applying Hertz contact mechanics to the O-ring other seals were reviewed to determine whether Hertz Contact mechanics could feasibly be applied to describe the sealing function of the seal component. When looking at seal designs which are not o-rings the analysis of the literature showed that the stresses in the sealing component was judged to be of the same form as that predicted by the application of the theory of Hertz contact mechanics. The same stresses in the seal and in the Hertz contact mechanics theories making it an appropriate to assume that the application of the theory to achieving a seal with the seal component is a sound judgement. The application of contact mechanics in the literature in this section is limited to basic geometries with simplistic loading conditions, to apply these theories to the interaction of the ball and seat components of a floating ball valve would require a significant degree of adaption due to the complex geometries involved in the floating ball valve component design. The design of the floating ball valve seat has been shown to typically be of an axis-symmetric nature, the application of hertz contact mechanics, a linear calculation method, to the geometry is likely to result in parameters from the geometry not being taken into account. The application of the load to the seat component by the ball is not in the same manner as in the equations describing the Hertz contact mechanics. While it appears possible to derive a suitable applied load this load may not take into account all the relevant factors which will affect the contact pressure value determined.

2.2.5 Theoretical Functional Model (Torque)

The torque of a floating ball valve is typically defined by the design of the seats among other factors. The following table comprises of equations that are currently used to evaluate the torque of a floating ball valve, each equation is applicable to a different component of the operating torque as shown.

Thrust Component	Equation	Sign	Opening Stroke		Closing Stroke	
			Fully Open	Fully Closed	Fully Open	Fully Closed
Packing Load	$T_P = F_{PL} \frac{D_S}{2}$ $F_{PL} = G_{stress} \cdot v \cdot \pi \cdot D_S \cdot H_P \cdot \mu_P$ $G_{stress} = 1.5 P_{sys} \text{ or } 1500\text{psi}$	always positive	+	+	+	+
Static Seat Torque	$T_S = \text{From Manufacturer's Data}$		+	+	+	+
Dynamic Seat Torque	$T_{DS} = \frac{\Delta P \cdot \left(\frac{\pi}{4}\right) \cdot d_{MS}^2 \cdot d_B}{\sqrt{d_B^2 - d_{MS}^2}} \cdot \mu_S \cdot \frac{d_B + \sqrt{d_B^2 - d_{MS}^2}}{48}$	always positive	+	+	0	0
Hydrodynamic torque	$T_H = \left(\frac{1}{12}\right) \cdot \Delta P \cdot \left(\frac{HTF}{100}\right) \cdot d_P^3$		+	0	+	0
Total Thrust (lbs):						

Table 4 - Tabulation of Torque Evaluation (EPRI, 1999)

If the elements in Table 4 that are related to the seat design are taken in isolation then it is found that “the effect of the seats on the valves operating torque shall be determined by the evaluation of the static seat torque and the Dynamic seat torque”, (EPRI, 1999). Of the two elements relating to the torque of the valve that are determined by the design of the seats the static seat torque is undefined; therefore, a theoretical model for the static seat torque will be required to make this a complete and acceptable model.

To evaluate the static seat torque a model may be built from the valve and seat geometry combined with the sealing theory as discussed on page 32 of section 2.2.1 and page 44 of section 2.2.4 respectively. Based on the work done in these sections in establishing the seat as a form of dynamic seal it is proposed to explore the theories relating to torques and thrusts of dynamic seal to see if they are applicable to the ball valve model. The theory used for dynamic seals is defined as being where in “dynamic seals the load generated by the seal must be multiplied by the coefficient of friction to obtain the dynamic load to move the seal assembly, which is effectively a ‘power loss’” (Warring, 1981) this power loss seems a logical method of defining the torque required to turn the ball through the seats.

In dynamic seals “friction is obviously proportional to a function of the actual contact pressure, although the actual coefficient of friction involved may vary with speed, time etc. as well as material and surface finish” (Warring, 1981), while this may be true in practice when considering a theoretical model this generates too many variables to generate a model comparable with the existing EPRI equations. For the purposes of defining the static seal torque the coefficient of friction between the ball and the seat shall be maintained as that already used in the dynamic seat torque equation. Based on the simplification of the coefficient of friction “seal friction is proportional to the effective contact pressure, i.e.

$$\text{Seal friction} = \mu \cdot P_e \cdot ab$$

Equation 21 - Seal Friction Equation

Where:

μ – coefficient of friction

P_e – Effective contact pressure

a – seal face contact width (inches)

b – Seal face contact length (inches) - $\pi \cdot d$ for a circular seal, where d is the contacting diameter” (Warring, 1981).

The seal face contact length, b in Equation 21, can be used for a circular seal becoming $\pi \cdot d$ however to make this applicable to a ball valve seat this needs tying to the valve geometry. Looking at the dynamic seat torque equation in Table 4 the load has been evaluated over the mean seat seal diameter, d_{ms} , therefore b should be determined in the following manner:

$$b = \pi \cdot d_{MS}$$

Equation 22 - seat friction contact length

It is proposed that the width of the seal face contact width, a , can be related back to Hertz contact mechanics for a cylindrical body on a flat plane where “the area of contact is a narrow rectangle of width $2b$ and length, l ” (Budynas & Nisbett, 2015), applying this to

Equation 22 would make 'a' equal to '2b' and 'b' equal to 'l'. The contact pressure, P_e , can be determined in accordance with Hertz contact mechanics for the interference load or preload of the seat as the dynamic seat torque deals with this aspect of the seat load, this contact pressure is the same value as the sealing contact pressure therefore it is logical to use the same method of determining the value in sealing and torque evaluation methods.

By making the assumptions of the previous paragraph it appears possible to apply a theoretical model for the seal friction of a dynamic seal to the undefined parameter of the static seat load. With this being applied model the assumptions made by drawing parallels with the contact model reviewed in the previous chapter may not hold true. To validate the outcome of any theoretical model which describes the torque of a floating ball valve it would be considered sensible to perform a series of tests to verify the components which make up the complete valve torque, both in their elemental form and in their combined form.

The seat design has an influence on the functional performance of the valve, most obvious of these influences are the influence of the seat design on the operating torque of the valve. To measure the torque of a floating ball valve there is a standardised method which forms part of API 591. API 591 is a recommended practice in the petrochemical industry, where it is recommended to perform the test detailed in the following section to validate any theoretical torque values. The requirement to test an assembled ball valve to determine the correlation between the theoretical torque and the actual torque for the valve, the test method in API 591, Clause H.6 is shown in the following quote.

"H.6 Torque/Thrust Functional Testing

The maximum torque or thrust required to operate ball, gate or plug valves shall be measured at the pressure specified by the purchaser for the following valve operations:

- a) Open to closed with the bore pressurized and the cavity at atmospheric pressure, if applicable to the valve design;
- b) Closed to open with both sides of the obturator pressurized and the cavity at atmospheric pressure;
- c) Closed to open with one side of the obturator pressurized and the cavity at atmospheric pressure;
- d) As item c) but with the other side of the obturator pressurized.

Torque or thrust values shall be measured with the seats free of sealant except where sealant is the primary means of sealing. If necessary for assembly, a lubricant with a viscosity not exceeding that of SAE 10W motor oil or equivalent may be used." (American Petroleum Institute, 2009). When the testing has been completed, "Thrust and torque or thrust results shall be recorded and shall not exceed the manufacturer's documented breakaway torque/thrust." (American Petroleum Institute, 2015) these quotes highlight a lack of a correlation between the theoretical torque values and the measured torque values within the petrochemical industry.

Despite the application of Equation 21 to a floating ball valve seat to describe the static seat load generated by the seat component, this is still simply a load applied to a component. Further work would be required to take the applied load and generate an expression where the static seat load is expressed as a torque which must be overcome to operate the valve. With a static seat torque theoretical model it should be possible to validate the model in its entirety through torque testing similar to that discussed in this section to ensure that the theoretical models match any results obtained through physical testing.

2.2.6 Section Outcomes

This section reviews the current theoretical models which are used or proposed through research to be used for the design of floating ball valve seats. In reviewing the theoretical models of the seat designs the models presented were found to be qualitative in nature describing the mechanics in broad terms with generalised equations. From the descriptions of the designs reviewed it was possible to identify common trends in the approach to the analysis of the designs. In all of the designs where a degree of flexibility is present in the seat design the loading of the seat was separated into a pre-load and a pressure-load, this was highlighted by the case where finite element analysis was carried out on the pre-load, pressure load and the combined load. Where the seat designs considered the interaction between the ball and seat components it was only considered through the use of plain stress analysis, this is contradicted by the finite element analysis of the rubber seat and the Metso seat design which clearly demonstrate the more appropriate theoretical model to describe the interaction is the Hertz contact model. There is limited available evidence that contact mechanics have been applied to the evaluation of a floating ball valve seat design, therefore this is a gap in the knowledge which is currently available. There was some evidence that the mechanics of achieving a seal had been investigated in the seat design works, however the lack of definition and constraints on valve size and pressure sealed which are applied to the models provided in these works limit the usefulness of such theories in achieving the aims of this thesis.

Where the literature describing the theoretical models of other seal types were reviewed the works demonstrated a number of mature and well-developed theoretical models. The achievement of a seal with a gaseous media is defined by a comprehensive equation which is not limited by the size of the seal or the pressure applied to the seal assembly. This relationship between the required sealing pressure, the process media pressure and the dimensions of the contact achieving the seal fills a gap in knowledge from the review of the floating ball valve seat literature. The mechanics of the face seal designs are observed being applied to the designs of floating ball valve seats where a ore-load is applied to the floating ball valve seat on assembly. The description of the contact between the seal face and the metallic counter-face added no knowledge as this interaction is typically two flat surfaces which are loaded therefore making it suitable to use plain stress equations of a load over an area. Therefore, the knowledge describing the interaction between the ball and seat components is still a significant gap to be addressed in this thesis.

The review of literature regarding the definition of the theories defining the contacts identifies Hertz contact mechanics as the most appropriate theoretical model to apply to a seal with a non-conforming sealing face design. The review of literature on pressure-energised dynamic seal and O-rings shows the application of Hertz contact mechanics to determine the contact pressure at which a seal would be leak-tight. Despite demonstrating the achievement of a seal by the application of Hertz contact mechanics to an O-ring, significant assumptions and modifications would need to be applied to the Hertz contact theory to make it applicable to the axis-symmetric geometry of a floating ball valve seal. This literature has identified an applicable theory for this thesis however it has not filled the gap to which it relates as it needs modification to make it applicable to the aim of establishing a theoretical model.

The requirements of the performance of a floating ball valve seat from the literature defining these requirements have been reviewed a part of this section. While not a part of the theoretical model these requirements define what is required from the outputs of the design methodology and therefore what requirements the theoretical models must be able to satisfy.

The literature related to the torque of the floating ball valve and the relationship of the operating torque of the valve to the design of the seat components was reviewed. The literature identified a theoretical model which has been published that defines the majority of terms for determining the torque of a floating ball valve. The published theoretical model was short of a model which describes the static seat torque. The literature related to other

seal types where a frictional load was determined have been reviewed. Through the comparison of the function dynamic seals to floating ball valve seats it is possible to identify applicable theoretical models which could be modified to be applied to the floating ball valve seat in a similar manner to the other theories identified in this literature review.

The review of the literature in this section has identified a number of theoretical models which add value to the analysis of the existing knowledge and create guidance on the development of a theoretical model describing the mechanics of the floating ball valve seat. Where theoretical models have been identified they have not been directly applicable to the requirements of this solution. The theoretical models identified will require development to allow them to be applied to the mechanics of the floating ball valve seat in a manner which adequately describes the interaction and response of the component.

2.3 Analytical Methods and Validation

This section reviews the analytical methods that are used to assess ball valves both in part, as an assembly and seal designs where a similar function has been identified in the previous section. Once the analysis in the works reviewed is complete the use of the information generated by the analysis for the purposes of validating the work is assessed.

The analysis of a radial lip seal by the application of finite element analysis to the component was achieved through applying simplifications to the model, "due to the axisymmetric structure of the radial lip seal" (XiaoHong, et al., 2014) as shown in Figure 25. It shall be possible to develop an axisymmetric, two-dimensional model in an appropriate finite element package.

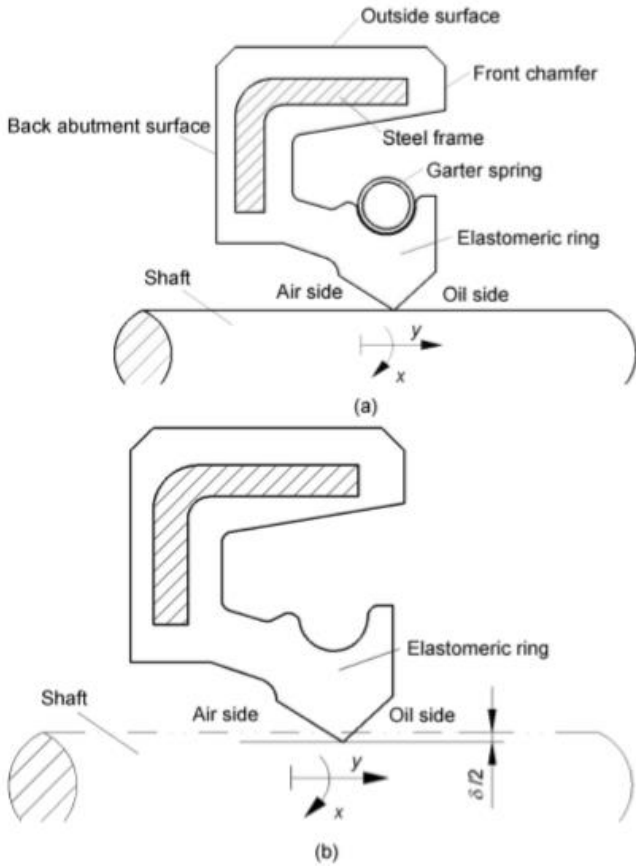


Figure 25 – Radial Lip Seal Schematic diagram (a), interference of seal lip and shaft (XiaoHong, et al., 2014)

Through the application of the axisymmetric simplification to the geometry allows for the reduction of computing time while maintaining the accuracy of the results of the gained from the computational model. The resulting mesh for an axis-symmetric finite element analysis model is shown in Figure 26.

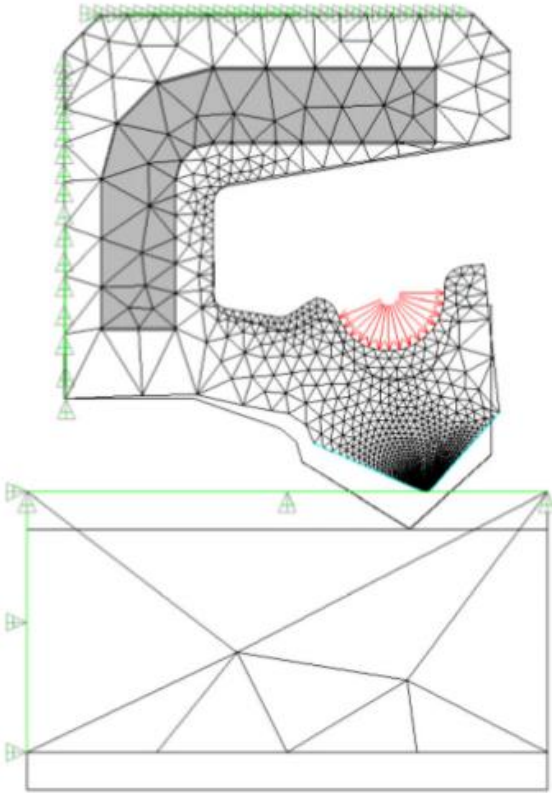


Figure 26 – Finite element Model (XiaoHong, et al., 2014)

When setting up the analysis, “The analysis is performed in two load steps.” (XiaoHong, et al., 2014) The first step takes the shaft and moves it “upward to the seal by applying the displacement.” The effect of moving the shaft upwards is equal “to the difference in radius between unsprung seal lip and shaft” (XiaoHong, et al., 2014) “As a result, the pre-stresses between the contact surfaces are produced.” “In the second step, the spring force is applied on the spring groove as a surface pressure.” (XiaoHong, et al., 2014). The application of the loads in two steps represents the loads being applied to the seal accurately. Despite the representative results gained through application of the two loads representing the combined loading conditions of the seal it is unlikely that the application of loads in this manner will be applicable to the floating ball valve seats. The application of the pressure over the area of the ball will result in varying loads being applied to the ball component itself. In applying a load to the ball, it would be impossible to apply a deflection to this component or the seat and achieve a stable model with a fixed component.

The computational model for the analysis of the floating ball valve with a nitrile rubber seat as shown in Figure 27 was assessed to optimise the profile of the seat component.

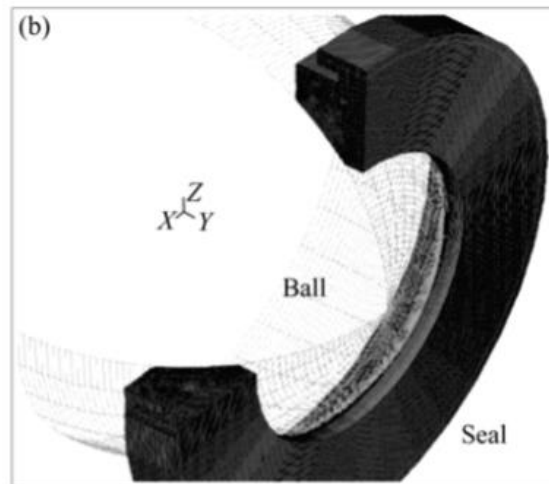


Figure 27 - 3D Modelling of ball valve and seat (Song, Wang, & Park, 2009)

In Figure 27 the valve is simplified to the ball component and a single seat, the body, closure and stem components are not included in the analysis of the valve and seat components. No constraints are discussed that are being applied to the modelled components to generate the effect the removed components will have on their behaviour under the loads applied. In modelling the ball, it is "represented by means of rigid elements, meaning that there are no deformations compared with the initial shape." (Song, Wang, & Park, 2009) While the use of rigid elements ensures the ball does not deform and reduce the load which is applied to the seat in anyway, the use of rigid elements does not represent the real-world conditions of the components where the differences in material properties may have an impact on the analyses of the seat. When simplifying the geometry being analysed "the axial symmetry constraint was taken into account for simulating the real model." (Song, Wang, & Park, 2009) based on the work presented in this paper the 2D axisymmetric simplification was successfully applied to a floating ball valve seat component.

Figure 28 shows the results gained from applying load condition A and load condition A+B to the simplified model shown in Figure 27.

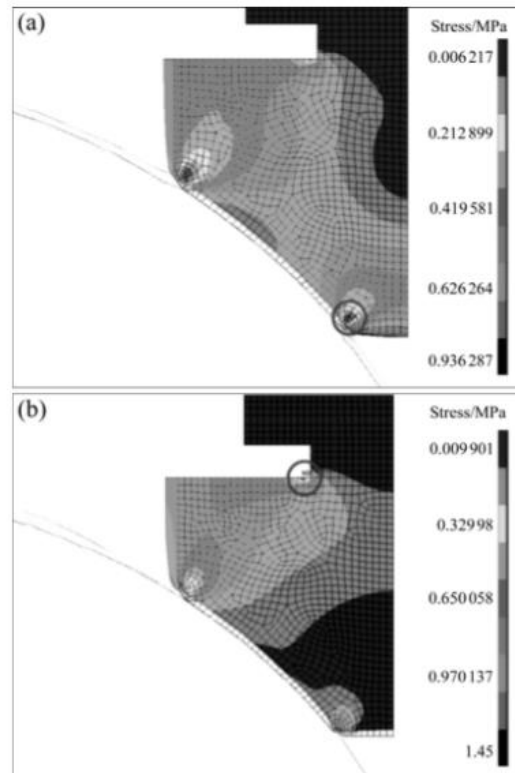


Figure 28 - Von Mises Stress under Load condition A (a), and Load condition A+B (b) (Song, Wang, & Park, 2009)

The results gained were discussed following plotting the contact stresses on the surface in contact with the ball. These results obtained and plotted from the analysed are the basis from which the seat is to be optimised. There is little presented in this paper which forms an objective basis through which changes were made to the seat design. "The purpose of the seal optimization is to find a good cross section that can provide the best trade-off between leakage prevention and material abrasion." By plotting the results of the contact stresses taken from the computational model and the re-running of the analyses with variations in the seat design this allows for the changes in the seat design to be analysed against a baseline set of results. By comparing the new results to the original results, the changes can be quantified to enable to solutions to converge on the objectives of the optimisation aim. This method of comparing and modifying the design manually would be a very labour-intensive process, and a process which would require significant understanding of the part being optimised to allow for manual changes to be made in a considered manner.

The works reviewed in this section identify that there have been successful analyses of floating ball valve seats and general seal designs through the application of finite element analysis. The geometries analysed in the review presented were simplified to the greatest extent possible, however there were some cases where this had been taken beyond what could reasonably be reflective of the real-world situation. In all the cases where an axisymmetric problem was found the 2D simplification for this problem was applied, in every situation including the analysis of the floating ball valve seat it was found that the results gained from the 2D model did not result in a loss of accuracy or relevance. In applying constraints to the models it is possible to replicate the behaviour of the bodies when used in a simplified simulation. There was minimal evidence of applying constraints to the floating ball valve model to achieve this aim. The stem component was removed from

the computational model however no constraint was identified which replaced the function through which the stem maintains the balls alignment and prevents it from rotating while contact the seat component. The application of loads to the shaft in the case of the seal creates a form of pre-load, this was identified as not possible using this and a pressure load as a stable model which is fixed in space would not be achievable as this would translate to a translation of the seat and a load acting on the ball resulting in free-body motion of the assembly.

Following the collection of the results of the analyses conducted on the computational models, these results were either used as the final output or used as part of an iterative process through which an optimal result was obtained. Neither of the two methods mentioned demonstrate a development of the understanding of the subject matter rather the use of the finite element analysis as a tool through which the problem is solved. The aims of this thesis are to understand and therefore optimise the process through which a floating ball valve seat is designed, therefore the use of finite element analysis must provide value in developing the understanding. By using the results of the finite element analysis to develop the understanding of the subject matter it will be possible to validate any theoretical model against this information. Evidence of the use of finite element analysis being used to validate the design of a seal theory was limited in the works reviewed.

2.3.1 Section Outcomes

This section has reviewed the analytical methods employed by previous works as well as how these works were used in the validation of any other components of the papers they are taken from.

Through applying analytical methods to seat and seal designs there is a common analytical method applied, finite element analysis. Through the application of finite element analysis to the component being analysed it has been shown that it is possible to investigate the mechanics involved in governing the response of the component to the applied boundary conditions. When considering the seals and seats to which these finite element analysis method is applied it is found that these are typically considered as axisymmetric models and therefore simplified to a two dimensional analysis of the computational model with constraints applied to the components. It is possible to apply constraints to the components where they are analysed in three dimensions but the model input to the analysis is of two dimensions. To allow the analysis to be completed in three dimensions specific symmetry constraints are applied to the model, these constraints are typically considered as axisymmetric constraints which allows for a two-dimensional slice of an axisymmetric model to be analysed while retaining the three-dimensional characteristics. The application of various constraints to the model of the subject area being analysed the most significant constraint which is applied to each of the computational models is the one which prevents free-body motion of the parts being analysed to create a stable model for the analysis to be performed on. The loads applied to the models have been applied in such a manner as to reflect the realistic condition of the models without allowing free-body motion from occurring. The best illustration of applied load is that of the radial lip seal, the creation of the pre-load by moving the shaft towards the seal creates the effect of the deflection while allowing for the seal to be fixed in a different location to stop the free body motion. The application of the loads to a computational model shall be considered to be representative of the realistic conditions which they are aiming to replicate while still allowing for a sound analysis to be completed. The final component of the analysis which is covered in the literature reviewed concerns the creation of a mesh which allows for the obtaining of accurate results while not becoming a data intensive process. The analyses presented in this section use a mesh which is finer (reduced distance between nodes) at the point of contact and coarser in areas where there is less interest in the result or where appropriate results

can be gained without the application of a finer mesh. The application of different sizes of mesh to the same analysis can be seen clearly in the mesh applied to the radial lip seal, here it is shown that the area of interest is the lip of the component, therefore at this location the size of the mesh is much finer than around the back of the seal where it is a standard size mesh. Through the application of the previously mentioned approaches and the synthesis of appropriate methods from these approaches it shall be possible to devise a finite element analysis where the constraints and loads applied to the model shall be representative of the real world response of the floating ball valve seat component to the loads applied to it.

The most common use of a computational model is for the generation of numerical results from a set of defined conditions; the numerical results are typically interpreted, the model refined and then re-run in an iterative process. Through applying an iterative process to the evaluated the subject area until an improved result is achieved.

The most significant finding of this section is the lack of the use of the analytical results as a means for validating other work undertaken in each of the works reviewed. The computational models are considered to be representative of the realistic interaction being investigated, however, there is limited evidence that the computational models have been used to validate any other works completed describing the same subject area.

2.4 Design Methodologies

This section of the literature review looks at the methodologies that are used to determine a process through which the theoretical model is established from which the parts are designed. These methods shall be reviewed for their effectiveness and applicability to the derivation of a sound theoretical model, validation of the theoretical model and establishment of a design methodology for the floating ball valve seat.

To start with a basic definition, "Engineering design has been defined as "...the process of applying the various techniques and scientific principles for the purpose of defining a device, a process or a system in sufficient detail to permit its realization."" (Norton, 2012), this creates context for the design process with regards to its place in this thesis. When applying the basic definition to the design methodology for the floating ball valve seat it shows that the design methodology developed should be a process through which the various principles and techniques are applied in order to develop sufficient detail to allow the seat design to be realised.

The design process can include all of the following sections in its scope, the process can be applied to determining the principles however it may also be applied to defining the system and then to creating sufficient detail about the seat component to permit its realization. Therefore, the design method can "be any procedures, techniques, aids or 'tools' for designing. They represent a number of distinct activities that the designer might use and combine into an overall design process." (Chakrabarti, 2002). The broad nature of the design process and its applicability to a wide range of subjects means that the use development of the design methodology to design the floating ball valve will need to be focused on the particular elements of the design process from which it is possible to create an optimised and robust process.

The design process can be broken down into a number of individual steps that when followed creates a series of steps that go from a specification to a realised product, as seen by the following list.

1. "Identification of Need
2. Background Research
3. Goal Statement
4. Performance Specifications
5. Identification and Invention
6. Analysis
7. Selection
8. Detailed Design
9. Prototyping and Testing
10. Production" (Norton, 2012)

While this list is considered as a design process it can be used to form an applied methodology from to which it would possible to create a framework of the process through which a floating ball valve seat can be designed. If it is considered that the subject areas of the identification of the need and review of the background material have been previously when developing the design process and therefore not applicable to the design methodology itself. When the designing a floating ball valve seat the goal statement is a straightforward statement of achieving a floating ball valve seat design where the functional aspect of the seat design are achieved. The performance specification can be considered as the specifications related to the seat component which need to be achieved by the design created, for a floating ball valve this can be the pressures at which the seat will achieve a seal at as well as the torque which the seat generates from the valve. Taking steps 5, 6 and 7 as a single group, this relates to the process through which the design rules can be applied to the development of the floating ball valve seat component, through the identification of the relevant information to input into the design methodology, the analysis of the information input through the design methodology and the selection of the output from the design methodology and the use of the output from the design methodology. Should the output from the design methodology not meet the performance specifications then a repeat of the three steps, step 5, 6 & 7, is a logical step to take and repeat until the performance specifications are achieved by the output of the three steps. The detailed design step appears to be a straightforward step in the application of the process to any component, where the output of the previous steps is converted into detailed drawings of the components developed by the process. Step 9, the prototyping and testing step is present to test the solution, however through the development of the design methodology in this thesis there should be no need to test the designs as they are developed from a sound theory. The final step is the manufacturing of the solution gained from the design methodology, this should be considered as the process which follows the design of the component as it has no relation to the design methodology presented or the one this thesis seeks to develop.

The process to develop a design methodology can be described in two broad steps, analysis and synthesis. "In writings on design theory and methodology the processes of "synthesis" and "analysis" are understood in two different ways. In one view synthesis and analysis are phases of the design process; in another view synthesis and analysis are functions that should be fulfilled by any problem-solving process." (Chakrabarti, 2002) Analysis is generally understood to be the process through which a scenario is assessed. Typically, an analysis of a complex system is completed by breaking the subject of the analysis down into its component parts. Through the analysis and understanding of the component parts it is usually possible to gain a deeper understanding of the whole subject area analysed. From the analysis of the subject area it should be possible to create a good working hypothesis of the subject area being analysed.

Synthesis is generally considered as the process through which a solution is synthesised; there are a number of definitions for synthesis, five of which follow.

“Synthesis as designing;

Synthesis as problem solving;

Synthesis as design solution generation;

Synthesis as design problem and solution generation;

Synthesis as exploration” (Chakrabarti, 2002)

From this application of synthesis there are two major directions from which it would be possible to synthesise a solution from, “composition from scratch, and building on an existing design. Whereas compositional synthesis is often believed to enable generation of more innovative ideas, retrieval-based approaches are seen to be more efficient.” (Chakrabarti, 2002), in the context of this thesis based on the literature reviewed so far it would appear as though it would be prudent to follow a retrieval-based approach leveraging the information current available which is applicable and filling the gaps in the knowledge with a compositional approach where applicable. It would be possible to include the matching design principle whereby the problem is matched to a similar problem and make use of the solution used in the match problem. Synthesis covers the identification and invention as well as the selection steps of the product realisation process; in this step the output of the analysis step is developed on to a solution to the problem by identification and selection of the solution from the analysis of the previous step. The synthesis step requires the use of ‘real knowledge’ whereby the problem must be defined by a finite number of inputs which can be verified by observing them or measuring them experimentally with instruments.

When considering the application of analysis and synthesis to the design methodology of the floating ball valve seat there appears to be a need for both processes to be applied to achieve the desired outcomes from the design methodology. When applying the theory of analysis to this thesis it appears logical that analysis would be appropriate to be used to develop an understanding of the mechanics which defined the function of the floating ball valve seat component. Through the use of analysis in this thesis it should be possible to understand the elements which combine to create the overall function of the seat component; while analysis creates the idea of numerical analysis it is entirely possible that a hypothetical analysis through the application of theories to develop a theoretical understanding may be applicable to the subject area concerned. From the understanding created from the analysis of the floating ball valve seat it would be possible to apply synthesis as an exploration tool initially to synthesise solutions and develop methods through which these solutions can be designed. Synthesis could also be applied in the design solution generation where it is possible to take the information gained from the analysis and synthesise a design methodology from which it is possible to design floating ball valve seats.

2.4.1 Section Outcomes

This section identified a number of design methodologies which may address in whole or in part the methodology of designing the floating ball valve seat. The basic description of the design methodology is a good place to start from when creating the design methodology as an outcome of this thesis; the description of a design methodology calls for the application of scientific principles to be applied to define the component being designed. The application of scientific principles means that the theoretical function of the floating ball valve seat component must be understood at a fundamental level to enable the scientific principles describing the mechanics of it to be applied to the design methodology. As seen on page 29

through page 38 of section 2.2.1 of this literature review there are limited works which demonstrate the application of scientific principles to the design methodology through which a floating ball valve seat is designed. Through the application of scientific principles to the design of floating ball valve seats by the work in this thesis this would demonstrate a significant increase in knowledge that it is possible to define the seat component using scientific principles.

The process of this thesis through which the design methodology is derived can make use of the application of both analysis and synthesis to achieve the aims of the thesis. The use of analysis has already been highlighted as the means through which the understanding of the fundamental mechanics and scientific principles describing the floating ball valve seat can be understood. With the application of synthesis being a tool in creating a design methodology from the understanding of the principles and mechanics describing the floating ball valve seat. Through synthesising design equations and a design methodology can be established which accurately describes the floating ball valve seat.

The design methodology described in steps in this section can be applied in part to the development and function of the design methodology. By describing the steps through which a design is arrived at in the methodology it would allow a structured approach to the derivation of the optimal design methodology. The steps discussed previously offer a good foundation from which steps could be identified where applicable and arranged in a manner which allows for the achievement of a design methodology that follow a structure through which the design of a floating ball valve seat is achieved in an optimal manner.

While the literature reviewed in this section is not directly applicable to the design of a floating ball valve seat on its own, when combined with the design methods for ball valve seats reviewed on pages 29 through 38, this provides the appropriate context from which it is possible to evaluate the current literature.

The ball valve seat design literature reviewed does not seem to apply scientific principles which govern the mechanics through which the design should be achieved to the subject of their methodologies. In most cases the ball valve design methodologies reviewed apply simplified and unsuitable theoretical models which do not match the scientific principles which are shown as present in various literature sources. While there are some examples of the use of analysis and synthesis in the previous literature regarding ball valve seats the application of these methodologies is typically limited to the analysis of the subject to gain a set of data from which an improved solution is synthesised. The iterative process of analysis and synthesis does not function to provide the necessary understanding allowing for the optimal design to be achieved; the iterative process simply repeats until a solution which satisfies the requirements is achieved.

2.5 Summary

In summary the literature review has identified a number of areas where there is applicable knowledge available however there are significant gaps in this knowledge which need to be addressed in order to create a satisfactory design methodology.

When reviewing the open literature on the mechanics which are currently used to describe the floating ball valve seat component a wide variety of literature sources were found. Where literature describing the mechanics of the seat were available they described seats that were not in keeping with the industry requirements; one seat design used O-rings to provide a preload to the seat, while another design used springs to provide the preload. The industry requirements made by the International Association of Oil and Gas Producers on page 34 sets the requirement that the seat component is to be wholly made from a single material or composite material, neither of the previously mentioned seat designs met that requirement and therefore cannot be considered as knowledge which is applicable to this thesis. The seat designs which would be directly applicable to this thesis provided broad descriptions of the theoretical function of the floating ball valve seat but did not offer any theoretical knowledge which is directly applicable to the subject area of this thesis. The main outcome of the review of the literature was the understanding developed that all the ball valve designs reviewed made use of a preload, generated by various means, and a pressure-generated load to achieve a seal between the ball and seat components. Where the theoretical ball valve models reviews described the interaction between the ball and seat components it was seen that in all the instances it was assumed that the seat and ball components were conforming surfaces, whereas previously it was stated in a number of quotes that the surfaces are typically tangential and therefore non-conforming surfaces. In the application of conforming surfaces an idea scenario is used rather than a realistic one, in literature reviewed it is seen through stress plots that the contact between the surfaces may not be conforming and there may be more mechanics involved to describe this interaction. The review of the literature directly applicable to ball valve seats fails to produce applicable knowledge that is applicable to the subject area of this thesis, the useful knowledge gained is the common methods of design used, however, the mechanics that describe the achievement of an appropriate design were limited in the available literature reviewed.

When extending the literature reviewed into the wider subject area of seals there is little more knowledge gained from the available literature which is applicable to the floating ball valve seat design. Through the definitions of various types of seals, the function of the floating ball valve seat is considered to be a type of seal of the dynamic seal category, this leads to the review of literature related to dynamic seals. A number of seal designs are described with mechanics and contexts for the design methodology applicable to the seal system, these methods are not considered applicable to floating ball valves as variables such as balance ratios would typically be associated with the seat design of a trunnion mounted ball valve which resembles the face-seal designs reviewed. Through the review of the literature related to seals it is seen that there are theoretical models which link a number of variables including the applied pressure, seal contact width and contact pressure to the achievement of a seal between components in contact. The literature reviewed in this section identifies knowledge which may be applicable to the subject area of this thesis; knowledge on the requirements to achieve a seal. However these requirements for conditions to achieve a seal will not be useful unless the contact between the ball and the seat can be adequately described.

In the initial review of the floating ball valve seats there are assessments made based on conforming contacts between the ball and seat components, however these are contradicted by a finite element analysis stress plot which does not match the proposed design methods. When reviewing the methods the predominate interaction between the ball and seat components is that of two non-conforming surfaces, through the review of the contact theories it was found that Hertz contact mechanics could be applied to the description of a

pair of non-conforming bodies in contact, however these bodies are typically both metallic. Looking at the application of contact mechanics revealed that these mechanics have previously been successfully applied to the interaction of a spherical metal body acting against a non-metallic plane. The modifications made to the original theory indicates that it is possible to apply Hertz contact mechanics to a metallic and non-metallic body in contact; therefore, these mechanics may be applicable to the interaction between the ball and seat components. When looking at the interaction of seals and their counter-faces it was found that a number of investigations have been completed on the subject area, although these works used finite element analysis and iterated the design based on the results; the results indicate that there may be commonalities between the application of Hertz contact mechanics to seals and the metallic/non-metallic adaption of the Hertz contact theories. When looking for the application of contact mechanics to seals it was found that a paper published a method through which the contact pressure created through the compression of an O-ring in a housing was used to determine whether the O-ring would seal the pressure or not. When the design methodology for the O-ring was compared to the Hertz contact mechanics a number of similarities were found between the two theories. The similarities between the O-ring design method and the Hertz contact mechanics make it possible that the application of the Hertz contact mechanics to the interaction between the floating ball valve seat and the ball component could be a suitable model from which to determine whether a seal has been achieved.

From the literature reviewed in this section of the literature review it is clear that a general philosophy of how a floating ball valve seat works has been established. There is little knowledge which describes the fundamental mechanics of the design philosophy; there should be a preload, however there is no knowledge on how to create a preload or what its magnitude should be. It is proposed that there should be a pressure-generated load, however there is little knowledge which describes how the load is determined or applied to the valve. There are a number of methods applied to current design methods for the interaction between the ball and seat, however these do not adequately describe the realistic mechanics shown by finite element analyses of floating ball valve seats and other seals. A floating ball valve seat should seal, yet there are a few methodologies which can be applied to describe the achievement of a seal. The lack of the preceding mechanics means the input variables to method to describe the achievement of a seal are currently unobtainable.

The methods through which the design of floating ball valve seat components have been verified is quite limited due to the minimal amount of work that has been completed previously in this subject area. The analytical tool used in each of the works reviewed is finite element analysis. The use of finite element analysis to create a realistic model from which data is obtained and analysed is prevalent in these works, however the data is not used to validate a theoretical model but rather analysed to modify the model which is then analysed again. The use of finite element analysis to optimise the rubber floating ball valve seat demonstrates the limited application of the approach, in this work it is used to determine the current state to the seat component being optimised, following this the profile of the seat component is modified and the analysis repeated. When considering the approach used to optimise the rubber ball valve seat there is little development of understanding to achieve the optimised seat profile presented, this sort of approach to developing a validation for theoretical models would not be appropriate for this thesis. The analysis of the radial lip seal provides a differing perspective on the use of finite element analysis with the model setup to generate data in a manner which could be used to evaluate the mechanics of the seal, the dense mesh in the location of contact between the seal and the shaft will provide sufficiently accurate data from which analysis would allow for an understanding of the mechanics of this interaction to be developed.

In setting up the computational models in the finite element analysis software these two papers adopt similar approaches. Both problems are considered as axisymmetric problems, the axisymmetric simplification is proven in the case of the ball valve analysis but applied to both of the works shown. The setup of the fixtures and loads differ due to the geometries of the components involved, with the lip seal the heel of the seal is fixed whereas the back of the ball valve seat is fixed this has consequences when applying the loads. Both seals have initial deflection preloads applied to them, the radial lip seal has the initial deflection applied as a movement of the shaft towards the seal whereas the ball valve has an additional load added to the load applied to the ball to create this initial deflection of the seat component as the ball cannot be deflected and have a load applied to it at the same time.

The analytical methods reviewed in this section show that there are prior works which have analysed similar subject areas and as such there is transferable knowledge. The use of finite element analysis has not been employed as a validation tool allowing for the comparison of the realistic condition to the theoretical model but just for interpretation of the realistic condition. In using the learnings of the previous works it will be possible to use finite element analysis to simulate the realistic condition of the floating ball valve seat component, this will provide accurate data against which it will be possible to validate any theoretical model.

As seen in the first section of this literature review there are few design methodologies available for review which relate to the design of a floating ball valve seat component. Those design methodologies which are available do not follow a methodology through which it is possible to design a seat component but rather follow the derivation of the equations from which the mechanics can be described and point to using these equations to design the seat component. Design methods such as previously described are not demonstrated through the use of case studies nor are they shown to work in practice to give a valid and robust model from which it is possible to design the seat component of a floating ball valve.

The design methodologies reviewed identify a number of methodologies through which designs are achieved, while these are not specific to floating ball valves the methodologies are reviewed in the context of the design of the floating ball valve seat component. The general theory behind the development of a design methodology is that it is a mechanism through which the science which describes the mechanics of the part being designed can be applied in a methodical way through which the component is designed. As seen previously in this literature review the scientific principles which govern the design of the floating ball valve seat component are not currently well understood therefore it would be extremely difficult to take what knowledge currently exists and create a sound design methodology. From the design methodologies reviewed it was found that the application of the principles of analysis and synthesis in combination with the scientific understanding of the mechanics governing the design would allow for an iterative process through which the design of a floating ball valve seat component could be achieved. Through the understanding of the fundamental mechanics describing the seat component and the application of the design methodology principles identified in this section of the literature review it would be possible to develop a floating ball valve design methodology that does allow for the design of the seat component in a methodical manner with the scientific principles describing the mechanics of the seat component applied.

2.6 Scope of the Work

The following list of work is included in the scope of the work for this thesis:

- Analysis of the mechanics of the ball and seat components
- Development of theoretical models describing the seat mechanics
- Effects of variables on the solution
- Seat Design methodology

The scope of work has been selected to fill the gaps in knowledge which currently exist in the available knowledge that are providing a barrier to the creation of a comprehensive design methodology for the design of a floating ball valve seat. In filling the gaps in the existing knowledge an improved understanding of the functions and therefore design of the floating ball valve seat is achieved.

The following list of work is to be considered outside scope of work for this thesis:

- The optimisation of the material properties of both the ball and seat components.
- The design of the valve that the seat works in.
- The specific value of a stress to affect sealing between the ball and seat

The above items which are outside of the scope of this thesis require the application of additional work which does not align with the scheme of the work for this thesis. The material properties are usually defined by the material supplier. For this thesis the material properties used shall be selected as generic material properties for the given materials. Optimising material properties is a complex issue which requires specialist knowledge which is typically considered as confidential by material manufacturing companies. The design of the valve the seat sits in has many forms which can be considered, in addition to this there are many papers available where the design optimisation of the metallic components of a floating ball valve have been considered. Because of the existing work on the design of the metallic components of the floating ball valve there are few gaps in knowledge which could be addressed by this thesis on the subject area. The specific value for the sealing stress of a given material under specific conditions would require a series of physical tests to be carried out. While completing these tests would be possible the results would not add value to this thesis. The design methodology created by this thesis shall be flexible enough to adaptable to the required sealing stress specified making the work determining the sealing stress for a given material irrelevant in achieving the aims of this thesis.

2.7 Specific Research Objectives

The specific research objectives shown below have been selected to develop knowledge to either fill gaps that are present in the literature review or build on the knowledge that is present in the literature review to achieve the three aims of this thesis that were previously specified.

1. Development of mechanistic theoretical models based on current theoretical models.

1.1. Development of mechanistic theoretical model of the effect of the pressure-load on the seat component by use of established theoretical models.

1.2. Development of mechanistic theoretical model of seat deflection using established theoretical models.

1.3. Development of bending stress mechanistic theoretical model based on established theoretical models.

The research objectives selected for this aim break the overall aim down into the basic components which can be developed in isolation. As seen in the literature review there is no comprehensive design methodology, however there are applicable theories which can be developed into a single theory. Each of these aims will take a single component of the overall model and develop an existing theoretical model to a point where it is applied to the floating ball valve seat design. The initial component of the pressure-load is not considered by the typical floating ball valve seat design methodologies reviewed however the effect of the pressure differential acting over the sealed area will create a load which generates a load which will need to be assessed to determine its influence on the design of the seat component. The deflection of the floating ball valve seat was identified as a method through which the seats are designed to create a sealing load therefore the relationship between the load applied and the deflection of the seat needs to be defined to develop a comprehensive model. The bending stress within the seat component was highlighted as an area which needs to be assessed. The bending stress in the seat is understood to be the limiting stress in the seat, if the bending stress exceeds the yield stress then the seat will yield and no longer function as designed. By developing these theoretical models the key features of the seats function will be defined numerically, as there is no accepted mechanistic model for the function of the floating ball valve seats, these theoretical models developed from these objectives fill these gaps in knowledge.

2. Validation of theoretical models through the application of finite element analysis.

2.1. Finite element analysis of the theoretical model.

2.2. Comparison of finite element analysis result to the theoretical models.

2.3. Modification of the theoretical models based on the assumptions and results from the finite element analysis model.

The objectives for the second aim take the theoretical model and compare it to the outcomes of an analytical model of the same geometry. By comparing the theoretical and computational models it allows for any assumptions and modifications made to the theoretical models in the previous chapters to be assessed and modified if necessary, to bring it in-line with the results from the computational models. In completing a finite element analysis of the ball and seat geometry it is possible to determine a detailed picture of the deflection of the seat, the contact pressure between the seat and ball components as well as the bending stresses in the seat component. By comparing the computational and the theoretical models any differences between the two models can be assessed and a

solution found which fits the results of the computational models. By ensuring the correlation of the theoretical model to the computational model the theoretical models are validated against the detailed results the finite element analysis provides. In achieving the objectives for the second aim the theoretical models in either its original or modified form become validated theoretical models. By validating the theoretical models it increases the accuracy of the results that the models give. The validated theoretical models further fills the gaps identified in the knowledge by demonstrating the theoretical models describe the key features of the seat function numerically. The description of the key features as defined by the computational model results provide the basis from which it is possible to create a comprehensive design methodology.

3. Development of a design methodology.

3.1. Propose design equations based on chapters 1 and 2.

3.2. Develop a design methodology.

3.3. Application of the design methodology to a case study.

As identified in the literature review there is no single design process which allows the floating ball valve seat component to be designed in a complete and theoretically sound manner. Unlike the design theories laid out in the literature review the design methodology developed by the objective of the third aim shall consider all the key features of the floating ball valve seat design as identified and defined in the previous objectives. The design methodology is developed by initially taking the mechanistic theoretical models describing the key features of the seat function and re-arranging them in a way which allows them to be used to calculate the required seat performance variables from defined inputs. The second objective takes the design equations developed in the first objective and arranges and combines them in a manner which creates a comprehensive design methodology. The design methodology created allows shall allow for the design of seat components in a logical manner. The final objective takes the design methodology and applies it to an example case study where the design method shall be used to define the seat component. In achieving these objectives a design methodology is developed from a theoretically sound set of design equations and the design methodology is tested in a practical setting.

Chapter 3 – Research Methods

This chapter discusses the research methods used in this thesis, their application to the problem and their applicability in their use to achieve the aims of the thesis. The application of research methods is described in this chapter and how they are implemented to reflect the practical situation which they are being used to simulate. The various inputs, process methods and associated properties are explained to demonstrate a sound process is being followed to achieve the required output. Lastly the post-processing methods which are applied to the research methods are described to ensure that the data created through the application of these methods is handled in a way which allows it to maintain its validity in applying it to the subject area of this thesis.

3.1 Finite Element Analysis

The use of finite element analysis in this thesis is to generate sets of data based on the realistic conditions of the components and interactions described through the application of theoretical models. By applying the material properties and loads applied to the theoretical models combined with the realistic application of constraints this will allow the computational model to demonstrate how the components perform in a realistic manner. From the data obtained from the computational model it shall be possible to validate the theoretical models used against the realistic situation thereby proving them valid. Where the finite element analysis shows differences between the theoretical and computational models it allows for the modification of the theoretical models to more accurately describe the realistic condition of the seat component under the loads assessed. The validation of the theoretical models through the use of finite element analysis enables any design methodology produced from the theoretical models to be demonstrably sound. In addition to achieving sound theoretical models the assessment of the case study through the application of finite element analysis will be able to demonstrate the applied design methodology achieve the overall aims of this thesis in allowing the floating ball valve seat to be designed through a theoretical model.

Where Finite Element Analysis is used in this thesis, the method used shall be as per the method as laid out in this section. The finite element analysis in this thesis shall be based around the properties of an ASME Class 150 floating ball valve. The geometry analysed and the load applied to this geometry shall be representative of a typical 2" (DN50) ASME Class 150 floating ball valve by selecting these geometries and associated loads (pressure-based) for the computational models the output of the analyses shall be representative of the stresses, and deflections a typical floating ball valve with a soft seat.

3.1.1 Analysis Steps

The general approach to performing finite element analysis in this thesis shall be based on the best practices taken from the approaches reviewed in the literature review. The most appropriate approach was seen applied by Song et al where the load is applied to the seat by applying the load to the ball component and fixing the seat component. In the previous method, through the load applied the reaction of the seat component is determined. The other sealing models (like the lip seal), to which finite element analysis is applied had the capacity to both fix the seal component and apply a deflection and load to the parts. With the geometry and function of the seat component it means that it is not possible to both fix the seat component and have a load applied to it. The method of applying the load to the model will look to use the method use in the paper by Song et al, and apply the load to the ball component.

The following flowchart shows the steps undertaken when finite element analysis is used in this thesis.

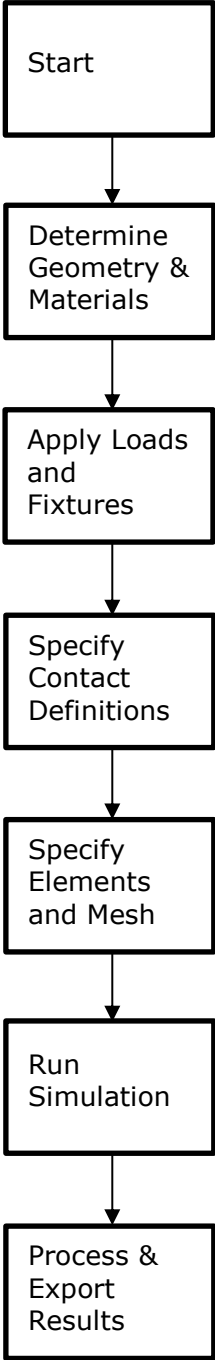


Figure 29 - Finite element analysis process flowchart

The process shown in Figure 29 first analyses the geometry of the valve and seat being assessed. Through analysing the geometry of the valve where components that aren't necessary for the analysis are present they can be removed from the analysis and replaced with constraints replicating their effect on the components being analysed. By removing

components from the analysis the mesh can be setup to give increased an accuracy in the areas of interest without having to apply the mesh to components outside the areas of interest. The materials applied to the components shall be realistic and based on those applied to a valve when a floating ball valve is manufactured. The properties of the materials applied to the components shall be based on publicly available properties where these are available. By applying known material properties to the components of the analyses the results gained will be representative of the realistic responses gained from the actual materials from which the valve would be manufactured from. The material properties are a significant input to the analyses being completed by finite element analysis; particularly the material properties of the seat component as these properties will govern the reaction of the seat component to the loads applied to it.

The loads and fixtures which are applied to the model must be representative of the realistic conditions of the valve. The fixtures applied to the valve must be representative of the restraints which the removed components apply to the components being assessed. Care must be taken in applying the fixtures to the valve to ensure that the fixtures applied to the components to not over-constrain the movement of the parts. The loads applied to the ball component shall be justified in terms of the realistic nature of the magnitude of the load being applied. Through the justification of the magnitude of the load applied to the components the response seen in the seat component can be assured to be representative of the realistic response as the load applied is a realistic load. The fixtures and loads applied to the model are critical inputs to the analyses, the loads and fixtures must be representative of the realistic conditions that the actual valve would be subject to, to give results which are also realistic.

The following step is to specify the contact definitions of the two components at the point where they come into contact. By selecting a contact definition which accurately reflects the interaction between the ball and seat components. These contact definitions applied to the model in this analysis will have a significant impact on the results gained from the simulations completed, therefore the selection of the contact definition will be required to be based off of the contact model applicable to the surfaces in contact with each other.

The type of elements selected for the mesh will have an effect on the accuracy of the results gained from the analyses; the selection of the elements should be undertaken to allow them to be generated in a manner which fits the geometry of the components being analysed. Further to the standard mesh properties it is possible to apply mesh refinements to the areas of interest of the model. Through the application of mesh refinements it is possible to apply a finer mesh to the areas of interest while allowing a coarser mesh to the remainder of the model, this approach allows more data to be obtained from the area of interest; for this thesis the area of interest will be the contact between the ball and seat components.

After running the simulation, the results gained will need to be processed to obtain the information from which it is possible to assess the response of the seat component to the applied loads. The outputs from the analyses which are expected to be assessed include the stress, von mises stress, in the seat component as well as the deflection of the seat component. The methods through which the results are assessed will be required to sample in a manner which uses a sample size large enough to avoid localised stress raising effects while being small enough to be representative of the local area being assessed. The trends displayed in results shall be assessed for consistency and patterns relating the inputs to the outputs as well as the change in outputs with relation to the change in inputs.

The following sections add more depth to each of the steps through which the finite element analysis passes to obtain the realistic results from the analyses.

3.1.2 Study Properties

With the models being representative of the interaction being assessed by a simulation (referred to as a study in Solidworks Simulation), shall be setup; the simulation type must be representative of the problem being solved. For the contact problem in this thesis a static non-linear simulation shall be used as “the contact area and the stiffness of the contact zone are unknown prior to the solution” (Dassaut Systems, 2010), the compression of the seat component while under load determines the contact half-width and the final stiffness of the material therefore the final values of these two elements of the model are unknown at the beginning of the analysis. The final stiffness of the plastic material and the size of the contact half-width are determined through the processing of the computational model in the simulation. When the seat component is loaded we can expect a degree of compression of the seat and therefore a change in the stiffness matrix whereas a linear problem will fix the stiffness matrix at a set value throughout the entirety of the simulation.

3.1.3 Geometry of the Valve

Based on the assessment of the various current seat designs in the literature review the seat design shown in Figure 30 shall be taken forward to be used as a basis for determining the mechanics governing the function and therefore the design of the seat component. This design has been arrived at following the comparison of current designs and the attached either claimed or demonstrated functionality. The previously reviewed designs each have their own advantages and disadvantages, rather than taking an existing design this thesis has taken the Velan design form of an internally and externally supported seat and simplified the profile of the seat from an arcuate profile to a flat profile. By taking a seat design that is not a currently available design and of a simplified profile, the work completed in this thesis demonstrates that the development of a design methodology to suit this seat design is possible thereby allowing for future work of the same nature to be completed on other specific profiles.

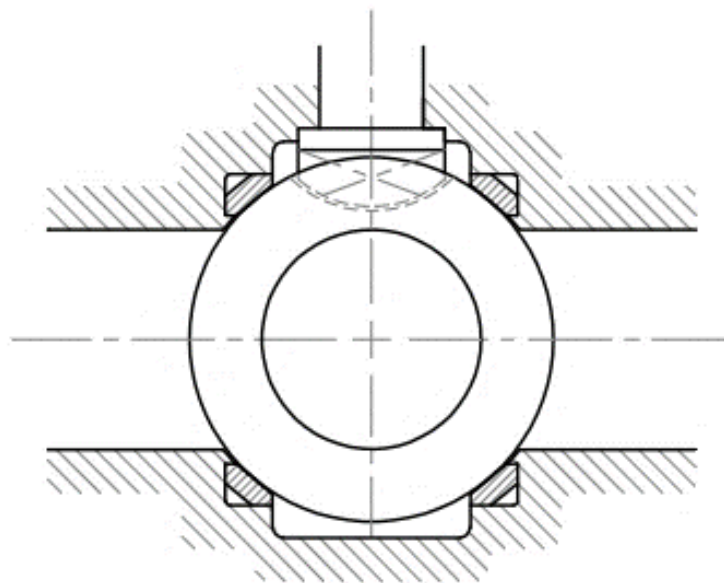


Figure 30 – General Seat Design Layout to be Optimised

The seat design shown in Figure 30 has a contact area which is approximately in the middle of the seat face with flexible regions extending from each side of the point of contact to the point where the seat contacts the housing. The contact between the seat and the ball has been kept as a tangential contact as with the flexible seat and jam seat shown in the literature review, by maintaining this contact geometry on an increase in load the contact area shall be predictable; based on Hertzian contact mechanics the contact area is expected to consist of a half-space on each side of the point of contact.

The geometry selected reflects a seat design which reflects the dimensions of the design of a typical seat component, these have been applied to the design philosophy chosen to give the design shown in Figure 31.

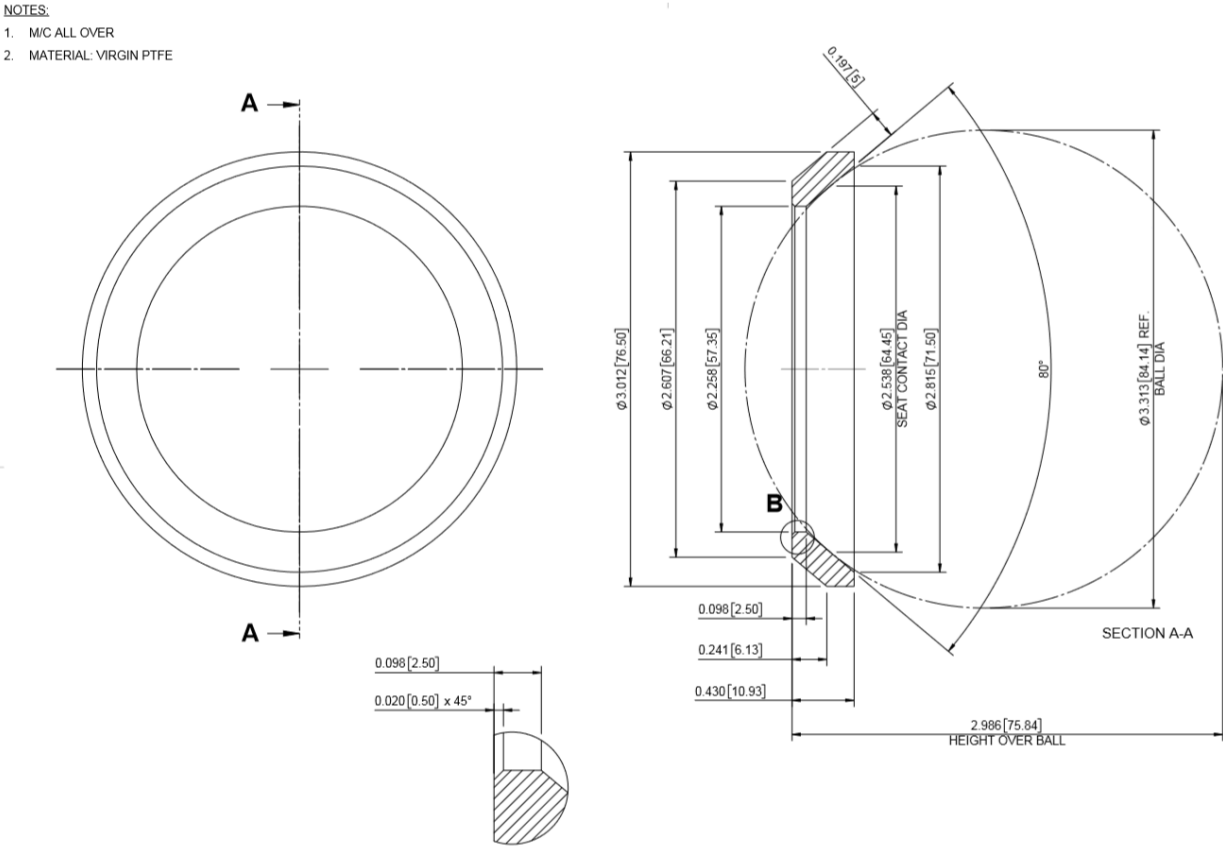


Figure 31 - Seat Design Detail Drawing

With supplemental dimensions shown in Figure 32.

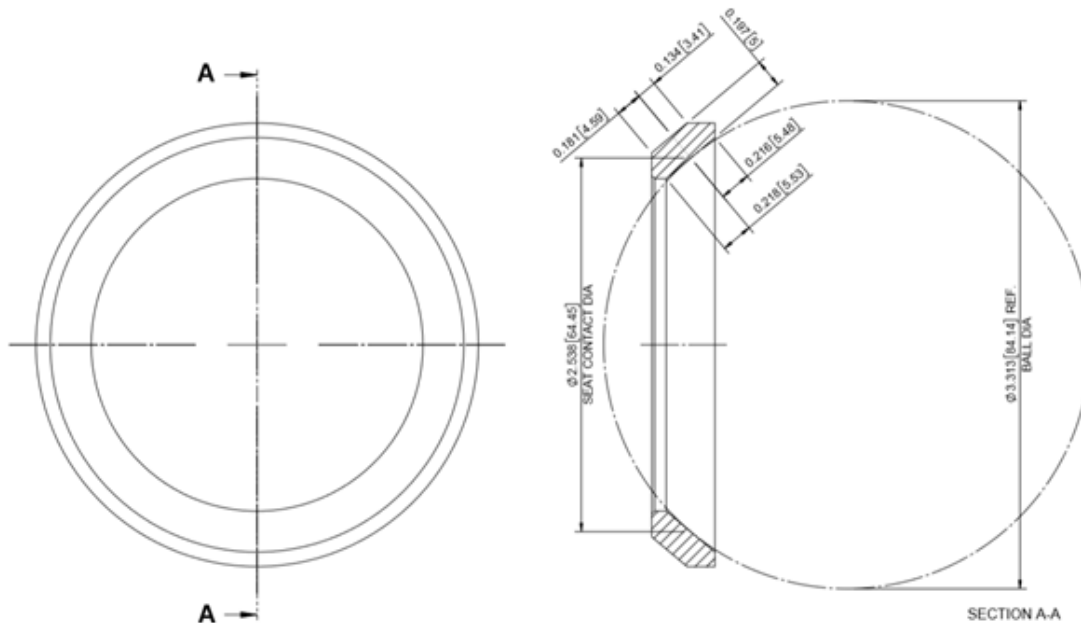


Figure 32 - Supplementary Seat Dimensions

Before starting any analysis on the models, the seat component part needed to be assessed for any features outside the area of interest that can be removed to simplify it and reduce the element count. When looking at Figure 31 the only element that needed to be removed was an internal chamfer, this chamfer is needed for the assembly of the valve as the location of this sits in a machined location that will always have a tool radius present. To allow the seat to press against the end of the housing recess as shown in Figure 30 this chamfer must be present. By removing this chamfer the complexity of the mesh in this region is reduced, therefore the simulation will be processed faster, also the reduced complexity of the mesh means there will be no mesh-induced errors effecting the model caused by high aspect ratio elements being present in the mesh where it has been fitted around the unnecessarily complicated profile.

The geometry involved in the simulation shall only consider the 'downstream' seat, however this is the highest stressed seat component, as discussed earlier the ball is pushed off of the upstream seat and not the downstream seat when pressure is applied to the valve; therefore the load acting on the downstream seat is the preload plus the pressure-load. The method of analysing the 'downstream' seat in isolation is a proven method having been used in the paper 'Analysis and optimization of nitrile butadiene rubber sealing mechanism of ball valve' (Song, Wang, & Park, 2009). In this paper it defines load condition A as the assembly load whilst load condition B is defined as the pressure load, the simulation is completed under load condition A+B. In the paper published by Song et al both the load conditions were known whereas in this thesis only one condition is known which can be applied to the model. As the magnitude and profile of the load acting on the seat cannot be accurately predicted the known load shall be applied to the seat by means of a ball component of the dimensions shown in Figure 31. The 'upstream' half of the ball shall be removed to reduce the size of the component that needs to be meshed; this 'upstream' half of the component does not have any function in the simulations being run therefore it is irrelevant in the outcomes of the studies of this thesis.

As the geometry of the parts being analysed are all axis-symmetric a 2D axis-symmetric simplification can be used to reduce and simplify the model being analysed to only in-plane elements. The axis-symmetric simplification is valid because the only non-axis-symmetric load that could be considered would be gravity and, in this simulation, that load has been removed from the simulation. This is due to the application of the load created by the action of gravity is negligible in its magnitude when compared to the axial loads applied. With all the results from the previous analyses of floating ball valve seats reporting the stresses and deflections found in the seat component of the three-dimensional models to be consistent around the axis of symmetry. As the results have been shown previously to be consistent about the axis of symmetry there is no need to analyse the valve in three-dimensions, there is no additional information which can be gained from the three-dimensional analysis which won't be visible in the two-dimensional analysis.

3.1.4 Material

Whilst the materials involved in the simulation are not the subject of this thesis however the response of the components to the load applied to them requires representative materials to be applied to each of the components. The ball is always a metal component therefore it shall have a typical metal applied to it, the properties of this metal are shown in Table 5; in this case the material chosen is ASTM A182 F316, a forged version of 316 Stainless Steel. ASTM A182 F316 is typically applied to the ball component of valves which are of a stainless steel construction, usually the ball component may be of a cast, bar or forged material. With the material properties of ASTM A351 CF8M (cast) and ASTM A479 S31600 (bar) being the same as ASTM A182 F316 the superior mechanical properties of a forging over a casting and a piece of bar for the ball component typically results in it being used for manufacture. With a casting there may be issues with porosity and increased tooling costs to hold the cast ball to machine the component. With a piece of (usually rolled) bar the grain structure of the material due to the forming process has been known to be attacked and weakened through repeated thermal cycling.

Property	Value	Units	Value	Units
Elastic Modulus	1,000,000	psi	6,894.8	N.mm ⁻²
Poisson's Ratio	0.3	N/A	0.3	N/A
Mass Density	0.288	lb-in ³	7.97 x 10 ⁻⁶	kg.mm ⁻³
Tensile Strength	75,000	psi	517.1	N.mm ⁻²
Compressive Strength	30,000	psi	206.8	N.mm ⁻²
Yield Strength	30,000	psi	206.8	N.mm ⁻²

Table 5 - ASTM A182 F316 Material Properties

While other papers have conducted material testing to derive the properties of the material used and therefore applied to the component this thesis used the typical materials properties for PTFE as shown in Table 6. PTFE is a well understood material, therefore the material properties of a typical PTFE can be easily sourced without the need for testing the material. These material properties shall be applied to the seat component in the computational model. The use of PTFE is selected due to its prevalence in having floating ball valve seats manufactured from it, being chemically inert to most fluids and having a wide operating temperature range lend the use of PTFE to most low pressure applications, therefore making it an appropriate material to use for the seat material in the analyses of this thesis.

Property	Value	Units	Value	Units
Elastic Modulus	80,640	psi	556.0	N.mm ⁻²
Poisson's Ratio	0.47	N/A	0.47	N/A
Mass Density	0.368	lb-in ³	1.02 x 10 ⁻⁵	kg.mm ⁻³
Tensile Strength	4,975	psi	34.3	N.mm ⁻²
Compressive Strength	4,975	psi	34.3	N.mm ⁻²
Yield Strength	2,975	psi	20.5	N.mm ⁻²

Table 6 - PTFE Material Properties

The use of realistic material properties applied to the components used in the analysis of the floating ball valve seat ensures that the results gained from the analyses are realistic and therefore an accurate representative of the reaction of the components in a physical valve subject to the same loads as the analysis.

3.1.5 Loads and Fixtures

The loads chosen to be applied to the valve in the simulation are of the same order of magnitude as those which would be applied to a manufactured valve with the seats being assessed installed in.

Using the commonly accepted theory shown in the literature review that a pressure acting over a sealed face acts over the mean diameter of that sealing face an area over which pressure acts creating a load can be determined as shown in the following figure.

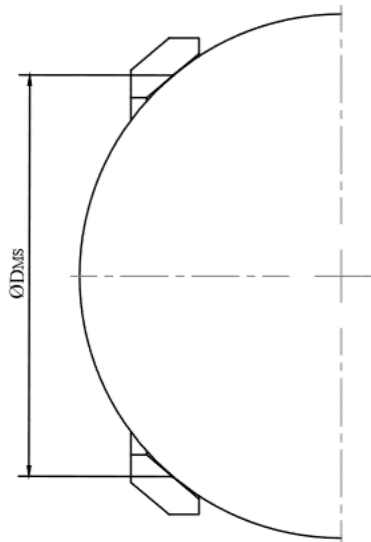


Figure 33 - Mean seal diameter

From the supplementary dimensions shown in Figure 32, the contact diameter, 'D_{MS}', is found to be 2.538in (64.47mm). As the shown from the standards reviewed on pages 42 and 43 of section 2.2.3 the range of pressures the seats must work at ranges from 6barg, to 22barg. The full range of pressures shall be evaluated to determine the mechanics of the seat across the full range of loads which could be applied to the component.

With the diameter that the pressure is acting over defined and the extents of the pressures applied to the valve known it is possible to use this information to derive a load that is applied to the ball by the pressure and therefore transferred to the seat. The following equation links the pressure applied to the valve to the contact diameter giving a load that is being applied to the ball.

$$F_{PL} = P \cdot \left(\frac{\pi \cdot D_{MS}^2}{4} \right)$$

Equation 23 - Pressure Load Equation

When evaluating Equation 23 at the minimum and maximum applied pressures the loads that are calculated are a minimum of 440.14lb-f (1957.8N) and a maximum of 1613.82lb-f (7178.63N). While it is impractical to use these loads as absolute maximum and minimum limits due to their irregular nature, they can be used to set reasonable limits with suitable intervals between them. A minimum load of 400lb-f (1779.3N) and a maximum of 1600lb-f (7117.2N) with a simulation carried out at 200lb-f (889.6N) intervals will cover a substantially similar range of loads while providing sufficient information to validate reliability of the results gained across the range.

The loads which have been determined shall be applied to the model as per the arrow shown in Figure 34.

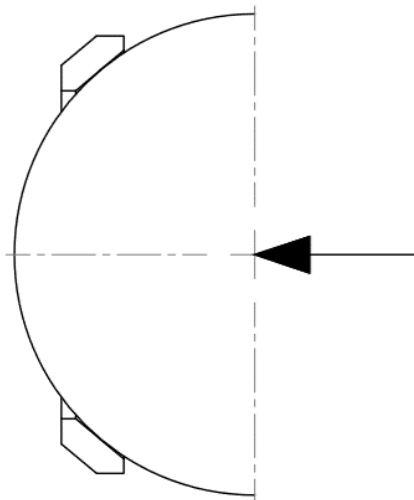


Figure 34 - Applied Load

The applied load is created by a pressure drop acting across a sealed area, as pressure acts perpendicularly to the surface here it is applied acting perpendicularly to the bound area it is acting over. The manner in which the pressure acts means that it is acting in an axial direction through the valve. When applied to the simulation the load is applied to the flat face of the ball where the upstream side has been removed, this defines the load as acting perpendicularly to that face; the application of this load to the model is shown in Figure 35.

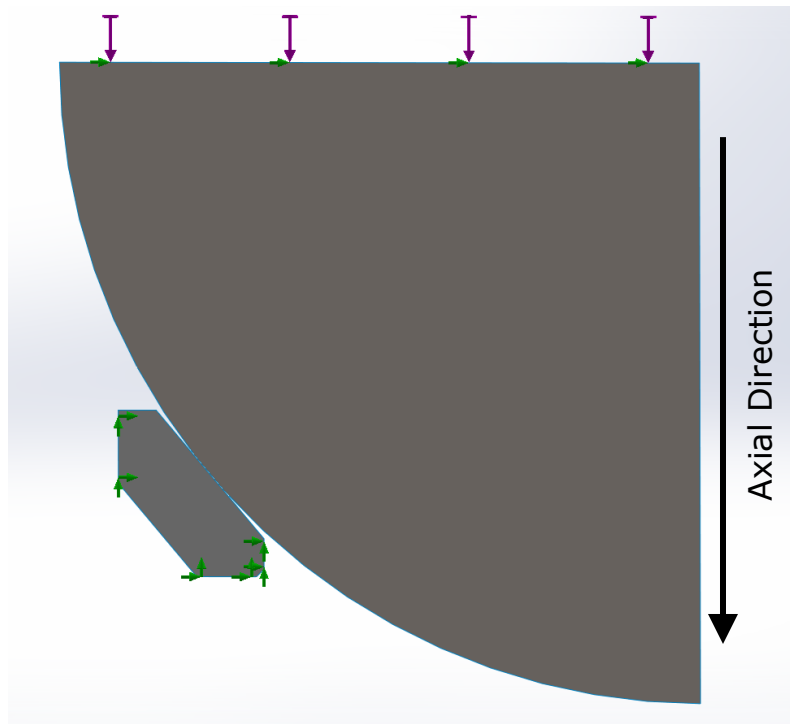


Figure 35 - Loads and Fixtures Applied to Model Geometry

The constraints applied to the model shall be representative of the function of the parts in practice, in addition to this the model shall be constrained to avoid free-body motion and to replicate the constraints applied to the parts by the components which have been removed to simplify the simulation.

There is a constraint shown in Figure 35 applied to the flat surface of the ball component, this is an advanced fixture constraint which constrains the motion of the ball so that it can only move in the axial direction. The constraint placed on the ball ensures that the even loading, as would be expected with a pressure load is achieved on the seat component.

There are three fixed constraints applied to the seat shown in Figure 35, these constraints replicate the effect that the housing has on supporting the seat. The seat component is shown in the housing in Figure 36. Figure 36 shows the seat where it is assembled into the housing by pressing it into the seat housing in the axial direction. The inner edge of the seat component sits against two faces of the body constraining the motion of the seat in both directions but still allowing the central section to bend. The external face of the seat is against the internal face of the seat pocket, this has the effect of fixing the external edge of the seat, however, the central section of the seat is still unsupported thereby allowing it to bend.

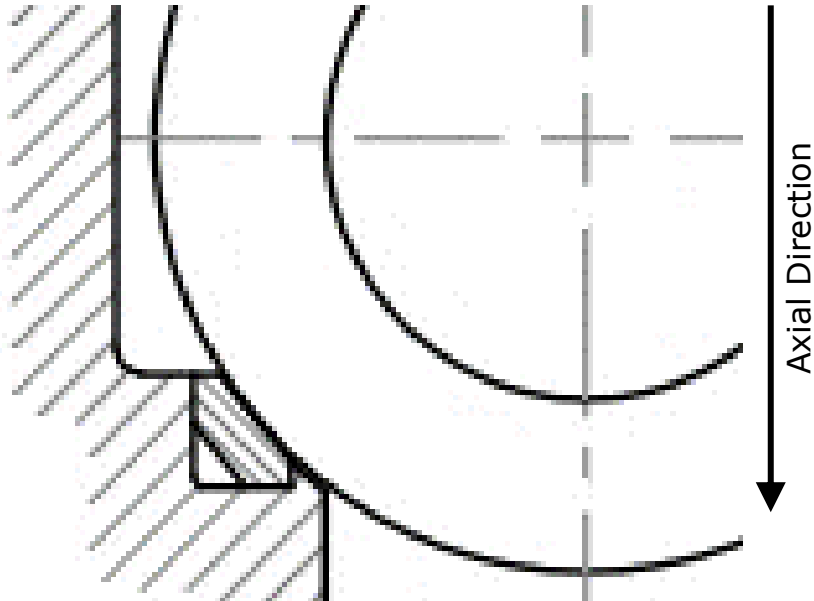


Figure 36 - Diagram of seat component being supported by housing

The two located around the lower and inner faces of the seat replicate the housing outside the firesafe seat and the inner face of the housing, with this forming a corner it will effectively 'wedge' the seat component into the corner fixing it in place preventing any movement of the seat component. The final constraint applied to the seat is on the outer edge of the part and is representative of the outer edge of the machined seat pocket supporting the seat. Initially this constraint was a roller-slider constraint that allowed the edge to move up and down, however this extra degree of freedom presented an unstable model that gave inconsistent results over a number of simulations. As a result, this constraint was amended to be a fixed constraint, the effect of a fixed constraint achieves the representative restrictions of the outer housing face while creating a stable model.

3.1.6 Contact Definitions

In addition to defining the behaviour of the contact between the ball and seat components the way the ball and seat mesh interact are required to be defined, for this the below table is referenced.

	Works with						Speed	Accuracy			Robustness
	No initial contact	Incompatible mesh	Vertices or edges as source entities	Large displacement in Static analysis	Drop test studies	Nonlinear studies		In general	With sliding or large rotations	Tiny contact area (line or point)	
Node-to-node	✗	✗	✗	✗	✗	✓	●	●	●	●	●
Node-to-surface	✓	✓	✓	✓	✓	✓	●	●	●	●	● or ●
Surface-to-surface	✓	✓	✗	✓	✗	✓	●	●	●	●	● or ●

● or ● = very model-dependent.

Legend:
 Good Not so good

Figure 37 - Finite Element Solver Comparison (Courtesy of SolidSolutions)

As discussed previously the problem is being defined as a non-linear static line contact problem, from looking at the table shown in Figure 37 above the most appropriate mesh interaction is the node-to-surface option; therefore all simulations run shall use the node-to-surface solver.

The contact of the two components defining the interaction will need to be representative of the assumptions made in the Hertz contact mechanics; therefore the contact shall be defined as a global 'no penetration' contact rather than a bonded one. The no penetration contact set does not allow one body to pass through another however it does allow the surfaces to slide along each other where required whereas the bonded option bonds the two meshes together effectively fixing the two surfaces together. With the bonded contact selected the nodes on each of the surfaces in contact at the start of the simulation will be paired, therefore where the ball moved the bonded nodes on the seat will be moved to too; this bonded contact model is not representative of reality as where the ball pushes into the PTFE, the PTFE will flow around the metallic sphere this 'flow' of PTFE can only occur if it is not bonded to the ball component. To accurately replicate Hertz contact mechanics the contact between the ball and seat shall be defined as a friction-less contact, as this is one of the assumptions previously defined as a requirement to use this contact model. When applying the constraint to the interaction of the ball and seat surfaces the coefficient of friction shall be disabled to ensure the interaction is representative of Hertz contact mechanics.

3.1.7 Elements and Mesh

When applying a mesh to the model the mesh shall follow the method laid out in the paper 'spherical indentation of elastic-plastic solids' (Fleck, 1998) where the mesh shall take a form similar to that shown in the following figure. The use of the mesh refinement in the contact area between the two bodies increases the density of nodes in the area of interest. As the contact mechanics that are expected to occur in the contact area may present some non-uniform stress profiles therefore increasing the density of nodes in this area will increase the accuracy of the results gained in this area.

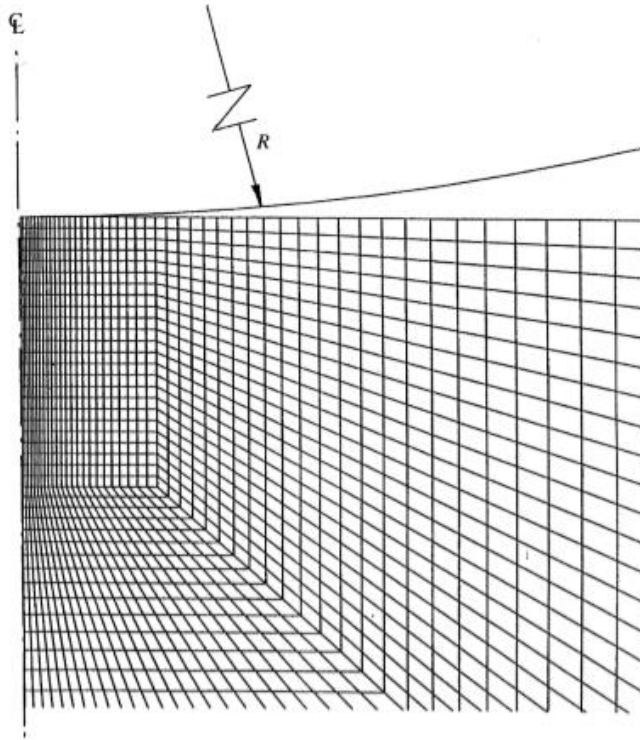


Figure 3. Typical finite-element mesh, composed of second-order isoparametric axisymmetric elements. The distance between nodes at first contact is $0.0005R$.

Figure 38 - Spherical Indentation Mesh (Fleck, 1998)

Here we see that the size of the elements in the area of interest have been reduced to increase the accuracy of the results gained while further from the area of interest the element size is much larger. While Solidworks Simulation cannot create a mesh comprised of second-order isoparametric axisymmetric elements it does offer the ability to add mesh refinements to areas of interest; this mesh refinement can be used to create the same effect as seen in Figure 38.

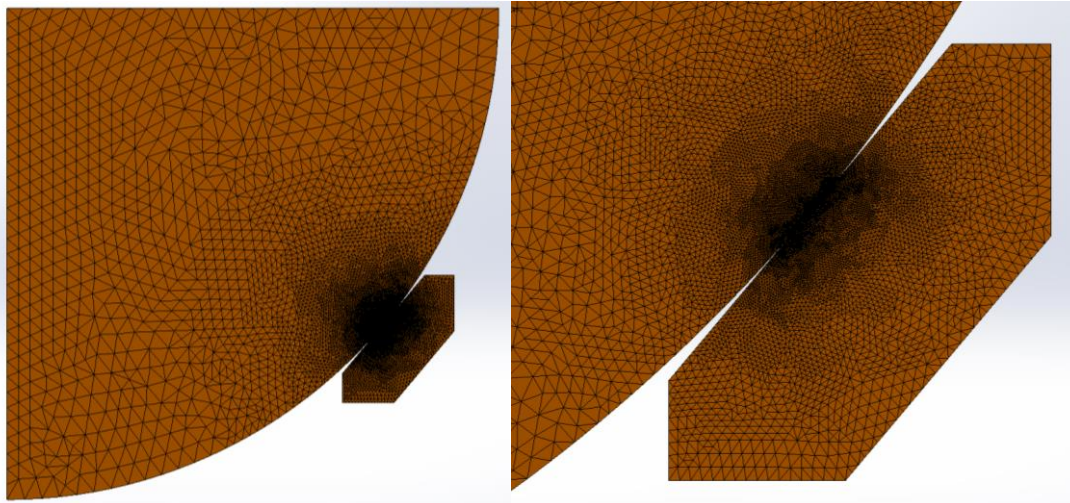


Figure 39 - Mesh Applied to Model Geometry

To ensure the results collected from the simulation are correct the each of the different mesh types available shall be applied to the model and in each case a mesh independence study completed. In each mesh independence study the global mesh shall be defined as the standard mesh of that type, the mesh refinements shall then be adjusted by reducing the element size for each run of the simulation. The results of the mesh independence studies shall be plotted as the total number of elements against the results gained from each of the meshes; the most stable, reliable and accurate mesh from these studies shall be used for the simulations where the results are recorded. Prior to running simulations the quality of the mesh shall be assessed to ensure there are no areas where issue with the mesh may generate spurious results based on the deformation of the mesh.

3.1.7.1 Convergence Study / Mesh Independence

To ensure the simulations are not influenced by the geometry of the mesh, a mesh independence study was completed as detailed in this section. There are a number of mesh options available in Solidworks, Standard Mesh, Curvature-Based Mesh and a blended Curvature-Based Mesh, in each case a convergence study was completed for the mesh following the method outlined below.

The global mesh applied to the model was the Solidworks standard mesh element size. As discussed in the previous section the Coarse mesh applied globally to the model, mesh refinement applied to the contact width was slowly decreased in size over the course of a number of simulations with the results recorded after each simulation was complete. After running a standard analysis of the meshes through the reduction of the size of the elements in the mesh refinement it through comparison of the results it was decided that the Curvature-based mesh yielded the most consistent results across the largest span of results and in the region where the mesh size matched the suggested element size from Figure 38.

To determine the level of accuracy needed for the simulations to provide reliable data the curvature-based mesh was modified to reduce the element growth ratio from the standard 1.5 to 1.25, and then to 1.1. By reducing the element growth ratio of the size of the elements there will be more elements of a smaller size around the contact area potentially increasing the accuracy of the results of the simulations. It was found that the most accurate results were achieved with a 1.1 element growth ratio as shown in convergence study in Figure 40

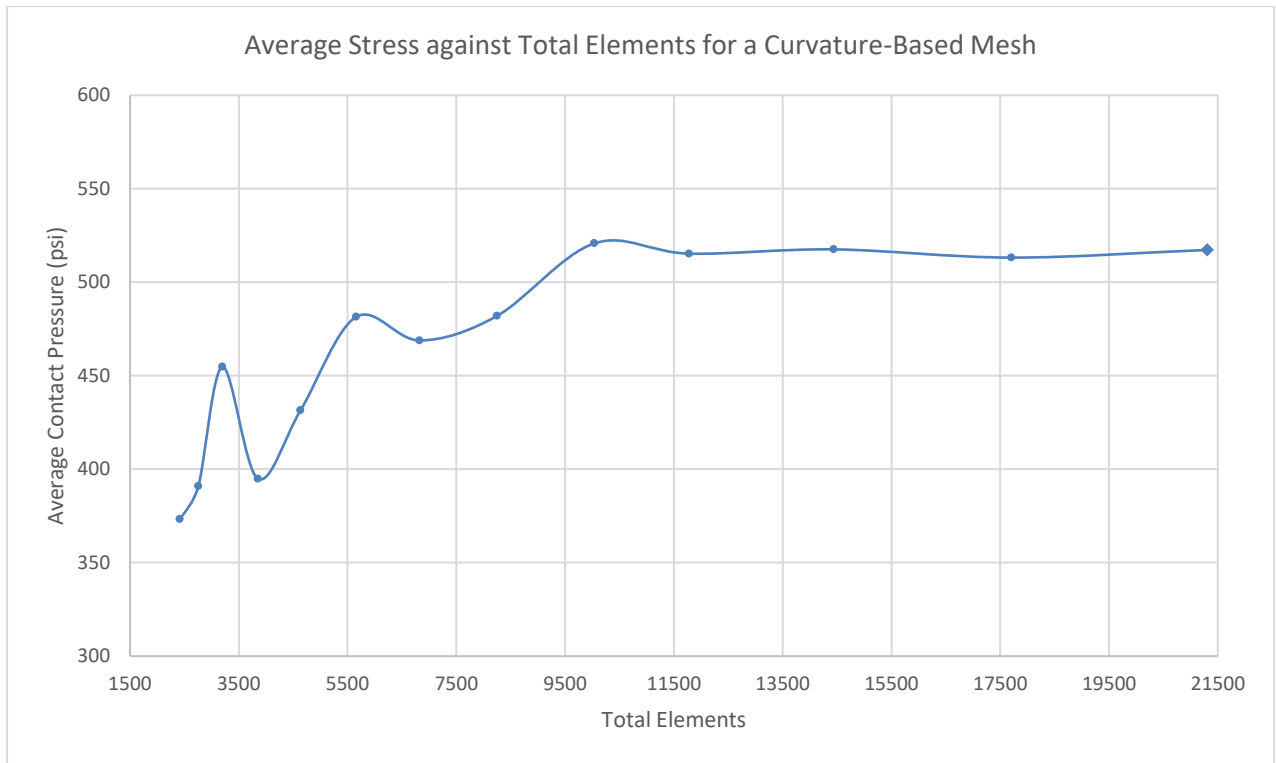


Figure 40 - Curvature-Based Mesh Convergence Study with Element Growth Ratio of 1.1

Figure 40 shows the reduction in size of the elements results, the figure shows a significant increase in the number of elements over a few reductions in the element size. After 10 simulations and element size reductions the results enter a relatively stable region, however the variation in results is only minimised over the last three simulations. The last three simulations have element sizes that match those shown as the required element size in the text of Figure 38, or are of a smaller size. The stability of the results gained over the final three meshes of the convergence study show that the results have converged within a suitable range to consider the results of the analysis to be independent of any effects caused by the size of the elements of the mesh. To ensure the highest accuracy in the contact region between the ball and seat components is achieved the smallest mesh refinement size of the three results which demonstrated the independence from the mesh shall be used for the analyses in this thesis.

3.1.8 Results Processing

The results expected from the analysis carried out by the simulation are to be stress and deflection values for the ball and seat components. With the subject area of this thesis being with regards to understanding the mechanics related to the seat the results of the seat component are to be considered the results which will be of most interest. The results of the simulation shall be plotted as an image. When evaluating the information obtained from the simulations the data shall be taken over more than one node to ensure the data is taken from nodes of more than a single element, the data collected from the nodes shall be mean averaged to determine a value which can be compared to the theoretical results. By averaging across a number of nodes in an area greater than a single element's size any distortion to a single element or node will not affect the data collected. All the results collected shall be plotted on graphs to determine trends shown in the results; by plotting the results in a graphical form it will also allow the results to be graphically interrogated to determine whether any results are inconsistent or whether any set of results is inconsistent with the overall trends. The data obtained from sampling across nodes in the areas of interest shall be evaluated to determine numerical values for the key outputs of the

theoretical models. The determination of the key variables based on the computational model allows for the comparison of the realistic data from the analyses to the theoretical values of the same output.

3.1.9 Instrumental Uncertainties

Across the final three iterations of the convergence study there can be seen that there is a 0.86% and a 0.79% change in the values recorded from the simulations. The minimal variation between the final three values in the convergence study clearly shows a convergence on a mesh which will provide reliable and accurate results from the analyses performed.

While there are minimal uncertainties in this method, the main factor creating uncertainty would be the discontinuities in the mesh however in creating a mesh as detailed previously in this section the discontinuities in the mesh will be located away from the areas of interest on the computational models analysed.

3.1.10 Instrumental Developments

The use of finite element analysis for assessing stress and deflection in this paper does not include any developments to the processing of the model or the code used to solve the problem being analysed.

Chapter 4 – Theoretical Mechanistic Model Development

In this chapter a series of theoretical models are developed through the application of the existing theories to the geometry of the floating ball valve. The theories that are developed are able to describe the mechanics of the seat component. The mechanics of the floating ball valve where theoretical models are developed are the response of the seat to loads being applied in respect to the contact stresses developed in the seat and the deflection of the seat component. Also, the bending stresses in the seat are described and related to the load applied to the seat component. By developing these theoretical mechanistic models it will allow the function of the seat component to be described numerically in terms of the load applied.

4.1 Pressure-load theoretical mechanistic model development

This section develops a theoretical model for the condition where the pressure is acting over the area bound by the contact between the ball and seat components. By the application of modelling, numerical methods and established theories the model developed links the pressure applied to the valve to the contact pressure developed in the seat by contact with the ball components. In developing this theoretical model, it is assumed that there are no system losses, therefore where a load is applied to a body it is assumed that the entire load is transmitted to the body in contact with the loaded body.

The ball and seat geometry produces a diameter where the ball and seat components are in contact, should this be a contact band rather than a point contact the mean diameter is taken rather than the diameter of the point of contact. An illustration of the contact diameter is shown in Figure 41.

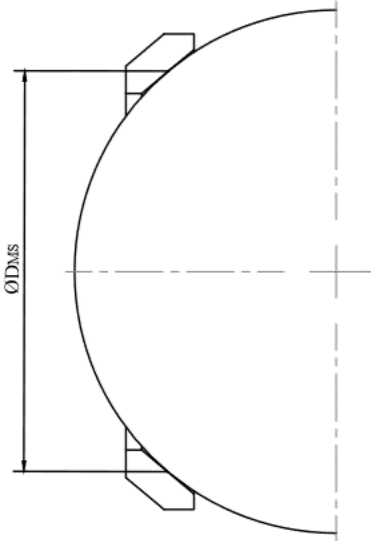


Figure 41 - Mean Seat Contact Diameter

It is assumed that the pressure acts across the mean seat contact diameter, denoted as D_{MS} . The effect of the pressure acting over the mean seat contact diameter is the generation of a pressure differential across the area bound by the diameter. With a pressure differential across the circular area a load is generated equal to the product of the pressure and the area. The pressure load is assumed to act entirely in the direction of the seat bore.

While the pressure load is assumed to act entirely in the axial direction of the seat bore, the face of the seat is set at an angle to this load. The axial load will not be acting on the seat face as the seat face is at an angle to the direction that the pressure load is acting. To determine the proportion of the pressure load which is acting directly on the seat and as a load acting in shear across the seat face. The components of the axial load are shown in Figure 42.

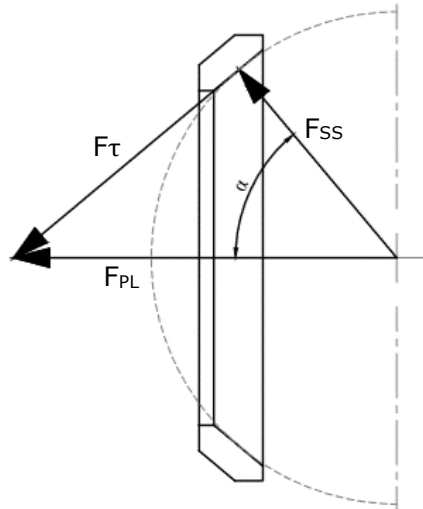


Figure 42 - Pressure Load Components

Figure 42 shows the splitting of the single pressure-based load into two components based on the angle, α . The magnitude of the load components is defined by the angle, α . Based on this, the sealing load, F_{SS} , can be defined as shown in Equation 24.

$$F_{SS} = F_{PL} \cdot \cos \alpha$$

Equation 24 - Sealing Force Component Calculation

As F_{SS} acts perpendicular to the seat face which in turn runs at a tangent to the surface of the ball. It would be reasonable to define the angle in terms of the seat face angle; this angle is defined as β in Figure 43.

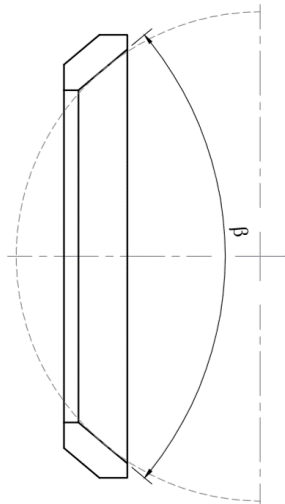


Figure 43 - Seat Angle

Based on the sealing load acting perpendicularly to the seat face it is possible to use complimentary angle geometric relationship within a triangle to relate the sealing load angle, α , to the seat angle, β as shown below.

$$\alpha = 90 - \frac{\beta}{2}$$

Equation 25 - Relationship between Alpha and Beta

The seat sealing load, F_{SS} , is required to be translated into a load per unit length to enable it to be applied to the contact mechanics equations shown in Table 2.

The length of the contact in an axis-symmetric case can be based on the equivalence between the O-ring and the line contact cases, as shown on page 49. To make this numerical model applicable to the ball and seat geometry parallels are found between this geometry and the previous application of the numerical models. The diameter at which the ball and seat make contact is equivalent to the mean diameter of the O-ring, therefore, the length of contact is determined as the contact diameter between the ball and seat multiplied by pi. Using this definition of the contact length it is possible to describe the load per unit length as shown in Equation 26.

$$P_1 = \frac{F_{SS}}{\pi \cdot D_{MS}}$$

Equation 26 - Load per unit length calculation

From line contact equations of Table 2 and Equation 14 from the O-ring numerical method, we find that there are two half-contact width equations from different sources, substituting the pressure load into these equations gives the following two equations.

$$a = \sqrt{\frac{4 \cdot P_1 \cdot R}{\pi \cdot E^*}}$$

Equation 27 - Pressure load contact half-width (Hertz)

and

$$b = \sqrt[3]{\frac{4 \cdot R_e \cdot F}{\pi \cdot L \cdot E^*}}$$

Equation 28 - Pressure load contact half-width (O-Ring)

Both of these equations for the half-contact width were evaluated for the pressure loads applied to the model and compared to the results, as shown in Appendix 1, the outcome of this is that Equation 28 produced the half-contact width that is the closest match to the results from the numerical model of the actual geometry, therefore subsequently in this thesis the half-contact width, 'a', shall refer to Equation 28.

When the pressure load is then applied to the maximum contact pressure equation it gives the following.

$$p_0 = \frac{2 \cdot P_1}{\pi \cdot a} = \sqrt{\frac{P_1 \cdot E^*}{\pi \cdot R}}$$

Equation 29 - Pressure load, max. contact pressure

In these equations the following definitions apply.

R – ball radius (mm)

E* - Equivalent seat material modulus (N.mm⁻²)

$$E^* = \frac{1 - \nu^2}{E}$$

Equation 30 - Single material reduced modulus

To compare the theoretical values to the results that are to be gained from the computational models the contact-pressure across the contact width will have to be reported as the mean contact pressure, this can be achieved by re-arranging Equation 12 to be in terms of the mean contact pressure rather than the maximum contact pressure; re-arranging Equation 12 gives Equation 31.

$$p_m = \frac{2 \cdot \pi \cdot P_1}{4 \cdot \pi \cdot a}$$

Equation 31 -Mean stress equation

This simplifies to:

$$p_m = \frac{P_1}{2 \cdot a}$$

Equation 32 - Simplified mean stress equation

From the range of pressures applied to the valve, as shown on page 84, and the geometry of the valve components, as defined in Figure 31 and Figure 32. The pressure loads applied to the valve can be determined by applying these values to Equation 23. When applying these loads and geometries to the theoretical model established on page 93 to page 96 of this section a numerical value for the mean contact pressure is found for each of the load cases. The numerical evaluation of each load case by the theoretical model of this section is shown in Appendix 4. Table 7, shows a summary of the results of these calculations.

Pressure Load (lb-f [N])	Mean Contact Pressure (psi [N.mm ⁻²])
400 [1779.3]	544.69 [3.76]
600 [2668.9]	714.03 [4.92]
800 [3558.6]	865.15 [5.96]
1000 [4448.2]	1004.11 [6.92]
1200 [5337.9]	1133.44 [7.81]
1400 [6227.5]	1256.03 [8.66]
1600 [7117.2]	1373.33 [9.47]

Table 7 - Theoretical contact pressures from the applied pressure load

The results shown in Table 7 show for each increase in load the mean contact pressure increases as well. For every percentage increase in the load applied there is an average increase of 93% in the mean contact pressure. The numerical values determined and presented in Table 7 will allow for the theoretical model from which these values were calculated to be validated. In validating the theoretical model the assumptions which were applied to the existing theories to make them applicable to the floating ball valve seat geometry can be evaluated.

This section developed a mechanistic theoretical model which links loads applied to the floating ball valve from pressure to the contact pressure developed in the seat component. The applied theoretical model was developed through the application of basic modelling techniques to break down the axial load into the component acting on the seat face in sealing. Following the derivation of the load acting on the seat in sealing the application of contact mechanics allow for the contact pressure in the seat component to be determined. By creating the theoretical model previously detailed there is a method which describes the mechanics through which an applied pressure creates a contact pressure in the seat face contacting the ball. The theoretical model links the pressure applied to the valve (input) to the mean contact pressure in the seat component (output). The establishment of this relationship is a key step in achieving an understanding the mechanics of the floating ball valve seat components.

4.2 Seat deflection theoretical mechanistic model development

This section contains the establishment of a theoretical model which defines the mechanics of the floating ball valve seat. The theoretical model relates the load applied to the seat component to the deflection of the seat component.

The load applied to the seat component is assumed to be acting in the axial direction of the seat component, therefore the method of breaking the load into sealing stress and shear stress components shall be applied to this model in accordance with the method from the previous section. In developing the theoretical model, it is assumed that all of the load applied to the ball is transmitted to the seat component. Initially the load is applied to the ball in the same manner as with the contact pressure model, therefore, the same model for the application of the load to the seat shall be used to determine the load acting on the seat component and causing it to deflect.

From looking at the geometry of the seat component being used in this thesis, as shown in 3.1.3, the seat can be described as an annular ring, set at an angle perpendicular to the load applied to it, creating the conical geometry shown. From defining the seat as an annular ring, the support of the internal and external edges of the ring will need to be considered so that a suitable theoretical model can be selected.

There are a number of variations on the theoretical model of an annular ring with both the internal and external edges supported. The variations of the theoretical model are typically in respect to the type of support the edges are provided with, whether the edge is fixed, simply supported or guided. Each of the edge conditions constrain the edge of the annular ring in a different way, these constraints effect the response of the ring to the load applied to it in different ways. The most appropriate theoretical models are discussed in the next part of this section, each of these models are taken from Roark's Formulas for Stress and Strain, the theories taken from this literature source have been long established and known for producing theoretically sound results when applied to the situation in the correct manner.

The first theoretical model applied is taken from table 11.2, case 1c, in this model the outer and inner diameter of the disc being assessed are considered to be simply supported, the simply supported constraint applied to the edges allows rotation from the point of support but does not allow any translation of the disc at the point of the support.



Figure 44 - Roark's theory of stress and strain, Table 11.2, Case 1c diagram

Figure 44 shows the location of the load applied is defined in the radial direction as variable, r_0 . The load applied to the annular ring is defined as ' w ', this is in the units of the load per unit length. Not shown in Figure 44 is the dimensions of the annular ring, the internal radius is defined as ' b ' with the external radius defined as ' b ' in these calculations.

By applying the table 11.2, case 1c model to the geometry of the floating ball valve seat it assumes that the internal and external diameters of the seat components are the locations where the seat pivots and the onset of bending in the seat component is located. Depending on the diameters of the seat component which are used to describe it this may be a valid model to use; should the locations at which the seat is supported but also pivots be chosen it is expected that the use of this model would accurately reflect the behaviour of the seat with regards to its deflection when a known load is applied to it. The point at which the seat pivots would be that where the seat is supported on one side of the chosen diameter and unsupported on the other side.

The second theoretical model applied is Table 11.2, case 1d. The model from Table 11.2, case 1d is formed from a combination of a simply support outer diameter with a fixed inner diameter; the inner diameter being fixed does not allow any rotation of the disc at the inner edge. Due to the change of the internal diameter of the annular ring from a simply supported edge to a fixed edge, the reaction of the disc to the load is shown in Figure 45.

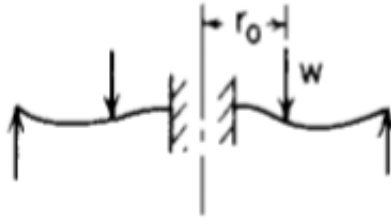


Figure 45 - Roark's theory of stress and strain, Table 11.2, Case 1d, diagram

The definitions of the variables shown and related to the annular ring theoretical model shown in Figure 45 are the same as those which describe Figure 44. With the internal diameter being fixed the internal diameter of the seat component does not pivot; the internal diameter is fixed and deflects by the ring bending at a location outside the inside diameter. In applying this model to the geometry of the floating ball valve seat there is a measure of uncertainty in the application of the fixed constraint to the internal diameter and the specific diameter of the geometry that this model describes accurately.

The final case the seat was evaluated using is case 1h, in this case both the inner and outer edges of the disc were constrained by fixed constraints. As can be seen from the below figure this removes completely the bending moments from both edges of the annual ring.

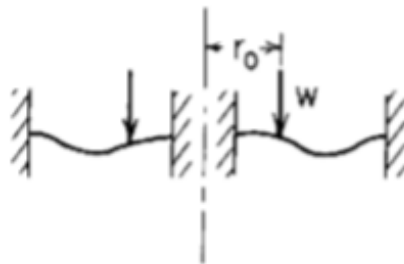


Figure 46 - Roark's theory of stress and strain, Table 11.2, Case 1h diagram

The variables shown in Figure 46 are defined in the same manner as those in Figure 44. With both the internal and external edges of the annular ring being fixed neither of the edges defined in this model have the ability to pivot and therefore allow the ring to rotate at its edges. As with the fixed edge in the previous model it is difficult to place the location of these edges with respect to the dimensions of the model of the seat component.

Of the three theoretical models presented on page 98 and page99 of this section the theoretical model which will be most applicable to apply to the seat geometry shown in Figure 31 is that of table 11.2, case 1c. The ability to identify the point at which the seat will pivot will allow for the matching of the theoretical model to the dimensions of the seat component to be completed successfully. The deflection of the seat component and bending shown by the table 11.2, case 1c model match that which is expected to occur with the seat at the pivot point of the annular ring of the seat component.

With the theoretical model identified the dimensions of the floating ball valve seat need to be determined in a manner which enables them to satisfy the conditions that are part of the table 11.2, case 1c model. The dimensions of the seat that will be considered for the theoretical deflection calculation shall have the dimensions defined in accordance with the following definitions.

- a – outer radius
- b – inner radius

These definitions are only applicable to the use of 'a' and 'b' in the equations for Roarks theories of stress and strain. 'a' and 'b' are defined based on the distance from the contact point D_{MS} of the seat to the extremities of the flexible area of the seat as shown in Figure 47. This is due to the load being considered as acting perpendicular to the seat surface where it contacts the ball.

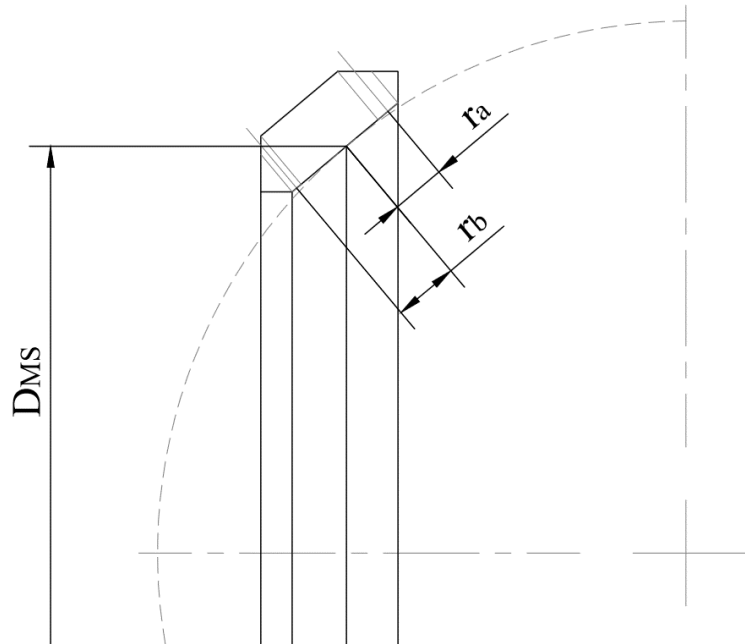


Figure 47 - Radial Seat Distance Definitions

Figure 47 shows the radial distances, 'ra' and 'rb', as being defined as the mean material condition, the lines inside the lines dimensioned represent the minimum material condition whereas the lines outside represent the maximum material condition, all these conditions shall be determined and evaluated. The method of determining the magnitude of 'a' and 'b' is shown in the following equations.

$$a = \frac{D_{MS}}{2} + r_a$$

Equation 33 - Outer seat radius

$$b = \frac{D_{MS}}{2} - r_b$$

Equation 34 - Inner seat radius

In addition to this the radius at which the load is applied at is given by:

$$r_0 = \frac{D_{MS}}{2}$$

Equation 35 - Seat load radial location

Based of measurements from the seat and ball components assembled as shown in Figure 32 and Figure 47 the dimensions for 'r_a' and 'r_b' in the various conditions are shown in the following table, Table 8.

Material Condition	Outer Radial length, 'r _a ' (mm)	Inner Radial Length, 'r _b ' (mm)	Seat Load Radius 'r ₀ ' (mm)
Maximum	5.48	5.53	-
Minimum	3.41	4.59	-
Average	4.45	5.06	
Actual	-	-	32.23

Table 8 - Theoretical seat material radial lengths

Applying these values to Equation 33 and Equation 34 gives following dimensions which have been be evaluated to describe the possible applicable theoretical material conditions for the seat component. The dimensions for the inner and outer radii of the annular ring are shown in Table 9.

Material Condition	Outer Radius, 'a' (mm)	Inner Radius, 'b' (mm)
Maximum	37.71	27.64
Minimum	35.64	26.7
Average	36.68	27.17

Table 9 - Theoretical radial seat dimensions

Based on the definitions applicable to the edge conditions in the theoretical model, and when reviewing the location of the material conditions shown in Figure 47 the minimum material condition is seen to be most appropriate material condition to use in the evaluation of the seat. The minimum material condition locates the edge of the material at the locations where the material outside the radial dimension is fully supported and the material within the radial dimension is completely unsupported. The support applied to the seat component in these locations identify these points as the pivot points of the seat when it is subject to bending.

The results of evaluating the annular ring in accordance with table 11.2, case 1c under the stated loads for the applicable material condition is shown in the Table 10.

Pressure Load (lb-f [N])	Min. Material Condition Deflection (in [mm])
400 [1779.3]	0.004 [0.10]
600 [2668.9]	0.007 [0.18]
800 [3558.6]	0.009 [0.23]
1000 [4448.2]	0.011 [0.28]
1200 [5337.9]	0.013 [0.33]
1400 [6227.5]	0.015 [0.38]
1600 [7117.2]	0.017 [0.43]

Table 10 - Roark's theory of stress and strain Table 11.2, Case 1c, deflection results

In Table 10 the results of evaluating the deflection of the seat component for each of the loads applied are shown. The results show that where the load applied increases the deflection of the seat component also increases. When the results are analysed it is found that for every percentage increase in load applied the deflection increases on average by the same percentage increase.

The section has developed a theoretical model that links the applied load (input) to the deflection of the seat itself (output). The applied theoretical models have been assessed with regards to their applicability to the geometry of the floating ball valve seat. The dimensions of the seat component have been evaluated to ensure the dimensions used in the theoretical model satisfy the requirements of the theoretical model as well as the expected mechanics of the components. As with the previous section the applied load has been broken down the axial load into components. The load component acting perpendicular to the seat face has been used as the load which is bending the annular ring defined by the seat. The theoretical model developed has been evaluated using the input of the loads as defined to be applied to the computational model to create outputs which are deflections of the seat component. The theoretical model defined in this section adequately describes the mechanics of the seat with regards to its deflection when a load is applied to it. By evaluating the deflection of the seat numerically it makes it possible to validate the theoretical model with either computational models or physical testing.

4.3 Bending stress theoretical mechanistic model development

This section contains the establishment of an applied theoretical model which relates the load applied to seat component to the bending stresses these loads generate in the seat component. The theoretical model will be established through the application of established theoretical models to the geometry of the floating ball valve.

In establishing the applied model, it is assumed that the full load acting on the ball is transferred to the seat. The load acting on the seat to bend it is a component of the total load acting on the ball which is perpendicular to the seat-face. As with the previous section, where the component of the total load was applied to the seat to determine the magnitude of the bending the same load is used to determine the bending stress within the seat itself.

The deflection of the seat has been determined by an adaption of Roark's theory of stress and strain, table 11.2, case 1c at the minimum material condition. The bending stress is related to the bending of the component, the greater the bending of the annular ring the greater the bending stresses in the annular ring will be. As the same conditions are present in the annular ring when determining the bending as are present when determining the bending stress it is a logical extension to use the bending stress model from Roark's theories of stress and strain, table 11.2, case 1c to evaluate the bending stress present in the seat component.

The following section contains the results of a set of theoretical calculations which are appropriate to determining the bending stress within the seat component. By applying the stress calculation from Roark's theory of stress and strain, table 11.2, case 1c the tangential and radial stresses shown in the following table are obtained.

Pressure Load (lb-f [N])	Radial Stress, S_r (psi [N.mm ⁻²])	Tangential Stress, S_t (psi [N.mm ⁻²])
400 [1779.3]	545.94 [3.76]	260.82 [1.80]
600 [2668.9]	818.43 [5.64]	390.99 [2.70]
800 [3558.6]	1091.89 [7.53]	521.63 [3.60]
1000 [4448.2]	1364.37 [9.41]	651.81 [4.49]
1200 [5337.9]	1637.83 [11.29]	782.45 [5.39]
1400 [6227.5]	1910.32 [13.17]	912.63 [6.29]
1600 [7117.2]	2182.80 [15.05]	1042.80 [7.19]

Table 11 - Radial and tangential stresses from Table11.2, Case 1c

The tangential and radial stresses are principal stresses and as such these stresses cannot be used on the own as individually they do not provide a full picture of the stresses within the seat component. The two principal stresses determined from the application of Roark's theories of stress and strain, table 11.2, case 1c theoretical model to the floating ball valve seat will need to be combined into an equivalent or von mises stress. The two principal stresses are combined into an equivalent stress by the use of Equation 36.

$$\sigma_v = \sqrt{\sigma_1^2 - \sigma_1\sigma_2 + \sigma_2^2}$$

Equation 36 – Equivalent Stress Calculation

The use of the Equivalent or Von Mises Stress allows for both of the principal stresses to be combined into a single equivalent stress that represents the total stresses the component is subject to. When applying Equation 36 to the principal stresses shown in Table 11 the results shown in Table 12 are found.

Pressure Load (lb-f [N])	Von Mises Stress, S_v (psi [N.mm ⁻²])
400 [1779.3]	472.95 [3.26]
600 [2668.9]	709.02 [4.89]
800 [3558.6]	945.92 [6.52]
1000 [4448.2]	1181.97 [8.15]
1200 [5337.9]	1418.87 [9.78]
1400 [6227.5]	1654.93 [11.41]
1600 [7117.2]	1890.99 [13.04]

Table 12 - Von Mises Bending Stress

As expected, and in-line with the deflections of the seat the Von Mises Stress increases where the magnitude of the applied load increases. The results show that the percentage increases in load are reflected in the percentage increases on Von Mises Stresses, again this matches the trends identified with the deflection of the seat being analysed.

This section has applied a theoretical model to the geometry being assessed to determine the bending stress within the seat component. The applied theoretical model is the corresponding model for bending stress to that used in the previous section for deflection. The constraints applied to the model reflect the limits of the seat where the pivot points of the seat component will be located; the edge conditions of the theoretical model used are representative of the pivot points of an annular ring. Again, the same application of geometric rules to the axial load applied to the ball to break the total load down into the component acting on the seat to cause the bending stresses. The theoretical model developed uses the input of the loads which shall be applied to the computational model and generates outputs of bending stresses of the seat component.

4.4 Conclusions

The aim of this chapter was to develop a set of theoretical models which describe the mechanics of the floating ball valve seat. The mechanics of the floating ball valve seat that required understanding as identified as the relationship between the contact pressure between the ball and seat and the pressure-based load applied to the valve, the mechanics describing the deflection of the seat component based on the load applied to it and the bending stresses generated in the seat by a load applied to it. Each of these mechanistic models have been described in a numerical manner by the application of theoretical models to the geometry of the ball and seat components.

The model established linking the pressure-load applied to the valve to the contact pressure between the ball and seat has a number of assumptions in it. The initial assumption made is

the basic use of numerical methods to derive the pressure-load, this is described as the area bound by the mean contact diameter multiplied by the pressure in the valve. The pressure-load assumes there are no pressure losses in compressing the seat and there is no pressure on the other side of the seat. The assumptions made in defining the pressure-load are considered to be of sound theoretical value. The pressure load was assumed to be acting down the axial direction of the valve, this assumption was made as pressure acts perpendicular to the surface it is acting on, in theory the area bound is perpendicular to the direction at which the pressure is acting. The direction the pressure-load is acting in is based on fundamental mechanics and is also considered as a safe assumption to make. The reduction in the axial load to the load acting perpendicular to the load acting on the seat face is an assumption based on the function of the load when acting at different orientations to the seat-face of the seat component, this assumption is considered theoretically sound however it may be an area of weakness and may need exploring when validating the theory. The application of the cylindrical-to-flat plane contact mechanics is based on the similar sources in the literature review; the seats are described as having an axisymmetric stress profile, therefore by un-revolving the floating ball valve geometry about the seat axis, the geometry becomes equivalent to that of the cylinder-to-flat plane geometry therefore making the contact model applicable to this application. The adaption and application of the contact mechanics may be an area of issue as there is limited information on the application of this theory to an axisymmetric problem. In addition to the limitations of information available the adaption of an axisymmetric problem to a non-axisymmetric model may have not considered the effects of the axisymmetric model which are not present in the cylinder-to-flat plane model. In applying the Hertz contact model to the interaction between the ball and seat components the effects of friction on the solution have not been considered. The Hertz contact theories consider both bodies to be smooth and frictionless, while this is an omission from the model there is prior work which justifies the use of this theory in describing the contact between two similar bodies in contact. This model achieves the objective of describing the contact pressure in the seat component in terms of the load applied, however the areas where assumptions have been made that are not proven to be justified by prior work, these assumptions will require validating for this model to be acceptable and used to numerically describe this relationship.

The aim of the second section was to create a theoretical model which describes the deflection of the seat component in terms of the load applied to it. In establishing this theoretical model, a selection of established numerical models have been assessed against the geometry of the seat component being evaluated. The evaluation of the applicable models and seat component material conditions used is considered to be appropriate to the application of describing the seat component accurately. By evaluating the theoretical models and the applicability of the theoretical models to describing the bending of the seat component it is possible to use a number of the elements from the work completed in the previous section to establish a theoretical model which relates the load applied to the deflection of the seat component.

The aim of the final section was to define the theoretical model which relates the load applied to the seat component to the bending stresses in the seat component. To establish this theoretical model the equivalent model to that used to describe the deflection of the seat was applied. In applying this model the same assumptions that are made in determining the deflection of the seat are made in determining the related bending stresses. While the application of the load to the seat is still in-line with the method used in the first section of this chapter and therefore subject to the assumptions made about that subject area. The theoretical model describing the bending stress in the seat component has been developed using a well established theoretical model and basic modelling techniques, therefore it is considered that the results from this model will be sufficiently accurate to describe the bending stresses within the seat component.

While all of the theoretical models have been established using appropriate and applicable assumptions to apply established theoretical models to the function floating ball valve seat these assumptions are not proven in published works and will need to be validated. By validating the theoretical models the assumptions made can be proven or where the results differ the assumptions can be modified to make the theoretical models a more accurate description of the mechanics of the floating ball valve seat.

This chapter achieves the aim of establishing mechanistic models for the contact pressure, deflections of the seat component and bending stress within the seat component. Each mechanistic model achieves the objective of relating the load applied to the relevant effect on the seat. The models established in this chapter form the basis from which the understanding of the effect of the load on these functions of the seat component can be described numerically. Once the assumptions made in these models have been validated, the theoretical models can be used to establish a complete theoretical model which describes the floating ball valve seat.

Chapter 5 – Validation of established theoretical models through the use of finite element analysis

In this chapter the theoretical models are validated through the application of finite element analysis to the floating ball valve mechanics defined in the previous chapter. By applying finite element analysis to the mechanics defining the components it is possible to evaluate the assumptions made in establishing the theoretical models and therefore the theoretical models defining the mechanics of the floating ball valve seat.

Through comparing the finite element analyses to the theoretical models of the mechanics the differences in the numerical outputs can be quantified, based on the differences between the models it is possible to refine the theoretical models where applicable. By modifying the theoretical models describing the mechanics of the floating ball valve seat it enables the validated model to accurately describe the mechanics.

From having a set of numerical equations which accurately describe the mechanics of the floating ball valve seat it will be possible to develop these into a design methodology.

5.1 Finite element analysis

In this section the application of finite element analysis to the mechanics of the previous section describing the pressure-load, deflection and bending stresses of the seat component. Through the application of finite element analysis to the behaviour of the floating ball valve seat component it is possible to develop a deeper understanding of the mechanics that are defining this part. By developing a deeper understanding of the governing mechanics in these three areas it shall be possible to either validate or refine the theoretical models describing the mechanics established in the previous chapter.

5.1.1 Pressure-load

This section looks at the mechanics of the seat with the ball subject to the pressure load on its own. This load is defined on page 84 of section 3.1.5 as the load acting on the seat due to the action of the pressure over the area bound by the contact between the ball and the seat; these loads are representative of the range of loads that a manufactured seat may be subject to for factory acceptance testing and in actual service. The outcome of this section is the validation of a mechanistic model that relates the pressure load to the contact pressure developed in the seat component.

5.1.1.1 Analysis Steps

The analysis of this component is conducted in accordance with the method shown in Figure 29. In this analysis the full range of pressure loads shall be applied to the ball, these pressure loads are turned into a load acting on the ball which is applied to the representative ball component in the computational model. The results gained from the analysis of the computational model will be the results of the contact pressure developed in the seat at the point of contact with the ball, in the analysis setup the contact pressure is reported as the Von Mises Stress in Solidworks Simulation. Solidworks Simulation reports the contact stress as a Von Mises Stress along the edge in contact with the corresponding body, therefore to investigate the contact pressure the Von Mises stress on the area in contact needs to be evaluated, these stresses will not produce a visible contour therefore sampling and plotting of the values will be required to demonstrate the exact values of the contact pressure.

5.1.1.2 Results

The results of the finite element analysis of the pressure-load acting on the seat component are taken from the von mises stress plots of the results, shown over the following pages.

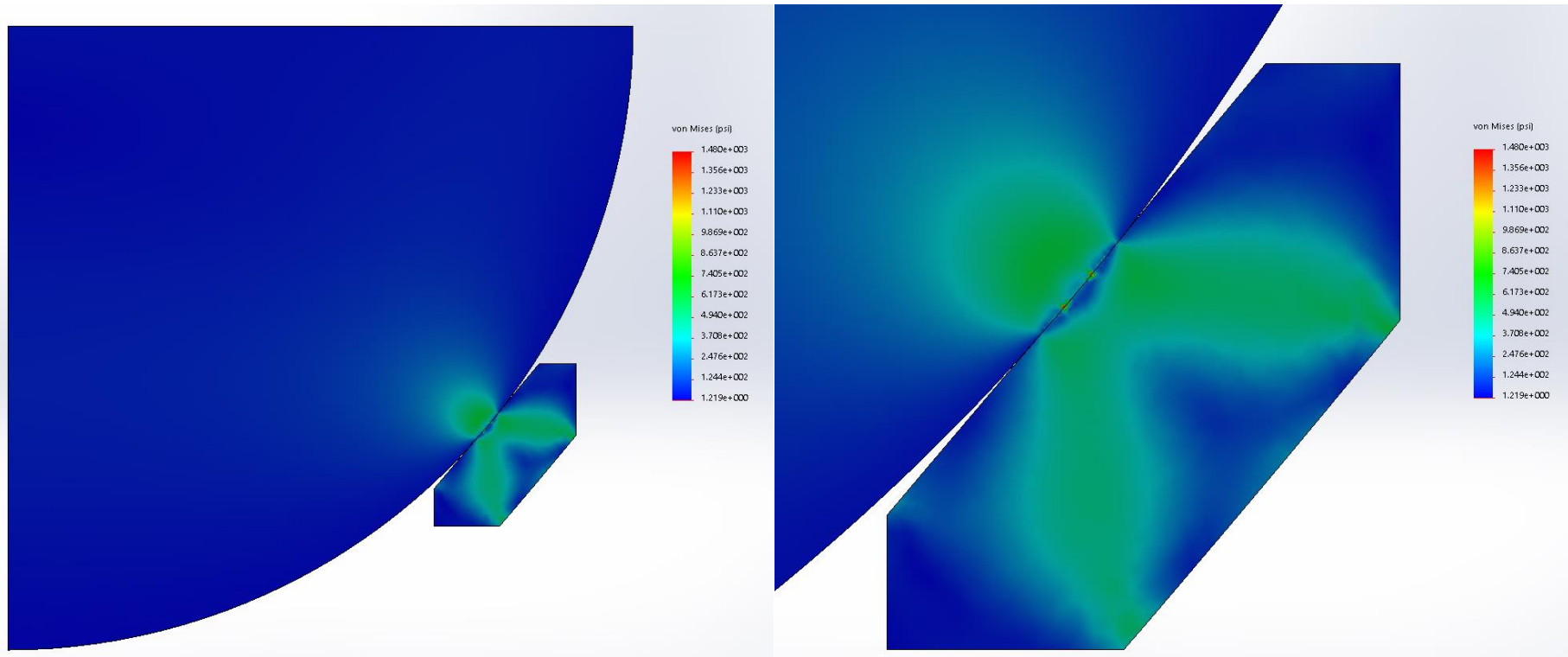


Figure 48 – A plot of the von mises stress from FEA when a 400lb-f (1779.3N) load is applied to the model

Figure 48 shows the stress plot with a 400 lb-f (1779.3N) load applied to the model. The stress field presented by the analysis is of a non-uniform nature. The stress at the point of contact is measured to be 215.10psi (1.48N.mm⁻²), the application of Hertz contact mechanics predicts this to be the greatest stress value. The maximum stress value, excluding anomalous readings, is measured as 257.50psi (1.78N.mm⁻²), this value is measured in the node next to the point of contact between the two bodies at a distance of 0.0008in (0.02mm) from the point of contact. At a distance of 0.02in (0.51mm) from the point of contact the stress value measured in the seat component is 232.10psi (1.60N.mm⁻²), this value is not what is predicted by the application of Hertz contact theory. The 232.10psi (1.60N.mm⁻²) reading amounts to an 8% increase on the stress at the contact point and a 90% reduction from the maximum stress value. The stress profile developed in the ball component it matches the profile predicted by Hertz contact mechanics and shown in Figure 24. There appears to be a similar pressure profile in the seat as shown in the ball but of a much smaller magnitude. The presence of bending stresses within the seat component appears to be the greater magnitude stress and are therefore distorting the stress profile in the seat component.

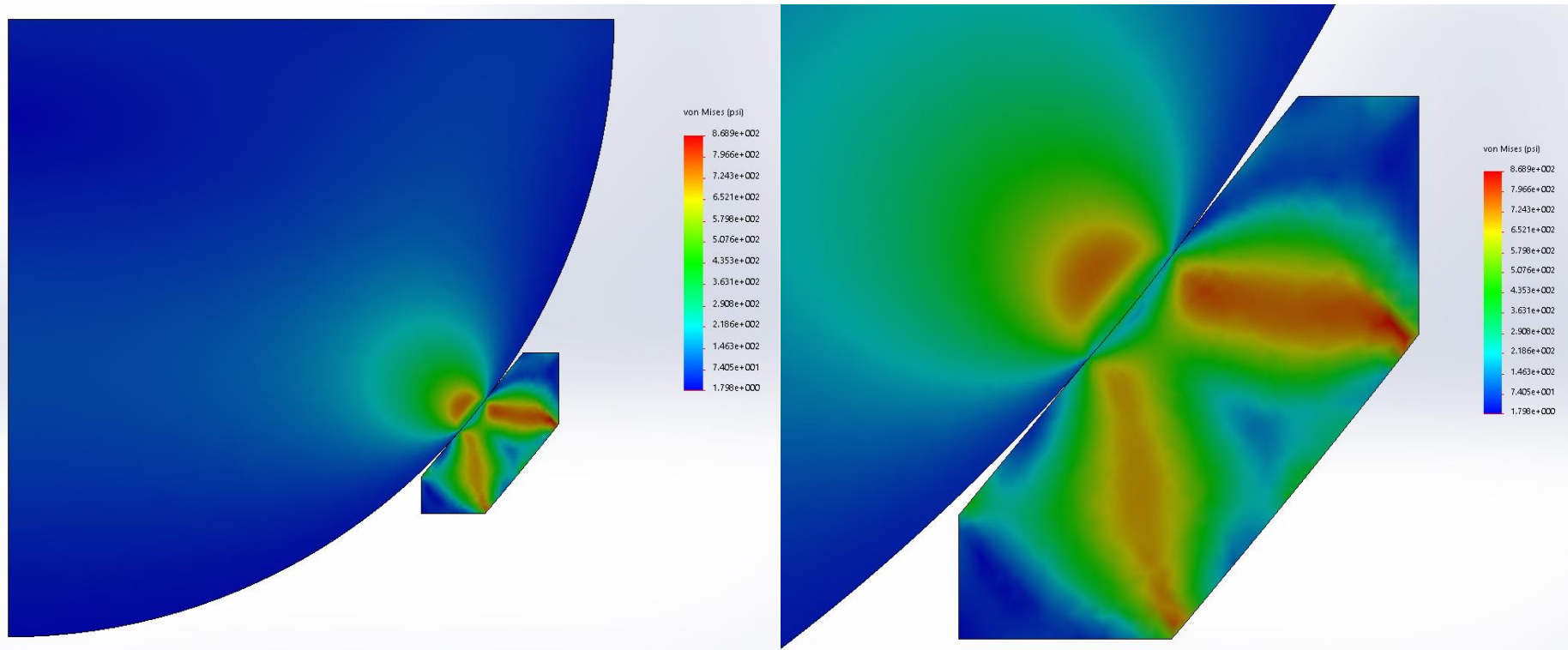


Figure 49 – A plot of the von mises stress from FEA when a 600lb-f (2668.9N) load is applied to the model

Figure 49 shows the stress plot when a load of 600lb-f (2668.9N) is applied to the model. In applying a 600lb-f (2668.9N) load, the load applied to the components has increased by 50%. The stress at the point of contact between the ball and seat is measured as 343.60psi (2.37N.mm⁻²), this is an increase of 60% when compared to the 215.10psi (1.48N.mm⁻²) reading and 33% when compared to the 232.10psi (1.60N.mm⁻²) reading taken from the previous analysis. The increase in the stress value at this point is not equal to the increase in load as the half-contact width will also increase with the load applied increasing the area across which the load is applied. At a distance of 0.02in (0.51mm) from the point of contact the stress value is found to be 298.32psi (2.06N.mm⁻²), this is a 29% increase on the value at the same position in the previous analysis. The increase in the stress at this location correlates with the 33% increase in stress at the point of contact. The stress measured at 0.02in (0.51mm) from the point of contact shows an 87% reduction in stress from the 343.60psi (2.37N.mm⁻²) measured at the point of contact, this compares with a 90% reduction of the corresponding values in the previous analysis, the reduction in stresses when measured from the same points on the stress plots identify a common stress profile along the edge in contact with the ball.

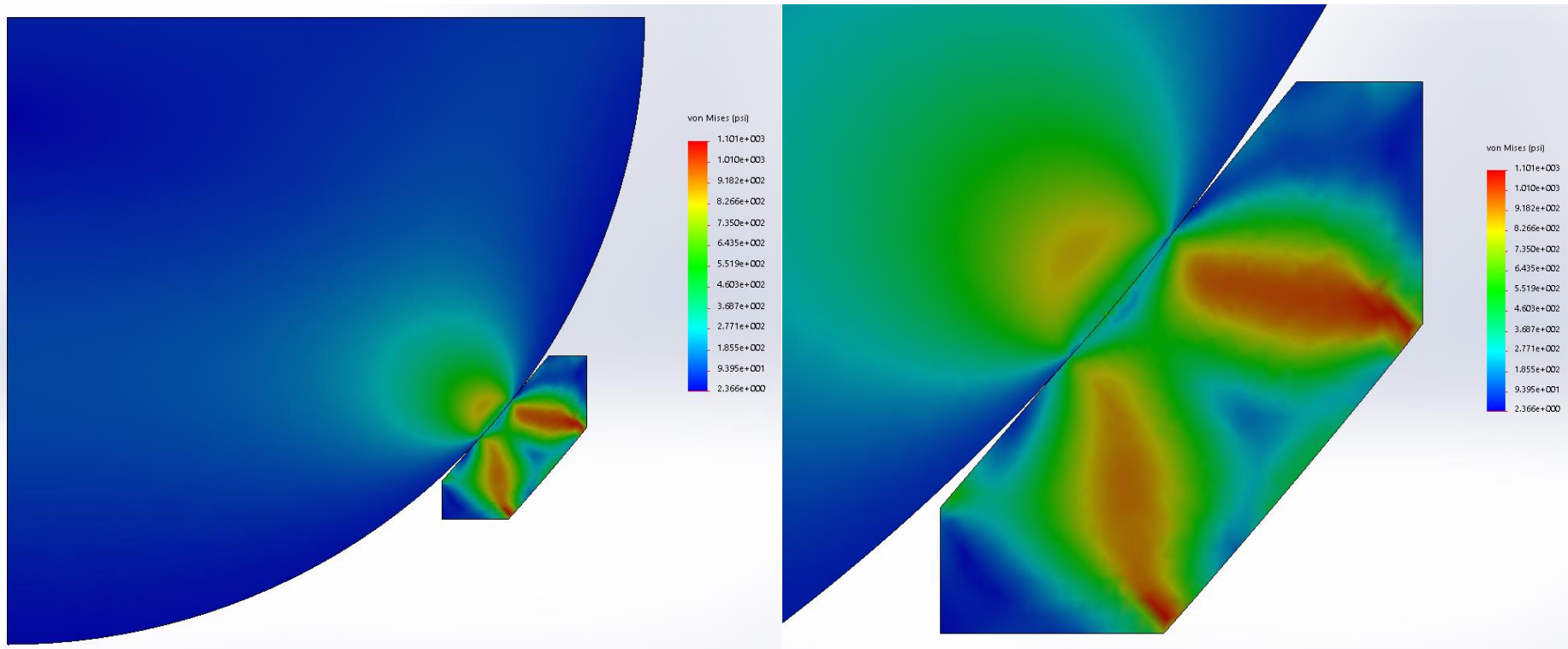


Figure 50 – A plot of the von mises stress from FEA when a 800lb-f (3558.6N) load is applied to the model

Figure 50 shows the stress plot when the load applied to the model is increased further to 800lb-f (3558.6N). The applied load of 800 lb-f (3558.6N) is an increase of 33% on the previously applied 600 lb-f (2668.9N). The stress at the point of contact is measured as being 445.30psi ($3.07\text{N}\cdot\text{mm}^{-2}$) this is a 30% increase on the stress at point of contact in the previous analysis. The stress at a distance of 0.02in (0.51mm) from the point of contact is measured as 389.77psi ($2.69\text{N}\cdot\text{mm}^{-2}$), this is an increase in the stress found at the same point in the previous analysis be by 31%. The increase in the stress at the set distance from the point of contact increases by approximately the same amount as the stress at the point of contact, this demonstrates the relationship across the stress profile is proportional to the applied load. The stress at 0.02in (0.51mm) from the point of contact was found to be 88% of the stress measured at the point of contact. When the relationship between the stress at the distance of 0.02in (0.51mm) from the point of contact and at the point of contact is compared to the same relationship from the previous analysis the percentage was approximately the same, (90% in the previous analysis), this demonstrates the stress profile along the edge in contact is common between the two stress plots.

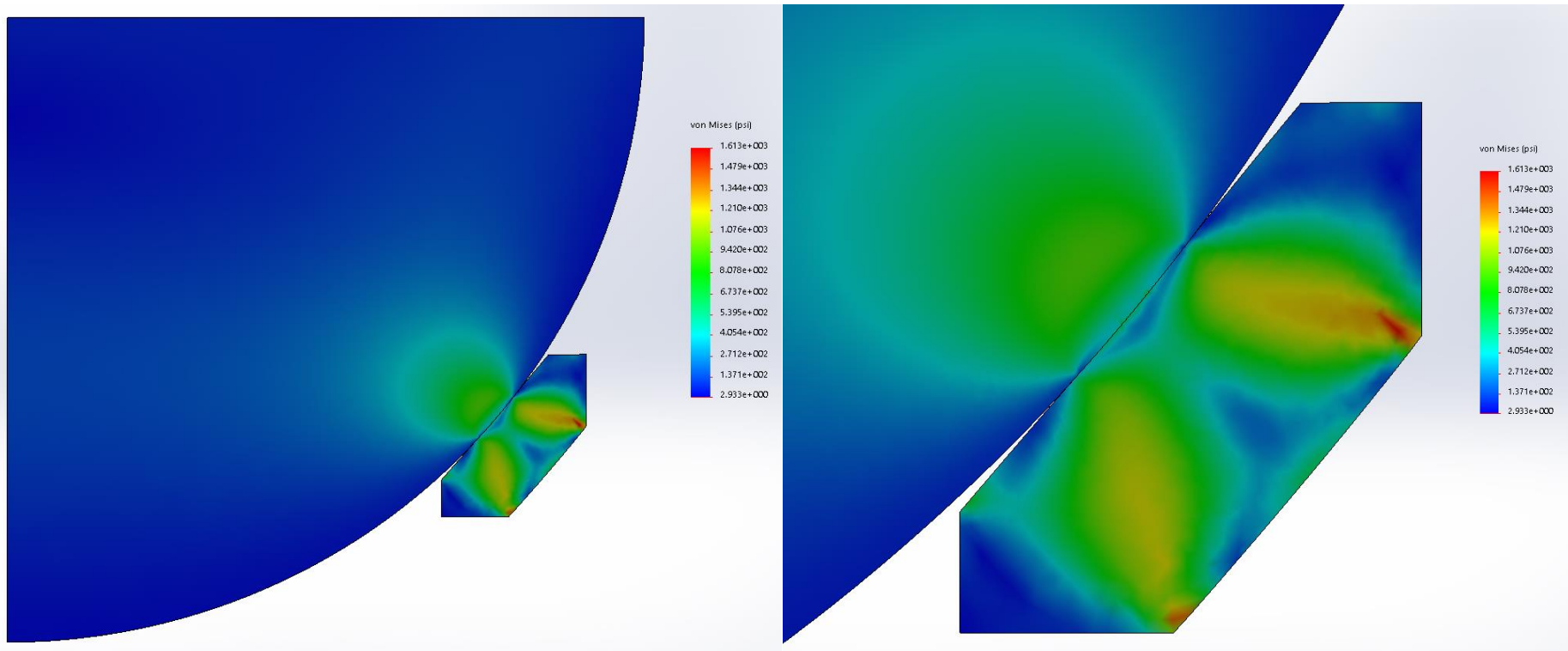


Figure 51 – A plot of the von mises stress from FEA when a load of 1000lb-f (4448.2N) is applied to the model

Figure 51 shows the stress plot when the load of 1000 lb-f (4448.2N) is applied to the model. The application of 1000 lb-f (4448.2N) is an increase in applied load of 25% on the previous analysis. With the increased load applied the stress at the point of contact is found to be 558.40psi ($3.85\text{N}\cdot\text{mm}^{-2}$). The stress at the point of contact is a 25% increase on the stress at the point of contact when the 800 lb-f (3558.6N) load is applied. The increase in the stress being proportional in this stress plot and the previous one show the increase in load resulting in an increase in the half-contact width by the increased load results in the load being spread over a larger area reducing the increase in stress to a proportional figure. At the distance of 0.02in (0.51mm) from the point of contact the stress is found to be 543.97psi ($3.75\text{N}\cdot\text{mm}^{-2}$), this is an increase of 40% on the stress in the same location from the previous analysis. The stress of 543.97psi ($3.75\text{N}\cdot\text{mm}^{-2}$) is also determined as 97% of the stress at the point of contact. These results are of the same order of magnitude as the trend seen previously however the values determined by the stress at this location do not hold true to these trends. An assessment of the entire stress profile with this load applied shall be undertaken to determine whether this result is a slightly spurious result or whether the trends identified do not hold true at this applied load.

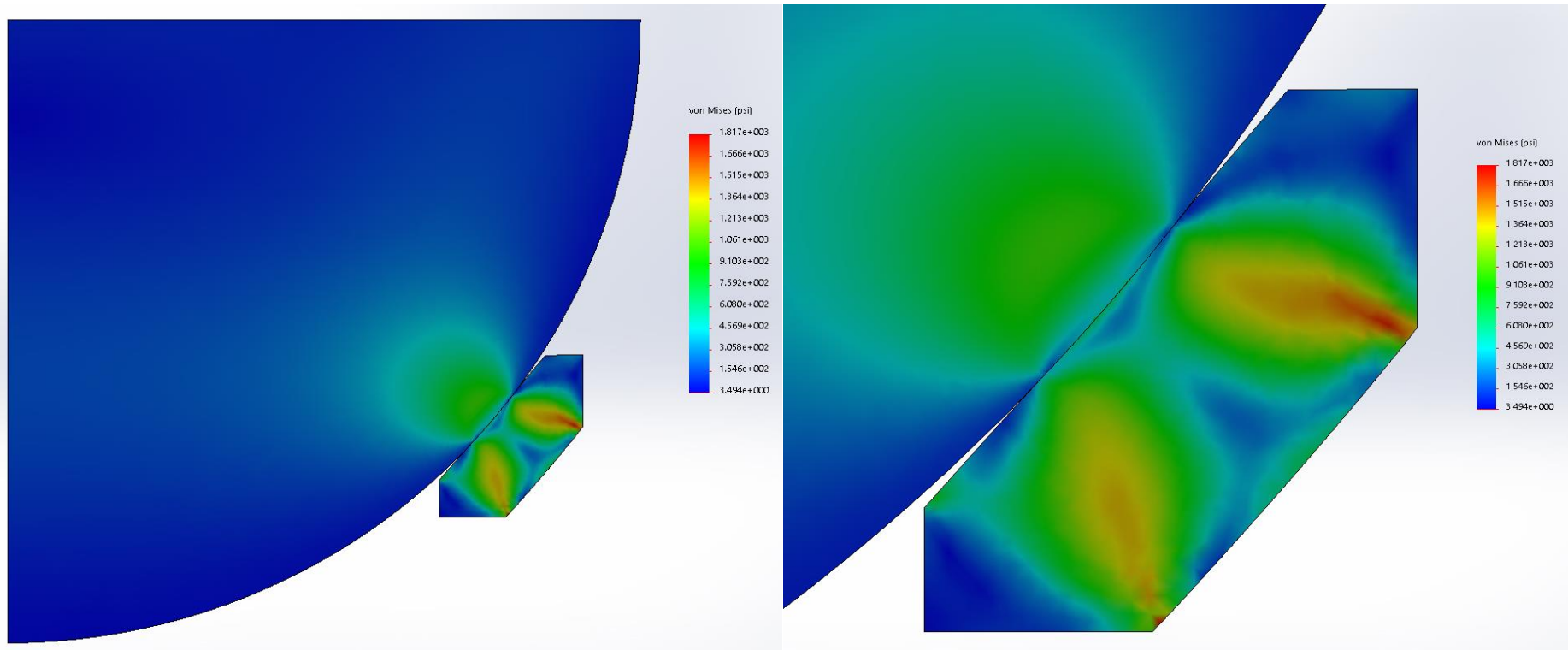


Figure 52 – A plot of the von mises stress from FEA when a load of 1200lb-f (5337.9N) is applied to the model

Figure 53 shows the stress plot obtained from the finite element analysis when the load applied was increased to 1200 lb-f (5337.9N). The load of 1200 lb-f (5337.9N) is an increase of 20% on the load applied in the previous analysis. The stress at the point of contact was found to be 660.20psi ($4.55\text{N}\cdot\text{mm}^{-2}$) with the 1200 lb-f (537.9N) load applied. The stress at the point of contact increased by 18% compared to that of the previous analysis, this is keeping with the established trend that the stress at this location and the increase in load increase at approximately the same rate due to the load determining the contact area as well as the stress. The stress along the contact surface 0.02in (0.51mm) from the point of contact was found to be 516.81psi ($3.56\text{N}\cdot\text{mm}^{-2}$), this stress is 85% of the stress at the point of contact. The relationship between the stress at 0.02in (0.51mm) and that of the stress at the point of contact is approximately the same as all the previous analyses with the exception of the 1000lb-f (4448.2N) analysis. As the previous analysis at the location of 0.02in (0.51mm) from the point of contact has been shown not to fit the trend it was not appropriate to determine the percentage change between these two analyses in this location.

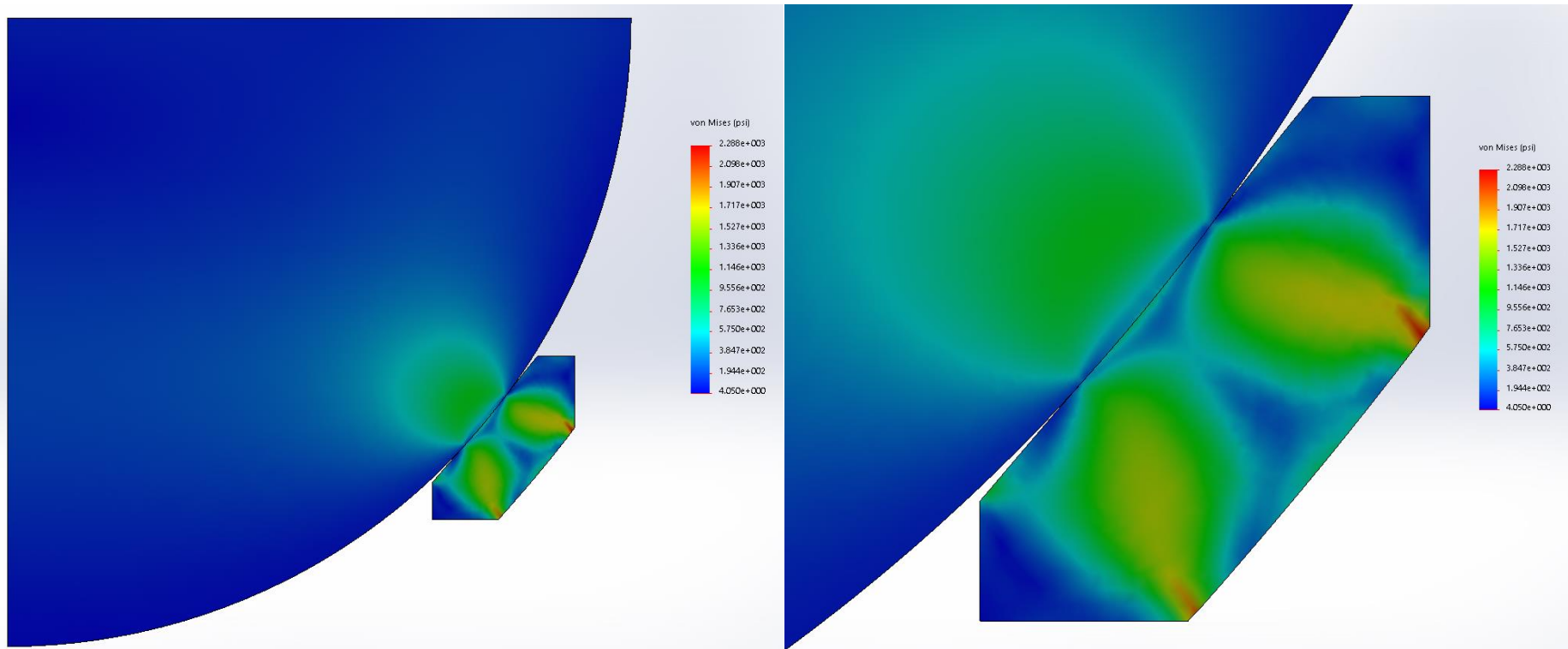


Figure 53 – A plot of the von mises stress from FEA when a load of 1400lb-f (6227.5N) is applied to the model

Figure 53 shows the stress plot when the load applied to the model is increased to 1400 lb-f (6227.5N). The increase in load from the previous analysis is 17% with the load increasing from 1200 lb-f (5337.9N) to 1400 lb-f (6227.6N). The stress at the point of contact was found to be 732.2psi (5.05N.mm⁻²), this is an 11% increase on the same stress from the previous analysis. The stress in the node next to the point of contact, 0.0008in (0.02mm) from the point of contact was found to be 764.30psi (5.27N.mm⁻²), this would be equivalent to an increase of 16% when compared to the stress at the point of contact from the previous analysis. These changes in the stress at this region of the stress plot show the trend of the stress increasing approximately in proportion to the increase in applied load holds true with this load applied to the model. When looking at the stress found 0.02in (0.51mm) from the point of contact it is found to have a value of 651.87psi (4.49N.mm⁻²). the load at the distance of 0.02in (0.51mm) from the point of contact has a value equal to 78% of the stress at the point of contact, this value shows that the general profile of the stress contour along the edge is approximately the same as seen in the previous stress plots. When compared to the previous analysis the stress at this location increases by 26%, this is not in-line with the general trend that all the stresses increase at the same rate and may suggest either there are variations in the values from comparing the values of two nodes and the possible errors from that method or that this trend does not apply to this area of the stress plots.

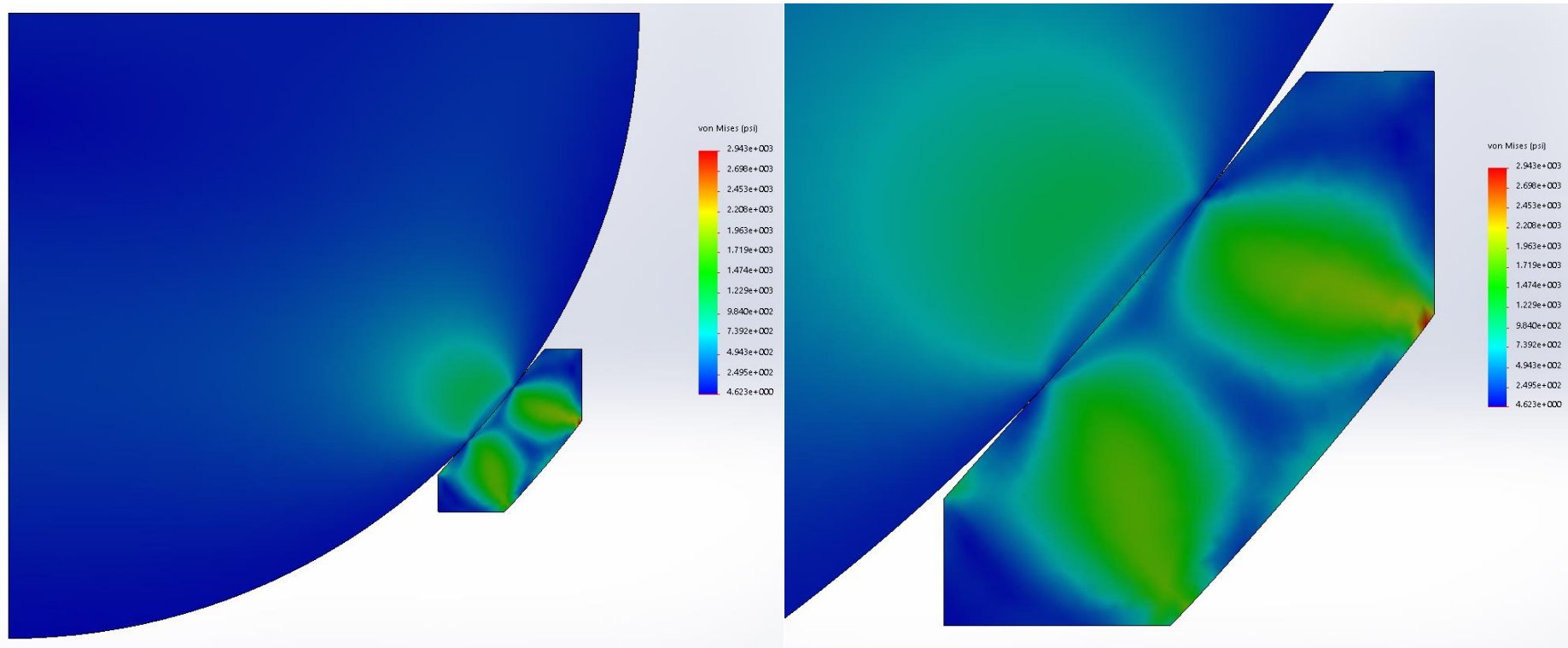


Figure 54 – A plot of the von mises stress from FEA when a load of 1600lb-f (7117.2N) is applied to the model

Figure 54 shows the stress plot obtained from finite element analysis where a load of 1600 lb-f (7117.2N) is applied to the model. The increase in load is found to be an increase of 14% on the load from the previous analysis. The stress at the point of contact was found to be 820.70psi (5.66N.mm⁻²), this is an increase of 12% on the stress at the contact point of the previous stress plot. The increase in stress is again approximately equal to the increase in load applied to the model. The effect increasing the load has on both contact half-width as well as being a component which is divided by the area defined by the contact half-width sees the load increase and stress increase approximately equal in magnitude. The stress at the point 0.02in (0.51mm) from the contact point was measured as 724.40psi (4.99N.mm⁻²), this was found to be equal to 88% of the stress at the contact point. The stress at the location 0.02 (0.51mm) was once again less than that at the point of contact showing a similar stress profile to the previous analyses. The increase in stress at this location compared to the previous analysis is 11% this is approximately equal to the increase in load between this analysis and the previous analysis.

The plots shown in Figure 48 through Figure 54 identify a number of trends supported by the mechanics of the previous chapter. It was identified that the stress found at the point of contact increases by approximately the same amount as the increase in load applied to the model. The equal increase in load and stress is considered to be due to the loads function in determining the contact half-width. As the load increases so too does the contact half-width, when the load is distributed over the area bound by the contact half-width the proportional increase between the two parts of the equation become equal to the magnitude of the increase of the load. The comparison of the stresses at a set distance from the point of contact initially appeared to find a trend with this value being approximately 90% of that at the point of contact. Through the increasing number of plots examined the initial trend did not match the data measured off the stress plots. The analysis between the two points in the stress plot are comparing the values at two nodes to each other, there is the possibility that one or more of the nodal value compared could be subject to errors or be increased or decreased in value by effects which aren't apparent at this point in the analysis of the results presented from the computational models.

The numerical results from the finite element analysis have been taken by sampling the result at the nodes of the split face representing the half-contact width of the contact and taking the average value of these results; the mean average is used to minimise the effect of any spurious results at a specific node. Where values are present that do not fit the trend they shall have a minimal effect on the value of the average stress determined from the stress profile data taken from the stress plots as the number of data point taken from stress plot is sufficiently high. The accuracy of the results is vastly improved by sampling across the nodes included in the entire contact half-width as the number of nodes is greater therefore a few spurious results will have little impact on the overall results gained from the analysis. When determined numerically, the mean average stresses are shown in Table 13 against the pressure load applied.

Pressure Load (lb-f [N])	Average Contact Pressure (psi [N.mm ⁻²])
400 [1779.3]	384.6 [2.65]
600 [2668.9]	326.2 [2.25]
800 [3558.6]	417.6 [2.88]
1000 [4448.2]	517.3 [3.57]
1200 [5337.9]	602.0 [4.15]
1400 [6227.9]	685.7 [4.73]
1600 [7117.2]	748.8 [5.16]

Table 13 – Average contact pressure from stress profile from FEA results (pressure load)

The results presented in Table 13 shows the numerical data extracted from the finite element analyses. This data clearly shows an issue with the data collected when the 400 lb-f (1779.3N) load is applied to the model when compared to the rest of the data extracted. It would be expected that the average contact pressure increases with the increasing load applied. This trend of the stress increasing in line with the load increase was shown in the stress plots, so it is expected that this trend will show itself in this set of data also. Table 14 looks to quantify the change in the variables reported to determine if any of the other data sets show significant variance.

Pressure Load (lb-f [N])	% Increase in Pressure Load	Average Contact Pressure (psi [N.mm ⁻²])	% Change in Average Contact Pressure
400 [1779.3]	-	384.6 [2.65]	-
600 [2668.9]	150	326.2 [2.25]	-85
800 [3558.6]	133	417.6 [2.88]	128
1000 [4448.2]	125	517.3 [3.57]	124
1200 [5337.9]	120	602.0 [4.15]	116
1400 [6227.9]	117	685.7 [4.73]	114
1600 [7117.2]	114	748.8 [5.16]	109

Table 14 - Percentage change in average contact stress from the stress profile of the FEA results

The analysis presented in Table 14 shows the percentage change in the average contact pressure (recorded as Von Mises Stress in FEA), against the increase in the load applied to the model. With the exception of the 400lb-f (1779.3N) results, the remaining results show a trend of increasing loads and increasing contact pressures. The percentage increase in load is shown as being approximately equal to the percentage increase in the average contact pressure. The percentage increase of the increase in load and average contact pressure decreases in the data shown as the load applied to the model increases and the relevant step increase in load becomes a smaller percentage increase. As the effect of the proportion increase in load shows a reducing percentage change in the load applied and the average contact pressure measured the following table, Table 15, shows the percentage change in average contact pressure per percentage change in applied load. The results shown in the table have removed the effects of the magnitude of the load and the average contact pressure from the values presented.

Pressure Load (lb-f [N])	% Increase in Pressure Load	% Change in Average Contact Pressure	% Change in Average Contact Pressure per % Change in Load
400 [1779.3]	-	-	-
600 [2668.9]	150	-85	-57
800 [3558.6]	133	128	96
1000 [4448.2]	125	124	99
1200 [5337.9]	120	116	97
1400 [6227.5]	117	114	97
1600 [7117.2]	114	109	96

Table 15 – Percentage change in average contact pressure per percentage change in load from stress profile FEA results

From Table 15 the exception to the general trend is the change between the 400lb-f (1779.3N) load and the 600lb-f (2668.9N) load, as the change between the 600lb-f (2668.9N) and 800lb-f (3558.6N) load is in accordance with the general trend it points to the average contact pressure for the 400lb-f (1779.3N) load being inconsistent with the remaining values. The identification of the results from the 400lb-f (1779.3N) load being applied being inconsistent with the other results shows this is an area which needs further investigation. From the results with a load of 600lb-f (2668.9N) to 1600lb-f (7117.2N) applied the results show that the percentage increase in load is matched by approximately the same increase in average contact pressure. Based on the assumption that Hertz contact mechanics is the applicable mechanism through which the mechanics of the contact are described, the determination of the contact area is determined by the application of the load and component geometries to an equation to determine the contact half-width. To determine the average contact pressure the load applied is the numerator while the contact half-width is a part of the denominator. The evaluation of these variables is in such a way where there proportional increase can be achieved in a consistent manner. This effect of proportional increase is realistic when the mechanism of the contact are considered, with a greater load acting on the ball component the force applied will create a greater contact area, through the flattening of the two surfaces in contact.

To gain further insights into the exact stress profile along the edge of the seat component in contact with the ball the data extracted from the stress plots are shown in the following figures.

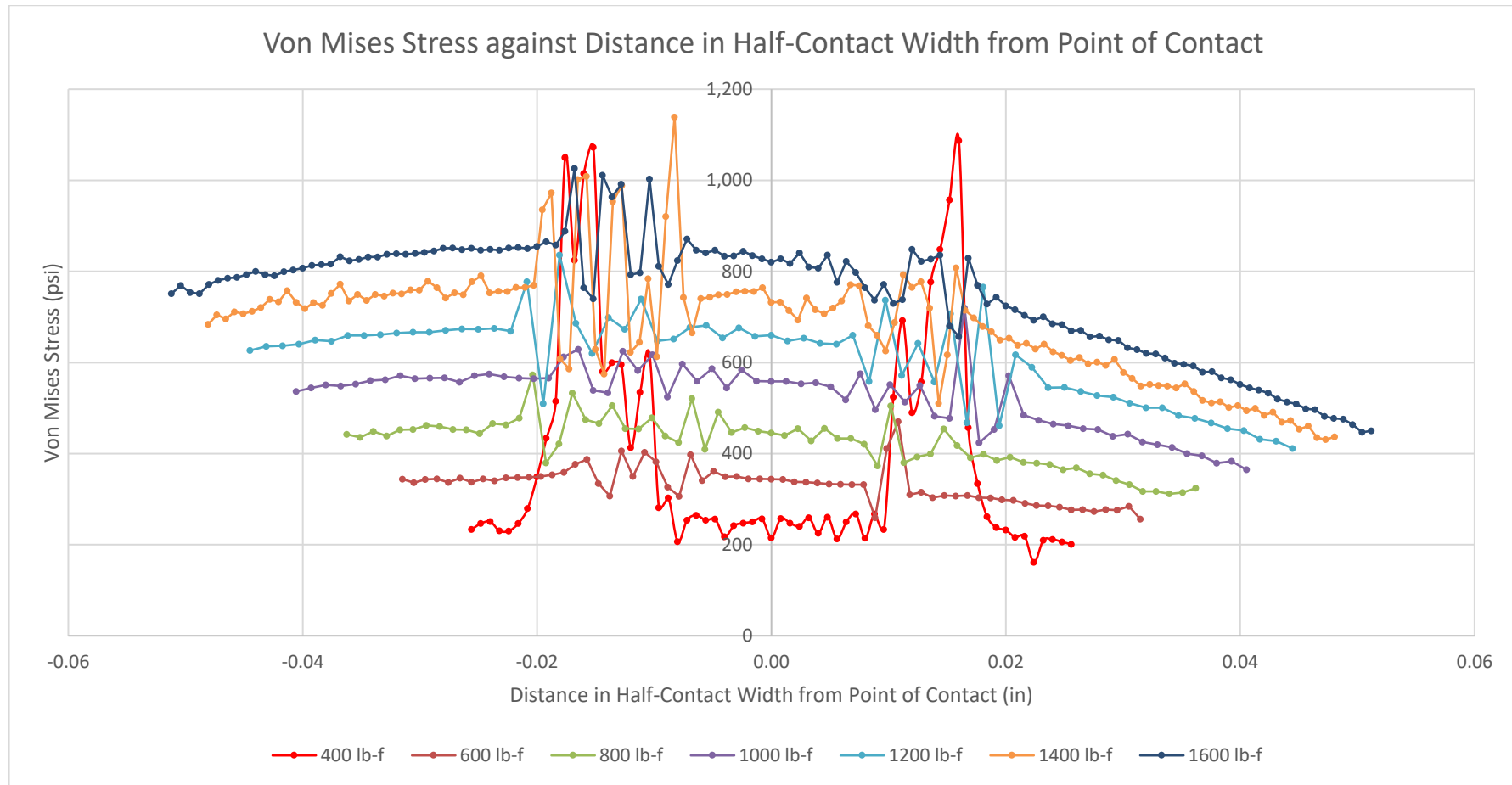


Figure 55 – Contact Pressure against Location of Stress in Half-Contact

Figure 55 shows the plot of the contact pressure (von mises stress) against the distance from the central point of contact, as expected the greater the load acting on the seat the greater the magnitude of the contact pressure is that is created in the seat component. The left hand side of the graph holds a slightly higher stress than the right, this is to be expected as this side represents the internal portion of the seat which will be subject to slightly more load than the external portion of the seat due to the conical nature of the seat profile. It is clear that the 400lb-f (1779.3N) plot has some significant stress discontinuities in it as the profile of the contact pressure plot is not in line with the others in two locations.

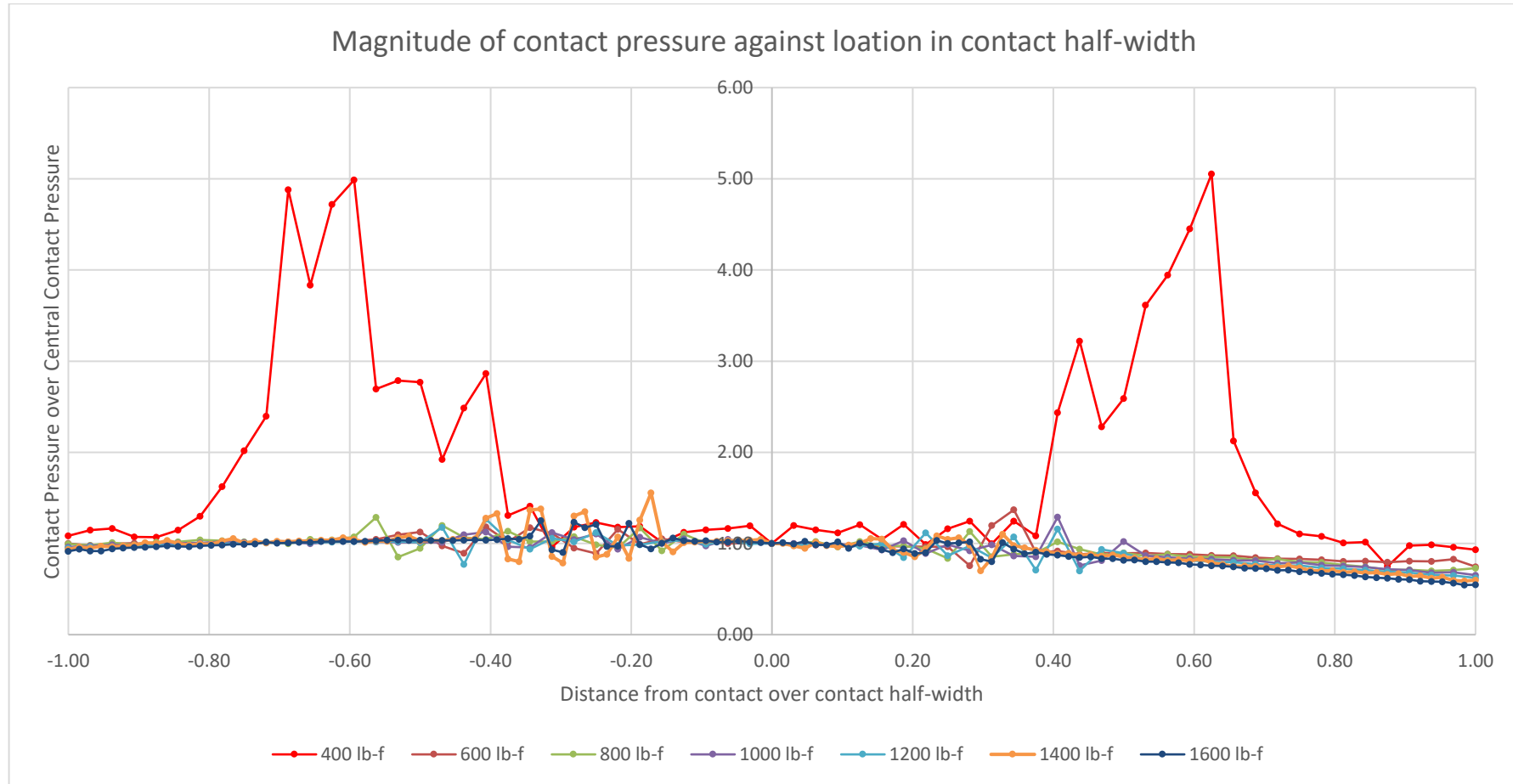


Figure 56 – A plot of the magnitude of contact pressure against location in contact half-width

Figure 56 shows the results recorded for each node as a proportion of the contact pressure at the point of contact against the location of the node as a distance from the point of contact. The ideal outcome of this figure would have been all the plots falling within a small margin from each other; this is the case for all the plots except for the 400lb-f (1779.3N) plot. The similarities in the majority of the plots shows a consistent response of the model to the loadings that were applied this therefore demonstrates that only the 400 lb-f (1779.3N) is influenced by any spurious results. Looking at the 400lb-f (1779.3N) plot in against the other data clearly shows two distinct regions where the results do not fit the trends established by the loadings that are being applied. The loads determined in the previous method section shows the minimum load to be applied to the ball is 440.14 lb-f (1957.8N) therefore the 400 lb-f (1779.3N) simulation shall be re-run at 440 lb-f (1957.2N) to establish whether the results at this load are not influenced by spurious values at the nodes shown.

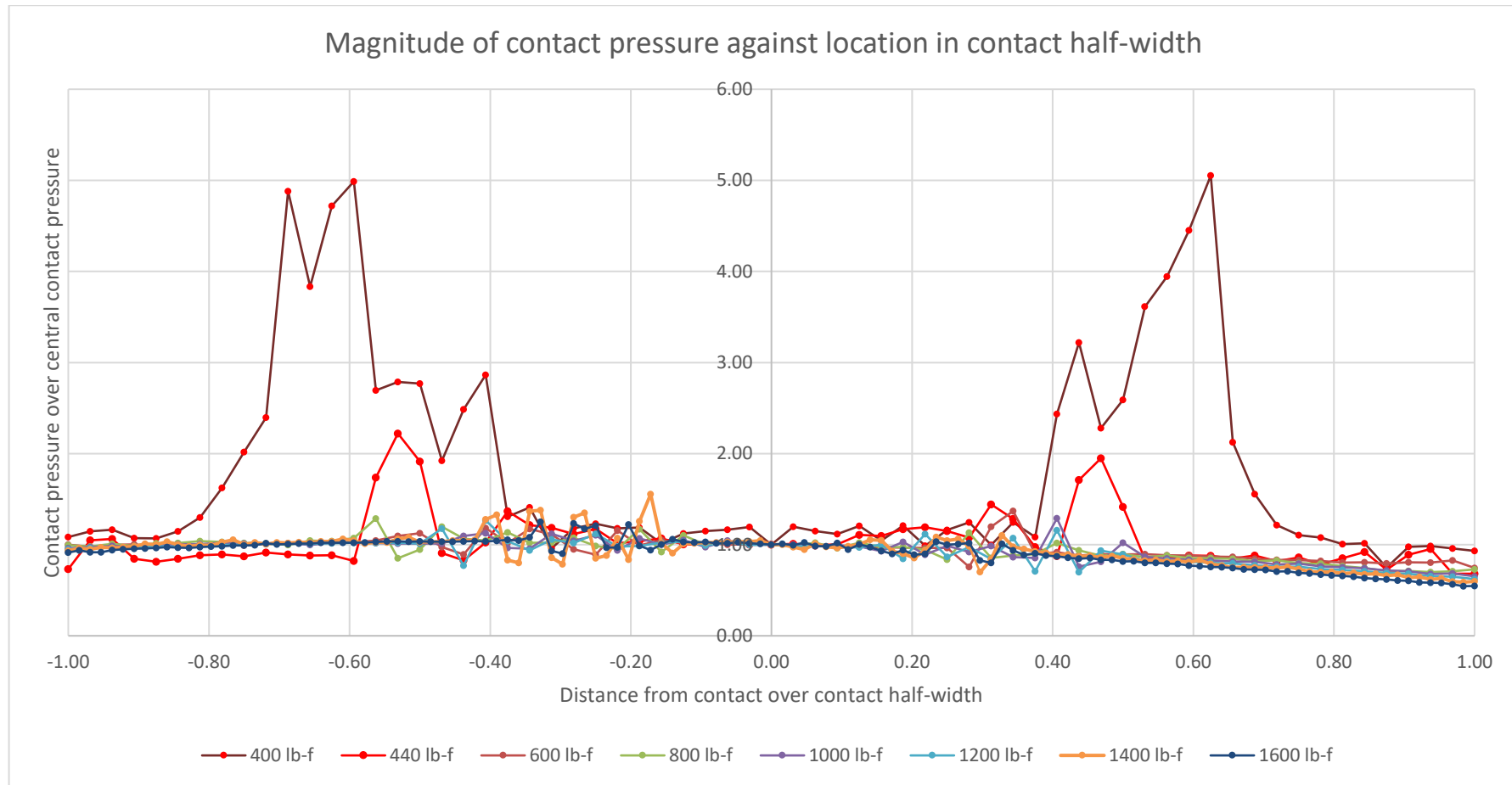


Figure 57 – A plot of the magnitude of contact pressure against location in contact half-width, including 440lb-f (1957.2N) data

Figure 57 shows the plot of the magnitude of the contact pressure against the location in the contact half-width as shown in Figure 56 with the addition of the results from the additional 440lb-f (1957.2N) load included. The two regions identified in Figure 56 where the 400lb-f (1779.3N) plot does not match the trend shown by the other plot are reduced in the 440lb-f (1957.2N) load plot, however, this plot still does not match the trends shown by the plots with greater loads applied. Due to the differences in the stress plots presented, in the preceding figures and the variation shown in the average stresses calculated it is considered that the mechanics governing the response of the seat at these loads may be different from those at the higher loads. This thesis shall only consider the data that follows the identified trend, further work is recommended to determine the exact mechanics through which the loads identified affect the response in the seat component.

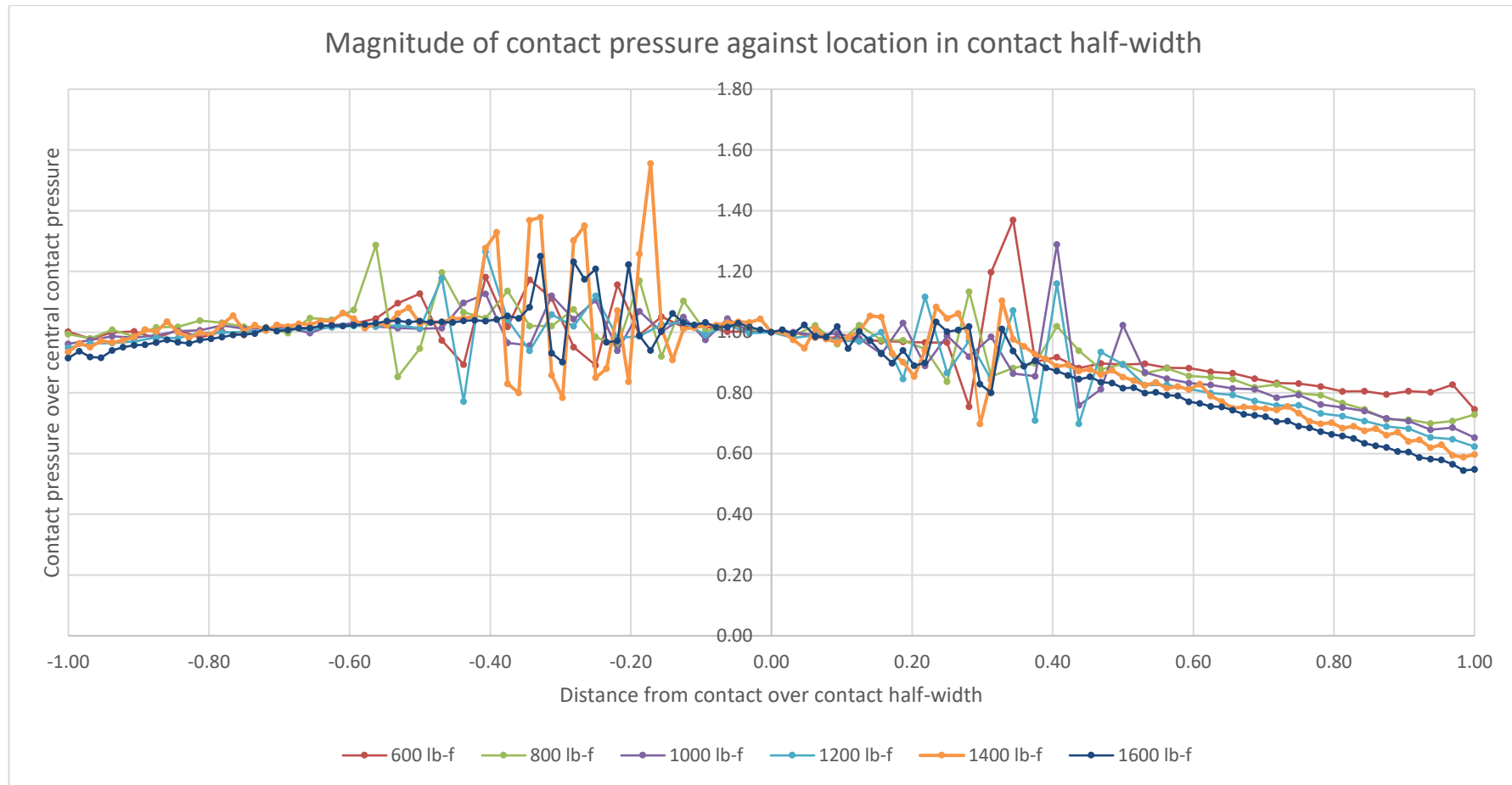


Figure 58 – A plot of the magnitude of contact pressure against location in contact half-width determined from the FEA stress profile

The plot shown in Figure 58 shows the magnitude of the contact pressure against the location of that magnitude in the contact half-width for the loads 600lb-f (2668.9N) through to 1600lb-f (7117.2N). These non-dimensional plots show two locations where there are discontinuities shown in the figure. The discontinuities in the plots are considered to be caused by shear stresses caused by the surface of the ball sliding against the face of the floating ball valve seat. The profiles of the non-dimensional plots show a common trend among the loads assessed, these common trends for the plots shown show that it shall be possible to describe the stress profile numerically by the derivation of a numerical model from the stress profiles shown.

Following the establishment that the applied loads of the magnitude of 600lb-f (2668.9N) through 1600lb-f (7117.2N) give analytical results showing a stress profile of a common trend it is possible to evaluate the numerical data these plots were created from to enable a numerical analysis and comparison with the theoretical model to be made. To ensure the results from the computational models are of the highest possible accuracy and reduce the effect of outliers on the results compared to the theoretical model the mean average contact pressure for the applicable loads shall be determined. The average contact pressures determined from the stress profiles gained from the finite element analyses are presented in Table 16, these results are presented for each of the loads considered.

Pressure Load (lb-f [N])	Average Contact Pressure (psi [N.mm ⁻²])
600 [2668.9]	326.2 [2.25]
800 [3558.6]	417.6 [2.88]
1000 [4448.2]	517.3 [3.57]
1200 [5337.9]	602.0 [4.15]
1400 [6227.5]	685.7 [4.73]
1600 [7117.2]	748.8 [5.16]

Table 16 – Table of average contact pressures determined from contact stress profile FEA results

The data presented in Table 16 shows the average contact pressures for each of the loads applied to the model. While these results show that the average contact pressure increases when the load applied to the model increases there is no way of determining whether this increase follows a trend as shown previous in the plots and to what degree these values follow this trend. By determining the percentage change in applied load and average contact pressure it will be possible to determine the magnitude of these changes between the applied loads, the results of this analysis is shown in Table 17.

Pressure Load (lb-f [N])	% Increase in Pressure Load	Average Contact Pressure (psi [N.mm ⁻²])	% Change in Average Contact Pressure
600 [2668.9]	-	326.2 [2.25]	-
800 [3558.6]	133	417.6 [2.88]	128
1000 [4448.2]	125	517.3 [3.57]	124
1200 [5337.9]	120	602.0 [4.15]	116
1400 [6227.5]	117	685.7 [4.73]	114
1600 [7117.2]	114	748.8 [5.16]	109

Table 17 – Table of the percentage change in load an average contact pressure from FEA data

The results of the analyses to determine the percentage change of the loads and average contact stresses are shown in Table 17. The percentage changes in the loads and contact pressures decrease as the load applied increases, this is thought to be a function of the magnitude of the increase and the magnitude of the load applied. As discussed in the analysis of the stress profile plots the change in average contact pressure is shown to be approximately equal to the change in applied load. To evaluate the change in average

contact pressure in a non-dimensional manner it is possible to numerically determine the percentage change in the average contact pressure per percentage change in the applied load. By completing this analysis, it shall be possible to determine the variance in the changes of load and therefore average contact pressure. Through completing this analysis, it will be possible to determine whether the general trend identified previously is applicable to all of the loads considered. Table 18 shows the result of completing this analysis on the data from Table 17.

Pressure Load (lb-f [N])	% Increase in Pressure Load	% Change in Average Contact Pressure	% Change in Average Contact Pressure per % Change in Load
600 [2668.9]	-	-	-
800 [3558.6]	133	128	96
1000 [4448.2]	125	124	99
1200 [5337.9]	120	144	97
1400 [6227.5]	117	114	97
1600 [7117.2]	114	109	96

Table 18 - Percentage change in contact pressure per percentage change in applied pressure load

By removing the effect of the magnitude of the applied loads it is possible to determine a directly comparable change in percentage of contact pressure per percentage change in load as shown in Table 18. From the results presented it is possible to see that the percentage increase in average contact pressure per percentage increase for the applied loads considered fall within a 3% range. Considering the effect of outliers on the averaging of the stress profiles these results suggest a common numerical equation would be applicable to describing the results of these applied loads. As there was limited available literature on the application of contact mechanics to the description of a sealing interface these results cannot be compared to a literature source to determine whether this outcome is in line with previously published work.

From the results shown in Figure 58 the following equation has been determined which allows for the determination of the stress at any point within the contact half-width.

$$y = -0.2149x^2 - 0.1639x + 1.0119$$

Equation 37 - Stress magnitude determination within contact stress profile

To apply this equation, it is necessary to determine the stress at the point of contact and multiply this by the outcome of Equation 37. Through the analysis of the stress profile data from the finite element analyses it was found that there involvement of a significant number of contact mechanics equations prevented an equation being formed which links the applied load to the stress at the contact point and therefore the stress at a given point within the stress profile.

This section has presented a series of analyses which have been completed through the application of finite element analyses to the geometry and with the applied loads determined in the previous chapter. Through the evaluation and analysis of the results from the finite element analyses it was identified that a general trend was being presented by the results, this general trend was identified to be the proportional increase in the contact stresses reported with respect to the applied load. The 400lb-f (1779.3N) applied load was seen not to follow the same trends as the loads of higher magnitudes. To determine whether the applied load was being influenced by a high number of outlying results in the data for that specific applied load the load was increased to 440lb-f (1957.2N), this was identified as the minimum load a floating ball valve seat should be subject to therefore it would be appropriate to use the data from this analysis in place of the 400lb-f (1779.3N) data if the results matched the general trends. When the plot of the stress profile for the 440lb-f (1957.2N) load was compared to the general trends established by the loads of higher magnitudes it was found that a closer match was presented however significant differences were still present. Based on the differences between the 400lb-f (1779.3N), 440lb-f (1957.2N) applied loads and those of higher magnitudes it is considered that the mechanics which govern the mechanics at these loads may be different from those governing the higher magnitude loads. This thesis considers the stress profiles where there is an established trend, it is recommended that further work is undertaken to develop an understanding of the mechanics that govern the response of the seat to these lower magnitude applied loads.

The applied loads, 600lb-f (2668.9N) through 1600lb-f(7117.2N), have been assessed to determine the level of the applicability of the general trends to each of these applied loads. Through the assessment of the plotted stress profiles it is found that the general trends of proportionality hold true within an acceptable tolerance. While there are a few outliers in each of the stress profile plots these are considered to be generated by shear stresses which are a reality of the application of the profile of the ball to the angled seat face but which are not considered in the ideal model of Hertz contact mechanics. The general profile of the stress plots are demonstrated to hold true with the exception of the one load where an outlying result is present at the location used to compare the profiles, this identifies the same form of mechanics is applicable to all of the results gained with the varying loads applied.

By taking the sets of data presented in the stress profile plot and determining the mean average it allows the accuracy and reliability of the results of the analytical stress values are increased due to the reduction in the effect of outliers on the stress values used. It was possible through the assessment of the change in the values of loads applied and average stresses measured to validate the relationship of proportionality between the applied load and the average contact pressure. Though the validation of the relationship between the applied load and the average contact pressure it is possible to derive and apply a general equation which defines the magnitude of the stress value within the stress profile of the contact half-width with respect to the stress value at the point of contact.

This section achieves the aim of demonstrating that a single form of mechanics is applicable to the definition of the contact pressure through the derivation of a single numerical model describing the stress profile measured from the computational model which represents the realistic evaluation of the selected geometry and applied loads. By determining the average contact pressures, it allows for the realistic computational model to be compared to the ideal theoretical model derived in the previous chapter. The inputs to the computational model are the same as the theoretical model with the outputs being in the same form also, the outputs have been gained through the application of real-world dynamics to the selected geometry.

5.1.2 Seat deflection

This analysis looks at defining the initial deflection of the seat in terms of the load applied to it in isolation from the pressure load; by isolating the initial deflection the effects this has on the seating component can be understood without having to consider the relative effects of other variables.

As seen in the literature review a pre-load is usually applied to the contact between the ball and seat. As with other floating ball valves the pre-load of the seat is achieved by an initial deflection of the seat component. In linking the seat deflection to the load applied it is possible to link the initial seat deflection to an initial contact pressure (before pressure is applied).

5.1.2.1 Analysis Steps

The analysis of the component in the computational model is conducted in accordance with the method shown in Figure 29. The analysis is run using the loads derived from the pressure acting over the ball being applied to the ball component. As this section is investigating the deflection of the seat the output of the analysis is required to be the resultant deflection of the components. From the load and the deflections, it shall be possible to investigate the relationship between the applied load and the deflection of the seat component.

5.1.2.2 Results

The 400lb-f (1779.3N) and 440lb-f (1957.2N) applied loads are not being considered in this thesis with respect to contact pressure this is due to the consideration that the results show the mechanics that describe the response of the seat when these low magnitude loads are applied may be different to those of the higher magnitude load. As the mechanics are considered to be different these loads shall not be considered in this section when evaluating the mechanics relating the deflection of the seat to the applied load.

The results from the finite element analysis of the load acting on the seat component are taken from the resultant deflection plots of the results, shown in the following figures.

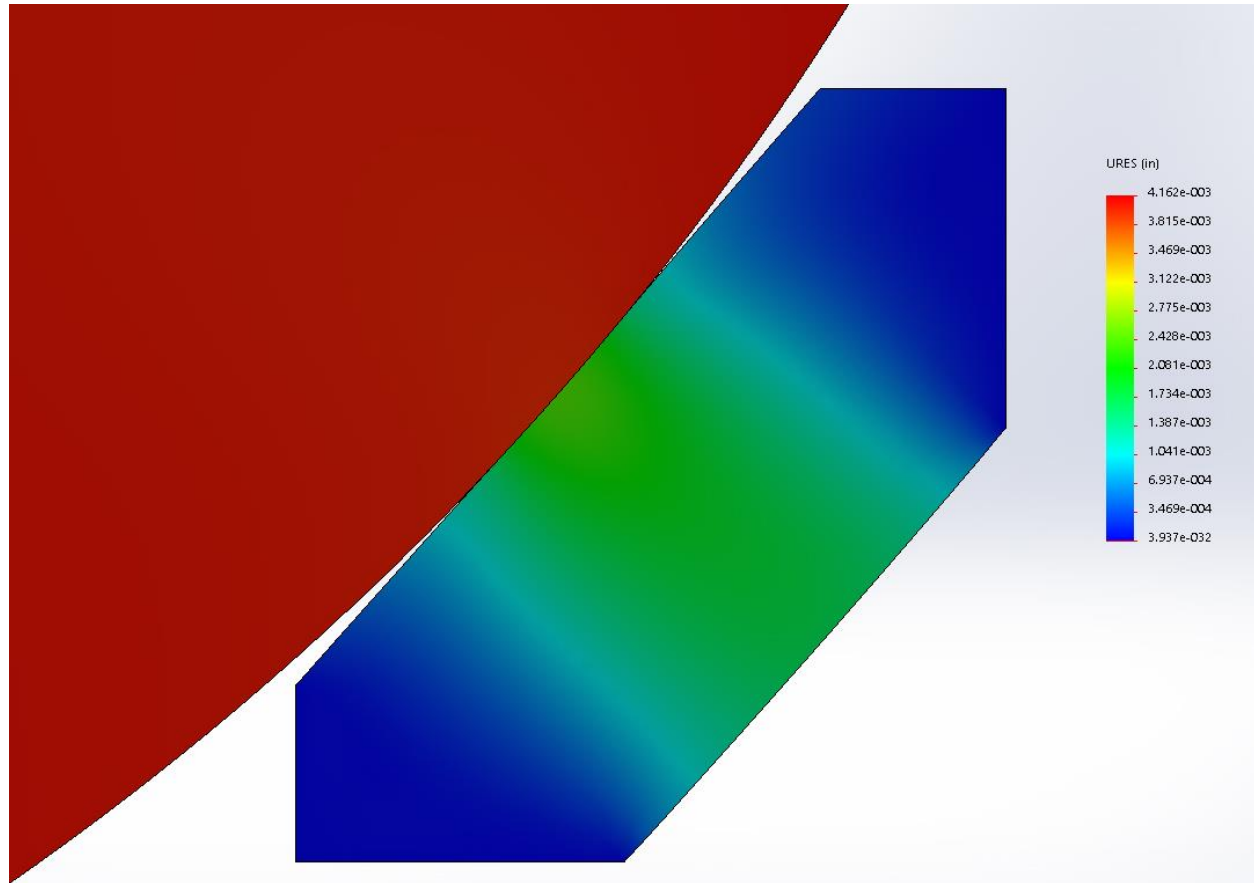


Figure 59 – A plot of the seat deflection from FEA when a 600lb-f (2668.9N) load is applied

Figure 59 shows the deflection of the seat component when a load of 600 lb-f (2668.9N) is applied to the model. The deflection of the seat is constrained to the flexible section of the seat component with the greatest magnitude measured at the point of contact as being 0.0024in (0.061mm). The deflection of the seat component is found to be 55% of the movement of the ball in the axial direction, the movement of the ball was measured as 0.0042in (0.107mm). As discussed in the theoretical model when determining the components of the total load acting on the seat component the ball is subject to the total load whereas the seat is only subject to a component of this therefore the seat deflection is proportional to the ball deflection by the amount of the total load acting on reach of the bodies. The average deflection in the contact half-width was found to be 0.0023in (0.059mm).

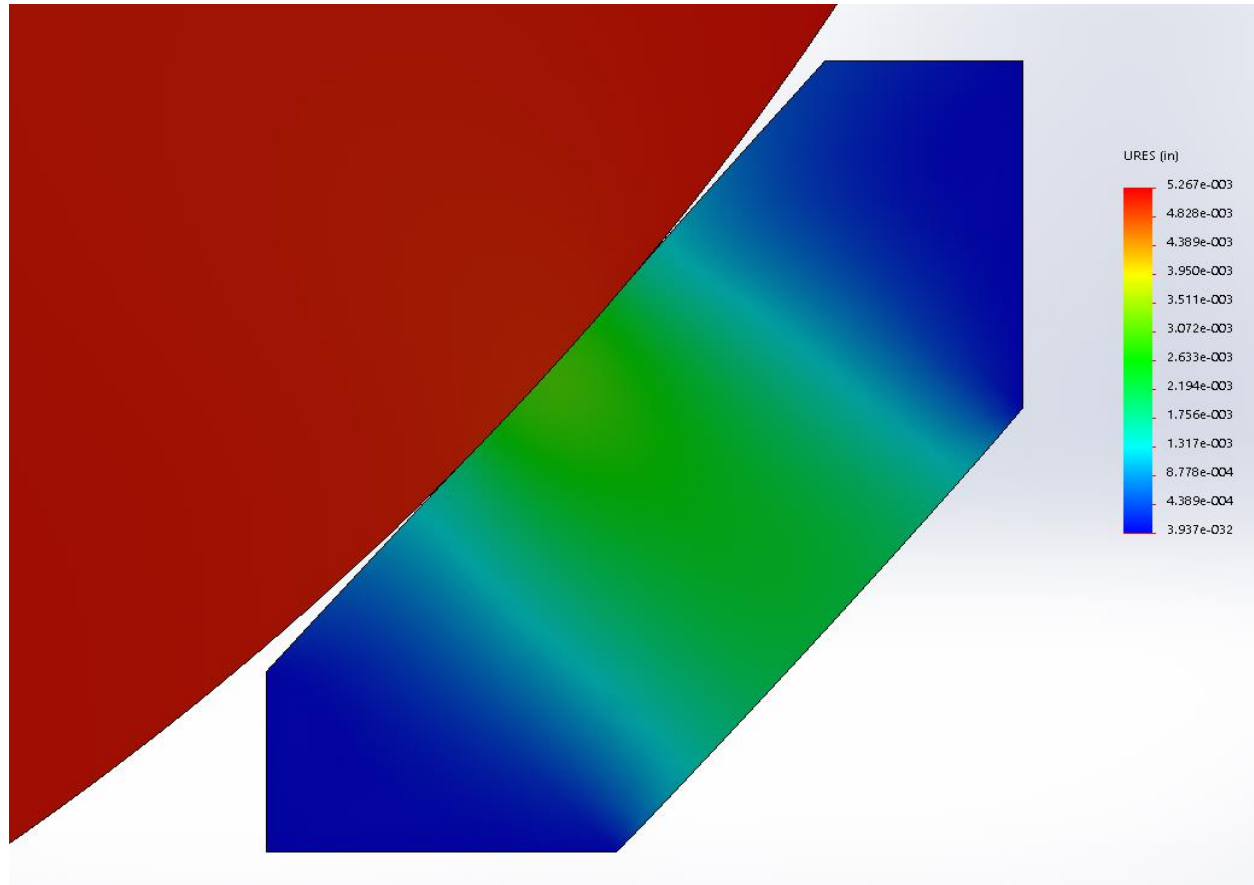


Figure 60 – A plot of the seat deflection from FEA when a 800lb-f (3558.6N) load is applied

Figure 60 shows results from the finite element analysis when the applied load is increased from 600lb-f (2668.9N) to 800lb-f (3558.6N), the applied load is increased by 33% when compared to the previous analysis. The deflection of the seat at the point of contact was measured as being 0.0031in (0.078mm), this is an increase of 29% when compared to the maximum deflection of the previous analysis. The movement of the ball in the axial direction was measured as being 0.0053in (0.135mm), therefore the deflection of the seat is 58% of that of the ball deflection. As the same geometry and proportion of load is maintained from the previous analysis the expectation that the deflection of the seat is the same proportion of the deflection of the ball was expected and maintained in the results of this analysis. The average deflection of the seat in the contact half-width is found to be 0.0029in (0.075mm), this is a 26% increase on the average deflection of the 600lb-f (2668.9N) analysis.

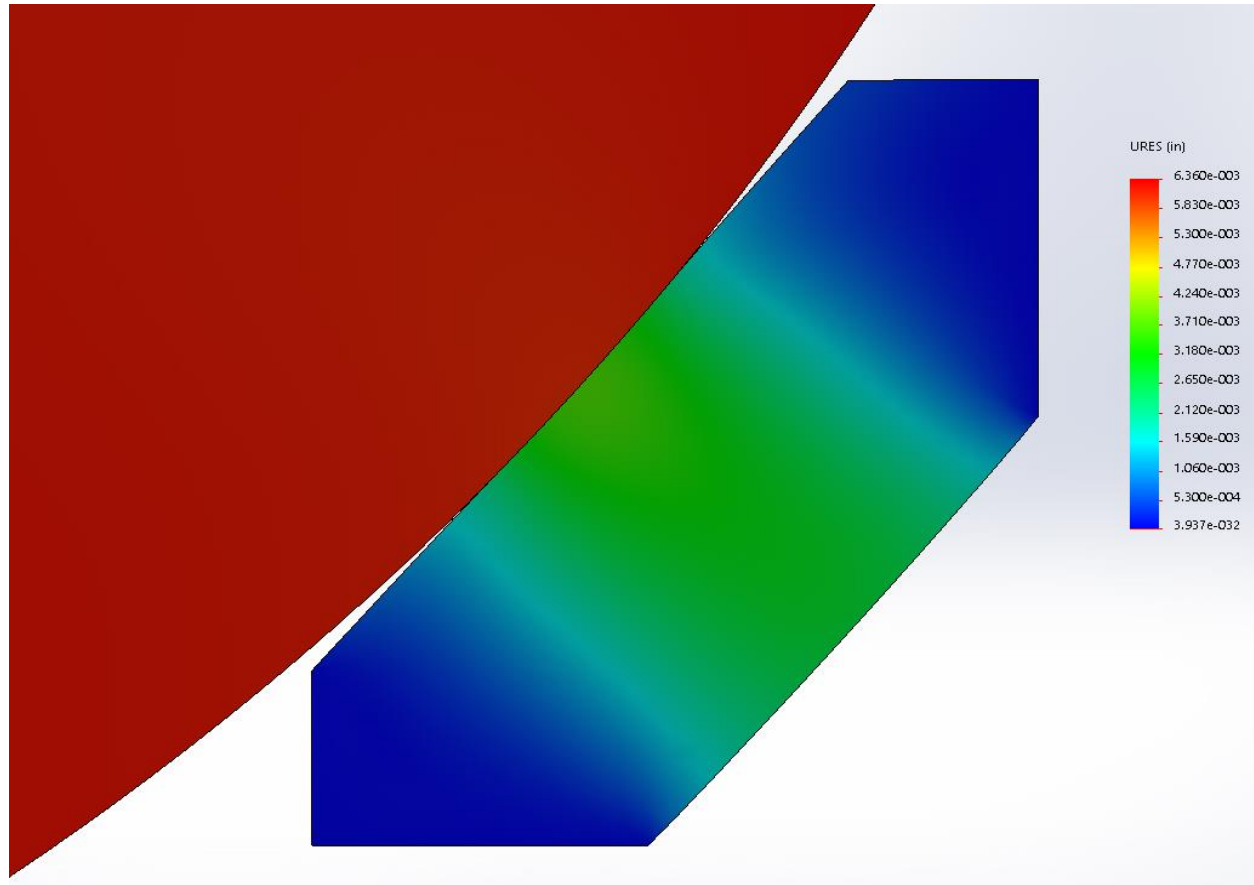


Figure 61 – A plot of the seat deflection from FEA when a 1000lb-f (4448.2N) load is applied

The results of the analysis presented in Figure 61 shows the deflection of the seat component with a 1000lb-f (4448.2N) load applied to it. The application of a 1000lb-f (4448.2N) load is a 25% increase in applied load from the load applied in the previous analysis. The maximum deflection is found at the point of contact between the ball and seat components here the deflection was measured as being 0.0037in (0.094mm). the increase in maximum deflection on the previous analysis is 19%, this follows the general trend of both deflections increasing by a value approximately equal to the increase in applied load. The movement of the ball in the axial direction was found to be 0.0064in (0.163mm), the maximum deflection is 58% of the movement of the ball. The relationship between the ball movement and seat deflection is maintained from the previous analysis showing a common trend developing based on the relative geometries of the components involved. The average deflection of the seat component under 1000lb-f (4448.2N) load is found to be 0.0035in (0.089mm).

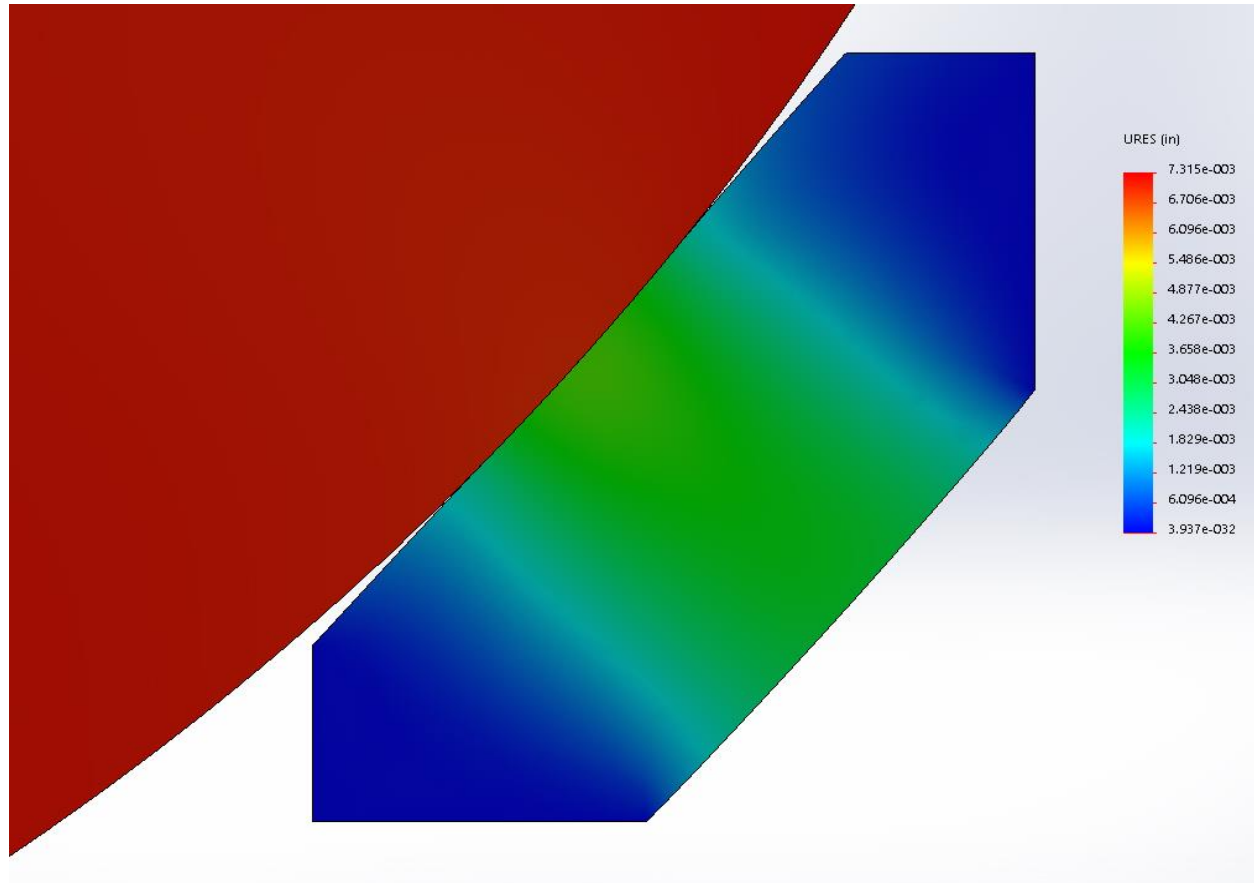


Figure 62 – A plot of the seat deflection from FEA when a 1200lb-f (5337.9N) load is applied

Figure 62 shows a plot of the deflection of the seat component when the applied load is 1200lb-f (5337.9N). The load of 1200lb-f (5337.9N) is a 20% increase on the load applied in the previous analysis. The maximum deflection of the seat is found at the point of contact where it is measured as being 0.0042in (0.107mm). The maximum deflection has increased by 14% from the previous analysis following the general trend that the where the applied load increases the deflection of the seat component increases too. The axial movement of the ball was measured at 0.0073in (0.185mm).The maximum deflection is found to be 58% of the movement of the ball component once again maintaining the relationship governed by the relative geometries of the components being analysed. The average deflection of the seat component was found to be 0.0041in (0.104mm), the average deflection is a 17% increase on the same figure in the previous analysis.

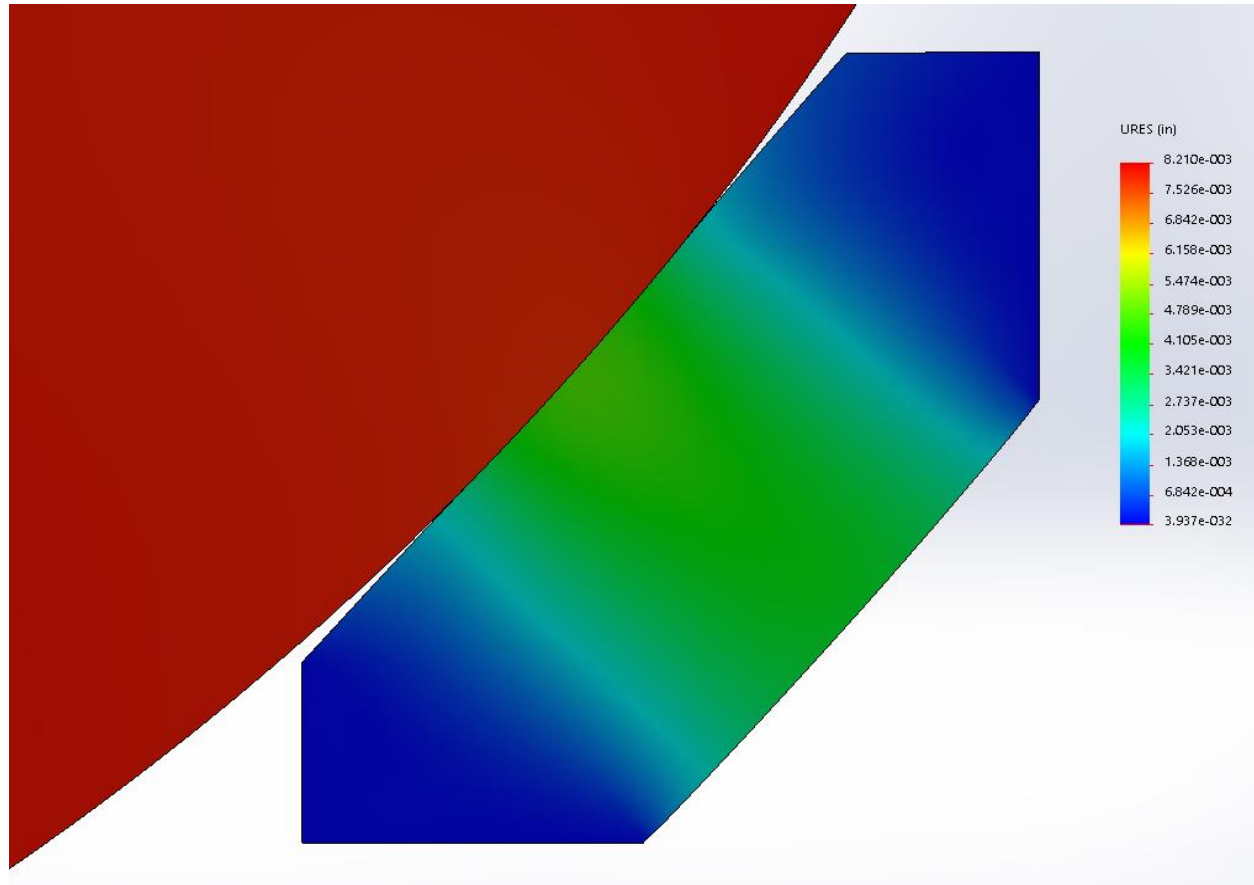


Figure 63 – A plot of the seat deflection from FEA when a 1400lb-f (6227.5N) load is applied

The deflection plot shown in Figure 63 shows the deflection of the seat component when a 1400lb-f (6227.5N) load is applied to the seat component, the applied load equates to a 17% increase on the load used in the previous analysis. The maximum seat deflection is found at the point of contact between the ball and seat components, the value of this deflection is 0.0048in (0.122mm), when compared to the deflection of the preceding analysis it is found to be a 14% increase. The percentage increase in applied load and maximum deflection are found to increase by a similar factor. The movement of the ball component in the axial direction is found to be 0.0082in (0.208mm). The maximum deflection is determined as being 59% of the movement of the ball component and therefore maintaining the relationship set by the geometry of the ball and seat components supposed previously. The average deflection of the seat component in the contact half-width is calculated from the data as being 0.0045in (0.114mm), this is a 10% increase on the average deflection of the previous analysis.

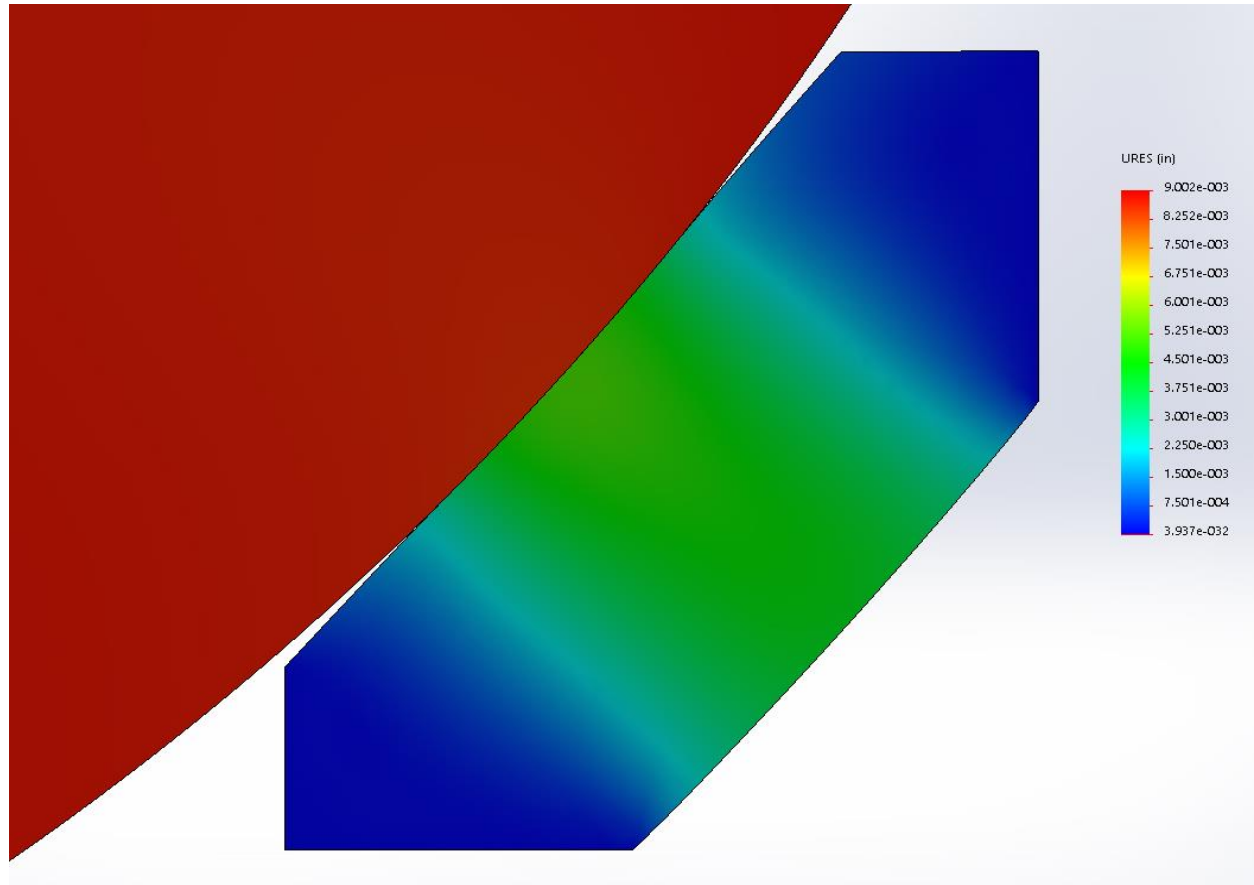


Figure 64 – A plot of the seat deflection from FEA when a 1600lb-f (7117.2N) load is applied.

Figure 64 shows the deflection of the seat component when an increased load of 1600lb-f (7117.2N) is applied to the model, increasing the load to 1600lb-f (7117.2N) results in a 14% increase in the load applied to the model. As the applied load increases the maximum deflection of the seat component increases to 0.0052in (0.132mm), this is an increase of 8% on the deflection measured in the previous analysis. The movement of the ball in the axial direction is measured as 0.0090in (0.229mm), therefore the deflection of the seat is 58% of this deflection maintaining the relationship between the deflection of the seat and the movement of the ball that has been seen throughout the evaluation of the analyses completed, it is considered that this relationship is maintained due to the geometry of the valve components and components of force acting on the relevant components. The average deflection of the seat in the contact half-width of the seat component was determined at being 0.0050in (0.127mm), this is an 11% increase on the average deflection of the previous analysis.

The following figures contain plots of the deflection profile of the seat component taken from the edge of the analysis shown in the previous figures. By plotting the deflection profile from the data taken from the analyses it is possible to see in more detail where the trends which are currently considered to be present from the evaluation of the deflection plots are consistent across the full range of data available. From the plots of the results from the finite element analyses it is expected that a trend showing a greater deflection of the seat where a larger load is applied shall be seen.

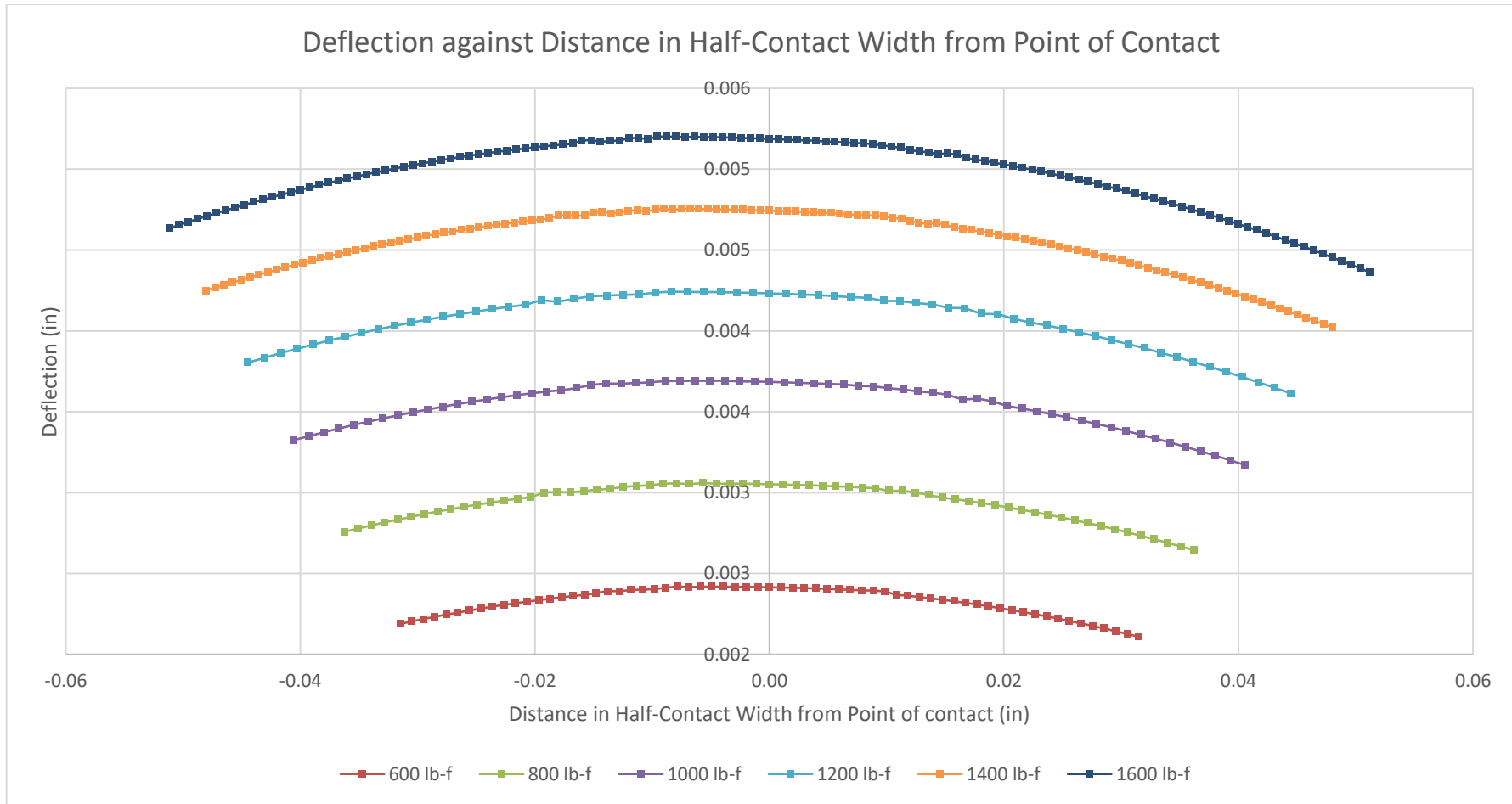


Figure 65 – A graph showing the deflection results plotted against distance of the result from point of contact

Figure 65 shows the deflection of the seat as measured at each node at the distance that node is from the point of contact. Looking at the trends presented in this plot the expected pattern is displayed as the load increases so too does the magnitudes of the deflection; while the magnitude and width of the area subject to deflection increases the profile of the deflection does not change. As considered in the previous section the greater the load applied to the model the greater the contact half-width becomes. The deflection profiles shown in the figure show the proportionality of the deflection profile of the seat, as the load increases the magnitude of the maximum deflection increases as does the rate at which the deflection decreases from the point of contact.

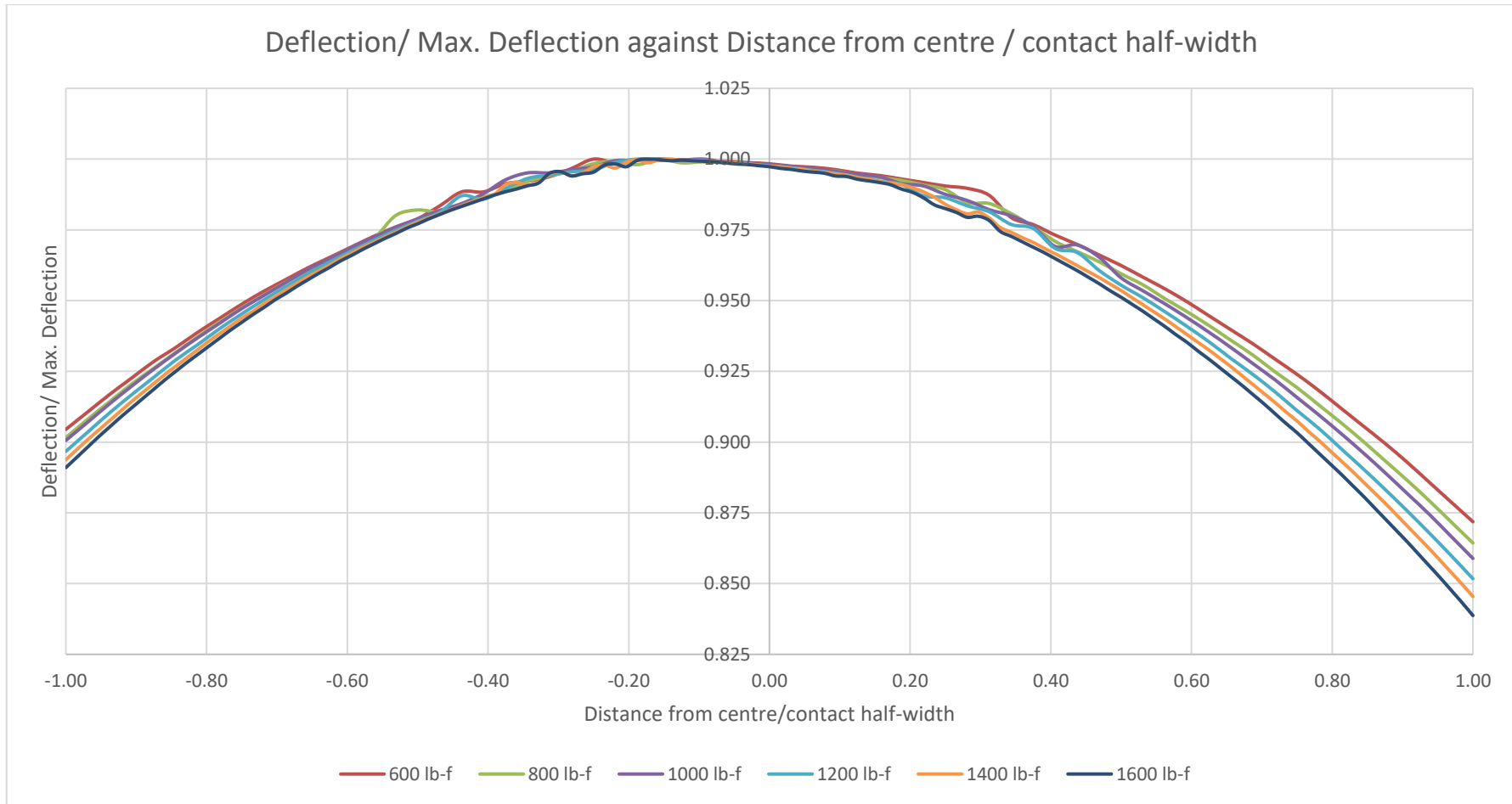


Figure 66 – Graph showing a plot of deflection/max. deflection against distance from centre/contact half-width

Figure 66 shows the plot of deflection/maximum deflection against distance from centre/contact half-width, this plot is completely free from the effects of the magnitude of the variables being assessed therefore allowing for a direct comparison between the data that has been collected from the analyses. The general trend of the deflections shown are, the greater the load applied to the seat component the greater the rate of change of the deflection within the contact half-width.

Unlike with the contact pressure graphs the profiles of the deflections shown in Figure 65 and Figure 66 show well defined sets of data with minimal variances and no variances that would result influence the outcome of averaging the results in a negative manner. The corresponding theoretical model established in the previous chapter calculates the maximum deflection of the seat therefore to achieve a comparable set of data it will necessary to determine a reliable maximum deflection value from the analyses completed in this section. The results for the maximum and average deflections are shown in the following table, Table 19.

Pressure Load (lb-f [N])	Average Deflection (in [mm])	Maximum Deflection (in [mm])
600 [2668.9]	0.0023 [0.058]	0.0024 [0.061]
800 [3558.6]	0.0030 [0.076]	0.0031 [0.079]
1000 [4448.2]	0.0035 [0.089]	0.0037 [0.094]
1200 [5337.9]	0.0041 [0.104]	0.0042 [0.107]
1400 [6227.5]	0.0045 [0.114]	0.0048 [0.122]
1600 [7117.2]	0.0050 [0.127]	0.0052 [0.132]

Table 19 - Finite Element Analysis Deflection Results

The results shown in Table 19, show a general correlation between the load applied to the ball and the deflection recorded in the seat component. The general trend shows that when the load increases so too does the deflection of the seat component, this trend is present in both the average deflection and maximum deflection results. Considering the plot of the data shown in Figure 65 shows there are no outliers which will affect the use of the maximum deflection as well as the maximum deflection being located in a small band of deflections around the point of contact of the same value justifies its use from the data gained from the finite element analyses. The small differences between the average and maximum deflections presented in Table 19 as well as the results with which these results are being compared the theoretical maximum deflection results would make the use of the maximum deflection the most appropriate values to use for further analysis. Taking the raw data from Table 19 and evaluating it to determine the change in deflection an applied load will allow for this data to be more objectively assessed.

Pressure Load (lb-f [N])	Percentage Change in Load	Maximum Deflection (in [mm])	Percentage Change in Average Deflection
600 [2668.9]	-	0.0024 [0.061]	-
800 [3558.6]	133	0.0031 [0.079]	133
1000 [4448.2]	125	0.0037 [0.094]	116
1200 [5337.9]	120	0.0042 [0.107]	114
1400 [6227.5]	117	0.0048 [0.122]	114
1600 [7117.2]	114	0.0052 [0.132]	108

Table 20 - Percentage change in FEA deflection results

The analysis shown in Table 20 shows the increase in load applied and the deflection measured is roughly equivalent in each case analysed. The general trend is that the percentage increase decreases as the loads applied get greater, this is considered to be due to the increase being proportionally smaller amount of the load applied to the geometry. To make direct comparisons of the analyses made in Table 20 the effects of the magnitude of each of the loads shall be removed from the calculations, as shown in Table 21.

Pressure Load (lb-f [N])	% Change in Load	% Change in Average Deflection	% Change in Average Deflection per % Change in Load
600 [2668.9]	-	-	-
800 [3558.6]	133	133	100
1000 [4448.2]	125	116	93
1200 [5337.9]	120	114	95
1400 [6227.5]	117	114	97
1600 [7117.2]	114	108	95

Table 21 - Percentage change in maximum deflection per percentage change in applied load

The results shown in Table 21 remove the magnitude of the load as a factor effecting the result of the calculations allowing a direct comparison between the results. The outcome of the calculations demonstrates that the deflections across the range of loads applied to the analytical model are consistent within the variances expected from a finite element analysis data set and therefore valid to be used as a basis from which to validate a theoretical model against.

This section has conducted a series of finite element analyses of a model of the ball and seat geometry which represent accurately the realistic interaction between the ball and seat and the deflection of the seat which is created by the applied load. The data extracted from the analyses undertaken show a consistent data series with limited outliers of any significance identified. Through the assessment of the data it was found that the deflection of the seat component is related proportionally to the load applied to the model. In determining the data required to validate the theoretical model the assessment of the data showed that the use of the maximum deflection value to the most appropriate data to use due to the small range of values and high quality of the data available from the analysed. Through the evaluation and validation of the data generated from the analyses the proportionality of the application of the load and the maximum deflection was shown both graphically and numerically.

This section achieves the aim of demonstrating that a single theory can be employed to describe the deflection of the seat component with respect to the applied load, due to the common deflection profiles and relationships established between applied load and seat deflection. From the data provided from this section is shall be possible to validate the theoretical model established in the previous chapter for the deflection of the seat by the load applied to it.

5.1.3 Bending Stress

Based on the research into contact mechanics it is clear that any contact between the ball and seat will need to be assessed in accordance with Hertz contact mechanics where the contact pressure (measured as the von mises stress) does not exceed the yield stress of the component.

As mentioned on page 23, the design of seats shall be such that there shall be no permanent gross deformation of the material therefore the yield stress shall not be surpassed by the von mises stress in the component when under the maximum load applied to the component. This section aims to take the same von mises stress plots and develop a mechanistic model to determine the maximum stress being developed in the seats when the maximum load is applied to it. By determining a theoretical model that allows for the prediction of the maximum bending stress in the seat it is possible to ensure that the seat doesn't yield (deform) therefore ensuring that the mechanics determined in the previous sections are still applicable.

5.1.3.1 Analysis Steps

The analysis of this component is conducted in accordance with the method shown in Figure 29. The analysis is run using the loads derived from the pressure acting over the ball being applied to the ball component. As the section is investigating the bending stress in the seat the output of the analysis is required to be the von mises stress in the seat component. From the loads and bending stresses, it shall be possible to investigate the relationship between the applied load and the bending stresses in the seat component.

As with the determination of the seat deflection the minimum load considered in this section shall be 600lb-f (2668.9N), this is due to the lack of continuity found in the results shown on page 121 of section 5.1.1 at the lower magnitude loads which have led to these loads being excluded from the scope of this thesis.

5.1.3.2 Results

The results of the finite element analysis of the pressure-load acting on the seat component are taken from the von mises stress plots of the results, shown in the following figures. In each of these figures the maximum stress in the seat component is expected to be at the middle of the seat thickness, therefore a line has been drawn to show this location and the stress plots probed where the contour shows the highest stress in this region.

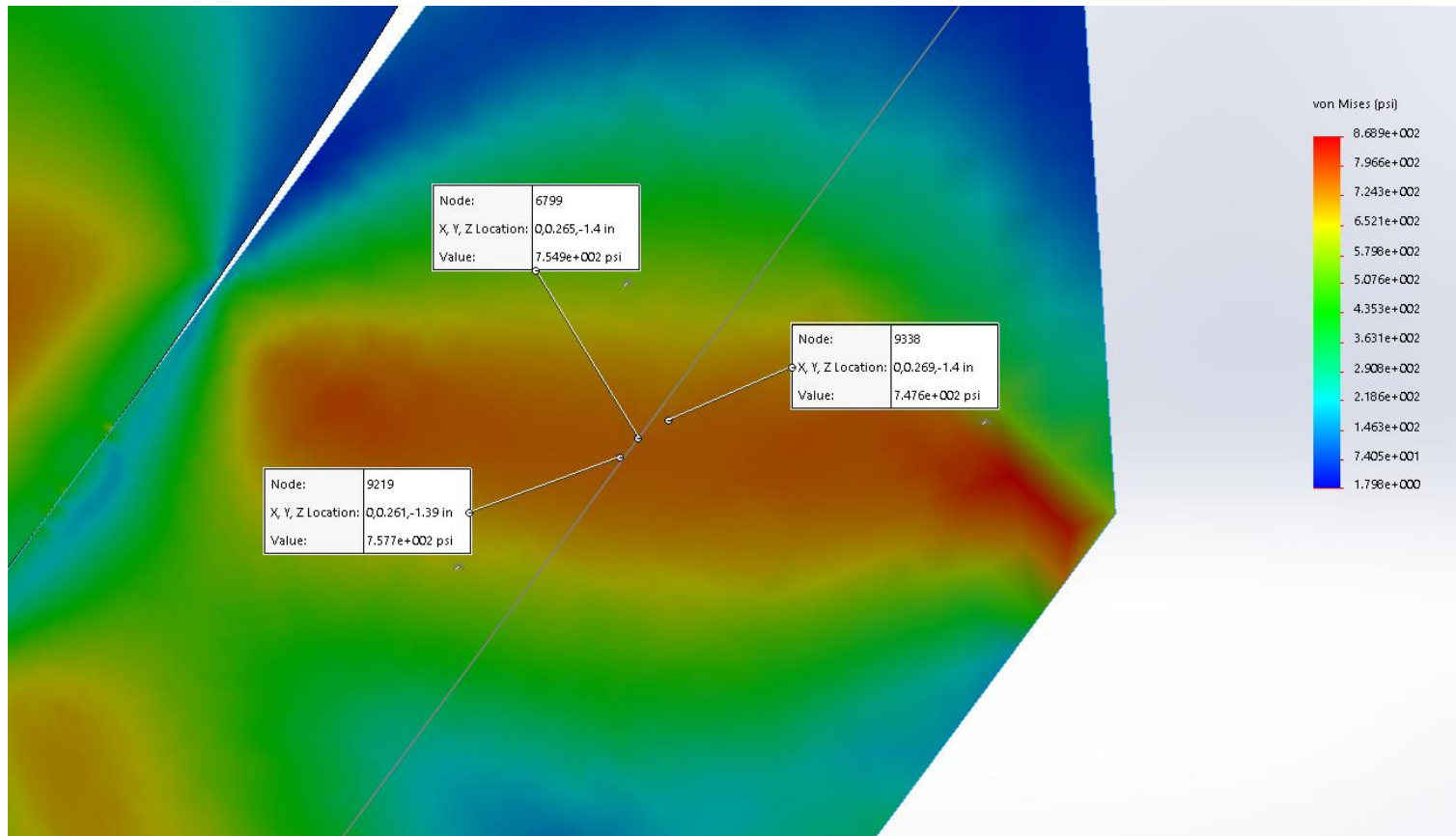


Figure 67 – A plot showing the probe of von mises stresses when a load of 600lb-f (2668.9N) is applied

Figure 67 shows the probe of the stress plot gained when a load of 600lb-f (2668.9N) is applied to the model. In this plot the contours shown are highly non-uniform. The area probed shows the highest stress along the middle of the seat thickness, two of the stress values at the probe locations fall within a close proximity of each other while the third is a lower value. When looking at the figure the lower stress value point looks to be from an area next to lighter shaded contour. In this plot there is an increase in stress from the corner of the seat, this is a stress raising effect which is caused by the concentration of stresses in this location as well as the application of a fixed constraint to the model to create a model which is stable for the analyses to be completed. While this stress raiser and does not reflect the actual condition of the component it does not appear to have a significant effect in influencing the values of stresses measured. The increase in stress due to the contact mechanics in this plot are shown to be minimal with the stress contour being slightly darker than at the region probed.

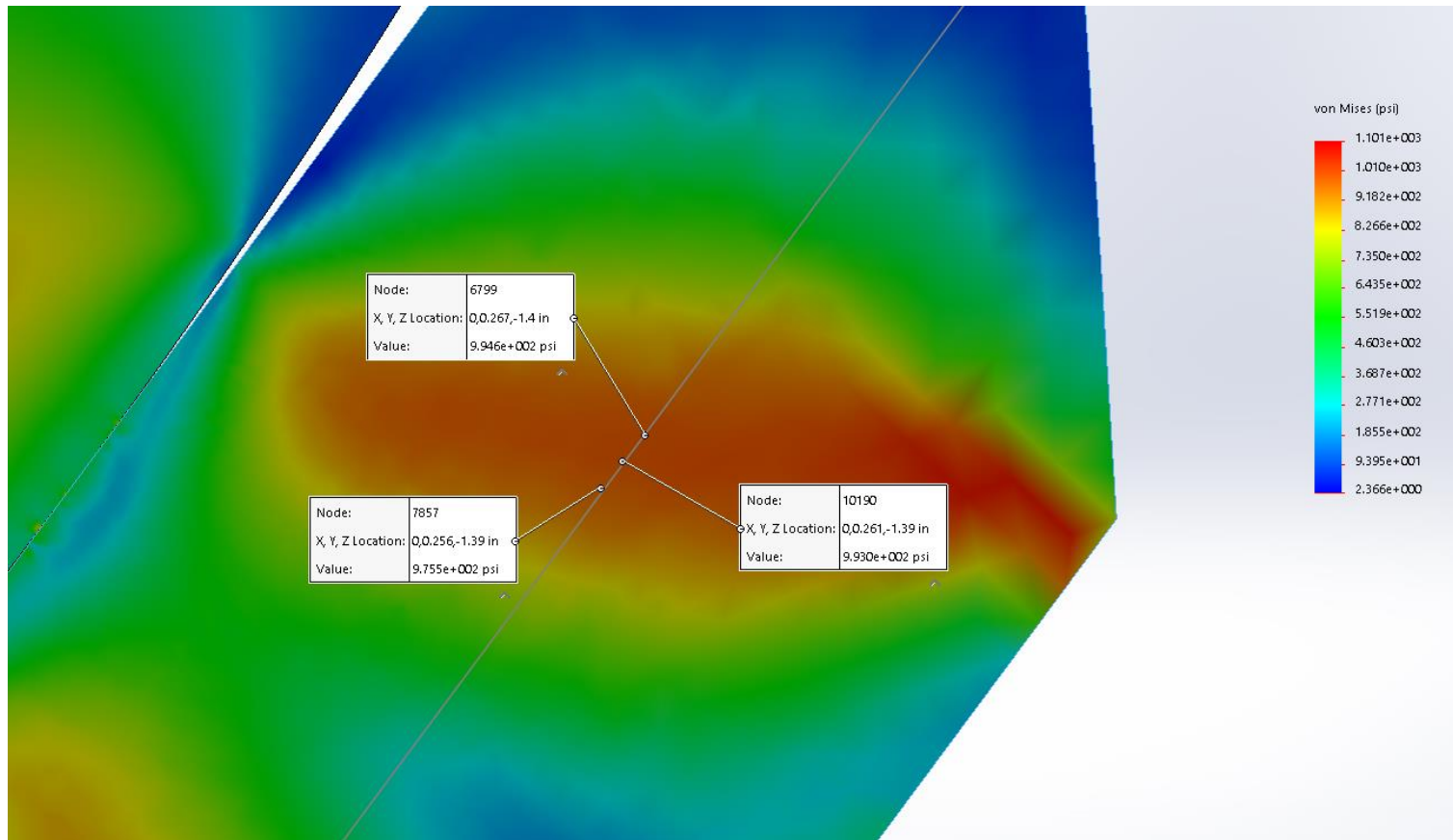


Figure 68 – A plot showing the probe of von mises stresses when a load of 800lb-f (3558.6N) is applied

Figure 68 shows the probe of the stress plot gained when a load of 800lb-f (3558.6N) is applied. The region in the centre of the seat thickness where the highest stress in the component is has become more defined than in the previous figures. The stresses at two of the points probed are close to each other in terms of value whereas the third point is of a lower value. The lower value of the point probed sits in a lighter colour contour outside the darker contour of the highest stress on the central point of the seat's thickness. The effect of the contact mechanics on the seat stress is not visible in this plot as the colour of the plot towards the area where the contact mechanics are the dominant effect shows no increased past the maximum stress caused from the seat bending. The stress plot towards the corner of the seat shows an increase due to the stress raising effect of constraining this corner of the seat.

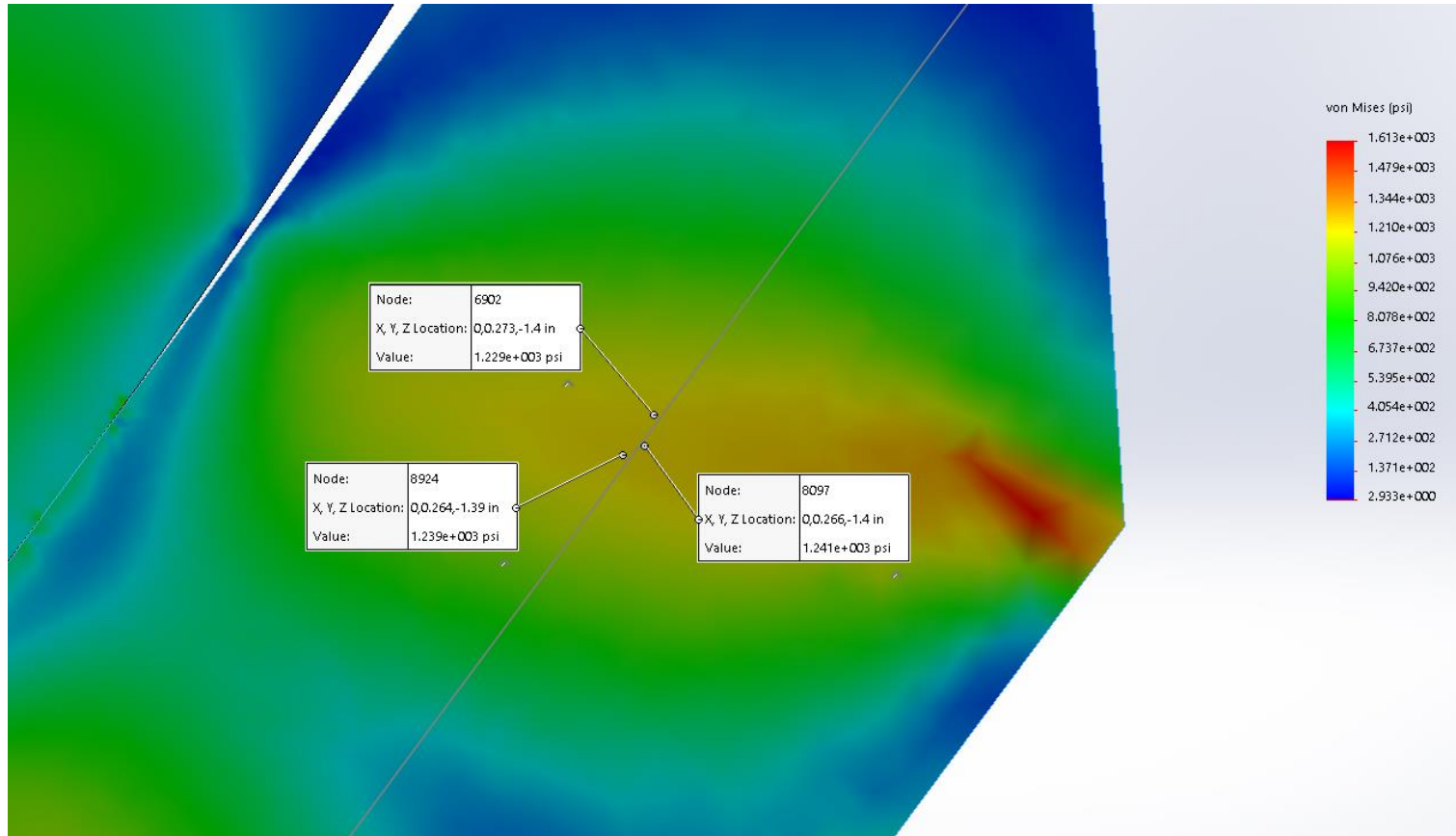


Figure 69 – A plot showing the probe of von mises stresses when a load of 1000lb-f (4448.2N) is applied

Figure 69 shows the probe of the stress plot gained when a load of 1000lb-f (4448.2N) is applied. The stress plot has become much closer to the typical plot that would be expected when a component is subject to bending with a high stress at the middle of the component's thickness and this stress decreasing away from this point. All three of the probe points are within a reasonable range, this correlates to the all being located within the high stress area along the middle of the seats thickness. The effect of the contact of the ball on the seat shows no impact on the stress in the seat due to bending as the stress contours in the plot show a reduction in the stress from the middle of the seat towards the contact with the ball. The stress raising effect of the corner of the seat component is still present in this plot however its effect is not influencing the results gained from the probes at the middle of the thickness of the seat.

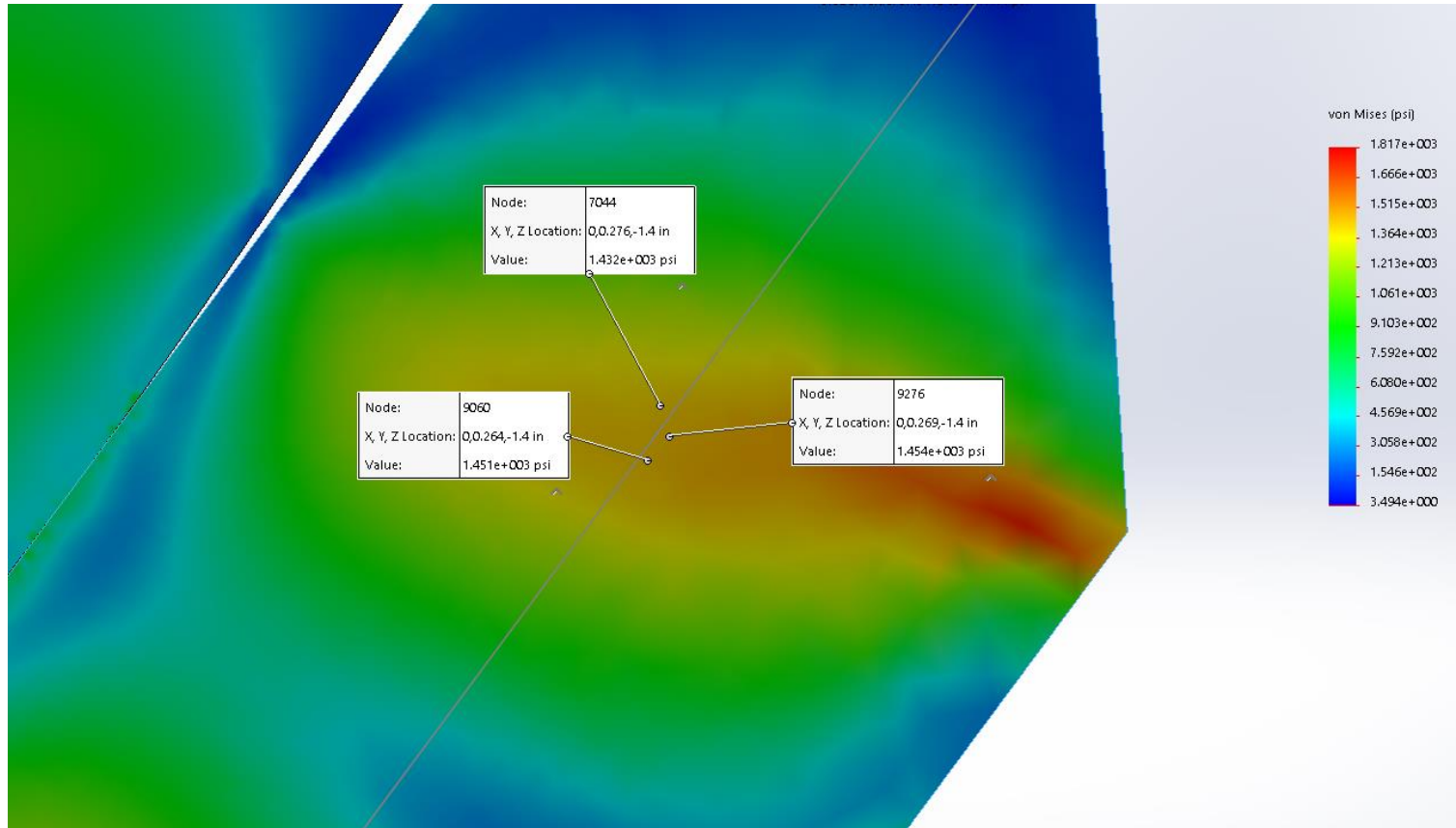


Figure 70 – A plot showing the probe of von mises stresses when a load of 1200lb-f (5337.9N) is applied

Figure 70 shows the probe of the stress plot gained when a load of 1200 lb-f (5337.9N) is applied. The stress plot has once again developed towards a standard contour which would be expected from a stress plot of an annular plate subject to bending. Two of the three probe points are within a reasonable variance however the third probe point is a significantly lower value which is reflected by the colour of the contour from which the point is measured. The two points showing agreeing values are located in the darker region of the plot with the third in a light region where the stress result would be expected to be lower. As with the previous figure there is no influence on the bending stress of the seat component by the contact mechanics governing the reaction of the seat to the ball. The stress raising effect of the corner of the seat being fixed does not affect the outcome of the stress at the middle of the thickness of the seat component.

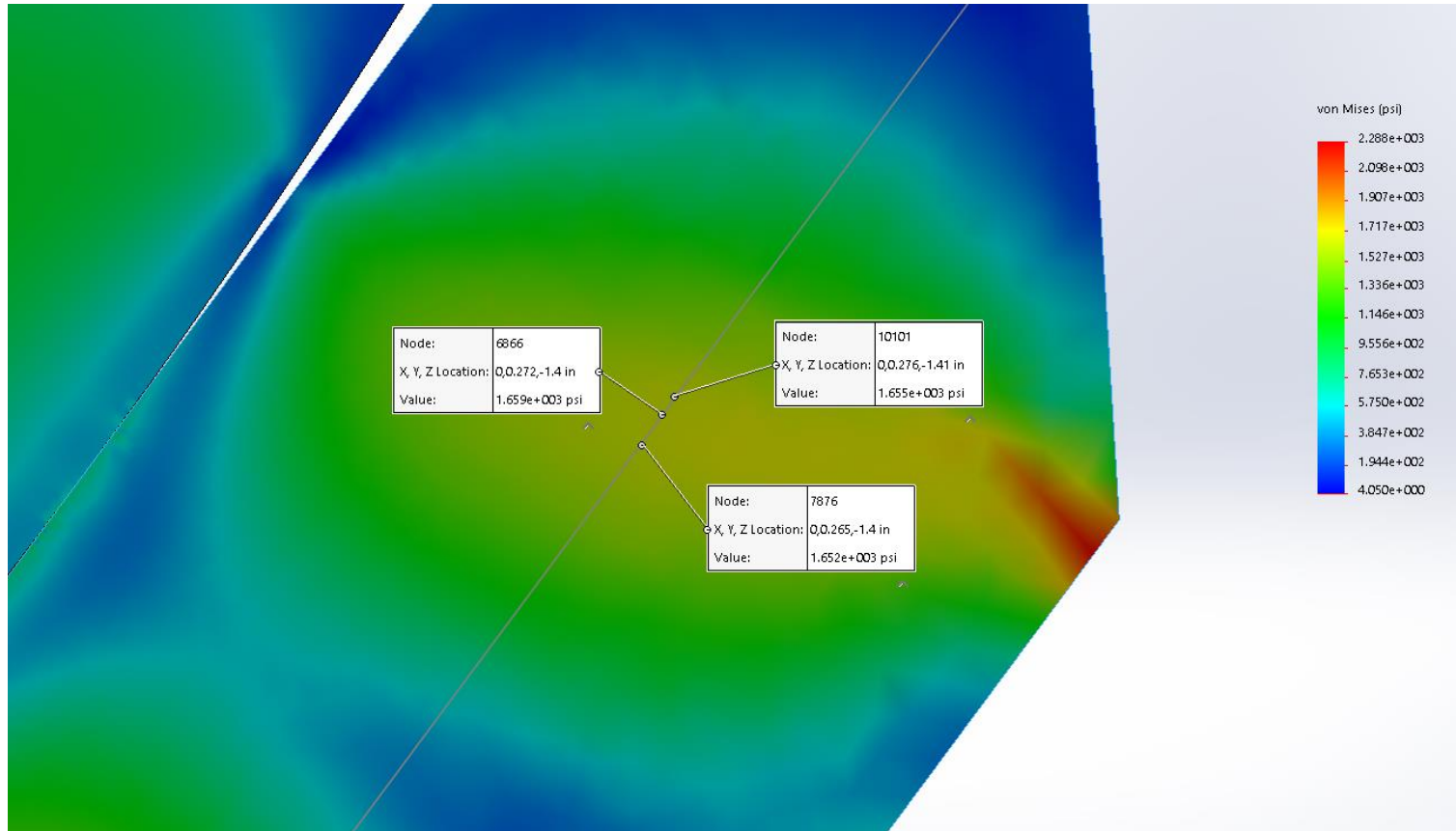


Figure 71 – A plot showing the probe of von mises stresses when a load of 1400lb-f (6227.5N) is applied

Figure 71 shows the probe of the stress plot gained when a load of 1400 lb-f (6227.5N) is applied. The stress plot shows the contours have maintained the same shape as shown in the previous plot. All three of the points probed are within a few psi of each other showing a consistently high stress at the centre of the thickness of the seat. The stress raising effect of the fixed corner of the seat is having less of an effect on the overall stress plot than shown in previous plots although it does not have any effect on the stress at the mid-point of the seat component. The effect of the contact stress on the bending stress in the seat component is negligible with the stress contour similar to that of the regions with no stress raising effects present.

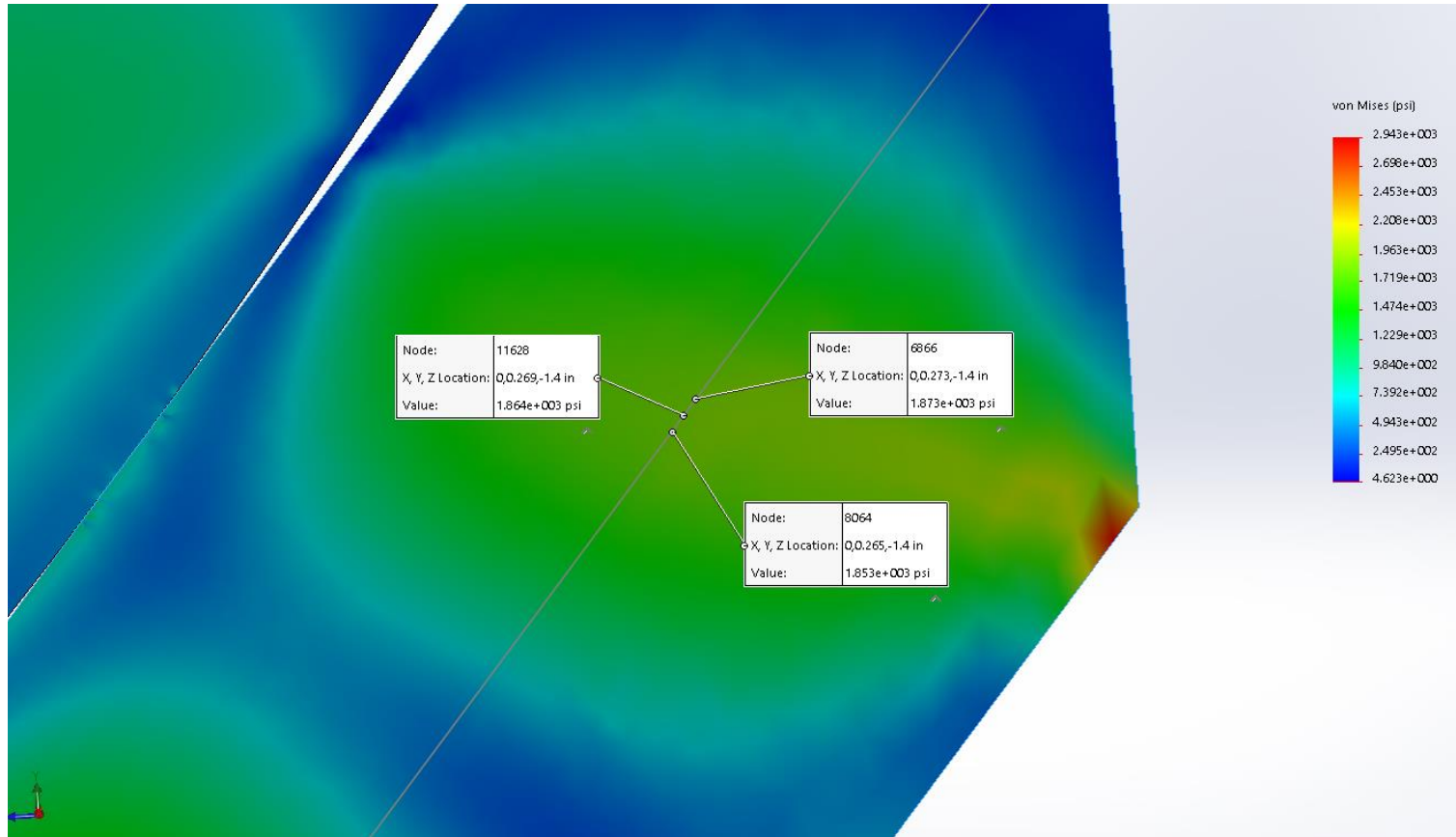


Figure 72 – A plot showing the probe of von mises stresses when a load of 1600lb-f (7117.2N) is applied

Figure 72 shows the probe of the stress plot when a load of 1600 lb-f (7117.2N) is applied. The stress plot contours are of the same shape as shown in the previous figures. The three points probed in the stress plot are all within a couple psi of each other defining a high stress region in the middle of the section of the seat component. The influence of the contact stress from the interaction between the ball and the seat has no impact on the stress found in the centre of the seat component. The stress raising effect of the corner of the seat has increased in its intensity but still does not have an effect on the outcome of the stress in the middle of the section of the seat component.

The results at each of the points probed in the previous figures have been collated and are shown in Table 22.

Pressure Load (lb-f [N])	Point 1 Stress (psi [N.mm ⁻²])	Point 2 Stress (psi [N.mm ⁻²])	Point 3 Stress (psi [N.mm ⁻²])
600 [2668.9]	757.7 [5.23]	754.9 [5.21]	747.6 [5.16]
800 [3558.6]	994.6 [6.86]	993.0 [6.85]	975.5 [6.73]
1000 [4448.2]	1239 [8.54]	1241 [8.56]	1229 [8.47]
1200 [5337.9]	1451 [10.00]	1432 [9.87]	1454 [10.03]
1400 [6227.5]	1652 [11.39]	1659 [11.44]	1655 [11.41]
1600 [7117.2]	1853 [12.78]	1864 [12.85]	1873 [12.91]

Table 22 – Tabulated stress values from probes of von mises stress plots at each load increment

In Figure 67 through Figure 72, where the stress values were shown being obtain by probing the von mises stress plot, an assessment of the figures was made. As these stress figures have been gained from probing the von mises stress plot of the middle of the seat component each of the values are taken from the nearest node to the location selected. Some of the nodes which were selected have values which are not in line with the greatest magnitude of stress at that location and therefore need to be removed from the data to avoid them influencing the average stress to be determined. The von mises stress data from probing the stress plots of each of the applied loads with the spurious values removed is shown in Table 23.

Pressure Load (lb-f [N])	Point 1 Stress (psi [N.mm ⁻²])	Point 2 Stress (psi [N.mm ⁻²])	Point 3 Stress (psi [N.mm ⁻²])
600 [2668.9]	757.7 [5.23]	754.9 [5.21]	-
800 [3558.6]	994.6 [6.86]	993.0 [6.85]	-
1000 [4448.2]	1239 [8.54]	1241 [8.56]	1229 [8.47]
1200 [5337.9]	1451 [10.00]	-	1454 [10.03]
1400 [6227.5]	1652 [11.39]	1659 [11.44]	1655 [11.41]
1600 [7117.2]	1853 [12.78]	1864 [12.85]	1873 [12.91]

Table 23 – Filtered stress values from probes of von mises stress plots at each load increment

To get a single value for the bending stress the values shown in Table 23 shall be mean averaged. By applying the mean average across this data it reduces the reliance on the data gained from a single node therefore reducing the possibility that this data could be influenced by effects localised around the specific nodal value used. The stresses have therefore been mean averaged to determine an average bending stress as shown in Table 24.

Pressure Load (lb-f [N])	Average Bending Stress (psi [N.mm ⁻²])
600 [2668.9]	756.3 [5.22]
800 [3558.6]	993.8 [6.85]
1000 [4448.2]	1236.3 [8.52]
1200 [5337.9]	1452.5 [10.01]
1400 [6227.5]	1655.3 [11.41]
1600 [7117.2]	1863.3 [12.85]

Table 24 - Average bending stress values determined from the results of the probe data

The results presented in Table 24 show the general trend that an increasing load applied to the component results in an increased bending stress within the seat component. While this general trend is visibly consistent across the data presented in Table 24 there are no means of quantifying it, therefore additional analysis must be carried out on the data to present it in a manner where it is possible to quantify the change in average bending stress. The following table, Table 25 determines the change in load and average bending stress between the loads assessed.

Pressure Load (lb-f [N])	Percentage Change in Load	Average Bending Stress (psi [N.mm ⁻²])	Percentage Change in Average Bending Stress
600 [2668.9]	-	756.3 [5.22]	-
800 [3558.6]	133	993.8 [6.85]	131
1000 [4448.2]	125	1236.3 [8.52]	124
1200 [5337.9]	120	1452.5 [10.01]	118
1400 [6227.5]	117	1655.3 [11.41]	114
1600 [7117.2]	114	1863.3 [12.85]	113

Table 25 - Percentage change in average bending stresses from probing von mises stress plots

From the results of the percentage changes determined in Table 25 it can be seen that the changes in load and the respective change in average bending stress are roughly equal throughout the loads which have been evaluated. While the trend is the larger the load applied the smaller the percentage change of both load and average bending stress it is not possible to make direct comparisons between various loads in the table. To make direct comparisons the magnitude of the load which is creating the scaling effect will need to be removed, in doing so the data shown in Table 26 is produced.

Pressure Load (lb-f [N])	Percentage Change in Load	Percentage Change in Bending Stress	% Change in Bending Stress per % Change in Load
600 [2668.9]	150	145	-
800 [3558.6]	133	131	98
1000 [4448.2]	125	124	99
1200 [5337.9]	120	118	98
1400 [6227.5]	117	114	97
1600 [7117.2]	114	113	99

Table 26 – Percentage change in bending stress per percentage change in applied load

When looking at the results shown in Table 26 the outcome from evaluating the percentage changes per percentage change in load the variance in the results is 2%. The small magnitude of the variance in the result in outputs presented demonstrates a highly aligned set of data across all the loads where this set of data can be used with confidence to derive and validate a theoretical model to describe the mechanics of the bending stresses in the seat component.

This section has presented a series of computational models in which the bending stresses in the seat have been determined from the analysis completed for each of the loads applied. The data from the analyses has been processed to remove spurious results which would skew the results of that dataset. The datasets for each pressure load are averaged to enable a single value to be the output from the analyses allowing a direct comparison to the results of a theoretical model.

The bending stresses presented in this section have been determined from the analyses completed, these results do not provide a description or a theoretical model which links the applied load to the bending stresses within the seat component. The bending stresses were not discussed beyond their effects in damaging the seat component should they pass the yield strength, therefore the any theoretical model will have to derived by modelling the computational model in a theoretical manner by applying relevant applicable models to achieve a compliant solution that links the applied load to the deflection of the seat.

5.2 Comparison of finite element analysis results to theoretical results

This section compares the results gained from the finite element analyses to those obtained through the numerical analysis of the theoretical model. Through the comparison of the sets of results it shall be possible to validate the theoretical models against the results gained from the computational models.

5.2.1 Pressure-load

This section compares the numerical outputs of the theoretical model describing the mechanics relating the applied load to the contact pressure in the seat component to the results from the computational model for the same condition.

Table 27 shows the average contact pressure results from both the theoretical model and the computational model. The additional column shown in Table 27 is the factor of difference between the two sets of results, this factor is determined by dividing the theoretical result by the computational result; the ideal outcome, which shows the agreement of both models is where the factor of difference is equal to one.

Pressure Load (lb-f [N])	Computational Results (psi [N.mm ⁻²])	Theoretical Result (psi [N.mm ⁻²])	Factor of Difference
600 [2668.9]	326.2 [2.25]	714.03 [4.92]	2.19
800 [3558.6]	417.6 [2.88]	865.15 [5.97]	2.07
1000 [4448.2]	517.3 [3.57]	1004.11 [6.92]	1.94
1200 [5337.9]	602.0 [4.15]	1144.44 [7.89]	1.90
1400 [6227.5]	685.7 [4.73]	1256.03 [8.66]	1.83
1600 [7117.2]	748.8 [5.16]	1373.33 [9.47]	1.83

Table 27 – Comparison of theoretical and computational average contact pressure by applied load

The average difference found between the theoretical and computational results was found to be 1.96. The factor of difference is greatest where the lowest load is applied to the models. The factor of difference becomes a consistent factor of difference at the applied loads of greater magnitudes, it is considered that the effects of the rounding of variables in the theoretical model has a greater effect on the outcome of the calculations when the values used in the calculations are of a smaller magnitude.

The factor of difference between the theoretical and computational models is such that there will need to be a degree of modification made to the theoretical model through the assessment of the assumptions made to ensure that the theoretical model produces valid results when compared to the computational model.

5.2.2 Seat Deflection

This section compares the numerical results gained from the theoretical and computational models assessed in the previous section and chapter where these models have been applied to the description of the deflection of the seat component with respect to the load applied to the floating ball valve geometry.

The following table, Table 28, shows the deflection results from both the computational model and theoretical calculation. The factor of difference in the table is determined by dividing the theoretical result by the computational one. For the models to match each other the factor of difference across the range of loads applied shall be equal to or approximately equal to 1.00.

Pressure Load (lb-f [N])	Computational Results (in [mm])	Theoretical Result (in [mm])	Factor of Difference
600 [2668.9]	0.0024 [0.061]	0.0065 [0.17]	2.71
800 [3558.6]	0.0031 [0.079]	0.0088 [0.22]	2.84
1000 [4448.2]	0.0037 [0.094]	0.0110 [0.28]	2.97
1200 [5337.9]	0.0042 [0.107]	0.0130 [0.33]	3.10
1400 [6227.5]	0.0048 [0.122]	0.0150 [0.38]	3.13
1600 [7117.2]	0.0052 [0.132]	0.0170 [0.43]	3.27

Table 28 - Comparison of theoretical and computational maximum seat deflection by applied load

When looking at the factors of difference presented in Table 28 these increase in magnitude as the applied load increases in magnitude. There is an average factor of difference of 3.00 between the theoretical results and the computational results with the theoretical results being of a greater magnitude. The assumptions made to establish this model appear to have overlooked a factor which is affecting the numerical evaluation of the theoretical model.

The magnitude of the factor of difference between the theoretical and computational models is such that the assumptions made in establishing the theoretical model shall be evaluated to determine where the factor of difference has come from and establish a modification to the theoretical model to enable the values determined by it to match those of the computational model.

5.2.3 Bending Stress

This section compares the theoretical and computational results of the bending stresses. Through the comparison of the numerical values it is possible to understand whether the established theoretical model is appropriate in its current form to describe the realistic mechanics shown by the computational model.

Pressure Load (lb-f [N])	Computational Results (psi [N.mm ⁻²])	Theoretical Results (psi [N.mm ⁻²])	Factor of Difference
600 [2668.9]	756.3 [5.22]	709.02 [4.89]	0.94
800 [3558.6]	993.8 [6.85]	945.92 [6.85]	0.95
1000 [4448.2]	1236.3 [8.52]	1181.97 [8.15]	0.96
1200 [5337.9]	1452.5 [10.01]	1418.87 [9.78]	0.98
1400 [6227.5]	1655.3 [11.41]	1654.93 [11.41]	1.00
1600 [7117.2]	1863.3 [12.85]	1890.99 [13.04]	1.01

Table 29 - Table showing the comparison of theoretical and computational bending stresses

When looking at the results compared in Table 29 a general trend can be seen where the factor of difference approaches 1.00 as the load increases. It is considered that the increase in the magnitude of the values used to determine the theoretical results at the higher loads has had the effect of reducing the effect of errors in the rounding of values which will have an effect on the theoretical value. The average factor of difference between the computational and theoretical values is 0.97. Considering the error due to rounding which is present in the theoretical results the correlation between the results of the computational and theoretical models is of a sufficiently high degree to consider the models a match. An area of concern is the lack of correlation in the deflection model in the previous section considering the same established model has been applied to both the deflection and bending stress variables.

5.3 Modification of theoretical models

This section takes the results of the comparisons made in the previous section between the theoretical data and the data from the computational models, where applicable it assesses the assumptions made to establish the theoretical models. By evaluating and where applicable modifying the assumptions in the theoretical models this facilitates the alignment in results of the theoretical and computational models.

5.3.1 Pressure-load

When the results of the computational model are compared to those of the theoretical model, it is found that the theoretical models results were on average approximately twice those of the computational model.

When establishing the theoretical model, the total axial load, F_{PL} , was separated into components acting on the seat in shear, F_{τ} , and in a sealing action, F_{SS} , as shown in Figure 73 below.

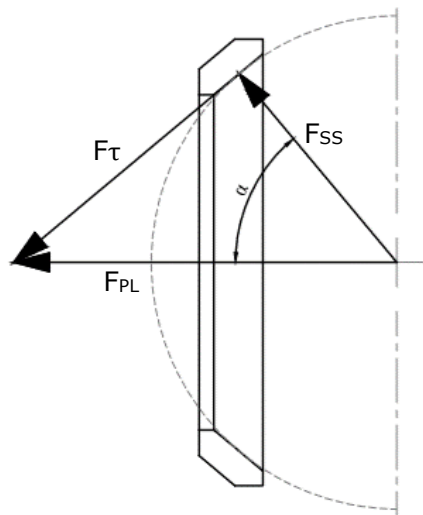


Figure 73 – Review of the load components

This assumption is still considered valid, however the action of the load in the sealing action is only considered to be acting on one side of the seat component. In reality the load F_{SS} will be acting over the same diametrically opposed areas at the same time, once the contact areas have been established. The action of the load over both sides of the seat will still be applicable even when the assembly is taken as a two-dimensional axisymmetric model.

To take into account the adjustment of the assumptions made in establishing the theoretical model the equation, Equation 32, where the contact pressure is determined will need to be modified. With the application of the modified assumption the equation to determine the mean contact pressure is updated as shown in Equation 38.

$$p_m = \frac{P}{4 \cdot a}$$

Equation 38 - Updated Mean Stress Equation

When applying this updated assumption to the theoretical model previously used the revised theoretical values are as shown in Table 30.

Pressure Load (lb-f [N])	Computational Results (psi [N.mm ⁻²])	Theoretical Results (psi [N.mm ⁻²])	Factor of Difference
600 [2668.9]	326.2 [2.25]	357.02 [2.46]	1.09
800 [3558.6]	417.6 [2.88]	432.58 [2.98]	1.04
1000 [4448.2]	517.3 [3.57]	502.06 [3.46]	0.97
1200 [5337.9]	602.0 [4.15]	572.22 [3.95]	0.95
1400 [6227.5]	685.7 [4.73]	628.02 [4.33]	0.92
1600 [7117.2]	748.8 [5.16]	686.67 [4.73]	0.92

Table 30 – Comparison of revised average computational contact pressures to analytical results by applied load

The results shown in the table above show the updated theoretical model reflects the computational model within to an acceptable level of accuracy. When the factors of difference shown in Table 30 are averaged the mean factor of difference is found to be 1.01, this much reduced factor of difference highlights the significant improvement in the accuracy of the modified assumptions applied to the theoretical model.

Applying the factor based off the updated assumptions to the maximum contact pressure, Equation 12, gives the following updated equation.

$$p_0 = \frac{P_1}{\pi \cdot a}$$

Equation 39 - Update Max. Contact Pressure (Pressure Load)

Due to the sensitivity of the computational model to variations from node to node, especially in the high stress areas, such as within the peak contact stress area probed results which would be required to determine the peak contact pressure would be unreliable. As the peak and mean stresses can be related to each other by a numerical relationship, as shown in the literature review, it is reasonable to apply the factor that was applied to the mean stress to the peak stress.

This section has taken the results of the comparison between the computational and theoretical models and the results gained and assesses considers the assumptions previously made which can be modified in order to address the differences identified previously. Through assessing the assumptions made in determining the contact pressure it was found that the sealing load is only considered to be acting over one face it is in contact with. When reviewing the interaction it was determined that once the contact half-widths have become established the load should be considered to be acting over both of these areas equally, in applying this assumption to the theoretical model the area related to the contact half-width was increased by a factor of two. In applying the factor of two to the theoretical model the results fall within an acceptable variance from the results obtained from the computational model.

5.3.2 Seat deflection

This section analyses the differences identified between the results of the theoretical model and finite element analyses. Through analysing the differences identified it is possible to modify the assumptions made to enable the theoretical model to accurately reflect the response of the seat as seen in the computational models.

The load applied to the seat component, acts over two surfaces at the same time however this is not taken into account in the original theoretical model. The application of this assumption to the theoretical model would be the first logical step to make in modifying the assumptions made. As there is not contact area considered in the determination of the deflection of the seat it would be appropriate to divide the applied load by two to replicate this effect. In applying the reduction of the applied load by two the following results, as shown in Table 31, are gained from the theoretical model.

Pressure Load (lb-f [N])	Computational Results (in [mm])	Theoretical Result (in [mm])	Factor of Difference
600 [2668.9]	0.0024 [0.061]	0.0033 [0.083]	1.38
800 [3558.6]	0.0031 [0.079]	0.0044 [0.111]	1.42
1000 [4448.2]	0.0037 [0.094]	0.0055 [0.139]	1.49
1200 [5337.9]	0.0042 [0.107]	0.0065 [0.166]	1.55
1400 [6227.5]	0.0048 [0.122]	0.0076 [0.194]	1.58
1600 [7117.2]	0.0052 [0.132]	0.0087 [0.222]	1.67

Table 31 - Comparison of the amended theoretical deflections to the computational results by applied load

The results shown in Table 31 do not show a significant improvement in the correlation between the computational and the theoretical results, the average factor of difference is found to be 1.52.

Considering the method of applying the load to the annular ring is not a point load as the model uses but by a spherical face, it is thought that taking this factor into account may more accurately reflect the realistic mechanics of the seat deflection. To take the spherical load into account it is proposed that the applied load which is divided by the contact diameter multiplied by pi to determine a load per unit length is further divided by pi making the equation as shown in Equation 40.

$$P_1 = \frac{F_{SS}}{\pi^2 \cdot D_{MS}}$$

Equation 40 - Revised load per unit length equation

Through the application of the revised load per unit length equation to the theoretical model for the determination of the seat deflection the results shown in Table 32 are obtained.

Pressure Load (lb-f [N])	Computational Results (in [mm])	Theoretical Result (in [mm])	Factor of Difference
600 [2668.9]	0.0024 [0.061]	0.0021 [0.053]	0.88
800 [3558.6]	0.0031 [0.079]	0.0028 [0.071]	0.90
1000 [4448.2]	0.0037 [0.094]	0.0035 [0.088]	0.95
1200 [5337.9]	0.0042 [0.107]	0.0042 [0.107]	1.00
1400 [6227.5]	0.0048 [0.122]	0.0049 [0.123]	1.02
1600 [7117.2]	0.0052 [0.132]	0.0055 [0.140]	1.06

Table 32 – Comparison of the revised theoretical deflections to the computational results by applied load.

The average factor of difference between the results from the computational model and the theoretical result is 0.97. Considering the finite element analysis model is a realistic model and the effect of rounding errors on the magnitude of the values which are being determined the modification of the applied load with respect to the deflection of the seat component is appropriate in consideration of the geometry of the components involved.

This section has taken the results of the comparison between the theoretical and computational models and considered the assumptions made previously to establish the model in order to revise the assumptions to establish a revised theoretical model where the result correlate to a higher degree. In applying the same assumption as on page 151 of section 5.3.1 it was found the results did not correlate with the computational results, the condition of the load acting over both the axisymmetric geometry is also already considered in the established equations applied. In modifying the applied load the spherical nature of the geometry which is applying the load is taken into account whereas the established model considers the load applied at a point location. Through the application of the modified applied load equation the correlation between the theoretical and computational results is vastly improved. Considering the differences in the values between the theoretical and the computational results as well as the magnitude of the figures involved the theoretical model developed in this section adequately describes the mechanics of the seat deflection with respect to the load applied to it.

This section takes the variations of the theoretical models developed in the previous section and by comparing them to the computational model determines the best model to be used to develop the theoretical model from. The theoretical model that best represents the mechanics of the seat described by the computational model is compared to the results of the computational model over the range of loads applied to it. The differences between the computational and theoretical results have resulted in a semi-empirical factor being derived to modify the theoretical equation to increase the accuracy of the theoretical models results when compared to the results gained from the theoretical model.

5.3.3 Bending Stress

The analysis of the difference between the computational and theoretical model for the relationship between the bending stress and the applied load showed a good correlation between both sets of data. As the correlation between the existing theoretical model and the computational results was high it is not required to amend the theoretical model to improve the description of the relationship between these variables.

5.4 Conclusions

This chapter takes the geometry of the floating ball valve seat and loadings applied to these components and develops a computational model representing the realistic response of the floating ball valve seat to validate the theoretical models describing the mechanics of the seat component.

The finite element analysis model was assessed for the contact pressures created in the seat component when a load is applied to it. Through applying the loads determined in the previous chapter to the computational model it was possible to determine the stress profile of the seat in contact with the ball. From establishing the stress profile in the contact half-width it is possible to evaluate the numerical data and then plot this data against the data gained from the analytical model to determine whether any trends were shown. From the evaluation of the data gained from the computational model it was found that the 400lb-f (1779.3N) load did not fit the trends shown by the other applied loads. In an effort to establish the minimum threshold to which the trend held with respect to the loads applicable to the seat component the analysis was re-run at 440lb-f (1957.2N). From the results of the 440lb-f (1957.2N) in addition to the previous data the trends were identified as being different with the low magnitude loads applied to the model. It was considered that there may be other theories governing the mechanics at these low magnitude loads, therefore the loads below 600lb-f (2668.9N) are considered outside of the scope of this thesis and are recommended as a topic of further work. From the remaining data it was possible to establish trends between the applied loads and the contact pressures measured and from the data determine a set of data against which it would be possible to assess the results of the theoretical model. Following the contact pressure, the deflection and bending stresses were measured from the finite element analyses and the results processed in the same manner, identifying trends and determining data against which the theoretical models can be assessed.

With a set of realistic data available the numerical results from the theoretical model are compared to the results from the computational model. Through comparing the results of the theoretical model to the computational model it is possible to determine whether the theoretical model accurately reflects the realistic mechanics of the floating ball valve seat under the same applied loads. For the theoretical models describing the contact pressure and deflection of the seat it was found that the numerical results did not match the computational results and these were therefore not representative of the realistic mechanics of the seat. Where the results differed, the differences were highlighted. In the case of the bending stresses of the seat component the theoretical model matched the data obtained from the computational model, from these results it was possible to say that the theoretical model adequately described the realistic bending stresses found in the seat component.

From the differences in the contact pressure and deflection models it is possible to modify the theoretical models describing these elements of the seat to more accurately reflect the realistic data obtained from the computational model. In modifying the theoretical models the assumptions made in applying the models to the geometry of the floating ball valve seat and the assumptions made by the established models applied were both considered before adjusting these assumptions to suit the computational results. Any changes in assumption

were justified prior to making the change to the theoretical model. On making the assumptions the theoretical models were re-calculated and the results compared against those of the numerical model. With the numerical and theoretical models providing data that matched within reasonable tolerances the theoretical models are considered validated by the realistic data of the computational models.

In achieving the computational models and sets of data from them this chapter has established the realistic response to the seat component in the level of detail required to validate the theoretical models established in the previous chapter. When validating the initial theoretical models, a number of assumptions in these models were found to be results which were not in-line with those of the computational model. On reviewing the assumptions made the theoretical models were re-evaluated and found to be valid against the realistic data from the computational models. With validated theoretical models describing the fundamental mechanics of the floating ball valve seat it shall be possible to formulate equations from which a floating seat can be designed.

Chapter 6 – Development of a Design Methodology

In this chapter the theoretical models which were modified and validated in the previous chapter are developed from describing the mechanics of the floating ball valve seat to being able to be used for the design of a floating ball valve seat. As identified in the literature review a ball valve seat is typically designed based on a load generated by the pressure acting inside the valve, and a pre-load of the seat component against the ball. Through the theoretical equations describing the mechanics it shall be possible to establish the equations through which the components are design and then to assemble these components into a coherent design methodology. With a design methodology established it will be possible to evaluate a case study to demonstrate the design methodology being applied to the design of a floating ball valve seat.

6.1 Proposal of design equations

This section makes use of the theoretical models from the previous chapter which describe the mechanics of the floating ball valve seat, these equations link the fundamental properties which describe the key functions of the seat. The inputs and outputs of the theoretical models may not be appropriate for the design of a seat, through developing these theoretical models the inputs and outputs to these equations can be developed in a way whereby it is possible to use the mechanics defined by the theoretical equations to design a floating ball valve seat.

6.1.1 Pressure Load

In this section the theoretical model describing the mechanics are used to describe a set of design equations through which it is possible to design the pressure-dependant part of the seat component.

The action of the pressure on the ball and seat geometry is a key part of the design of the floating ball valve seat design. The mean seat contact diameter of the seat as shown in Figure 74 must be measured to determine the area over which the pressure in the valve acts over.

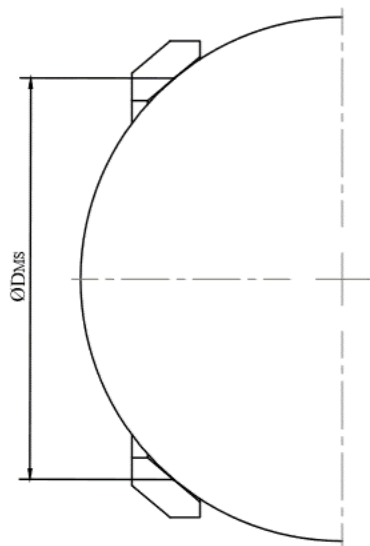


Figure 74 – Design Pressure-Area Definition

The mean seat contact diameter is defined as the point of contact between the ball and the seat. The mean seat contact diameter is taken as the diameter which defines the area over which the pressure acts. To define the load that the pressure and the area bound by the mean diameter creates Equation 41 shall be applied. Equation 41 combines the pressure in the valve with the mean seat contact diameter, whereas in the previous chapters the applied load applied to the valve seat was defined as a set of load this equation determines the load which is applied by the pressure being considered.

$$F_{PL} = P \cdot \left(\frac{\pi \cdot D_{MS}^2}{4} \right)$$

Equation 41 - Design Pressure Load

With the loads generated by the pressure applied to the valve determined the relative geometry of the ball and seat components acting in the axial direction of the valve. The load generated by the pressure is acting in the direction of the bore of the seat (and valve), the portion of this load which is acting on the seat face needs to be determined.

The factor which determines the portion of the axial load, F_{PL} , which is acting on the seat face in the action of creating a seal between the two components is determined by the angle of the seat. The seat angle is defined as the angle between the two faces in contact with the ball when a section through the seat is taken. The seat angle is measured as shown in Figure 75.

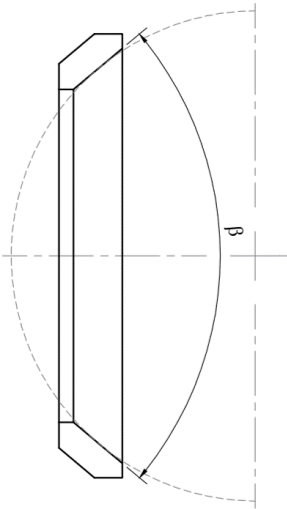


Figure 75 - Seat Angle for Design Calculations

The angle used to determine the component of the axial load, F_{PL} , which is acting perpendicular to the seat face and therefore acting to create a sealing load is determined from the seat angle, β , as measured in Figure 75. From the seat angle, β , the complimentary angle will need to be defined, this angle is the angle shown in Figure 76.

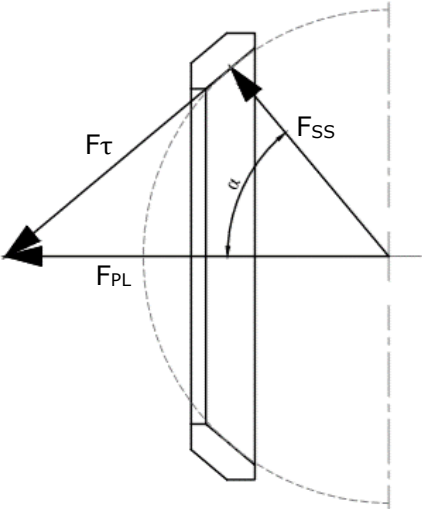


Figure 76 – Applied load components used for the determination of sealing mechanics

The complimentary angle, α , shown in Figure 76 is determined through the application of Equation 42. The complimentary angle is used to determine the proportions of the axial load, F_{PL} , which is acting on the seat in sealing, F_{SS} , and in shear, F_{τ} . The determination of the complimentary angle is achieved through the evaluation of Equation 42.

$$\alpha = 90 - \frac{\beta}{2}$$

Equation 42 - Design Complementary Angle

In the case of determining the sealing load applied to the seat the only component of the axial load that needs evaluating is that of the sealing load, F_{SS} . The determination of the sealing load, F_{SS} , is evaluated through the application of the complimentary angle and trigonometry to the geometry of the valve as was previously shown in Figure 76. The numerical evaluation of the sealing load is achieved through the application of Equation 43.

$$F_{SS} = F_{PL} \cdot \cos \alpha$$

Equation 43 - Design Sealing Load (Pressure Component)

With the sealing load, F_{SS} , acting on the seat determined by the application of Equation 44 the load needs to be converted into a format which is able to be used for the evaluation of the contact pressure, as achieved in the previous chapter. To convert the applied load into a usable format from which the contact pressure can be determined the load needs to be converted to a load per unit length. To convert the sealing load, F_{SS} , to a load per unit length it needs to be divided by the length over which the load is distributed. The diameter which the load is in contact with is the mean seat contact diameter, D_{MS} , therefore the reduction of the load to a load per unit length can be achieved through the division of the load by the mean seat contact diameter multiplied by pi. The conversion of the sealing load to a load per unit length is shown in Equation 44.

$$P_1 = \frac{F_{SS}}{\pi \cdot D_{MS}}$$

Equation 44 - Design Contact load per unit length (pressure)

Before processing the sealing load to determine the contact pressure in the seat by the action of the sealing load per unit length acting on the seat the material properties of the seat need to be considered. The material properties of the seat, particularly the material modulus of elasticity must be considered, and the reduced material modulus found. From the reduced material modulus the it is possible to apply contact mechanics equations. The reduced modulus of the seat component material is determined in accordance with Equation 45.

$$E^* = \frac{1 - \nu^2}{E}$$

Equation 45 – Reduced Material Modulus

With the determination of the reduced material modulus and the applied load in the form of a load per unit length it is possible to apply the contact mechanics equation for determining

the contact half-width. The contact half-width is determined in accordance with Equation 46, this equation determines numerically the dimensions of the contact between the ball and the seat components.

$$a_1 = \sqrt[3]{\frac{4 \cdot R \cdot P_1}{\pi \cdot E^*}}$$

Equation 46 - Half-contact width (Pressure Load)

With the evaluation of the contact half-width the dimensions of the contact between the ball and seat components has been defined it is possible to determine the maximum contact pressure. Through the review of the literature conducted earlier it was found that the parameter defined in a contact that aims to achieve a seal which determines whether a seal is achieved or not is the maximum contact pressure. To evaluate whether a seal has been achieved through the application of the pressure to the valve the maximum contact pressure needs to be valuated, this can be achieved through the application of Equation 47.

$$p_{01} = \frac{P_1}{\pi \cdot a_1}$$

Equation 47 - Design max. contact pressure

From the maximum contact stress determined it is possible to evaluated the whether a seal has been achieved or not, this is done through comparing the maximum contact pressure calculated to the maximum contact pressure required to achieve a seal. To determine the maximum contact pressure the media being sealed needs to be considered. When sealing a liquid the following relationship is applied to determine the maximum contact pressure required. Based on the sealing models from the literature review sealing gas and liquid will require the application of different theoretical models to determine the minimum contact pressure required to achieve a seal between the ball and seat. The sealing model to seal a gas is shown by Equation 48.

$$q = \frac{6.8 - 2.7 \cdot b}{1.8 - 0.7b} \cdot P_g^{0.12+0.4 \cdot b}$$

Equation 48 – Sealing contact pressure in terms of seal contact width (Bozhko, Kalabekov, Vinogradov, & Denisov, 1992)

The required sealing stress to seal the against a gas is determined based on the contact width, 'b', and the pressure of the gas, 'Pg' as shown in Equation 48. The width of the contact will therefore need to be based on the half-contact width 'a' with a multiple of two applied to increase it to the full width of the contact, making this substitution gives Equation 49 to be used to determine the required contact pressure to seal against a gas.

$$q = \frac{6.8 - 5.4 \cdot a}{1.8 - 1.4 \cdot a} \cdot P_g^{0.12+0.8 \cdot a}$$

Equation 49 - Sealing contact pressure based on half-contact width

The pressure of the gas being sealed shall be the same as the pressure acting over the area bound by the contact between the ball and seat components as it serves both purposes of energising the ball and being the medium that is required to be sealed against.

As discussed on page 53 in the literature review the requirement to seal a liquid is considered much simpler than that for a gas whereby the sealing stress is simply required to be at least greater than that of the medium being sealed. With legacy valve designs it is generally considered that a factor should be added to this figure to give a safety margin, typically this factor is 50%, considering the more accurate nature of this approach in determining whether a seal is formed or not this factor shall be reduced. To ensure the valve does achieve a seal a safety factor of 5% shall be added to the sealing stress in this instance. This safety factor ensures that the contact pressure determined by the design method is greater than the pressure to be sealed while taking into account the variances which could affect the outcome of this result. To ensure there are no manufacturing tolerances which effect the ability of the valve to affect a seal between the ball and the seat the analysis shall be completed with the worst case dimensions used, this would typically be the ball at minimum limit, the seat at minimum thickness limit and the retaining parts, i.e. body and adaptor at maximum limits where they retain the seats. At these material conditions the interference between the ball and seat components would be at the minimal condition, where the provision for achieving a seal would be at it worst.

With the maximum contact pressure in the seat component determined for the pressure applied it shall be compared against the criteria for evaluating whether a seal is formed or not; where the medium is gas Equation 50 shall be used, for pressures where the medium is a liquid Equation 51 shall be used.

Equation 50 shall be evaluated using the pressure of the gas acting within the valve as well as the previously calculated half-contact width that correspond to the relevant pressure.

$$p_{gs} = \frac{6.8 - 5.4 \cdot a_1}{1.8 - 1.4 \cdot a_1} \cdot P^{0.12+0.8 \cdot a_1}$$

Equation 50 - Design gas sealing stress

Equation 51 shall be evaluated using the pressure of the liquid acting within the valve, it shall be evaluated for the relevant pressure it is being compared to.

$$p_{ls} = 1.05 \cdot P$$

Equation 51 - Design liquid sealing stress

The required contact pressures shall be compared to the calculated maximum contact pressures previously calculated. Where the maximum contact pressure is greater than the required contact pressure it is considered that a seal will form under those conditions.

This section takes the theoretical equations describing the mechanics of the relationship of the applied load and the contact pressure and applied them to the floating ball valve seat in a manner which determines whether the pressure-load applied to the seat achieves a seal between the ball and seat components.

6.1.2 Initial Deflection – Seat Preload

This section takes the theoretical model describing the deflection of the seat with regards to the load applied. From the equations and theoretical models established in chapter 5 which describe the deflection of the seat this section creates a set of design equations to describe the load applied to the seat by a deflection of the seat thereby creating a preload.

The deflection of the seat in terms of applied load is defined on pages 153 and 154 in the previous chapter by a validated theoretical model. The model was validated against the computational model through which the realistic response of the seat can be quantified. When designing a floating ball valve, like other types of ball valves, a preload is typically applied to the seat component in addition to the pressure load determined in the previous section. When designing a valve, it is impractical to select a deflection and design a seat which has the corresponding deflection designed into the components; this is impractical due to the irrational nature of the output of the theoretical model. To allow a floating ball valve seat preload to be designed into the components in a rational way the preload will have to be determined in terms of the selected deflection of the seat component. To achieve the design equation proposal of this section the validated theoretical model needs to be defined in terms of deflection rather than load applied.

The equation which defines deflection in terms of applied load as verified in the previous section is shown by Equation 52.

$$y = M_{rb} \cdot \frac{r_0^2}{D} \cdot F_2 + Q_b \cdot \frac{r_0^2}{D} \cdot F_3 - w \cdot \frac{r_0^2}{D} \cdot G_3$$

Equation 52 - General seat deflection equation

Equation 52 is an equation form Roarks formulas of stress and strain however where specific conditions are applied to these models they can be simplified from the equation shown. Through applying the general equation to the Table 11.2 case 1c model the following conditions are applicable through the edge constraints selected. The conditions applied to the general model when applying it to the Table 11.2, case 1 c model are:

$$Y_b = 0$$

$$M_{rb} = 0$$

These conditions applied to the model shows that there is no deflection of the annular ring at point b (the inner edge of the annular ring), this is shown through $y_b=0$. The condition $M_{rb}=0$ demonstrates that there is no bending moment found at the inner edge of the annular ring. The same conditions apply to the outside edge of the annular ring, where there is no deflection or bending moment, however these variables are not evaluated in the equation used to determine the deflection of the annular ring. By applying these conditions to Equation 52 it allows for the removal of the first term of the equation as this is multiplied by M_{rb} and therefore the entire term is equal to 0, therefore Equation 53 is formed from the application of the conditions to Equation 52.

$$y = Q_b \cdot \frac{r_0^2}{D} \cdot F_3 - w \cdot \frac{r_0^2}{D} \cdot G_3$$

Equation 53 - Simplified general seat deflection equation

To establish the load applied in terms of deflection the equation needs to be re-arranged to make the applied load per unit length, 'w', the subject of the equation. To achieve the re-arrangement of the equation the following steps are taken. Common factors have been identified in the terms on the right-hand side of Equation 53, this allows the equation to be factorised as shown in Equation 54.

$$y = (Q_b \cdot F_3 - w \cdot G_3) \cdot \left(\frac{r_o^2}{D}\right)$$

Equation 54 - Factorised general seat deflection equation

By dividing through by common factors and subtracting the term 'Q_b.F₃' it is possible to isolate a single term including the applied load per unit length, 'w', as shown in Equation 55.

$$\frac{y \cdot D}{r_o^2} + Q_b \cdot F_3 = w \cdot G_3$$

Equation 55 - Re-arranged general seat deflection equation

Finally dividing through by the term 'G₃' allows the applied load per unit length 'w' to be isolated, making it the subject of the equation, as shown in Equation 56.

$$w = \frac{y \cdot D}{r_o^2 \cdot G_3} + \frac{Q_b \cdot F_3}{G_3}$$

Equation 56 - Load per unit length in terms of deflection

Equation 56 gives the load per unit length acting on the seat in terms of the deflection of the seat component itself. By creating a load per unit length output this load can be input into the contact mechanics equation to determine the half-contact width and therefore the contact pressure the load per unit length generated by the initial deflection creates. While the load per unit length can be used to determine the contact pressure through the application of contact mechanics as seen in the previous section the function of this equation is to determine the load per unit length created by the pre-load of the seat therefore when designing the floating ball valve seat this value should be evaluated with the load per unit length generated by the pressure-load. The development of the theoretical model in this section allows an initial deflection to be selected which is a rational number and therefore relatively simple to be designed into the components when they interact on assembly. From the initial deflection designed into the floating ball valve seat through the application of the calculations in this section it is possible to determine the preload this applies to the contact between the ball and seat components.

6.1.3 Bending Stress

This section looks to apply the theoretical model describing the bending stresses in terms of the applied load to the design of a floating ball valve seat design. The theoretical model describing the bending stresses which was validated in the previous chapter against the computational model which provides a realistic model of the interaction of the ball and seat component and the bending stresses developed within the seat during this interaction. Through the application of the theoretical model describing the bending stresses in the seat as shown in the previous the stress in the seat can be analysed and where the loads applied to the seat do not allow the stress in the seat to surpass the yield strength. Should the stress in the seat component pass the yield strength the seat would become deformed and would therefore no longer function in the manner in which it is designed.

In the theoretical model the bending stress in the seat component was determined through the evaluation of the bending stress formulas from Roarks formula for stress and strain, table 11.2 case 1c. In the application of this numerical model and associated formulas in the previous chapters it was seen and verified that the calculation of the equivalent stress from the principal stresses determined from the table 11.2, case 1c model matched the values established from the computational model. In establishing a match between the theoretical model and the computational model this validates the method through which the bending stresses are determined as being representative of those in the realistic situation analysed.

While the theoretical model has been validated against the realistic mechanics shown in the computational model the fundamental nature of the bending stress in the function of the floating ball valve seat means that a greater degree of safety is required to ensure the seat component does not deform when in service. The extra degree of safety applied to the bending stresses determined can be seen in Equation 57 where a factor of 10% has been included in the previously validated equation.

$$\sigma_v = 1.1\sqrt{\sigma_1^2 - \sigma_1\sigma_2 + \sigma_2^2}$$

Equation 57 - Equivalent stress in seat component

Where the stress has been determined by both the radial and tangential moments as shown by Equation 58 and Equation 59.

$$\sigma_1 = \frac{6 \cdot M_t}{t^2}$$

Equation 58 – Radial stress in seat component

$$\sigma_2 = \frac{6 \cdot M_r}{t^2}$$

Equation 59 – Tangential stress in seat component

In establishing the application of the equations relating to the bending stresses to the design of the floating ball valve seat the final component of the mechanics is applied to the component in a manner through which the design of the component may be achieved. Through the calculation of the bending stress from the applied load to the seat component it is possible to ensure the bending stresses in the developed design is maintained within acceptable stress limits that allows the seat to function as intended.

6.2 Develop of design methodology

In this section the proposed design equations of the previous section are formed into a design methodology. The design methodology takes the proposed equations from section 6.1.2 and chapter 5 and arranges them in a manner through which the design of the seat is analysed and developed to ensure it meets the requirements laid out previously. As discussed in the literature review the design of a valve of any type is typically an iterative process, therefore the methodology of this section is also an iterative methodology.

6.2.1 Initial Analysis (Step 1)

The initial step in designing the floating ball valve seat is to identify the spherical diameter of the ball component. The design of the ball component in a floating ball valve is outside of the scope of this thesis but is typically determined by the application of numerical methods.

With the ball diameter established a sketch of the seat component where the sealing face runs at a tangent to the spherical face of the ball is established. The initial design of the seat includes no pre-load and therefore no deflection of the seat component on assembly. The seat design must fit within the envelope of the valve housing and enable the location of a firesafe seat and other related features to be located in the required locations about the seat component.

At this point of designing the seat the initial analysis of the seat is undertaken. To determine the function of the seat, first the media and pressures which define the conditions under which it is required for the seat to seal under must be defined. With the conditions for sealing defined the application of the numerical method for the analysis of the seat can be started.

The contact pressure generated by each of the pressures at each of the defined sealing conditions shall be assessed as the initial analysis. The mean contact diameter, measured off the drawing of the ball and seat assembled as the diameter at which tangential contact is made between the ball and seat component, as show previously in Figure 74 is applied to the following equation with each of the applied pressures in-turn to establish a set of pressure loads which are acting on the seat.

$$F_{PL} = P \cdot \left(\frac{\pi \cdot D_{MS}^2}{4} \right)$$

Equation 60 - Initial pressure load

With the range of applied pressure loads determined, these loads need to be converted from axial loads to the component of the axial load which is acting on the seat face in the sealing action. To establish the component of the axial load the seat angle selected must be measured. The seat angle, β , is measured from the seat component in accordance with Figure 75. From this seat angle the complimentary angle, α shall be found by the application of Equation 61.

$$\alpha = 90 - \frac{\beta}{2}$$

Equation 61 - Complimentary angle of sealing load component

With the complimentary angle of the sealing load component determined, the application of this value to Equation 62, this equation needs to be evaluated for each value of the applied pressure load, F_{PL} determined in previously.

$$F_{SS} = F_{PL} \cdot \cos \alpha$$

Equation 62 - Sealing load component of the pressure load

Each of the pressure loads are now converted into sealing loads generated by the specific pressures applied to the valve. To make these pressure sealing loads applicable to the Hertz contact mechanics the pressure sealing loads will need to be converted to pressure sealing loads per unit length. The conversion from pressure sealing load to pressure sealing load per unit length is achieved through the application of Equation 63, this conversion uses the mean seat contact diameter measured off of the model earlier in the design methodology.

$$P_1 = \frac{F_{SS}}{\pi \cdot D_{MS}}$$

Equation 63 – Pressure sealing load per unit length

With the pressure sealing load per unit length determined the outstanding variable to be established to allow the evaluation of the Hertz contact mechanics is based on the material properties of the seat component. The reduced modulus is determined in accordance with Equation 64, this requires the material properties of the seat material to be established and available for use.

$$E^* = \frac{1 - \nu^2}{E}$$

Equation 64 – Seat material reduced material modulus

With the reduced material modulus and the pressure sealing load per unit length established these values can be applied to the Hertz contact mechanics along with the radius of the ball component. The contact half-width shall be determined for each of the pressure sealing loads per unit length determined from Equation 63. When considering the inputs to this calculation the pressure sealing load per unit length is the only variable which will change between the evaluations made for each of the applied pressures as the geometry of the valve does not change depending on the pressure applied to the valve.

$$a_1 = \sqrt[3]{\frac{4 \cdot R \cdot P_1}{\pi \cdot E^*}}$$

Equation 65 – Applied pressure load, contact half-width

From the contact half-widths determined from Equation 65 and the pressure sealing loads per unit length determined from Equation 63 it is possible to determine the maximum contact pressure for each of the conditions that the floating ball valve seat is required to operate in. The evaluation of the maximum contact pressure under the pressure sealing load is determined by the application of Equation 66, this calculation shall be completed for each of the pressures that the floating ball valve seat is considered to seal at.

$$p_{01} = \frac{P_1}{\pi \cdot a_1}$$

Equation 66 – Applied pressure max. contact pressure

With the maximum contact pressures determined for each of the conditions the floating ball valve seat is required to seal at it is necessary to determine whether the valve will seal with the calculated contact pressures. Where the conditions for sealing are specified on a gaseous media Equation 67 shall be used to determine the sealing stress required to achieve a seal. To determine the required sealing stress the pressure of the gaseous media, P_1 , is required as well as the contact half-width determined by Equation 65 for the condition being assessed.

$$p_{gs} = \frac{6.8 - 5.4 \cdot a_1}{1.8 - 1.4 \cdot a_1} \cdot P^{0.12+0.8 \cdot a_1}$$

Equation 67 – Applied pressure gaseous media sealing stress

The evaluation of the sealing stress shall be carried out in accordance with Equation 67 for each condition where the media applied to the valve is gaseous. Where the media applied to the valve is a liquid the required sealing stress shall be determined by the use of Equation 68, to evaluate this equation the pressure of the liquid that is applied to the valve under each condition with a liquid media is required.

$$p_{ls} = 1.05 \cdot P$$

Equation 68 – Applied pressure liquid sealing stress

With the maximum contact pressures determined in accordance with Equation 66 and the required sealing stress for gases and liquids determined by Equation 67 and Equation 68 respectively it is possible to determine whether a seal is achieved or not. Where the maximum contact pressures are greater than the required sealing stress a seal is achieved, where this is not the case a seal has not been achieved. Typically, without a preload from the seat component a seal will not be achieved, therefore it is expected that all the designs will fail to achieve a seal and step 2 will be required to increase the maximum contact pressure. However, where valves do meet the sealing requirements without the addition of a preload step 2 would not be applicable.

6.2.2 Application of a Seat Preload (Step 2)

This step is an iterative step whereby the initial deflection of the seat is selected and the load per unit length is calculated and combined with the pressure load. By combining the preload and the pressure load it is possible to determine whether the combined loads generate a contact pressure of sufficient magnitude to affect a seal between the ball and seat components under the applied pressures and media.

To determine the preload which is applied to the seat the dimensions of the seat component as previously defined as the minimum material condition on page 100 and page 101 must be measured from the seat component. With the dimensions and material properties of the seat component determined these values must be applied to the formulas found in Appendix 5 to determine the constants and factors shown in Equation 69. On completion of the calculation of the constants and factors a deflection value shall be chosen at which the seat shall be set to generate the preload. The seat deflection, calculated constants and factors are applied to Equation 69 to determine the load per unit length that is generated by the initial deflection of the seat component.

$$w = \frac{y \cdot D}{r_0^2 \cdot G_3} + \frac{Q_b \cdot F_3}{G_3}$$

Equation 69 - Load per unit length in terms of deflection

This load does not achieve a seal on its own, the preload is to be combined with the pressure-load to determine the combined load from which the sealing stress is generated. To evaluate the combined load step 3 shall be followed.

6.2.3 Evaluation of the Combined Load (Step 3)

In this, the third step, the pressure-load that determined in step 1 from the pressures which are applied to the valve is combined with the specified preload of the previous step. This part of the methodology determines whether the action of the combined loads on the floating ball valve seat is sufficient to achieve a seal between the ball and seat components.

The first part of evaluating the combined load is the determination of the total load applied to the seat, the total load applied to the seat, P_3 , is found through the application of Equation 70 to the results of Equation 63 and Equation 69. The output of the two equations combined are in load per unit length form, the load per unit lengths applicable to each of the pressures applied to the valve need to be combined with the preload determined to determine a total load for each sealing condition identified. Due to the inputs to the equation the output of Equation 70 is in the form of a load per unit length.

$$P_3 = P_1 + w$$

Equation 70 - Total Load Summation

Both the pressure load per unit length, and the deflection load per unit length are the loads acting perpendicular to the seat face therefore meaning that no calculation of components of an axial load is required. By combining the load per unit lengths determined previously the value of the total load per unit length is in the correct format to allow it to be applied directly to the Hertz contact mechanics equations. The first variable from Hertz contact mechanics to be determined is the contact half-width, this is determined by the application of Equation 71. The same reduced modulus and ball radius, as used in step 1, shall be applied, and a contact half-width will need to be determined for each of the sealing conditions identified.

$$a_3 = \sqrt[3]{\frac{4 \cdot R \cdot P_3}{\pi \cdot E^*}}$$

Equation 71 - Contact Half-space, Total Load

With the contact half-width determined it shall be possible to find the maximum contact pressure in the seat for each of the sealing conditions previously identified. Equation 72 allows the evaluation of the maximum contact pressure when the load per unit lengths determined in Equation 70 and the contact half-width evaluated in Equation 71 are applied. The inputs previously determined for each of the sealing conditions will need to be applied to Equation 72 to find the maximum contact pressure for each of the sealing conditions identified.

$$p_{03} = \frac{P_3}{\pi \cdot a_3}$$

Equation 72 – Max. contact pressure developed under the combined load

As with step 1, the maximum contact pressures determined from the previous equation must be compared against a required sealing stress to establish whether a seal is achieved or not. The sealing conditions identified and evaluated must be separated for the purposes of determining the required sealing stress. The required sealing stress for a gaseous media is determined by a different method to that of a liquid media. The application of Equation 73 is required to determine the required sealing stress of a gaseous media.

$$p_{gs} = \frac{6.8 - 5.4 \cdot a_3}{1.8 - 1.4 \cdot a_3} \cdot P^{0.12+0.8 \cdot a_3}$$

Equation 73 – Combined load gaseous media sealing stress

With the required sealing stress for the gaseous media conditions determined, the same values must be determined for the sealing conditions where the media applied to the valve is a liquid. To determine the sealing stress for the conditions where the media is a liquid the pressure of the liquid at the sealing conditions is applied to Equation 74.

$$p_{ls} = 1.05 \cdot P$$

Equation 74 – Combined load liquid media sealing stress

With the required sealing stresses determined for each of the sealing conditions, in accordance with Equation 73 and Equation 74 these values must be compared to the maximum contact pressures determined from Equation 72. Where the maximum contact pressure is greater than the required sealing stress for each condition the floating ball valve seat is considered to seal against the ball component. Where there is at least one sealing condition where the required sealing stress is greater than the maximum contact pressure the process completed in step 2 shall be repeated for an increased deflection of the seat, following the load per unit length increase from the increase in deflection the process completed in this step shall be re-evaluated with the increased load per unit length values. Should all the maximum contact pressures be greater than the required sealing stresses then the design shall move onto the next step, step 4 of the design methodology.

6.2.4 Validation of Bending Stress in Seat Component (Step 4)

Following the achievement of the previous step, step 3, in achieving a seal in the floating ball valve seat, this step verifies that in achieving the seal the seat does not yield and therefore become permanently deformed. By becoming deformed the seat will fall outside of the specified requirements and cease to function as it has been designed to.

To determine the bending stress in the component first the bending moments applied to the seat must be calculated. These bending moments for both the radial and tangential conditions require variables and constants to be calculated from the dimensions and loads applied to the seat component. When evaluating the variables and constants required the maximum applied load from step 3, 'P₃', is applied, the value of this shall be the greatest value determined from all of the identified sealing conditions. When all the variables and constants have been determined the values shall be applied to Equation 75 and Equation 76 to calculate the bending moments.

$$M_r = \theta_b \cdot \frac{D}{r} \cdot F_7 + Q_b \cdot r \cdot F_9$$

Equation 75 - Simplified Radial Moment Equation

$$M_t = \frac{\theta \cdot D \cdot (1 - \nu^2)}{r} + \nu \cdot M_r$$

Equation 76 - Tangential Moment Equation (Young & Budynas, Roark's Formulas for Stress and Strain, 2002)

Once the bending moments have been evaluated, the bending moments are combined with the thickness of the seat component to determine the principal bending stresses. The radial and tangential bending stresses are determined by the application of Equation 77 and Equation 78 respectively.

$$\sigma_2 = \frac{6 \cdot M_r}{t^2}$$

Equation 77 - Principal radial bending stress in seat component

$$\sigma_1 = \frac{6 \cdot M_t}{t^2}$$

Equation 78 - Principal tangential bending stress in seat component

From the principal stresses calculated it is possible to determine an equivalent stress, the equivalent bending stress combines both the stresses acting in different directions to determine a single value for the bending stresses in the seat component. The bending stress is determined through the application of the principal bending stresses to Equation 79.

$$\sigma_v = 1.1 \sqrt{\sigma_1^2 - \sigma_1 \sigma_2 + \sigma_2^2}$$

Equation 79 - Equivalent bending stress in seat component

The equivalent bending stress is compared to the yield strength of the material used for the construction of the floating ball valve seat. Should the equivalent bending stress be less than the material yield strength then the seat is considered as an acceptable design. Should the yield strength of the seat material be less than the equivalent bending stress, then the seat design will need to be modified to enable it to meet the criteria of this step. Should the dimensions of the seat component in contact with the ball need to be modified then the process shall start from step 1. Should the modification of the seat not affect the dimensions of the seat component in contact with the ball, typically thickness only, then the methodology should be started from step 2.

6.2.5 Determination of Valve Torque (Step 5)

The functional performance defined and analysed through the application of the previous 4 steps in the design methodology. This step takes the information generated by the preceding steps and utilises that information to determine a theoretical torque prediction. This step shall be considered as a supplemental calculation to the design methodology.

As discussed in the literature review and shown in Table 4 there is currently a partially complete theory in place for the determination of a floating ball valves operating torque, however the static seat torque component is undefined. Equation 21 and Equation 22 show it is possible with the application of Hertz contact mechanics to determine the resistance ('power loss') of the seat.

To begin with Equation 21 and Equation 22 shall be combined together with the application to the floating ball valve design made in the literature review to give Equation 80.

$$\text{Seat load} = \mu \cdot P_e \cdot a \cdot \pi \cdot d_{MS}$$

Equation 80 - Seat frictional load equation

This equation is only considering the static load acting on the ball as set by the preload of the seat, the preload of the seat was determined in step 2 by Equation 69. Equation 80 only considering one seat at the moment it is assumed that the second seat will provide an equal and opposite load holding the ball in equilibrium; the load of both seats shall be addressed at a later point in this design method.

The preload, w , from Equation 69 is applied to Hertz contact mechanics it is possible to determine the contact width required to be applied to Equation 80. The following equation shows the determination of the half-space width in accordance with load per unit length, w , and Hertz contact mechanics:

$$a_2 = \sqrt[3]{\frac{4 \cdot R \cdot w}{\pi \cdot E^*}}$$

Equation 81 - Contact half-width developed from the application of the seat preload

To make this contact width applicable to Equation 80 it will need to be doubled as shown in Figure 21 the half-space width is only half the total contact width, therefore applying this to Equation 80 gives Equation 82.

$$Seat\ load = 2 \cdot \mu \cdot P_e \cdot \left[2 \cdot \left(\sqrt{\frac{4 \cdot w \cdot R}{\pi \cdot E^*}} \right) \right] \cdot \pi \cdot d_{MS}$$

Equation 82 – Static seat load including Hertz contact half-width

The effective contact pressure, P_e , shall also be determined by using Hertz contact mechanics and load per unit length, w , by substituting them into a modified version of the contact pressure equation from Table 2 as shown in Equation 83.

$$P_e = \frac{w}{\pi \cdot a_2}$$

Equation 83 - Effective contact pressure from Hertz contact mechanics from preload

The equation to determine the effective contact pressure is combined with the modifications made earlier by to the seat sealing contact pressure model to bring it in-line with the realistic computational model against which the theoretical model is validated. Following the evaluation of the static seat load, the static seat load needs to be combined with the other factors that affect the design of the valve as shown in Table 4 of section 2.2.5 to create the full torque for the valve when evaluated as full assembly.

6.2.6 Design Methodology Flowchart

The following flowchart takes the methodology laid out over the previous sections and shows it in the form of a flowchart. By presenting the methodology as a flowchart the interaction of the processes, inputs and outputs can be easily identified and the process easily followed.

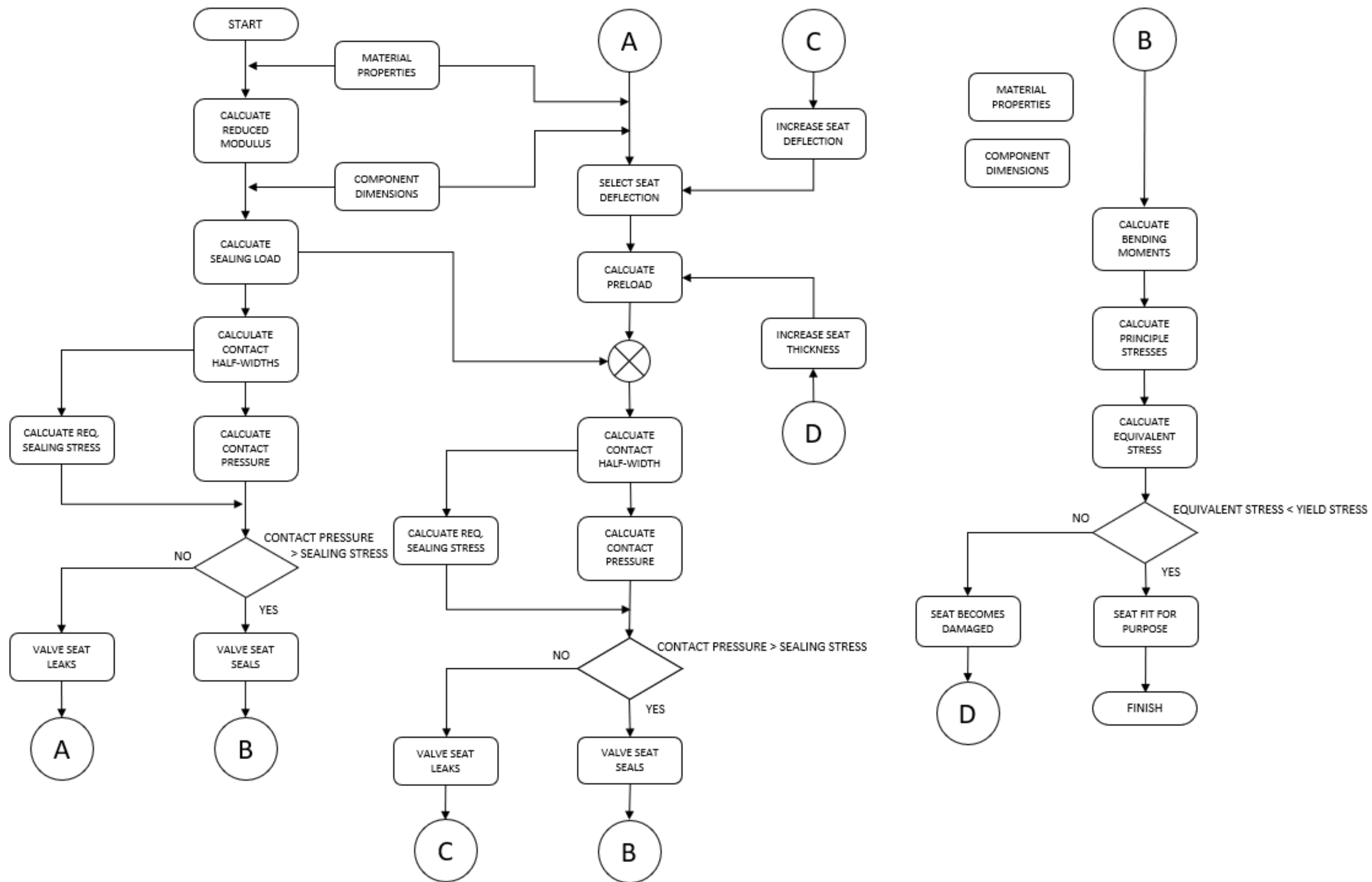


Figure 77 - Flowchart of the design methodology

The flowchart shows the design methodology described in sections 6.2.1, 6.2.2, 6.2.3, 6.2.4 and 6.2.5 in a visual format. From this flowchart it is possible to see the iterative process much clearer than from the previous section describing the methodology. The design methodology shown in the flowchart evaluates the floating ball valve seat design and in doing so determines whether the seat design will achieve a seal or not, whether the seat will become damage while in-service or not and what the predicted operating torque of the valve is. This process is highlighted as being an iterative process where parts of the process are repeated to if they fall outside of the requirements to enable the parameters to be adjusted allowing the design to achieve the desired outcomes.

Through the development of a design methodology it is possible to apply the equations developed to the design of a floating ball valve without applying differential equations, or complex numerical methods and without specialist knowledge being a pre-requisite to understand the full set of principles which govern the outputs of the design methodology.

6.3 Application of design methodology to a case study

In this section the design methodology shown in Figure 77 is applied to a case study of differing dimensions to those used to derive the original methodology. Through applying the design methodology to a case study it validates the functionality of the design methodology in achieving the outputs desired to assess the design of the floating ball valve seat. As the previous sections were based off of historical 'legacy' data in the form of the ball diameter and the housing dimensions were designed in imperial units, the design created in this section is not based on any historical design data and therefore shall be completed using metric units only.

The developed design methodology is to be applied to an initial geometry and then through the application of iterative process shown in the flowchart of the previous, refine the design to the optimal solution. The initial geometry of the valve used in the case study is shown in Figure 78.

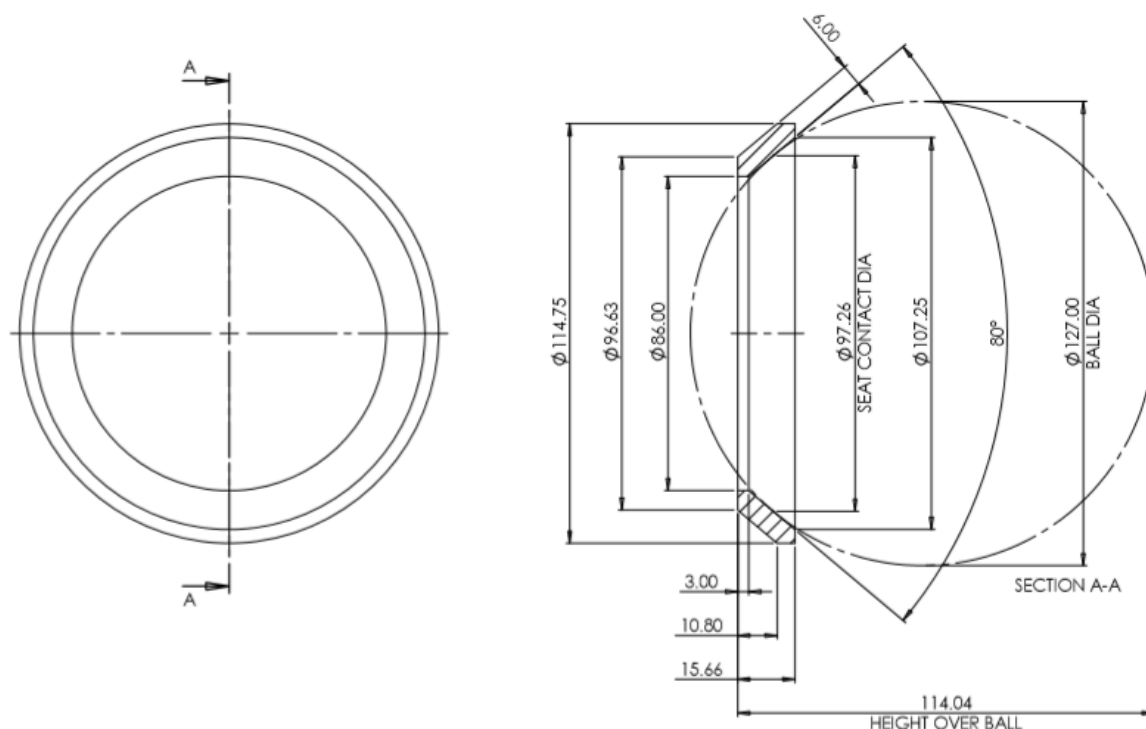


Figure 78 - Dimensions of seat and ball component for case study

The dimensions of the components are applicable to a 3" ASME Class 150 Floating ball valve. The design of the ball component is outside of the scope of this thesis, therefore a typical ball size has been used. In arriving at these dimensions, the ball was the initial starting point with the component defined through the application of the established numerical models to the materials and pressures considered to arrive at the size used for this design. The seat component was designed through the selection of the common seat angle with the previous work completed in this thesis, from this a point of contact the size of the seat was designed to fit outside the boundary of the profile of the firesafe seal and within the boundary of the typical seat pocket for a valve of this size and rating. The thickness of the seat was selected to maintain proportionality of the seat component, it is expected through the application of the design method to the seat component that the thickness may require modification to allow for the management of the stress developed within the seat itself.

The first step of the design method is to determine the contact pressure developed in the seat component through the application of pressure to the valve. The evaluation of the case study shall consider the valve is pressurised to the maximum cold-rated pressure of a Class 150 valve, 19.0 Barg (1.9N.mm⁻²) this applied pressure is in the form of a liquid acting on the valve. By applying the first equation the load the pressure generates in the axial direction by acting over the ball and seat component geometries is determined, this is shown in Equation 84.

$$F_{PL} = P \cdot \left(\frac{\pi \cdot D_{MS}^2}{4} \right) = 1.9 \cdot \left(\frac{\pi \cdot 97.29^2}{4} \right) = 14,124.7\text{N}$$

Equation 84 - Case study initial pressure load

Following the determination of the axial load acting on the seat it is required to determine the component of this axial load which is acting on the seat in a sealing function. To allow for the calculation of the sealing component the angle of the component must be determined from the seat geometry, to do this the seat angle is applied to Equation 85.

$$\alpha = 90 - \frac{\beta}{2} = 90 - \frac{80}{2} = 50^\circ$$

Equation 85 - Case study sealing load component angle

With the angle of the component calculated from Equation 86 it is possible to combine this with the axial load determined in Equation 84 and apply the equations of the next step of the process, as shown by Equation 86, through which the sealing load acting on the seat component is determined.

$$F_{SS} = F_{PL} \cdot \cos \alpha = 14,124.7 \cdot \cos 50^\circ = 9,079.2\text{N}$$

Equation 86 - Case study sealing load component of the pressure load

To convert the sealing load component to a value to be used in the applied Hertz contact mechanics part of the design methodology the sealing load component needs to be converted to a load per unit length. The sealing load per unit length is found through the application of the mean seat contact diameter and the sealing load component in the next calculation as shown in Equation 87.

$$P_1 = \frac{F_{SS}}{\pi \cdot D_{MS}} = \frac{9,079.2}{\pi \cdot 97.27} = 29.70\text{N} \cdot \text{mm}^{-1}$$

Equation 87 - Case study sealing load per unit length applied from pressure load

Reduced modulus of seat material would be determine as the next step in allowing the application of Hertz contact mechanics to the design methodology. As the reduced modulus of the seat material has been previously determined and the same material as used previously is being applied to the design of this component there is no need to re-evaluate the reduced modulus. The reduced modulus shall be taken as the value of 713.64 N.mm⁻², this was determined in the calculations performed previously. With the sealing load per unit length and the reduced modulus available the next part of step 1 of the analysis can be completed by evaluating the contact half-width, shown in Equation 88.

$$a_1 = \sqrt[3]{\frac{4 \cdot R \cdot P_1}{\pi \cdot E^*}} = \sqrt[3]{\frac{4 \cdot 63.5 \cdot 29.70}{\pi \cdot 713.64}} = 1.498 = 1.50\text{mm}$$

Equation 88 – Case study contact half-width under pressure load

With the sealing load per unit length and contact half-width determined from the previous analysis the final analysis to be completed for the given geometry is the evaluation of the maximum contact pressure, this is shown in Equation 89 for the case study being evaluated.

$$p_{01} = \frac{P_1}{\pi \cdot a_1} = \frac{29.70}{\pi \cdot 1.50} = 6.31\text{N}\cdot\text{mm}^{-2}$$

Equation 89 – Case study max. contact pressure under pressure load

With the maximum contact pressure in the seat component established the last calculation of step 1 is to evaluate whether the seat will create a seal against the applied pressure. As the fluid applied to the case study is considered to be water the equation applied uses a factor applied to the pressure to determine whether a seal is created between by the seat or not. The required sealing stress in the seat is determined through the application of the liquid pressure to the design methodology as shown in Equation 90.

$$p_{ls} = 1.05 \cdot P = 1.05 \cdot 1.9 = 2.00\text{N}\cdot\text{mm}^{-2}$$

Equation 90 – Case study required liquid sealing stress

With the calculations completed for step 1 it is possible to determine whether a seal has been achieved between the ball and seat components. The condition for achieving a seal as well as the comparison of the results of Equation 89 and Equation 90 are shown below.

$$P_{ls} > P_{01}$$

Therefore, applying the values calculated in this step:

$$P_{ls} = 2.00 > P_{01} = 6.31$$

The result of comparing the requires sealing stress against the maximum contact pressure for the condition analysed means that a seal is formed by the sealing rules applied by the application of pressure alone to the valve geometry of the case study.

As the floating ball valve seat analysed by this section has achieved a seal by the application of the pressure alone there is no requirement to assess the geometry in accordance with step 2. Step 2 would add additional load to achieve the required sealing stress, if it were applicable. As there is no additional load required and therefore generated by step 2 there is no requirement for step 3. Step 3 combines the load generated from the applied pressure, (step 1), with the load generated by an initial deflection, (step 2) and evaluates the contact pressure this generates, with the additional load being equal to zero

step 3 would be equal to step 1 if the evaluation were to be carried out, therefore making it a redundant step in this case study.

With the theoretical maximum contact pressure determined from the design methodology, the model used in the previous chapters was modified to the dimensions of the ball and seat used in the case study. Through evaluating the case study with finite element analysis, it is possible to create a realistic reaction of the floating ball valve seat component with the applied load taken from the calculations of the case study. In establishing the model for the case study the same process was followed as previously completed for the preceding chapters where finite element analysis is applied. With the same constraints and mesh applied to the model as previously used the results gained from the analysis are shown in Figure 79.

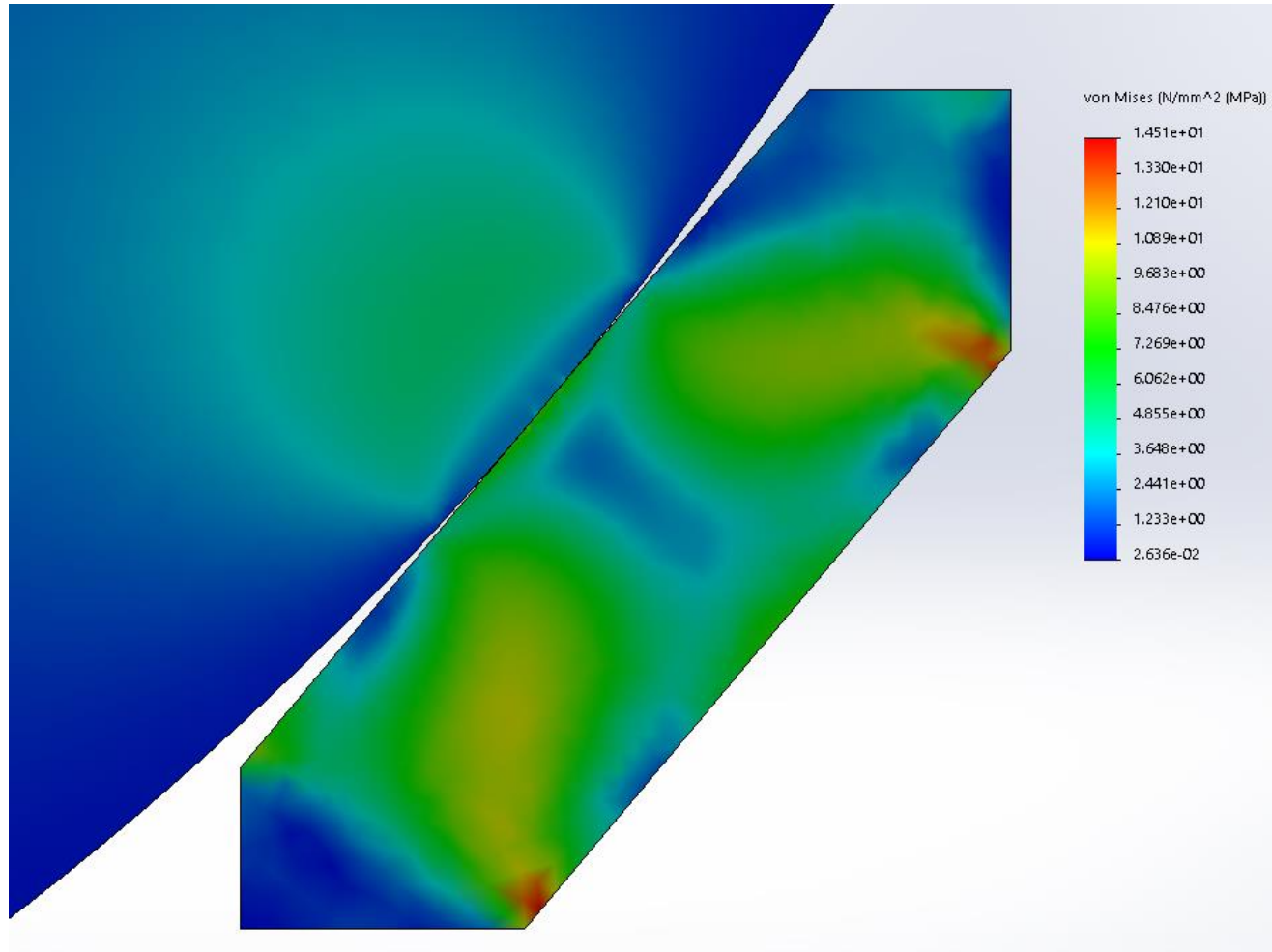


Figure 79 - Von Mises stress plot with case study geometry and applied loads

The results shown in the von mises stress plot of Figure 79 presents a non-uniform distribution of the stresses, as seen in the previous plots. The profile of the stress generated in the ball component once again matches the stress profiles predicted in metal components by Hertz contact mechanics. To facilitate the comparison of the theoretical results to the computaional ones the point of contact and nodes to the left and right of the point of contact were probed giving the 6.883N.mm^{-2} , 6.724N.mm^{-2} , 6.738N.mm^{-2} respectively. These values probed from the stress plot demonstrate that the results gained are in accordance with the theoretical values predicted.

The three values from the results of the analysis of the computational model shall be averaged to increase the accuracy of the value reported and compared with theoretical result. By sampling the point of contact and the nodes to each side the point of contact an average of the stress values at this point will have the highest magnitude of all the values as predicted by the theoretical equations, in addition using three nodes rather than the single node reduces the possibility of stress raisers at a particular node effecting the results gained from the analysis.

Node	Computational Results (N.mm ⁻²)
Node 1	6.883
Node 2	6.724
Node 3	6.738
Average Nodal Value	6.782

Table 33 - Case study max. contact pressure finite element analysis results

When the theoretical value, 6.310N.mm⁻², is compared with the average of the three most central nodes there is found to be a 7.5% variance between the two values with the computational results being of the higher value. Considering the small sample taken from the taken from the computational model, the small magnitude of the variance as well as the theoretical value being less than the computational value it is considered that the theoretical result provides a method that gives a sufficiently accurate representation of the realistic mechanics to allow the design to be completed with confidence that the outcome will meet the requirements. The small quantity of the nodes sampled represent the central location of contact between the ball and the seat it is possible there may be a localised stress raiser effecting these results making them slightly higher than predicted. While there is a possibility of error from the small sample, increasing the sample size reduces the representation of the sample of being the maximum contact pressure at the point of contact. With the variance being 7.5% and the contact pressure from the computational model being higher of the results this leads to the inclusion of a degree of conservatism when the design methodology is applied to the design of a floating ball valve, however the level of conservatism is not so great as to create a seat component which falls significantly far from the optimal design solution.

Following the achievement of a seal between the ball and the seat components, step 4 of the design methodology verifies that the seat component will not become damaged through the application to the previous design. The check on whether the seat becomes damaged is completed through the evaluation of the bending stress in the seat component.

To apply the calculations for step 4 of the design methodology additional dimensions of the seat component are required to define the annular ring dimensions which are to be assessed. The additional dimensions required are provided through measuring the case study seat component and are shown in Figure 80.

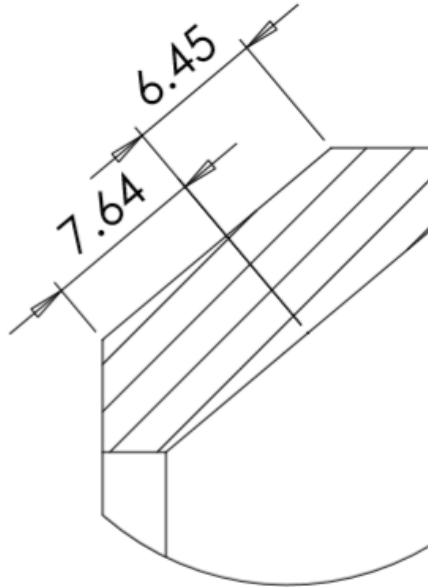


Figure 80 - Figure showing radial distances of the case study annular disc

The dimensions shown in Figure 80 equate to the internal and external radial dimensions from the point of contact to the extremities of the flexible region of the seat component. From the dimensions measured, 7.64mm is the internal radial width and 6.45mm is the external radial width. Both the dimensions measured must be combined with the diameter from Figure 78 to determine the dimensions for analysis, the determination of the geometry of the equivalent annular ring to be assessed is shown in the following equations.

$$a = \frac{D_{MS}}{2} + r_a = \frac{97.26}{2} + 6.45 = 55.08\text{mm}$$

Equation 91 - Outer radius of case study seat

$$b = \frac{D_{MS}}{2} - r_b = \frac{97.26}{2} - 7.64 = 40.99\text{mm}$$

Equation 92 - Inner radius of case study seat

$$r = \frac{D_{MS}}{2} = \frac{97.26}{2} = 48.63\text{mm}$$

Equation 93 - Radial load location of case study seat

From the dimensions determined in Equations 91, 92 and 93, it is possible to evaluate the bending stresses in the seat component for the case study. For the purposes of clarity the calculation of each of the constants and variables required to evaluate the radial and tangential moments of the bending equation are not presented. When applying the required information, the material properties applied to the case study are consistent with the previous work of this thesis as with the contact pressure calculation, to the bending moment equations the results for the case study are gained, as shown in Equation 94 and Equation 95.

$$M_r = \theta_b \cdot \frac{D}{r} \cdot F_7 + Q_b \cdot r \cdot F_9 = -0.009 \cdot \frac{12843.9}{48.63} \cdot 0.134 + 4.95 \cdot 48.63 \cdot 0.196 = 46.75$$

Equation 94 - Radial moment of case study seat

$$M_t = \frac{\theta \cdot D \cdot (1 - \nu^2)}{r} + \nu \cdot M_r = \frac{0.0013 \cdot 12843.9 \cdot (1 - 0.47^2)}{48.63} + 0.47 \cdot 46.75 = 22.25$$

Equation 95 - Tangential moment of case study seat

With the evaluation of moments complete when applying the case study loads to the geometry of the case study seat component when described as an annular ring it is possible to evaluate the principle stresses in the seat component. The principle stresses are evaluated by the application of Equation 96 and Equation 97.

$$\sigma_2 = \frac{6 \cdot M_r}{t^2} = \frac{6 \cdot 46.75}{6^2} = 7.792 \text{ N} \cdot \text{mm}^{-2}$$

Equation 96 – Principle radial bending stress in seat component

$$\sigma_1 = \frac{6 \cdot M_t}{t^2} = \frac{6 \cdot 22.25}{6^2} = 3.708 \text{ N} \cdot \text{mm}^{-2}$$

Equation 97 – Principle tangential bending stress in seat component

Following the determination of the principle stresses in the seat component these are combined to give the equivalent bending stress in the seat component. The evaluation of the equivalent bending stress component in the seat is completed by the application of Equation 98.

$$\sigma_v = 1.1 \sqrt{\sigma_1^2 - \sigma_1 \sigma_2 + \sigma_2^2} = 1.1 \sqrt{3.708^2 - 3.708 \cdot 7.791 + 7.791^2} = 7.425 \text{ N} \cdot \text{mm}^{-2}$$

Equation 98 - Equivalent bending stress in seat component

The application of the determination of the bending stresses through design methodology established in this thesis provides a value of $7.425 \text{ N} \cdot \text{mm}^{-2}$. When the value for the bending stress is compared to the von mises stress plot shown in Figure 79 it can be seen that in the region where the bending stresses are present and the stress raising effects created due to the constraints applied to the corners of the seat component are not influencing the stresses shown the values fall within the range of $7.269 \text{ N} \cdot \text{mm}^{-2}$ to $8.476 \text{ N} \cdot \text{mm}^{-2}$ as shown on the scale of the stress plot. The application of probing the stress plot would not be able to improve the comparison between the theoretical and computational values due to the small bands where measurements can be taken from and the coarseness of the mesh in this area. Through the general correlation between the values determined by both methods and the previous accuracy of the results obtained by this theoretical method it is possible to consider the results for bending stresses as being valid.

The torque prediction step, step 5, of the design methodology determined only the static seat torque component of the overall theoretical torque model. Without the application of step 2 previously there is no static seat torque developed from the preload of the case study as there is no preload value to evaluate this value from. As the theoretical model developed in this thesis is not applicable to this case study there is no benefit gained from evaluating the predicted torque of the case study floating ball valve.

In this section the design methodology of the previous section has been applied to a case study. The case study valve is of different dimensions to the valve from which the design methodology was originally derived, therefore should the design methodology be applied to case study and give results which are able to be validated thereby validating the design methodology developed in this thesis.

Through the application of the design methodology to the case study geometry for the ball and floating ball valve seat at the pressure specified for the case study the design methodology was able to predict the maximum contact pressure in the seat component as well as the bending stresses within the seat component. Through the application of finite element analysis to a model of the case study components with the same methodology used as used previously in this thesis it was possible to obtain results for both the contact pressure and the bending stress within the seat component. The theoretical values for contact pressure showed a slight variance when compared to the computational results. Despite showing slight variances between the theoretical and computational results, the methods used in calculating and sampling these results are considered to account for a significant portion of the difference therefore considering the design methodology valid for determining the contact pressure. From comparing the bending stresses determined from the design methodology to the von mises stress plot the theoretical value was found to fit within the appropriate range of values shown in the stress contour to be considered as a valid model in determining the bending stresses. Through the comparison of the theoretical values to the results gain from the computational model for the case study it is appropriate to consider the design methodology proposed in this thesis as a valid methodology.

6.4 Conclusions

This chapter has brought together the knowledge created and validated in the previous chapters into a design methodology which has been further validated through the use of a case study.

The knowledge created in the previous chapters was shown to describe the mechanics of the fundamental mechanics which govern the function of the floating ball valve seat component, this knowledge was not in a format which could be used for the design of the seat component. Through the first section of this chapter the knowledge created in previous chapters was combined with established knowledge with respect to achieving a seal and arranged in such a way as to facilitate the use of the proposed equations to design the seat component. The pressure load component knowledge was developed into a model where the application of pressure to the geometry of the valve can be evaluated to determine whether the contact pressure this develops in the seat component will enable a seal to be achieved between the ball and seat components. The determination of a seal is determined through the adaption of sealing theories to include contact half-width based sealing widths to allow a direct comparison between the contact pressure and the sealing stress required. The deflection of the seat was identified as utilising inputs and giving outputs which are difficult to apply to the design of the floating ball valve seat component. By re-arranging the equations relating the deflection of the seat component to the load applied to the seat it was possible to allow for the designing of a pre-determined compression of the seat component to be designed into the valve and the preload this generates determined from the design method. By modifying the deflection model allowing the load to be determined from the deflection this allows for the design of the initial deflection to be achieved through the use of rational number allowing for the creation of parts which can be manufactured in a repeatable fashion giving a robust output from the design methodology. The bending stress theoretical model was adapted in the application to the floating ball valve seat as the description of the bending stresses from the applied loads was found to be the most accurate of all the models. To enable the bending stresses to add conservatism into the

calculation to increase the robustness of the seat designed a factor of 10% was added to the mechanics previously established. The design equations proposed by this section create the knowledge through which it would be possible to design a floating ball valve seat component, this knowledge has previously been shown to be limited in its availability and completeness.

From the design equations proposed in the previous section, the second section of this chapter develops a design methodology through which it is possible to design a floating ball valve seat. This section identifies the application of each of the proposed design equations to a method where the inputs and outputs of the design equations are arranged and combined to achieve the design of a floating ball valve seat. In arranging the equations into a method this takes the design equations from a set of equations which could be applied in part or as a whole and creates a method which when followed provides a complete analysis of the fundamental features and mechanics of the seat providing a robust design solution. The achievement of a design methodology is also the creation of new knowledge which as seen from the literature review is very limited in its availability to date. Previously proposed design methods for floating ball valve seats showed the derivation of the equations alone with little applicability and even less methodology behind the application to the design.

The design methodology developed in the preceding section has been applied to a case study to validate the outputs of the design methodology against a computational model of the same geometry. Through the application of the design methodology to a case study it allows for the testing of the methodology with geometry that is different from that which it was developed from. Through the application of the design methodology to the case study geometry values for the contact pressure in the seat and the bending stress of the seat were found, this successful application of the design methodology shows the application of the design methodology to be successful in evaluating the design of a floating ball valve seat. To validate the results of the case study a computational model was created through the use of finite element analysis. The results gained from the finite element analysis are compared with the results from the application of the design methodology the correlation of the results demonstrated that the design methodology still produced valid results when applied to the different geometry of the case study and is therefore a valid design methodology.

This chapter has established a set of design equations which develop the mechanics previously established in this thesis into equations which determine the outputs from which the floating ball valve seat component can be defined. These equations are developed in a manner which provides a completeness of the description of the fundamental design features of the seat component to a level which was not previously available. The design methodology developed by from the design equations provides a process through which it is possible to design a floating ball valve seat component while assessing each of the fundamental features determined by the seat design, the level of analysis provided by the method of this chapter has not been seen previously to the level of completeness demonstrated in this thesis. With the design methodology established this methodology was applied to a case study to demonstrate the validity of the process, the correlation between the design methodology when applied to the case study and the analytical results from evaluating the case study with finite element analysis demonstrate that the design methodology provides valid outputs. Through the work completed in this chapter the aim of establishing a design methodology has been achieved both in completeness and in the validity of the design methodology itself.

Chapter 7 - Summary

This chapter provides a summary of the work conducted in this thesis highlighting the research aims and major achievements as well as providing recommendations for future work to be conducted to further the work completed.

7.1 Research Problem Synopsis

The purpose of undertaking this research was to establish an optimised design methodology for a floating ball valve seat component. As there was limited literature available to fully describe the mechanics of the seat component and less literature available on how to design the floating ball valve seat component based on established mechanics.

The research completed in this thesis has taken a set of abstract theories and combined them in a manner through which it has been possible to develop a practical design methodology. Work has been undertaken to establish a theoretical relationship between the fundamental aspects which describe the mechanics of the floating ball valve seat, these relationships were initial relating an applied load to the contact pressure on the sealing surface, the deflection of the seat component as well as the bending stresses within the seat component.

Each of the fundamental aspects which describe the function of the floating ball valve seat is described through the application of theoretical models to the geometry and loads involved in the relevant components. With the theoretical models established, the geometry and material properties of the floating ball valve seat and ball have been modelled in a 3D CAD software. Through the application of finite element analysis to the 3D CAD model of the valve components it was possible to develop a realistic computational model from which the data describing the effects of the mechanics of the floating ball valve seat can be obtained. By numerically evaluating the theoretical models established and processing the data obtained from the finite element analysis models it is possible to compare the theoretical model against the realistic scenario. From the differences between the theoretical models and the computational results it was possible to evaluate these differences and identify the assumptions made in applying the theoretical models to the floating ball valve seat which need to be modified to enable the theoretical models to describe the mechanics accurately. The set of validated theoretical models which describe the mechanics of the floating ball valve are developed into a set of equations through which the mechanics of the floating ball valve are used in combination with inputs to evaluate the design of the seat component. The design equations which have been derived to evaluate the design of the floating ball valve seat are developed and combined into a single design methodology. Through the application of the design methodology to the design of a floating ball valve seat an optimised and functional component can be achieved. To validate the developed design methodology it is applied to a case study, the application of the methodology shows its application in a real-world design scenario highlighting the knowledge created by this thesis as this sort of applied methodology was unavailable prior to this work being completed.

7.2 Research Aims and Major Achievements

With the intention of this thesis being to establish and optimised methodology for the design of the floating ball valve seat component it is required that this be achieved in a number of steps. Each step towards achieving the outcome of this thesis is described as an aim; to achieve the overall outcome three aims were identified. The three aims identified are discussed in term in the following section.

1. Development of mechanistic theoretical models based on established theoretical methods.

The initial aim of this thesis was to develop theoretical models from established methods which describes the mechanics of the fundamental features of the floating ball valve seat. To identify the mechanics applicable to the functions of the seats the design was broken down into the three components that were identified through the literature review as being the components used to design the ball valves seats in general. By separating out the load applied due to pressure, the generation of a preload through seat deflection and the bending stresses in the seat it was possible to identify the mechanics that need to be described to define the components used to design the seat component. The pressure load was determined to be related to the achievement of the sealing stress with the sealing stress described by Hertz contact mechanics, the linking of the applied load to a theoretical model describing the sealing stress through numerical methods is a major achievement which has not previously been achieved. Previously assumptions have been made about the area of the seat and ball components which are in contact with each other, compared to the method described in this thesis there is significant possibility of error in making assumptions compared to being able to calculate the parameters such as contact area. The application of theoretical models to describe the deflection and bending stresses of the components involved the derivation and simplification of the model in certain aspects to allow for the application of the appropriate theoretical models. Through the application of established theoretical models, it was possible to describe the function of the floating ball valve seat in terms of an applied load for each of the fundamental features of the floating ball valve seat. Through the literature review it can be seen that there are limited theoretical descriptions of any of the mechanics of the floating ball valve seat available. Through the achievement of this aim and the development of mechanistic theoretical models for the floating ball valve seat it has demonstrated that it is possible to describe the mechanics of the floating ball valve seat in a purely theoretical manner.

2. Validation of theoretical models through finite element analysis.

The application of finite element analysis to the geometry and material properties of the floating ball valve seat which is the subject of this thesis allows for a realistic set of numerical results to be gained from an analytical tool with a very high degree of accuracy. Through the development of the finite element analysis model and the data extracted from the model it is possible to validate the theoretical models developed under the previous aim. Through the validation of the theoretical models against the realistic computational data it was possible to evaluate where differences existed between the two sets of numerical data. From the differences between the two sets of data, the assumptions made to apply the established models to describe the floating ball valve seat mechanics were reviewed and where applicable modified to enable the numerical results from the theoretical model to correlate with those of the computational model. From the modification of the assumptions applied to the theoretical models the finalised theoretical models are considered validated against the data extracted from the computational model. The use of a computational model

creating realistic data describing the mechanics of the floating ball valve seat has been seen used in previous works, however in these previous works the data was generated, analysed and then used to modify the model before repeating the process; the work completed in this thesis takes the data obtained from the computational model and uses it to validate assumptions made in the theoretical models. By applying the data from the computational model to validating the mechanics defined in the theoretical it allows for the development in understanding the mechanics governing the floating ball valve seat. In developing the validated theoretical models the understanding of the mechanics which govern the features of the floating ball valve seat component can be fully understood.

3. Development of a design methodology

In achieving the previous aim a set of validated theoretical models were developed which describe the mechanics of the floating ball valve seat; while the description of the mechanics in terms of a applied load is a significant achievement it cannot be utilised in the development of the design methodology. The modification of the validated theoretical models to allow for the use in designing the floating ball valve seat was undertaken, the objective of this is to arrange the models in such a way as the inputs and outputs are taken from the various inputs to the design process and the outputs inform the next stage of the design or provide a validation of the completed stage of the design. In creating the design methodology the equations proposed in the previous section were developed into a coherent design methodology where the method could be followed through from an initial inception of the valve to a completed and valid design. Following the development of a methodology, the methodology is applied to a case study, through applying the methodology to the case study a measure of validation of the process through which the seat is designed is achieved. By achieving the design methodology and performing a case study on that methodology this aim achieves a complete design methodology based on valid theoretical models which is shown to be applicable to the actual design of a floating ball valve seat.

In achieving the aims of this thesis, a significant amount of knowledge has been both generated and applied to the subject area. Through generating and applying this knowledge it has allowed for the optimisation of the design of a floating ball valve seat.

7.3 Recommendations

Based on the outcomes of this thesis this section makes a number of recommendations for how to further develop the understanding of the subject area and work presented in this thesis.

In the evaluation and comparison of the pressure-load of the theoretical model it was found that when the lower applied loads were applied to the applied model results inconsistent with the rest of the applied loads were found. It is recommended that the lower loads be explored to determine whether the design methodology of this thesis is applicable or whether these loads are described by different mechanics.

It is recommended to investigate the theoretical models used to describe the mechanics which have been validated against the finite element analysis are further validated against a wider range of computational models. Through validating the theoretical models against a wider range of computational models it will allow for further validation of the range of applicability of the design methodology developed.

Although the theoretical models and therefore the design methodology have been validated against realistic data from computational models, to ensure that the performance of the valve matches that predicted by the calculations it would be reasonable to undertake physical testing of a seat component designed by the design methodology. Testing would need to involve pressurising the valve from one end and measuring the leakage from the other end in line with the testing standard discussed earlier in this thesis. As well as the sealing performance of the seat the torque model developed that linked the design of the seat to the numerical torque calculation could be validated by conducting tests on a prototype valve.

The cavity relief function of the ball valve seat was not considered in this thesis however developing and adding a cavity relief model to the seat design method would make the method complete in terms of the requirements applicable to the floating ball valve. As with the other numerical models it would also be recommended that the numerical model developed be validated through physical testing of the valve.

Lastly the element outside the scope of this thesis that would have the largest impact on the performance of the seal design is the effect of fatigue in the seat material due to cyclic loadings when the valve is put into service. It would be desirable to understand based on the seat design and the service conditions of the valve the duration for which the seat would remain within the functional parameters when subject to the in-service cyclic loadings.

Appendices

Appendix 1 – Contact Width Comparisons

The sealing width, 'b', used in Equation 20 is not defined therefore to create a satisfactory comparison between Equation 12 and Equation 18 it is necessary to seek a definition for it. Equation 18 deals with the compression of an O-Ring therefore it is assumed that the section to be compressed is circular. As an approximation to determine a comparable value to 'b' the chord of a circle with the same cross-sectional diameter.

The calculations contained in this appendix were completed using the dimensions of a 72-0945-30 O-Ring, the dimensions of this O-Ring are defined in the following table:

72-0945-30 O-Ring	
Variable	Value (mm)
Section, d_1	3.0
Inside Diameter, D_i	94.5
Outside Diameter, D_o	100.5
Mean Diameter, D_m	97.5

Table 34 - O-Ring 72-0945-30 Dimensions

From basic geometry the chord of the circle can be determined from the below:

$$L_c = 2 \cdot \sqrt{r^2 - d_2^2}$$

Equation 99 – Equation for the determination of the chord length

With the variables as defined the figure below:

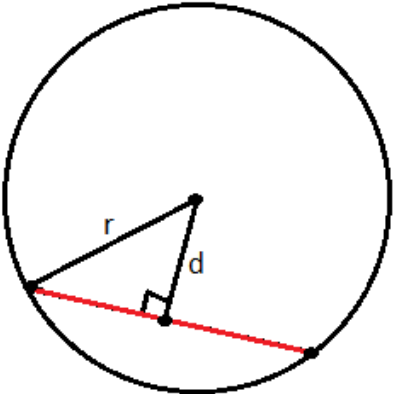


Figure 81 - Chord Length Variable Definitions (Tutor Vista, 2019)

This can be linked to the sealing width 'b', in Equation 18, of by defining 'd' as:

$$d_2 = r - x$$

Equation 100 - Distance to Chord Position

The below table shows the results of evaluating Equation 99 and the chord lengths for a 10%, 15% and 20% compression of the 3.0mm section O-Ring.

Compression (%)	x (mm)	d ₂ (mm)	Chord Length (mm)	b (mm)
10	0.30	1.20	1.80	0.72
15	0.45	1.05	2.14	1.08
20	0.60	0.90	2.40	1.44

Table 35 - Contact width results compared to chord lengths

From these results it is possible to determine that the contact width in Equation 18 is approximately equal to half of the chord length and therefore equivalent to the half-contact 'a' in Hertz Contact Mechanics.

Appendix 2 – O-Ring Load and Sealing Calculations

This Appendix contains the method and calculations for determining the load acting on and the maximum contact pressure developed by compressing a 72-0945-30 O-Ring of 70 Shore A hardness for varying amounts of compression. This is the same O-Ring as used in Appendix 1 to determine the sealing width 'b' for comparison, therefore these sealing widths shall be used in this Appendix.

The first step is to determine the compressive load required to achieve the compression of the O-Ring, this is achieved by using Equation 101 as shown below.

$$F = \pi \cdot d_1 \cdot D_m \cdot E \cdot \left[1.25 \cdot \left(\frac{x}{d_1} \right)^{1.5} + 50 \cdot \left(\frac{x}{d_1} \right)^6 \right]$$

Equation 101 - Compressive load on an o-ring (Hertz, 1979)

The compressive load at a set compression is then used with the sealing width, also determined for the same compression, to determine the maximum contact pressure in accordance with Equation 102.

$$f' = \frac{4 \cdot F}{\pi^2 \cdot b \cdot D_m}$$

Equation 102 - Max. contact pressure developed in an o-ring (Hertz, 1979)

Where a 70 Shore A O-Ring material has a Modulus of Elasticity equivalent to 1040psi / 7.171 N.mm⁻² Modulus of Elasticity. (Hertz, 1979). A Summary of the results gained from applying Equation 101 and Equation 102 to the dimensions of a 72-0945-30 O-Ring of a Shore 70 A material is given in Table 36.

Compression (%)	Load, F (N)	Max. Contact Pressure (N.mm ⁻²)
10	260.8	1.50
15	482.3	1.86
20	757.82	2.19

Table 36 – Tabulated max. contact pressure results for Hertz analysis of an o-ring

The results presented in the above table have been determined by the following calculations for various levels of compression of the O-Ring.

Equation 103 and Equation 104 shows the compressive load and max. contact pressure calculations when the O-Ring is subject to a compression of 10%.

$$F_{10} = \pi \cdot 3 \cdot 97.5 \cdot 7.171 \cdot \left[1.25 \cdot \left(\frac{0.3}{3.0} \right)^{1.5} + 50 \cdot \left(\frac{0.3}{3.0} \right)^6 \right] = 260.8N$$

Equation 103 - Compressive load when the o-ring is subject to 10% compression

$$f'_{10} = \frac{4 \cdot 260.8}{\pi^2 \cdot 0.72 \cdot 97.5} = 1.5 N \cdot mm^{-2}$$

Equation 104 - Max. contact pressure when the o-ring is subject to 10% compression

Equation 105 and Equation 106 show the calculations for the compressive load and the max. contact pressure when the O-Ring is compressed by 15%.

$$F_{15} = \pi \cdot 3 \cdot 97.5 \cdot 7.171 \cdot \left[1.25 \cdot \left(\frac{0.45}{3.0} \right)^{1.5} + 50 \cdot \left(\frac{0.45}{3.0} \right)^6 \right] = 482.3 N$$

Equation 105 - Compressive load when the o-ring is subject to 15% compression

$$f'_{15} = \frac{4 \cdot 482.3}{\pi^2 \cdot 1.08 \cdot 97.5} = 1.86 N \cdot mm^{-2}$$

Equation 106 - Max. contact pressure when the o-ring is subject to 15% compression

Equation 107 and Equation 108 show the calculations completed for a 20% compression of the O-Ring section for the compressive load as well as the maximum contact pressure.

$$F_{20} = \pi \cdot 3 \cdot 97.5 \cdot 7.171 \cdot \left[1.25 \cdot \left(\frac{0.6}{3.0} \right)^{1.5} + 50 \cdot \left(\frac{0.6}{3.0} \right)^6 \right] = 757.8 N$$

Equation 107 - Compressive load when the o-ring is subject to 20% compression

$$f'_{20} = \frac{4 \cdot 757.2}{\pi^2 \cdot 1.44 \cdot 97.5} = 2.19 N \cdot mm^{-2}$$

Equation 108 - Max. contact pressure when the o-ring is subject to 20% compression

Appendix 3 – Simulation Convergence Studies (Data)

The data shown in Table 37 includes the settings used and the results obtained from the convergence study conducted for the curvature-based mesh which was used in this thesis.

Main Mesh				Mesh Control				Simulation Result
Element Size		Min. Elements in a circle	Element growth ratio	Element Size Max. (in)	Element Ratio	Total Nodes	Total Elements	Average Von Mises Stress (psi)
Max. (in)	Min. (in)							
0.059947	0.059947	8	1.1	0.014987	1.1	1300	2419	373.2
0.059947	0.059947	8	1.1	0.011989	1.1	1478	2756	390.9
0.059947	0.059947	8	1.1	0.009592	1.1	1711	3201	454.7
0.059947	0.059947	8	1.1	0.007673	1.1	2044	3852	394.9
0.059947	0.059947	8	1.1	0.006139	1.1	2442	4636	431.5
0.059947	0.059947	8	1.1	0.004911	1.1	2970	5658	481.5
0.059947	0.059947	8	1.1	0.003929	1.1	3559	6826	468.9
0.059947	0.059947	8	1.1	0.003143	1.1	4283	8248	482
0.059947	0.059947	8	1.1	0.002514	1.1	5206	10038	520.8
0.059947	0.059947	8	1.1	0.002011	1.1	6095	11783	515.3
0.059947	0.059947	8	1.1	0.001609	1.1	7437	14441	517.6
0.059947	0.059947	8	1.1	0.001287	1.1	9113	17706	513.2
0.059947	0.059947	8	1.1	0.00103	1.1	10924	21307	517.3

Table 37 - Convergence Study Settings and Results

As can be seen from the table the results converged to less than 1% variance in the resulting average von mises stress measured from a single point on the computational model. These results were obtained using the 1000 lb-f load applied to the geometry of the valve and seat as used in the analyses conducted in this thesis.

Appendix 4 – Theoretical Mean Contact Stress Calculations

The following equations (Equation 109 and Equation 110), are the standard Hertz Contact mechanics equations to describe the contact of a cylindrical body and a flat surface.

The initial step in the calculation is determining the contact half-width as shown by Equation 109.

$$a = \sqrt[3]{\frac{4 \cdot R \cdot F}{\pi \cdot L \cdot E^*}} = \sqrt[3]{\frac{4 \cdot R \cdot P}{\pi \cdot E^*}}$$

Equation 109 – Contact half-width equation

With the contact half-width calculated by Equation 109 the result is used in Equation 110 to determine the mean contact stress.

$$p_m = \frac{P}{2 \cdot a}$$

Equation 110 – Mean contact pressure equation

When applying the values related to the loads applied to the model to the equations to determine the contact half-width and the mean contact stress.

Equation 111 and Equation 112 shows the contact half-width calculation and the mean contact stress equation when a 400 lb-f (1779.3N) load is applied to the geometry of the ball and seat.

$$a_{400} = \sqrt[3]{\frac{4 \cdot 42.07 \cdot 5.64}{\pi \cdot 713.64}} = 0.75 \text{ mm}$$

Equation 111 – Contact half-width calculation when subject to 400lb-f (1779.3N) applied load

$$p_{m400} = \frac{5.64}{2 \cdot 0.75} = 3.76 \text{ N.mm}^{-2} = 544.69 \text{ psi}$$

Equation 112 – Mean contact pressure calculation when subject to 400lb-f (1779.3N) applied load

Equation 113 and Equation 114 shows the contact half-width calculation and the mean contact stress equation when a 600 lb-f (2668.9N) load is applied to the geometry of the ball and seat.

$$a_{600} = \sqrt[3]{\frac{4 \cdot 42.07 \cdot 8.47}{\pi \cdot 713.64}} = 0.86 \text{ mm}$$

Equation 113 – Contact half-width calculation when subject to 600lb-f (2668.9N) applied load

$$p_{m600} = \frac{8.47}{2 \cdot 0.86} = 4.93 \text{ N.mm}^{-2} = 714.03 \text{ psi}$$

Equation 114 – Mean contact pressure calculation when subject to 600lb-f (2668.9N) applied load

Equation 115 and Equation 116 shows the contact half-width calculation and the mean contact stress equation when a 800 lb-f (3558.6N) load is applied to the geometry of the ball and seat.

$$a_{800} = \sqrt[3]{\frac{4 \cdot 42.07 \cdot 11.29}{\pi \cdot 713.64}} = 0.95 \text{ mm}$$

Equation 115 – Contact half-width calculation when subject to 800lb-f (3558.6N) applied load

$$p_{m800} = \frac{11.29}{2 \cdot 0.95} = 5.97 \text{ N.mm}^{-2} = 865.15 \text{ psi}$$

Equation 116 – Mean contact pressure when subject to 800lb-f (3558.6N) applied load

Equation 117 and Equation 118 shows the contact half-width calculations and the mean contact stress equation when a 1000 lb-f (4448.2N) load is applied to the geometry of the ball and seat.

$$a_{1000} = \sqrt[3]{\frac{4 \cdot 42.07 \cdot 14.11}{\pi \cdot 713.64}} = 1.02 \text{ mm}$$

Equation 117 – Contact half-width calculation when subject to 1000lb-f (4448.2N) applied load

$$p_{m1000} = \frac{14.11}{2 \cdot 1.02} = 6.92 \text{ N.mm}^{-2} = 1004.11 \text{ psi}$$

Equation 118 – Mean contact pressure calculation when subject to 1000lb-f (4448.2N) applied load

Equation 119 and Equation 120 shows the contact half-width calculations and the mean contact stress equation when a 1200 lb-f (5337.9N) load is applied to the geometry of the ball and seat.

$$a_{1200} = \sqrt[3]{\frac{4 \cdot 42.07 \cdot 16.93}{\pi \cdot 713.64}} = 1.08 \text{ mm}$$

Equation 119 – Contact half-width calculation when subject to 1200lb-f (5337.9N) applied load

$$p_{m1200} = \frac{16.93}{2 \cdot 1.08} = 7.82 \text{ N.mm}^{-2} = 1133.44 \text{ psi}$$

Equation 120 – Mean contact pressure calculation when subject to 1200lb-f (5337.9N) applied load

Equation 121 and Equation 122 shows the contact half-width calculations and the mean contact stress equation when a 1400 lb-f (6227.5N) load is applied to the geometry of the ball and seat.

$$a_{1400} = \sqrt[3]{\frac{4 \cdot 42.07 \cdot 19.75}{\pi \cdot 713.64}} = 1.14 \text{ mm}$$

Equation 121 – Contact half-width calculation when subject to 1400lb-f (6227.5N) applied load

$$p_{m1400} = \frac{19.75}{2 \cdot 1.14} = 8.66 \text{ N.mm}^{-2} = 1256.03 \text{ psi}$$

Equation 122 – Mean contact pressure when subject to 1400lb-f (6227.5N) applied load

Equation 123 and Equation 124 shows the contact half-width calculations and the mean contact stress equation when a 1600 lb-f (7117.2N) load is applied to the geometry of the ball and seat.

$$a_{1600} = \sqrt[3]{\frac{4 \cdot 42.07 \cdot 22.58}{\pi \cdot 713.64}} = 1.19 \text{ mm}$$

Equation 123 – Contact half-width when subject to 1600lb-f (7117.2N) applied load

$$p_{m1600} = \frac{22.58}{2 \cdot 1.19} = 9.47 \text{ N.mm}^{-2} = 1373.22 \text{ psi}$$

Equation 124 – Mean contact pressure when subject to 1600lb-f (7117.2N) applied load

Appendix 5 – Theoretical Seat Bending Stress Calculations

This Appendix contains the theoretical bending stress calculations for the seat component. The bending stress in the seat is described by the equations from Roark's theory of Stress and Strain this shall be determined in accordance with:

$$\sigma_v = 1.1\sqrt{\sigma_1^2 - \sigma_1\sigma_2 + \sigma_2^2}$$

Equation 125 - Equivalent Stress in Seat Component

The Equivalent stress is derived from the Radial and Tangential stress in the set component, these are determined in Equation 126 and Equation 130.

$$\sigma_1 = \frac{6 \cdot M_t}{t^2}$$

Equation 126 – Tangential Stress in Seat Component (Young & Budynas, Roark's Formulas for Stress and Strain, 2002)

The tangential stress calculation shown in Equation 126 is determined based on the tangential moment determined in Equation 127.

$$M_t = \frac{\theta \cdot D \cdot (1 - \nu^2)}{r} + \nu \cdot M_r$$

Equation 127 - Tangential Moment Equation (Young & Budynas, Roark's Formulas for Stress and Strain, 2002)

The tangential moment is evaluated in accordance with the equation shown in Equation 127, this requires the radial moment to be determined prior to this, this can be done in accordance with Equation 132 for this case. In addition to the radial moment the deflection angle needs to be determined in accordance with Equation 128.

$$\theta = \theta_b \cdot F_4 + M_{rb} \cdot \frac{r}{D} \cdot F_5 + Q_b \cdot \frac{r^2}{D} \cdot F_6 - w \cdot \frac{r^2}{D} \cdot G_6$$

Equation 128 - Deflection Angle Equation (Young & Budynas, Roark's Formulas for Stress and Strain, 2002)

$$\theta = \theta_b \cdot F_4 + Q_b \cdot \frac{r^2}{D} \cdot F_6$$

Equation 129 - Simplified Deflection Angle Equation

$$\sigma_2 = \frac{6 \cdot M_r}{t^2}$$

Equation 130 – Radial Stress in Seat Component (Young & Budynas, Roark's Formulas for Stress and Strain, 2002)

The radial stress calculation shown in Equation 126 is determined based on the radial moment determined in Equation 131.

$$M_r = \theta_b \cdot \frac{D}{r} \cdot F_7 + M_{rb} \cdot F_8 + Q_b \cdot r \cdot F_9 - w \cdot r \cdot G_9$$

Equation 131 - Radial Moment (Young & Budynas, Roark's Formulas for Stress and Strain, 2002)

The radial moment is simplified from that shown in Equation 131 to that shown in Equation 132 by the application of the following rules. One of the boundary conditions from this particular case in Roark's Formulas of Stress and Strain is that $M_{rb} = 0$, therefore any term which involves this variable is removed from the equation. The location of the load, r_0 and the location of the analysis, r , are the same location, therefore when analysing the 'G' variables these are all evaluated as being equal to 0 and therefore removed from the equation, this leaves the equation to be evaluated as Equation 132.

$$M_r = \theta_b \cdot \frac{D}{r} \cdot F_7 + Q_b \cdot r \cdot F_9$$

Equation 132 - Simplified Radial Moment Equation

The 'F' constants evaluated in the previous equations are determined by the use of the following equations.

$$F_4 = \frac{1}{2} \left[(1 + \nu) \cdot \frac{b}{r} + (1 - \nu) \cdot \frac{r}{b} \right]$$

Equation 133 - Constant, F4 (Young & Budynas, Roark's Formulas for Stress and Strain, 2002)

$$F_6 = \frac{b}{4r} \left[\left(\frac{b}{r} \right)^2 - 1 + 2 \cdot \ln \frac{r}{b} \right]$$

Equation 134 - Constant, F6 (Young & Budynas, Roark's Formulas for Stress and Strain, 2002)

$$F_7 = \frac{1}{2} \cdot (1 - \nu^2) \cdot \left(\frac{r}{b} - \frac{b}{r} \right)$$

Equation 135 - Constant, F7 (Young & Budynas, Roark's Formulas for Stress and Strain, 2002)

$$F_9 = \frac{b}{r} \left\{ \frac{1 + \nu}{2} \cdot \ln \frac{r}{b} + \frac{1 + \nu}{4} \cdot \left[1 - \left(\frac{b}{r} \right)^2 \right] \right\}$$

Equation 136 - Constant, F9 (Young & Budynas, Roark's Formulas for Stress and Strain, 2002)

Bibliography

- American Petroleum Institute. (2008). *API 591 - Process Valve Qualification Procedure*. Washington: API Publishing Services.
- American Petroleum Institute. (2009). *API 598 - Valve Inspection and Testing*. Washington: API Publishing Services.
- American Petroleum Institute. (2015). *API 6D - Specification for Pipeline and Piping Valves*. Washington: API Publishing Services.
- American Society of Mechanical Engineers. (2013). *ASME B16.34-2013*. New York: American Society of Mechanical Engineers.
- American Society of Mechanical Engineers. (2017). *ASME/BPVC VIII Division 1*. New York: ASME.
- API. (2008, April). *API 6D. Specification for Pipeline Valves*. Washington D.C., USA: API.
- Ben Jemaa, M. C., Mnif, R., Fehri, K., & Elleuch, R. (2011). *Design of a New Tribometer for Tribological and Viscoelasticity Studies of PTFE Valve Seats*. New York: Springer.
- Boiko, A. Y., Regush, L. A., Semenov, I. V., & Regush, L. A. (1986). Calculation of Polymer Seals for Ball Valves. *Design and Stress Analysis*, 529-531.
- Borrego, M. (2009). Quantitative, Qualitative and Mixed Research Methods in Engineering Education. *Journal of Engineering Education*, 53 - 66.
- Bozhko, G. V., Kalabekov, I. G., Vinogradov, G. G., & Denisov, S. M. (1992). *Conditions of Hermetic Sealing of Thermoplastic Surfaces*. London: Plenum Publishing Corporation.
- BP International Ltd. (2012). *BP GIS 62-012. Group Instruction for Supply*. BP International Ltd.
- BP International Ltd. (2012, May 11). *GIS 62-013. Group Instruction for Supply*.
- Brink, R. V., Czernik, D. E., & Horve, L. A. (1993). *Handbook of Fluid Sealing*. New York: McGraw-Hill.
- British Standards Institute. (1974). *BS 5159. Cast Iron and Carbon Steel Ball Valves for General Purposes*. London: British Standards Institution.
- British Standards Institution. (2015). *BS EN ISO 17292 . Metal Ball Valves for Petroleum, Petrochemical and Allied Industries*. Brussels: BSI Standards.
- Brown, M. W. (1990). *Seals and Sealing Handbook*. Oxford: Elsevier Science Publishers Limited.
- Budynas, R. G., & Nisbett, J. K. (2015). *Shigley's Mechanical Engineering Design*. New York: McGraw-Hill.
- BVAA. (2007). *BVAA Training Course Notes Valves & Actuators*. Banbury: BVAA.
- Campbell, F. C. (2012). *Fatigue and Fracture: Understanding the Basics*. Ohio: ASM International.
- Chakrabarti, A. (2002). *Engineering Design Synthesis*. London: Springer-Verlag.
- Chern, M.-J. (2007). Performance test and flow visualization of ball valve. *Experimental Thermal and Fluid Science* 31, 505-512.
- Dassault Systems. (2010). *Understanding Nonlinear Analysis*. Massachusetts: Dassault Systems.
- Dwyer-Joyce, R. S. (1997). *Tribological Design Data*. London: The Institution of Mechanical Engineers.
- EPRI. (1999). *Air-Operated Valve Evaluation Guide, TR-107322*. Palo Alto, CA.

- Fleck, S. D. (1998). *Spherical Indentation of Elastic-Plastic Solids*. Cambridge: The Royal Society.
- Fluid Sealing Association. (2008, May). What determines seal leakage? *Pumps & Systems*, pp. 48-50.
- G.V.Bozhko. (2000). Force Analysis for a Ball-Seating Valve with PTFE Seal. *Chemical and Petroleum Engineering, Vol. 36*, 11-12.
- Grant, A. (2019, May 25). *The Essential Role Of Ball Valves In Engineering Systems*. Retrieved from Spirit of Freedom: <https://www.spiritoffreedom.org.uk/the-essential-role-of-ball-valves-in-engineering-systems/>
- Hertz, D. L. (1979). *O-Rings for Low-Pressure Service*. New Jersey: Machine Design.
- International Association of Oil & Gas Producers. (2019). *Specification S-562 Supplementary Requirements to API Specification 6D Ball Valves*. London: International Association of Oil & Gas Producers.
- International Organisation for Standardization. (2008). *ISO 5208, Industrial Valves - Pressure testing of metallic valves*. Geneva: ISO Copyright Office.
- K.L.Johnson. (2003). *Contact Mechanics*. Cambridge: Cambridge University Press.
- Kim, C. K. (1997). Analysis of contact force and thermal behaviour of lip seals. *Tribology International Volume 30 Number 2*, 113-119.
- Lee, C.-Y. (2006). Simulation and experimentation on the contact width and pressure distribution of lip seals. *Tribology International 39*, 915-920.
- Lyons, J. L., & Askland, C. L. (1975). *Lyons' Encyclopedia of Valves*. New York: Van Nostrand Reinhold Company.
- Machine Design. (1993). Design Considerations for PTFE Seals. *Machine Design*, 156.
- Metso. (2011). *Advanced Sealing Technology*. Shrewsbury: Metso.
- Neale, M. J. (1995). *Drives & Seals - A Tribology Handbook*. Oxford: Butterworth-Heinemann Ltd.
- Nesbitt, B. (2001). *Guide to European Valves*. Chippenham: Professional Engineering Publishing.
- Ning, Z. (2015). Compressive and Sealing Characteristics of PTFE under Cyclic Loading-unloading. *Journal of Wuhan University -Mater. Sci. Ed.*, 181 - 184.
- Ning, Z., Qiang, L., Kang, H., & Qing, L. (2015). Compressive and Sealing Characteristics of PTFE under Cyclic Loading-Unloading. *Journal of Wuhan University of Technology-Mater. Sci. Ed*, 181-184.
- Norton, R. L. (2012). *Design of Machinery*. New York: McGraw-Hill.
- Ripert, R. L. (1964). *Canada Patent No. 3,384,341*.
- Rogula, J. (2011). The Influence of Seat Fatigue Test on the Leakage in Ball Valve. Elsevier Ltd.
- Skousen, P. L. (1997). *Valve Handbook*. New York: McGraw-Hill.
- Song, X.-G., Wang, L., & Park, Y.-C. (2009). *Analysis and optimization of nitrile butadiene rubber sealing mechanism of ball valve*. New York: Elsevier.
- Taylor, B. (2016). *Tutorial - Hertz Contact Stress*. Arizona: University of Arizona College of Optical Sciences.
- Tsai, C. C., Chang, C. Y., & Tseng, C. H. (2004). *Optimal design of metal seated ball valve mechanism*. Taiwan: Department of Mechanical Engineering, National Chiao Tung University.

- Tutor Vista. (2019, January 09). *Chord of a Circle*. Retrieved from Tutor Vista: <https://math.tutorvista.com/geometry/chord-of-a-circle.html>
- Velan Inc. (2014). *Valvac - General purpose ball valves*. Montreal: Velan Inc.
- Velan Inc. (2019). Memoryseal Resilient-seated ball Valves. Cote de Liesse, Montreal, Canada: Velan Inc.
- Warring, R. H. (1981). *Seals and Sealing Handbook*. Surrey: Trade & Technical Press.
- Weber, D., & Haas, W. (2007, February). Wear behaviour of PTFE lip seals with different sealing edge designs, experiments and simulation. *Sealing Technology*, pp. 7-8.
- XiaoHong, J., Fei, G., Le, H., LongKe, W., Zhi, G., & YuMing, W. (2014). *Effects of radial force on the static contact properties and sealing performance of a radial lip seal*. Beijing: Science China Technological Sciences.
- Young, W. C. (2002). *Roark's Formulas for Stress and Strain, Seventh Edition*. New York: McGraw-Hill.
- Young, W. C., & Budynas, R. G. (2002). *Roark's Formulas for Stress and Strain*. New York: McGraw-Hill.
- Zappe, R. W. (1998). *Valve Selection Handbook*. Houston: Gulf Publishing Company.
- Zoombd24. (2019, May 25). *Ball Valve*. Retrieved from Zoombd24: <http://www.zoombd24.com/ball-valve/>